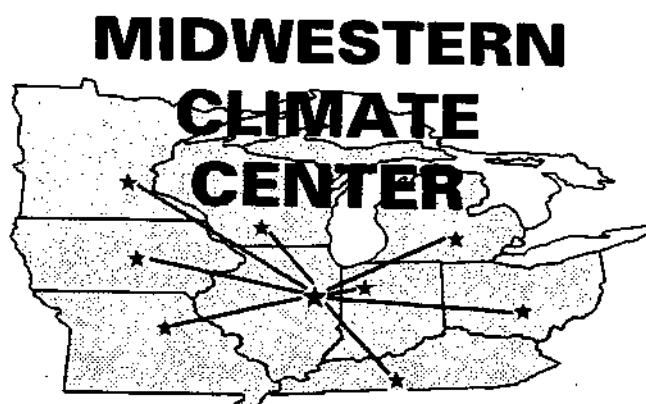


*Implementation of a Semi-Physical Model
for Examining Solar Radiation
in the Midwest*

Mary Schoen Petersen



**Research Report 90-01
December 1990**

Midwestern Climate Center
Atmospheric Sciences Division
Illinois State Water Survey
2204 Griffith Drive
Champaign, IL 61820-7495
(217) 244-8226

E.N.R. LIBRARY

DEMCO

The body of this report was printed on recycled paper.

Department of Energy & Natural Resources
325 West Adams
Springfield, Illinois 62704-1892

IMPLEMENTATION OF A SEMI-PHYSICAL MODEL
FOR EXAMINING SOLAR RADIATION IN THE MIDWEST

BY

MARY SCHOEN PETERSEN

B.S., University of Nebraska-Lincoln, 1987

Published by the

Midwestern Climate Center
Publication Number 90-01

Illinois State Water Survey
Richard G. Semonin, Chief
2204 Griffith Drive
Champaign, Illinois 61820-7595

December 1990

ABSTRACT

This study arose from the need for a detailed documentation of the solar radiation (SR) climate of the Midwest region. Because the network of SR measurements for this region is either sparse or lacking in longevity, a semi-physical SR model based on Meyers and Dale (1983) was implemented. A 40-year (1948-1987) data base of daily SR values was created for 53 stations in the Midwest.

The advantages of the model implemented include: 1) its dependence on standard hourly meteorological data (surface pressure, dew point temperature, and cloud height and fractional sky cover) as input; 2) its accommodations of the effects of Rayleigh scattering, absorption by water vapor and permanent gases, absorption and scattering by aerosols and clouds, and ground-to-cloud-to-ground reflectance; and 3) the fact that it is both computationally efficient and was previously found, as well as proven here, to give accurate results. Techniques were employed to insure the most complete possible SR data base for each station and, as a result, the daily SR data set generated is 93% complete for the 53 stations for 1948-1987.

The model generated SR values were compared and validated against several sets of measured SR data, including SOLMET (SOLar METeorological) and regression-extended SOLMET values. Comparisons indicated that the model generally tends to overpredict daily totals of SR on average, but more so in the cooler months (October-March) than the warmer months (April-September). The mean absolute error was approximately $1.6 \text{ MJ m}^{-2} \text{ day}^{-1}$, which translates to differences from 8-12% of the measured averages. Meyers and Dale (1983) obtained similar mean absolute error (8.7%) for the same model. Thus, the model produces results that are comparable to previous validations and are in very good agreement with observed SR. Comparisons of modeled data with regression-extended SOLMET data suggested that the regression-extended SOLMET data should be viewed with caution, which is in agreement to findings of the Solar Energy Research Institute (1990a).

Analysis of calendar monthly mean spatial SR patterns obtained from this newly developed 40-year data base revealed a pronounced near-zonal SR pattern during the fall and winter months, with more meso-scale features in the late spring and summer months. Evident from these meso-scale features are the effects of the Great Lakes (additionally seen in all seasons) and the effects of urban industrialization/pollution. Time series analyses of individual monthly SR means for all stations in the Midwest revealed a region-wide 40-year downward trend for the mid-season month of October; for many stations the trend was statistically significant at the >99% confidence level.

This strikingly coherent pattern was less visible for the other mid-season months, which displayed mostly positive trends.

These seasonal SR trends were noted to be consistent with previous results on the secular variation of Midwestern cloudiness, which found substantial percentage increases in the number of cloudy days occurring in autumn, and smaller increases in spring. Previously studied visibility trends were mostly associated with increasing SR, except in October when SR trends were also downward.

DEDICATION

I dedicate this work to the most important person in my life, Paul Petersen; to the memory of Burl Graff, my high school Math teacher, my friend, and my "second father"; to the memory of Bob Taylor, the weathercaster on Channel 10 in Lincoln, Nebraska as I was growing up; and to the memories of Sharon Carlson and Jim "Eggy" Kolterman who died while still in High School.

ACKNOWLEDGMENTS

This paper was submitted in partial fulfillment of the requirements for the degree of Master of Science in Atmospheric Sciences to be awarded in January 1991 by the Graduate College of the University of Illinois at Urbana-Champaign.

I thank the Climate and Meteorology Section of the Illinois State Water Survey for their scientific interaction and encouragement during the past 3 years. In particular, I thank Kenneth E. Kunkel, Robert R. Czys, and Peter J. Lamb for their time and encouragement, without which this thesis would not have been completed. I also thank Rebecca Runge very much for help in typing this manuscript, and John Brother for drafting a figure.

My family, especially my parents, deserve thanks for all their years of support, caring, and encouragement, which has led me to what and where I am today. I owe everything to Paul M. Petersen, my consultant, encourager, best friend, and husband, who has never stopped believing in me, and has helped me immensely in attaining this goal and finally finishing this thesis.

This research was supported under NOAA Grant NA87AA-D-CP119.

TABLE OF CONTENTS

CHAPTER	Page
I. INTRODUCTION	1
A. Background	1
B. Motivation	2
C. Objectives	4
II. MODEL IMPLEMENTATION AND VALIDATION	7
A. Semi-Physical Model	7
1. Description of Model	7
2. Model Input Data	10
a. Pre June 1951 Cloud Problems (CC51).	11
b. Post June 1951 Cloud Problems.	13
c. Miscellaneous Problems.	18
3. Model Sensitivity to Dew Point Temperature.	19
4. Model Sensitivity to Surface Pressure.	20
B. Validation of Model	21
III. COMPARISON WITH CORRECTED SOLAR RADIATION FROM SOLMET.	34
A. Background to SOLMET Data	34
B. Statistical Results	35
C. Comparing with Baker and Klink's Data	46
D. Extension of SOLMET using Regression Estimates.	51
E. Summary.	59
IV. ASPECTS OF THE SPATIAL AND TEMPORAL VARIABILITY OF SOLAR RADIATION IN THE MIDWEST.	63
A. Spatial Variability.	63
B. Secular Variation.	69
C. Comparison with Precipitation, Cloudiness, and Visibility.	82
V. CONCLUSION.	85
A. Summary.	85
B. Future Research	88
REFERENCES.	90
APPENDIX A: STATION NAMES AND IDENTIFIERS.	95
APPENDIX B: DATA BASE INFORMATION.	98
APPENDIX C: FIGURES FROM BENNETT (1965).	101
APPENDIX D: FIGURES FROM BAKER AND KLINK (1975).	114
APPENDIX E: MID-SEASON TIME SERIES.	120

LIST OF TABLES

Table 2.1.	values taken from Smith (1966).	9
Table 2.2.	Transmission coefficients, t_b , for indicated cloud height and coverage (from Meyers and Dale, 1983).	10
Table 2.3a.	Method of assigning the cloud height when observations give the sky condition (BKN or OVC) for one layer and the ceiling height (CLHT).	14
Table 2.3b.	Method of assigning cloud heights when observations give the sky condition (SCT, BKN or OVC) for two layers and the ceiling height (CLHT). The two possible combinations of sky conditions are demonstrated (CASES A and B). Two CLHT criteria (defined by superscripts and accompanying information) are used for CASE A, and three for CASE B.	14
Table 2.3c.	Method of assigning cloud heights when observations give the sky condition (SCT, BKN or OVC) for three layers and the ceiling height (CLHT). The three possible combinations of sky conditions are demonstrated (CASES A, B, and C). Three CLHT criteria (defined by superscripts and accompanying information) are used for CASE B, and four for CASE C.	15
Table 2.3d.	Method of assigning cloud heights when observations give the sky condition (SCT, BKN or OVC) for four layers and the ceiling height (CLHT). The four possible combinations of sky conditions are demonstrated (CASES A, B, C, and D). Four CLHT criteria (defined by superscripts and accompanying information) are used for each case.	16
Table 2.4.	Assigned cloud heights at a given layer, when no cloud height (layer or ceiling) information is known, but sky condition values are given as SCT.	18
Table 2.5.	Regression results of observed versus modeled SR for each of the four stations compared. All r^2 results were found to be significant at the greater than 99.9% confidence level.	26
Table 2.6.	Mean error, mean absolute error, and root mean square (rms) error for modeled solar radiation at Eau Claire (EAU) in 1986. Units are $\text{MJ m}^{-2} \text{ day}^{-1}$, and percent of measured average.	28
Table 2.7a.	As in Table 2.6, but for Columbus (OSU) in 1987.	28

Table 2.7b.	As in Table 2.7a, but measured data were increased by 5%.	29
Table 2.8.	As in Table 2.7a, but for Peoria in 1987.	29
Table 2.9.	As in Table 2.8, but for all of 1988 at Peoria	30
Table 2.10.	As in Table 2.9, except cloud heights were only available every 3 hours as model input (i.e., modeled data are a test of the interpolation scheme).	32
Table. 3.1.	Mean error, mean absolute error, and root mean square (rms) error of modeled solar radiation versus SOLMET a) OBS b) ENG, and c) STD data for Madison. Units are MJ m ⁻² day ⁻¹ , and percent of SOLMET average.	36
Table 3.2.	As in Table 3.1, but for Omaha	37
Table 3.3.	As in Table 3.1, but for Columbia	38
Table 3.4.	As in Table 3.1, but for Nashville, TN.	39
Table 3.5.	Coefficient of determination (r ²), slope (m), and intercept (b) for regression of SOLMET on modeled daily solar radiation (SR), for indicated SOLMET data sets and stations.	45
Table 3.6.	Percent error of daily, monthly, and annual totals computed from fitted SOLMET hourly SR values. Mean daily totals are in KJ m ⁻² day ⁻¹	58
Table 3.7.	Mean error, mean absolute error, and root mean square (rms) error of modeled versus regression-extended SOLMET SR for Indianapolis. Units are MJ m ⁻² day ⁻¹ , and percent of SOLMET average.	60
Table 4.1.	Slopes of regression multiplied by 1000 for SR (i.e., KJ m ⁻² day ⁻¹) and 100 for precipitation (i.e., hundredths of inches year ⁻¹) for the indicated stations and months. Numbers below slopes indicate level of statistical significance of the trend based on the Student's <i>t</i> test. Highly significant trends (>95% confidence level) are in bold.	79
Table B.1.	Summary of the modeled solar radiation data base produced for each station listed in Appendix A (listed alphabetically by station). Any day with Data, is listed either in Missing Data or Good Data. Good Data includes Flagged Data; days are flagged if no cloud heights were given during the day, and there was at least 1 hour with sky condition not clear (CLR). Stations for which there were separate data tapes (e.g., because of stations moves, etc.) are listed separately and identified.	98

LIST OF FIGURES

Fig. 1.1.	The 26 SOLMET (SOLar METeorological) stations in the United States.	3
Fig. 1.2.	Map of 10 solar climate regions of the United States, according to Willmott and Vernon (1980). Dots indicate station location.	5
Fig. 1.3.	Map of the solar climate regions of the United States, according to Balling and Vojtesak (1983). Squares indicate SOLMET stations, dots indicate derived data stations.	5
Fig. 2.1.	Map of midwest states showing location with identifiers of stations for which solar radiation (SR) was modeled. See Appendices A and B for further station information.	12
Fig. 2.2.	Scatter plot of modeled versus observed daily SR for 130 days in 1986 at Eau Claire (and Chetek), WI. Regression line of all days is dashed (see Table 2.5); the 1:1 line is solid.	22
Fig. 2.3.	As in Fig. 2.2, but for 361 days in 1987 at Columbus (and Delaware), OH.	23
Fig. 2.4.	As in Fig. 2.3, but for 136 days in 1987 at Peoria, IL.	24
Fig. 2.5.	As in Fig. 2.4, but for 286 days in 1988.	25
Fig. 2.6.	Same as in Fig. 2.5, except cloud heights were only available every 3 hours as model input (i.e., modeled data are a test of the interpolation scheme).	33
Fig. 3.1.	Scatter diagram of 3000 randomly selected pairs of modeled versus SOLMET daily data for Madison. Solid line is 1:1 line; regression line is dashed.	41
Fig. 3.2.	Scatter diagram of 3000 randomly selected pairs of modeled versus SOLMET daily data for Omaha. Solid line is 1:1 line, regression line is dashed.	42
Fig. 3.3.	Scatter diagram of 3000 randomly selected pairs of modeled versus SOLMET daily data for Columbia. Solid line is 1:1 line; regression line is dashed.	43
Fig. 3.4.	Scatter diagram of 3000 randomly selected pairs of modeled versus SOLMET daily data for Nashville. Solid line is 1:1 line, regression line is dashed.	44
Fig. 3.5.	Comparison of the climatological weekly averages of Baker & Klink's data (solid line) versus modeled output (dashed) for Madison, Omaha, and Columbia.	47

Fig. 3.6.	Comparison of the climatological weekly averages of Baker & Klink's data (solid line) versus the SOLMET data sets (dashed) for Madison	48
Fig. 3.7.	Comparison of the climatological weekly averages of Baker & Klink's data (solid line) versus the SOLMET data sets (dashed) for Omaha	49
Fig. 3.8.	Comparison of the climatological weekly averages of Baker & Klink's data (solid line) versus the SOLMET data sets (dashed) for Columbia	50
Fig. 3.9.	Comparison of the climatological weekly averages of the modeled output (solid line) versus the SOLMET data sets (dashed) for Madison	52
Fig. 3.10.	Comparison of the climatological weekly averages of the modeled output (solid line) versus the SOLMET data sets (dashed) for Omaha	53
Fig. 3.11.	Comparison of the climatological weekly averages of the modeled output (solid line) versus the SOLMET data sets (dashed) for Columbia	54
Fig. 3.12.	Scatter diagram comparing the climatological weekly averages of the modeled output versus the SOLMET data sets for Madison	55
Fig. 3.13.	Scatter diagram comparing the climatological weekly averages of the modeled output versus the SOLMET data sets for Omaha	56
Fig. 3.14.	Scatter diagrams comparing the climatological weekly averages of the modeled output versus the SOLMET data sets for Columbia	57
Fig. 3.15.	Scatter diagram of 3000 randomly selected pairs of modeled versus SOLMET daily data for Indianapolis. Solid line is 1:1 line; regression line is dashed	60
Fig. 3.16.	Comparison of the climatological weekly averages of a) Baker & Klink's data (solid) versus the modeled output (dashed); b) Baker and Klink's data (solid) versus the SOLMET data (dashed); and c) modeled output (solid) versus the SOLMET data (dashed) for Indianapolis.	61
Fig. 4.1.	Spatial variations in mean daily totals of SR for January, February, March, and April over the midwest region. Contour interval is 0.5 MJ m ⁻² day ⁻¹	64
Fig. 4.2.	As in Fig. 4.1, but for May, June, July, and August	65

Fig. 4.3.	As in Fig. 4.1, but for September, October, November, and December.	66
Fig. 4.4a.	Solid line is time series of monthly mean SR values for January at International Falls, Sault Ste Marie, Sioux City, and Madison. Dashed line is regression line; open circles are total precipitation. The number in the upper right-hand corner of each graph is the level of statistical significance of the SR time series.	70
Fig. 4.4b.	Solid line is time series of monthly mean SR values for January at Cleveland, Evansville, and Springfield. Dashed line is regression line; open circles are total precipitation. The number in the upper right-hand corner of each graph is the level of statistical significance of the SR time series.	71
Fig. 4.5a.	As in Fig. 4.4a, but for April.	72
Fig. 4.5b.	As in Fig. 4.4b, but for April.	73
Fig. 4.6a.	As in Fig. 4.4a, but for July.	74
Fig. 4.6b.	As in Fig. 4.4b, but for July.	75
Fig. 4.7a.	As in Fig. 4.4a, but for October.	76
Fig. 4.7b.	As in Fig. 4.4b, but for October.	77
Fig. 4.8.	Spatial coherency of SR trends for 1948-1987 for January, April, July, and October months. Relatively insignificant (<90%) positive and negative trends are shown with a + and -, respectively; significant (90-95%) positive and negative trends display a A and v, respectively; and highly significant (>95%) positive and negative trends are shown as and , respectively. Double solid triangles indicate significance at the >99% confidence level. No trend is signified by a 0.	80
Fig. C.1.	Mean daily insolation in langleys from 1950-1962 during January (from Bennett, 1965).	102
Fig. C.2.	As in Fig. C.1, but for February.	103
Fig. C.3.	As in Fig. C.1, but for March.	104
Fig. C.4.	As in Fig. C.1, but for April.	105
Fig. C.5.	As in Fig. C.1, but for May.	106
Fig. C.6.	As in Fig. C.1, but for June.	107
Fig. C.7.	As in Fig. C.1, but for July.	108
Fig. C.8.	As in Fig. C.1, but for August.	109
Fig. C.9.	As in Fig. C.1, but for September.	110
Fig. C.10.	As in Fig. C.1, but for October.	111
Fig. C.11.	As in Fig. C.1, but for November.	112
Fig. C.12.	As in Fig. C.1, but for December.	113

Fig. D.1.	Average daily radiation received at the 80-percent level of probability during a period of similar radiation pattern that lasts from February 21 - April 4 (from Baker and Klink, 1975).	.114
Fig. D.2.	Same as in Fig. D.1, except from April 5 - July 18.	.115
Fig. D.3.	Same as in Fig. D.1, except from July 19 - August 15.	.116
Fig. D.4.	Same as in Fig. D.1, except from August 16 - October 3.	.117
Fig. D.5.	Same as in Fig. D.1, except from October 4 - October 24.	.118
Fig. D.6.	Same as in Fig. D.1, except from October 25 - February 20.	.119
Fig. E.1.	Solid line is SR time series for indicated month and stations; dashed line is regression line. Number in upper right-hand corner indicates statistical significance of the regression line slope.	.121
Fig. E.2.	As in Fig. E.1	.122
Fig. E.3.	As in Fig. E.1	.123
Fig. E.4.	As in Fig. E.1	.124
Fig. E.5.	As in Fig. E.1	.125
Fig. E.6.	As in Fig. E.1	.126
Fig. E.7.	As in Fig. E.1	.127
Fig. E.8.	As in Fig. E.1	.128
Fig. E.9.	As in Fig. E.1	.129
Fig. E.10.	As in Fig. E.1	.130
Fig. E.11.	As in Fig. E.1	.131
Fig. E.12.	As in Fig. E.1	.132
Fig. E.13.	As in Fig. E.1	.133
Fig. E.14.	As in Fig. E.1	.134
Fig. E.15.	As in Fig. E.1	.135
Fig. E.16.	As in Fig. E.1	.136
Fig. E.17.	As in Fig. E.1	.137
Fig. E.18.	As in Fig. E.1	.138
Fig. E.19.	As in Fig. E.1	.139
Fig. E.20.	As in Fig. E.1	.140
Fig. E.21.	As in Fig. E.1	.141
Fig. E.22.	As in Fig. E.1	.142
Fig. E.23.	As in Fig. E.1	.143
Fig. E.24.	As in Fig. E.1	.144
Fig. E.25.	As in Fig. E.1	.145
Fig. E.26.	As in Fig. E.1	.146
Fig. E.27.	As in Fig. E.1	.147
Fig. E.28.	As in Fig. E.1	.148

Fig. E.29.	As in Fig. E.1149
Fig. E.30.	As in Fig. E.1150
Fig. E.31.	As in Fig. E.1151
Fig. E.32.	As in Fig. E.1152
Fig. E.33.	As in Fig. E.1153
Fig. E.34.	As in Fig. E.1154
Fig. E.35.	As in Fig. E.1155
Fig. E.36.	As in Fig. E.1156
Fig. E.37.	As in Fig. E.1157
Fig. E.38.	As in Fig. E.1158
Fig. E.39.	As in Fig. E.1159
Fig. E.40.	As in Fig. E.1160
Fig. E.41.	As in Fig. E.1161
Fig. E.42.	As in Fig. E.1162
Fig. E.43.	As in Fig. E.1163
Fig. E.44.	As in Fig. E.1164
Fig. E.45.	As in Fig. E.1165
Fig. E.46.	As in Fig. E.1166
Fig. E.47.	As in Fig. E.1167
Fig. E.48.	As in Fig. E.1168
Fig. E.49.	As in Fig. E.1169
Fig. E.50.	As in Fig. E.1170
Fig. E.51.	As in Fig. E.1171
Fig. E.52.	As in Fig. E.1172
Fig. E.53.	As in Fig. E.1173
Fig. E.54.	As in Fig. E.1174
Fig. E.55.	As in Fig. E.1175
Fig. E.56.	As in Fig. E.1176

CHAPTER I

INTRODUCTION

Radiant heat energy originating from the sun is a crucial input for many earth systems, both natural and humanly constructed. This energy is variously referred to as shortwave radiation, solar radiation (SR), global radiation, solar energy, or insolation, and will henceforth be designated by SR. The wide variety of systems for which SR is an important energy source results in there being a large number of actual or potential users of SR data, including those in agriculture, atmospheric science, building design, engineering, forestry, horticulture, hydrology, and land use planning. For example, an agriculturalist might be interested in using SR data to determine hay drying conditions; an engineer or building designer may use the data to plan the orientation of windows and solar panels; and an atmospheric scientist might use SR information to study the surface heating that induces convection. In many cases, such users require that the information be representative of the long term conditions.

This thesis deals with the SR climatology of the Midwest for 1948-1987. It first explains the procedure used to generate daily values of SR for 53 locations in 9 agriculturally important states (Minnesota, Iowa, Missouri, Illinois, Wisconsin, Michigan, Indiana, Ohio, Kentucky) for the 40 year period. Those data are then analyzed to provide information on the spatial and temporal variability of SR throughout the Midwest.

A. Background

The SR input to and its disposition within the plant system is of great interest to agriculturalists, horticulturalists, and foresters, since these factors have considerable influence on plant productivity. SR provides the reducing power within green leaves to convert CO₂ and H₂O into sugars (Moss, 1967). The CO₂ is supplied by the atmosphere and enters the leaf by diffusion. Light affects CO₂ diffusion by initiating photosynthesis which removes CO₂ at the chloroplast and establishes a diffusion gradient. In addition to field studies that seek an understanding of the physics of radiative transfer in crops, many scientists have been concerned with incorporating SR into empirical models that estimate crop productivity. SR can be incorporated into such models both directly and indirectly, with the latter being through its use in the calculation of evapotranspiration (Rosenberg *et al*, 1983).

As Neild *et al*. (1978) point out, summaries of weather normals over fixed time periods of one month or more are too coarse and out of phase with critical stages of crop development, with the result that their use in agriculture is limited. Daily averages and daily

accumulated values are much preferred as agroclimatic normals. They permit critical stages of plant development and associated agricultural operations to be oriented to climatic patterns on a phenological or bioclimatic time scale. Another important feature of these agriculturally oriented daily normals is their use in assessing seasonal crop weather conditions on a real time basis. When only monthly averages are available, it is necessary to wait until the end of the month to determine how the seasonal weather conditions (e.g., temperature, radiation, soil moisture, etc.) relate to other years and the long-term average. Current daily values compared against daily normals computed with 40 years of data permit such assessments to be made on a real time basis.

Agriculture, which is the most important economic activity in the Midwest region, is concerned with methods to achieve greater yields of specific products ~ high protein corn or prime beef, for example. The economic value of these products can, in large measure, ultimately be traced back to the input of SR to highly fertile soil. This thesis should therefore provide valuable background information for many aspects of the agricultural meteorology and climatology of the Midwest.

B. Motivation

The National Science Foundation's Research Applied to National Needs (NSF/RANN) program of the early 1970's initiated research and technological studies concerning the economic applications of solar energy. Consequently, a number of papers (reviewed below) have been published in the last two decades on SR and its temporal and spatial variation in the United States. The research they report is rather varied with respect to the number of years studied, the number and density of the stations utilized, the data sets used, and the methods of analysis employed and results obtained. Many studies used (rehabilitated) data from the only SR network in the United States, while others constructed new SR data sets using various techniques.

Publication of solar radiation data was stopped by the U. S. Weather Bureau in 1972 when it became clear that its network's routine observations contained errors of ± 5 to $\pm 30\%$ (Thekarhara, 1976). The available hourly radiation data were subsequently rehabilitated by the National Oceanic and Atmospheric Administration (NOAA) for 26 stations by applying a correction that largely accounted for a slow instrument deterioration. These stations, for which rehabilitated hourly radiation data are available for 1952-1975, are known as the SOLMET (SOLar METeorological) stations (see Fig. 1.1). The various versions of the SOLMET data are discussed more fully in Chapter III.

The aforementioned studies that examined long-term SR generally used the spatially sparse SOLMET data, as well as data generated by models that regressed SOLMET SR data



Fig. 1.1. The 26 SOLMET (SOLar METeorological) stations in the United States.

with more frequently observed meteorological parameters such as cloud cover or percent possible sunshine (i.e., regression-extended SOLMET). They documented the climatological spatial variations of SR in the United States (Bennett, 1975; Enmap Corp, 1980; Solar Energy Research Institute, 1981; Balling and Vojtesak, 1983) and established the secular trends (Balling, 1983; Balling and Cerveny, 1983). However, in some cases, long-term actual sunshine hours were used to achieve similar results in analyzing temporal and spatial variations (Bryson and Hare, 1974; U. S. Department of Interior, 1970; Angell and Korshover, 1975, 1978; Doehring and Karl, 1981). Some papers used short-term and highly reliable solar radiation measurements in studying short-term and spatial variations. In most cases, these short-term data were collected at special networks of stations in particular states or small regions within the United States - for example, California (11 stations; Granger, 1980); the Washington, D. C. area (3 stations; Pinker and Militana, 1981); the New England,

Mid Atlantic, and Georgia-South Carolina regions (7 to 8 stations each; Atwater and Ball, 1978); San Diego County, California (8 stations; Aguado, 1986); Arizona (6 stations); the Tennessee Valley Authority region (12 stations; Suckling, 1983); Wisconsin (17 stations; Kerr *et al.*, 1968a,b); and the intermountain region (37 stations; Bennett, 1964). The analyses of these small areas were based on data sets ranging in length from only 7 months up to 5 years, and focused on the meso-scale variability of SR from which an interpolation scheme could be developed for estimating insolation at locations where no measuring stations exist.

Only a few investigators (Terjung, 1970; O'Brien, 1978; Willmott and Vernon, 1980; and Balling and Vojtesak, 1983) have proposed various schemes to classify and regionalize SR data. Willmott and Vernon (1980) were the first to objectively classify solar climates for the contiguous United States. They identified the 10 solar climate regions shown in Fig. 1.2 by applying P-mode Principal Component Analysis and an optimized Ward's grouping procedure (Ward, 1963) to five years (1970-1974) of daily SR data for 60 stations. Balling and Vojtesak (1983) delineated the 18 solar climate regions shown in Fig. 1.3 by applying Principal Component Analysis and Euclidean Distance Cluster Analysis (Sneath and Sokal, 1973) to 24 years (1952-1975) of monthly SR data (rehabilitated SOLMET and regression-extended SOLMET) for 221 stations. The different results of these two studies are due to the contrasting time-scales (daily versus monthly) of the radiation data used and also the differences in the statistical techniques employed. Balling and Vojtesak (1983) suggest that a multitude of legitimate, defensible solar climatic structures could be developed for the contiguous United States; given some applicable problem, researchers must carefully and cautiously evaluate the appropriateness of the operational considerations used to generate a particular set of solar climate regions.

C. Objectives

As is evident from the papers described above and especially Figs. 1.2 and 1.3, the SR climate of the Midwest region, which includes the most important crop producing area in the United States, has yet to be documented *in detail*. Figure 1.2 suggests the Midwest region is split generally into two SR climate regions, while, in contrast, Fig. 1.3 presents the entire Midwest region as being similar in SR characteristics (i.e., one SR climate region). This thesis aims to address this deficiency by generating and analyzing detailed SR for a nine-state region (Minnesota, Iowa, Missouri, Illinois, Wisconsin, Michigan, Indiana, Ohio, and Kentucky).

In order to achieve this goal of examining insolation in the Midwest, a long-term SR data set needed to be created, since the network of available SR measurements, be they the SOLMET data or those from other localized networks, is either sparse or lacking in longevity. A semi-physical SR model is used to create the 40 year data base of daily SR

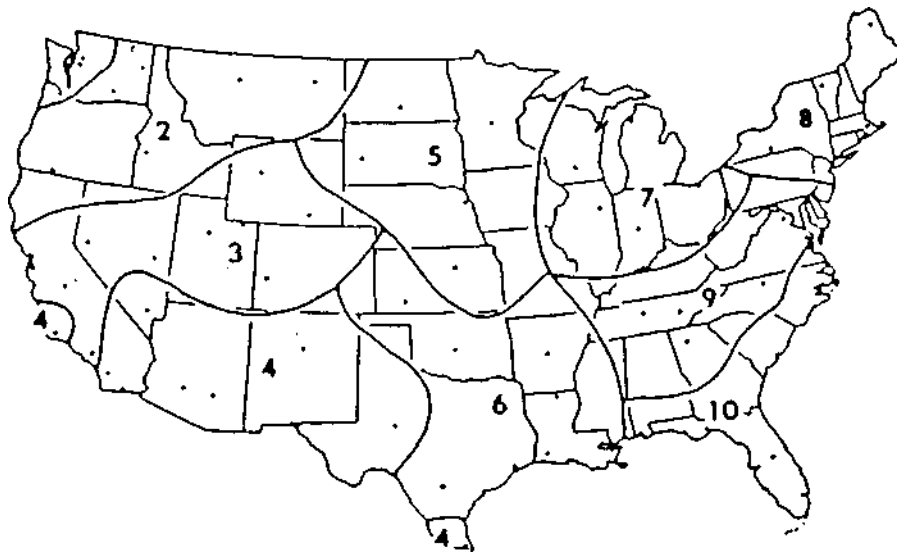


Fig. 1.2. Map of 10 solar climate regions of the United States, according to Willmott and Vernon (1980). Dots indicate station location.

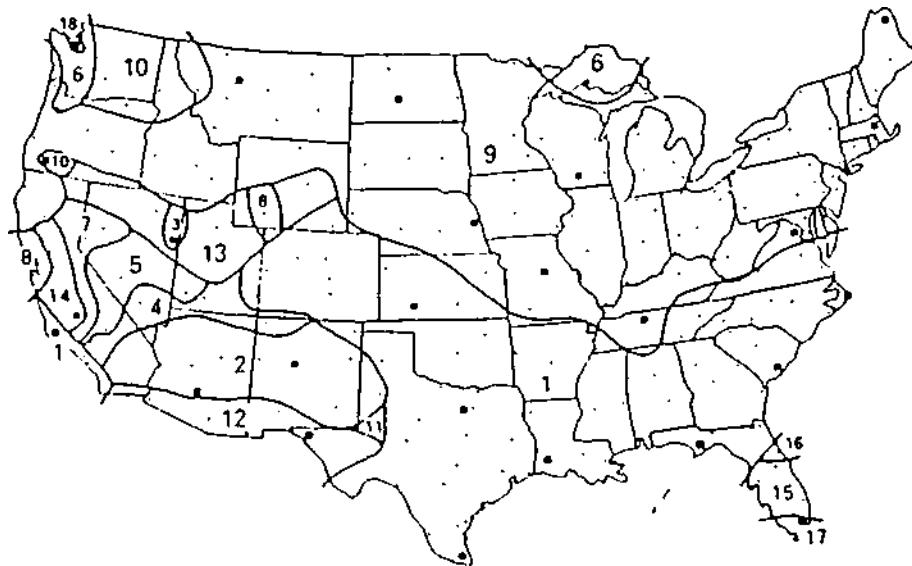


Fig. 1.3. Map of the solar climate regions of the United States, according to Balling and Vojtesak (1983). Squares indicate SOLMCT stations, dots indicate derived data stations.

totals. These data are then examined in order to document the spatial and temporal SR variability throughout the Midwest. The goal of this work is not necessarily to produce a map of the solar climate regions in the Midwest, as others have objectively attempted, but 1) to display climatological spatial variations of insolation across the Midwest, 2) to illustrate the fluctuations of SR over the past 40 years at stations in the midwestern region, and 3) to provide a long-term data base for the region which may be used in further research, not only on solar radiation, but also for studies in which solar radiation plays an important role or driving force (e.g., evapotranspiration, crop yield, or solar heating research).

The Midwestern Climate Center (MCC), one of six Regional Climate Centers that serve the 48 contiguous United States, provides a wide range of climate information to agribusinesses, water resource managers, and researchers in its region via an interactive computer system (Changnon *et al.*, 1990; Kunkel *et al.*, 1990a). The calculation of variables such as soil moisture, crop development, and yield depend on SR as input. The MCC provides information about these variables, such as soil moisture deviations from the long-term mean, as well as other climate information, to its clients. Thus, the MCC was in need of an historical SR data base in order to calculate historical data bases for other variables (e.g., soil moisture), and to provide timely crop yield assessments. This thesis research was specifically done to meet the need of an historical SR data base for the Midwest region.

Chapter II describes the semi-physical model used to create the data base, documents the input data, and validates the results of the model against four sets of measurements observed in Illinois, Ohio, and Wisconsin. Chapter III reviews the history of the SOLMET data and compares the model's output with data from four SOLMET stations, as well as compares the model results with one regression-extended SOLMET station. The modeled SR is also compared with the data analyzed and published by Baker and Klink (1975) for the North Central region of the United States. The spatial variability of the monthly climatological means are illustrated and discussed in Chapter IV. The 40 year trends are shown for 7 stations, as well as the spatial coherency of trends for all stations. Chapter V provides a summary of the comparisons between the modeled output and the various other SR data bases and summarizes the features of both the spatial and secular variability found in examining the SR data base created.

CHAPTER II

MODEL IMPLEMENTATION AND VALIDATION

Numerous models have been proposed and utilized for the estimation of SR from a wide range of parameters. For example, the models of Reddy (1974) and Schmetz and Raschke (1978) used cloud amount and type; Rangarajan *et al.*'s (1984) approach used cloud height and coverage; many models have employed sunshine duration (e.g., Glover and McCulloch, 1958; Schulze, 1976; Rietfeld, 1978; Biga and Rosa, 1980; Martinez-Lozano *et al.*, 1984); Bristow and Campbell's (1984) method utilized daily maximum and minimum temperatures; and Reddy (1987) attempted to use precipitation and latitude. In contrast to this situation, the present investigation uses a more sophisticated semi-physical model that has been under development since the mid-1970s (Atwater and Brown, 1974; Atwater and Ball, 1978; Atwater and Ball, 1981; Meyers and Dale, 1983). This chapter describes the model, outlines its data requirements, reports the results of some sensitivity testing, and concludes by validating the model against four small samples of pyranometer measurements made in Illinois, Ohio, and Wisconsin.

A. Semi-Physical Model

The advantages of this semi-physical SR model include the following -- its use of standard meteorological data as input; its accommodation of the effects of Rayleigh scattering, absorption by water vapor and permanent gases, absorption and scattering by aerosols and clouds, and the contribution from ground-to-cloud-to-ground reflectance; and the fact that it is both computationally efficient and has been found to give accurate results.

1. Description of Model

Following the discussion of Meyers and Dale (1983), the SR received at the earth's surface is given by

$$I = I_0(\cos Z)T_R T_g J_w T_a T_c \quad (2.1)$$

where I_0 is the extraterrestrial flux density at the top of the atmosphere on a surface normal to the incident radiation, Z is the solar zenith angle, and T_i denotes the transmission coefficients after Rayleigh scattering (R), absorption by permanent gases (g) and water vapor (w), absorption and scattering by aerosols (a), and cloud attenuation (c). Although this equation is strictly valid for monochromatic radiation, it has been used for broad-band models to approximate the real atmosphere (Atwater and Ball, 1981).

As a result of the annual changes in the earth-sun distance, the impinging radiation at the top of the atmosphere varies according to the following relation:

$$I_o = S_o \{ 1 + 0.034 \cos[2 (n-1)/365] \} \quad (2.2)$$

where S_o is the solar constant in W m^{-2} , which was taken to be 1353, and n is the (Julian) day of the year (1 through 366). The cosine of the solar zenith angle in Eq. 2.1 is computed from

$$\cos Z = \sin \phi \sin \delta + \cos \phi \cos \delta \cos H \quad (2.3)$$

where ϕ is the latitude, δ the solar declination angle, and H the hour angle. Walraven's (1978) procedure for accurately calculating δ and H was used to compute the position of the sun to an accuracy of 0.01° . The model employed an empirical relationship (see Kondratyev, 1969, p. 263, Eq. 5.10) for the solar attenuation by Rayleigh scattering and permanent gas absorption that considers the radiation scattered in the forward direction (Atwater and Brown, 1974). The relation is

$$T_R T_g = 1.021 - 0.084 [m(949p \cdot 10^{-5} + 0.051)]^{1/2} \quad (2.4)$$

where p is the surface pressure in kPa, and m is the dimensionless optical air mass at a pressure of 101.3 kPa given by

$$m = 35 (1224 \cos^2 Z + 1)^{-1/2}. \quad (2.5)$$

To compute the broad-band transmission after water vapor absorption, the expression

$$T_w = 1 - 0.077 (um)^{0.3} \quad (2.6)$$

was used, where u is the precipitable water vapor. Precipitable water can be estimated from the surface dew point with the expression from Smith (1966)

$$u = \exp [0.1133 - \ln(A + 1) + 0.0393 T_d] \quad (2.7)$$

where T_d is the dew point temperature ($^\circ\text{F}$) and A is a constant derived empirically for latitude and season. Values of A taken from Smith (1966) are shown in Table 2.1.

Table 2.1. values taken from Smith (1966).				
Latitude Zone	Winter	Spring	Summer	Fall
30-40	3.04	3.11	2.92	2.94
40-50	2.70	2.95	2.77	2.71

Aerosol attenuation is complex; therefore, a simple treatment of the form

$$T_a = x^m \quad (2.8)$$

was used. Here, m is again the optical air mass and x is a constant which Meyers and Dale (1983) derived empirically as a residual in the governing equation, Eq. 2.1, for clear sky conditions. They found x to be nearly constant at approximately 0.935 for all U.S. stations except for the extreme southern locations of Miami (Florida) and Lake Charles (Louisiana), where x was found to be 0.95. Therefore, for this study confined to stations in the midwest, the value 0.935 was used for x .

The transmission after cloud attenuation, including the contribution from ground-to-cloud-to-ground reflectance, R , is given as

$$T_c = \prod_{i=1}^{n_c} R_i [1 - c_i (1 - t_i)] \quad (2.9)$$

where n_c is the number of cloud layers, c_i the fractional sky coverage of the i th layer, and t_i the transmission coefficient for the (most abundant) cloud type in the layer. It is assumed that the reported cloud coverage between an observer (or pyranometer) and the sun averaged over time gives an effective cloud cover and cloud transmission. The individual cloud transmission coefficients, t_i , were taken from Meyers and Dale (1983), who generated populations of cloud transmission coefficients, and grouped them according to cloud base height and coverage. Their cloud height classifications were

- 1) < 1219 m (4000 ft)
- 2) 1219 – 3048 m (4000 – 10000 ft)
- 3) 3048 – 5486 m (10000 – 18000 ft)
- 4) > 5486 m (18000 ft)
- 5) > 5486 m (18000 ft) thin,

and the transmission coefficients found and used are shown in Table 2.2. For overcast (OVC) conditions, c_i was set equal 1.0, for broken (BKN) 0.7, for scattered (SCT) 0.3, and for clear skies (CLR) 0.0.

R_i in Eq. 2.9 is given, by

$$R_i = (1 - r_e r_{ci})^{-1} \quad (2.10)$$

where r_e is the earth's surface albedo and r_{ci} the i th layer's cloud albedo. Based on Meyers and Dale (1983), the surface albedo was assumed to be 0.2, but 0.65 with snow cover. The cloud albedo was assumed to be 0.5 for all clouds with bases less than 5486 m (18000 ft) and 0.0 for those greater than 5486 m.

Table 2.2. Transmission coefficients, t_i , for indicated cloud height and coverage (from Meyers and Dale, 1983).		
Height (m)	Scattered (SCT) or Broken (BKN)	Overcast (OVC)
<1219	0.63	0.31
1219 - 3048	0.53	0.41
3048 - 5486	0.52	0.46
>5486	0.66	0.67
>5486 thin	0.95	0.87

In using this model (i.e., Eq. 2.1), it was assumed that 1) the radiative properties of the atmosphere do not change significantly when clouds are introduced, 2) the hourly cloud observations are representative of the sky conditions during the time solar radiation was computed, and 3) the reported cloud layers are located between the observer (or pyranometer) and the sun.

2. Model Input Data

As can be seen from Eqs. 2.1-2.10 above, the input parameters required by the model are: time of day, day of year, latitude/longitude, surface pressure, dew point temperature, cloud height and fractional sky coverage, and the presence or absence of snow cover. It

would be ideal if these variables were reported every hour, especially the cloud information. This requires that the data come from the National Weather Service (NWS) first-order stations or the Federal Aviation Administration (FAA) stations. Although the NWS's Cooperative Observer Network is very dense across the country, their *daily* reports of precipitation and maximum and minimum temperatures do not meet the requirements of the hourly input parameters needed by the model. In order to document the spatial and temporal variability of SR across the Midwest, hourly surface observation data for sites throughout the Midwest (cf. Fig. 2.1) for (generally) 1948-1987 were given as input to the model.

The TD-3280 Surface Airways Hourly data were acquired on magnetic tape from the National Climatic Data Center (NCDC, 1986) for the stations and time periods listed in Appendix A. Care had to be taken when using these data for a number of reasons, and a significant effort was made to calculate the most accurate possible SR value for each day of a station's period-of-analysis.

The reporting times and intervals for each station were not constant during its period-of-analysis. Some stations may have reported every hour, while others reported every 3 hours, and this reporting procedure may have changed at one or more times during the period-of-record used. Intuitively, the absence of an element for one or more hours would normally indicate missing data. However, close examination of MF1-10 forms from Springfield, Illinois (e.g., July 5, 1951), in conjunction with NCDC's archive tape of Springfield data, indicated that the absence of the sky condition element during an entire day is informative in itself, indicating no clouds to report that day. Thus, this was assumed true for all stations.

Pertinent cloud information was available in four elements: ceiling height (CLHT); sky condition and cloud coverage for layer "x" (CLCx); cloud type and height for layer "x" (CLTx); and, for prior to June 1, 1951, a general sky condition category (CC51).

a. Pre June 1951 Cloud Problems (CC51)

For the time period previous to June 1, 1951, as much cloud information as possible was obtained from the CC51 element, which included fractional amount of the higher layer, fractional amount of the lower layer, and the height of the lowest scattered layer. However, preliminary tests indicated that the literal use of this information led to unrealistically low values of SR for this time period; in addition, the quality of this element is marred by many missing values. Subsequently, an attempt was made to use another element to estimate cloud heights. It was found to be successful and is now discussed.

As will be presented in Sections 3 and 4 of this chapter, if the other two input meteorological parameters (dew point and surface pressure) were unknown, either the mean of the available hours for the day or the climatological monthly mean was substituted to prevent missing hours as a result of these variables, which aided in creating complete SR data sets at each station. Therefore, rather than creating SR values believed to be too low or using the CC51 element which was often missing or invalid, ceiling height (CLHT) was used to determine cloud layer heights.

It was assumed there were 0, 1, or 2 layers of clouds, since the CC51 element basically only assumed 2 possible layers (a higher and a lower layer) as well. If there was a ceiling reported, the sky condition was chosen randomly to be either BKN or OVC. All random choices were based on a random number generator. If the ceiling was low (<5000 ft), it was assumed there was only 1 cloud layer. If the ceiling was above 5000 ft, either no lower layer was randomly chosen, or a lower layer of SCT was chosen and its corresponding height was 5000 ft less if the ceiling was < 12000 ft, or 10000 ft less otherwise. If the ceiling was unlimited (no ceiling), the sky condition of either SCT, with corresponding heights randomly chosen (i.e., 0, 2500, 5000, ... 25000 ft), or CLR was chosen at random for the 2 layers. If the ceiling information was unknown or missing, then the sky condition was also set to missing for that hour. As will be shown in Chapter IV, this method of estimating cloud information for pre June 1951 data did not appear to introduce any detectable biases in the SR data generated. It was found that at some stations the CLCx (sky condition) and perhaps the CLTx (cloud height) elements were also given prior to June 1951. Thus, in these cases, the CLCx and CLTx elements were used in place of the above estimates which were based on the ceiling information.

b. Post June 1951 Cloud Problems

Considerable examination of the data suggested that there was a mixture of reporting (or perhaps archiving) procedures between the stations concerning cloud information after June 1, 1951. Three possible combinations existed concerning the CLCx and CLTx elements: 1) both reported; 2) sky condition (CLCx) only reported; and 3) neither reported. Most of the time, both elements were given; however, on occasion neither element was given. In this instance, it was assumed that neither element was recorded/archived because there were no clouds during the day or hour to report. For some stations, however, the CLTx (cloud height) element was not given whether there were clouds or not. This situation led to the development of the following approach.

The CLCx (sky condition) element was used to determine the number of cloud layers and each layer's coverage for a given hour. Then ceiling height was used to estimate the height of these layers (see Table 2.3). For example, if there was a ceiling, and the number

Table 2.3a. Method of assigning the cloud height when observations give the sky condition (BKN or OVC) for one layer and the ceiling height (CLHT).	
	Layer 1
<i>Observed Sky Condition</i>	BKN or OVC
<i>Assigned Cloud Height</i>	CLHT

Table 2.3b. Method of assigning cloud heights when observations give the sky condition (SCT, BKN or OVC) for two layers and the ceiling height (CLHT). The two possible combinations of sky conditions are demonstrated (CASES A and B). Two CLHT criteria (defined by superscripts and accompanying information) are used for CASE A, and three for CASE B.		
	Layer 1	Layer 2
CASE A		
<i>Observed Sky Condition</i>	BKN	BKN or OVC
<i>Assigned Cloud Height</i>	CLHT	CLHT ¹ + 5000'
	CLHT	CLHT ² + 10000'
CASE B		
<i>Observed Sky Condition</i>	SCT	BKN or OVC
<i>Assigned Cloud Height</i>	CLHT ³	CLHT
	CLHT ⁴ - 5000'	CLHT
	CLHT ² - 10000'	CLHT
¹ observed ceiling height is 10000' ² observed ceiling height is > 10000' ³ observed ceiling height is 5000' ⁴ observed ceiling height is 10000' but > 5000'		

<p>Table 2.3c. Method of assigning cloud heights when observations give the sky condition (SCT, BKN or OVC) for three layers and the ceiling height (CLHT). The three possible combinations of sky conditions are demonstrated (CASES A, B, and C). Three CLHT criteria (defined by superscripts and accompanying information) are used for CASE B, and four for CASE C.</p>			
	Layer 1	Layer 2	Layer 3
CASE A			
<i>Observed Sky Condition</i>	BKN	BKN	BKN or OVC
<i>Assigned Cloud Height</i>	CLHT	CLHT + 5000'	CLHT + 10000'
CASE B			
<i>Observed Sky Condition</i>	SCT	BKN	BKN or OVC
<i>Assigned Cloud Height</i>	CLHT ³	CLHT	CLHT ³ + 5000'
	CLHT ⁴ - 5000'	CLHT	CLHT ⁴ + 5000'
	CLHT ² - 10000'	CLHT	CLHT ² + 10000'
CASE C			
<i>Observed Sky Condition</i>	SCT	SCT	BKN or OVC
<i>Assigned Cloud Height</i>	CLHT ³	CLHT ³	CLHT
	CLHT ⁴ - 5000'	CLHT ⁴ - 3000'	CLHT
	CLHT ⁵ - 8000'	CLHT ⁵ - 4000'	CLHT
	CLHT ⁶ - 16000'	CLHT ⁶ - 10000'	CLHT
<p>² observed ceiling height is > 10000'</p> <p>³ observed ceiling height is 5000'</p> <p>⁴ observed ceiling height is 10000' but > 5000'</p> <p>⁵ observed ceiling height is 18000' but > 10000'</p> <p>⁶ observed ceiling height is > 18000'</p>			

Table 2.3d. Method of assigning cloud heights when observations give the sky condition (SCT, BKN or OVC) for four layers and the ceiling height (CLHT). The four possible combinations of sky conditions are demonstrated (CASES A, B, C, and D). Four CLHT criteria (defined by superscripts and accompanying information) are used for each case.				
	Layer 1	Layer 2	Layer 3	Layer 4
CASE A				
<i>Observed Sky Condition</i>	BKN	BKN	BKN	BKN or OVC
<i>Assigned Cloud Height</i>	CLHT	$CLHT^3 + 6000'$	$CLHT^3 + 12000'$	$CLHT^3 + 18000'$
	CLHT	$CLHT^4 + 4000'$	$CLHT^4 + 4000'$	$CLHT^4 + 9000'$
	CLHT	$CLHT^5$	$CLHT^5 + 8000'$	$CLHT^5 + 8000'$
	CLHT	$CLHT^6$	$CLHT^6$	$CLHT^6$
CASE B				
<i>Observed Sky Condition</i>	SCT	BKN	BKN	BKN or OVC
<i>Assigned Cloud Height</i>	$CLHT^3$	CLHT	$CLHT^3 + 5000'$	$CLHT^3 + 10000'$
	$CLHT^4 - 5000'$	CLHT	$CLHT^4 + 5000'$	$CLHT^4 + 8000'$
	$CLHT^5 - 5000'$	CLHT	$CLHT^5 + 5000'$	$CLHT^5 + 8000'$
	$CLHT^6 - 8000'$	CLHT	$CLHT^6$	$CLHT^6$
CASE C				
<i>Observed Sky Condition</i>	SCT	SCT	BKN	BKN or OVC
<i>Assigned Cloud Height</i>	$CLHT^3$	$CLHT^3$	CLHT	$CLHT^3 + 5000'$
	$CLHT^4 - 5000'$	$CLHT^4$	CLHT	$CLHT^4 + 8000'$
	$CLHT^5 - 10000'$	$CLHT^5 - 6000'$	CLHT	$CLHT^5 + 8000'$
	$CLHT^6 - 13000'$	$CLHT^6 - 8000'$	CLHT	$CLHT^6$
CASE D				
<i>Observed Sky Condition</i>	SCT	SCT	SCT	BKN or OVC
<i>Assigned Cloud Height</i>	$CLHT^3$	$CLHT^3$	$CLHT^3$	CLHT
	$CLHT^4 - 5000'$	$CLHT^4 - 3000'$	$CLHT^4$	CLHT
	$CLHT^5 - 10000'$	$CLHT^5 - 7000'$	$CLHT^5 - 3000'$	CLHT
	$CLHT^6 - 18000'$	$CLHT^6 - 12000'$	$CLHT^6 - 6000'$	CLHT
³ observed ceiling height is 5000' ⁴ observed ceiling height is 10000' but > 5000' ⁵ observed ceiling height is 18000' but > 10000' ⁶ observed ceiling height is > 18000'				

of layers given by the sky condition was one, then the cloud height of that layer was equal to the ceiling height (Table 2.3a). If there were two layers given (Table 2.3b), then the sky condition indicated which layer was the ceiling (i.e., a ceiling must be either BKN or OVC). If layer 1 was the ceiling, then the cloud height at layer 1 was set equal to the ceiling height, and if that height was less than or equal to 10000 ft, the second layer's height was set equal to layer one's height (i.e., the ceiling height) plus 5000 ft. Otherwise, layer one's height was greater than 10000 ft and the second layer's height was layer one's height plus 10000 ft. If layer 2 was the ceiling, then its height became the ceiling height, and if that height was less than or equal to 5000 ft, layer one's height was set equal to layer two's height. If layer two's height was between 5000 and 10000 ft, layer one's height was set equal to layer two's height minus 5000 ft, and if layer two's height was greater than 10000 ft, layer one's height was set equal to layer two's height minus 10000 ft. The estimates of cloud height for combinations of 3 or 4 layers were similarly determined, as shown in Tables 2.3c and 2.3d.

If the CLCx (sky condition) element indicated 5 cloud layers, the heights for each layer were assigned as shown in Table 2.4, irrespective of whether a ceiling height was given. Table 2.4 also shows the cloud heights assigned to each layer if 3 or 4 cloud layers were reported and none was a ceiling. If 2 layers were reported, and the second layer was reported as thin (defined as a "-" preceding the coverage abbreviation; e.g., -OVC), the cloud height for layer 1 was set to 8000 ft while the height for the thin layer was set to 25000 ft. If the 2nd layer was not reported as thin, its height was randomly chosen (using a random number generator) to be either 12000 to 25000 ft, while layer 1 was then set to the height of layer 2 minus 10000 ft. If only 1 (SCT) layer was reported with no information on height given, the height of this layer was chosen at random to be either 0, 2500, 5000, 7500, 10000,..., or 25000 feet. Possible biases do exist from estimating cloud heights using the methods shown in Tables 2.3 and 2.4 when no height is given, and will be shown and discussed in Chapter IV.

If the CLCx (sky condition) element indicated 5 cloud layers, the heights for each layer were assigned as shown in Table 2.4, irrespective of whether a ceiling height was given. Table 2.4 also shows the cloud heights assigned to each layer if 3 or 4 cloud layers were reported and none was a ceiling. If 2 layers were reported, and the second layer was reported as thin (defined as a "-" preceding the coverage abbreviation; e.g., -OVC), the cloud height for layer 1 was set to 8000 ft while the height for the thin layer was set to 25000 ft. If the 2nd layer was not reported as thin, its height was randomly chosen (using a random number generator) to be either 12000 to 25000 ft, while layer 1 was then set to the height of layer 2 minus 10000 ft. If only 1 (SCT) layer was reported with no information on height given, the height of this layer was chosen at random to be either 0, 2500, 5000, 7500, 10000,..., or 25000 feet. Possible biases do exist from estimating

Table 2.4. Assigned cloud heights at a given layer, when no cloud height (layer or ceiling) information is known, but sky condition values are given as SCT.					
No. of Layers	Cloud Layer				
	1	2	3	4	5
1 ^A	RAND	—	—	—	—
2 ^B	8000'	25000'	—	—	—
2 ^C	2000' 15000'	12000' 25000'	—	—	—
3	5000'	10000'	20000'	—	—
4	2000'	8000'	12000'	20000'	—
5	2000'	5000'	9000'	14000'	20000'
^A Randomly chosen among 0', 2500', 5000'....25000' Used when layer 2 is thin Randomly chosen between when layer 2 is not thin					

cloud heights using the methods shown in Tables 2.3 and 2.4 when no height is given, and will be shown and discussed in Chapter IV.

c. Miscellaneous Problems

Ideally, a SR value was calculated for each hour during the day, and then summed to produce the total SR for that day. However, if any input parameter was missing for a given hour (with the exception of sky condition as described above), the SR value for that hour was initially also set to be missing. Even though most of the time both the sky condition and cloud height elements were reported during a day, the cloud heights were rarely reported every hour, as the sky condition usually was, but rather every 3 hours. This resulted in periodic hours of missing SR. To fill in these hours, interpolation was needed. Due to the discontinuity in the location of clouds from one hour to the next, which encompasses the fact that, at one hour, the height of layer 1 may be the height of last hour's layer 2 since layers can disappear from hour to hour, the T_c variable was interpolated between given hours rather than the layer's height or layer's t_i . A linear

interpolation scheme with step interpolation at the ends was used, but if more than 2 consecutive daylight hours were missing, those hours were left missing/unknown.

It was found that frequently when a station reported the sky condition to be partially obscured, the corresponding height was reported as unknown/missing. To minimize the possible number of interpolations and perhaps missing daily SR values, the cloud height was set to 900 feet when the sky condition was given as partial obscuration, since phenomena which partially obscure the sky occur close to the ground.

On occasion, the reported sky condition did not match the reported cloud cover for the same hour (CLR = 0 tenths, SCT = 1 to 5 tenths, BKN = 6 to 9 tenths, OVC = 10 tenths). For example, the 7:00 am observation on July 5, 1951 at Springfield, Illinois reported cloud information as follows:

	Sky Condition	Actual Tenths Coverage	Height of Layer (in ft)
Layer 1:	SCT	2/10	7000
Layer 2:	-OVC	0/10	18000
Layer 3:	CLR (no clouds/unknown)	8/10	25000
Layer 4:	CLR (no clouds/unknown)	0/10	unknown

Clearly, layer 2 and 3's sky condition and tenths of cloud coverage do not match. Thus, it was assumed that when a sky condition other than CLR was reported at the same layer as 0 tenths cloud coverage for a given hour, the sky condition was taken to be that of the next higher layer. In other words, in the example above, it was assumed that layer 1 was SCT (2/10) at 7000 ft, layer 2 had no clouds (0/10), and layer 3 was -OVC (8/10) at 25000 ft (i.e., 2 layers total of clouds for this hour).

Actual snow cover data were used for each day at each station, if available. If it was not available at that station on a given day, the next closest station with available data was used. If no other nearby station had data, a climatology of snow cover for the station was used. That is, for a given day of a given week, snow cover was assumed if climatology (based on the years 1948-1987) indicated 50% or more of the time there was snow cover for that week.

3. Model Sensitivity to Dew Point Temperature

Missing hours of dew point temperature during the day will result in missing hourly values of SR, which results in missing daily totals since it is required to have a SR value for each hour before they are summed to give a value for the day. It was common for hours to occur for which the dew point temperature was missing. In order to eliminate this potential for missing daily SR totals, it was hypothesized that substituting

an average of the available hours of dew point temperature on that day or substituting a monthly climatological average of dew point temperature for the missing hours, would prevent missing daily SR totals caused by missing dew point temperatures without introducing significant biases in the data. Thus, the sensitivity of the model to variations in dew point temperature was tested. An example is illustrative. The range of dew point temperatures during June, at Peoria (Illinois, 40.67 ° N, 89.68 ° W) is approximately $T_{d1} = 30^{\circ} \text{ F}$ (1.11° C) to $T_{d2} = 80^{\circ} \text{ F}$ (26.67° C). From Eq. 2.7 and Table 2.1, $u_1 = 0.97$ and $u_2 = 6.89$. At 1200 CST, from Eq. 2.3, the cosine of the Zenith is 0.95 ($Z = 18.7^{\circ}$), which from Eq. 2.5 gives $m = 0.0317$. Then from Eq. 2.6, the transmission coefficient after absorption by water vapor at 30° F is $T_{w1} = 0.97$; and at 80° F , $T_{w2} = 0.95$. Similarly, at an hour close to sunset when the Zenith angle is large, Eq. 2.5 yields an $m = 4.51$, and Eq. 2.6 yields $T_{w1} = 0.88$ and $T_{w2} = 0.78$. Therefore, with all other variables held constant, the transmission coefficient after water vapor changes by only 2.08% of the average value around solar noon and about 12.05% close to sunrise and sunset. However, the maximum absolute changes are approximately $3.6 \text{ MJ} \times 0.0208 = 0.07 \text{ MJ m}^{-2} \text{ hr}^{-1}$ around solar noon on a clear day in summer, and $0.4 \text{ MJ} \times 0.1205 = 0.05 \text{ MJ m}^{-2} \text{ hr}^{-1}$ close to sunset or sunrise in summer. Thus, it was considered justified to substitute averages of the available dew point temperatures for occasional missing hours during a day, or the station's monthly (climatological) averages for each hour if all hours of the day were missing, in order to reduce the number of missing SR values due to missing dew point temperatures and not introduce detectable biases in the data.

4. Model Sensitivity to Surface Pressure

Similarly, occasional hours of missing surface pressure would have resulted in missing daily totals of SR; thus, the model's sensitivity to surface pressure was tested to determine the likelihood of introducing errors in the SR data if daily or monthly means were used to replace missing hours of surface pressure. Surface pressure is found to range from $p_1 = 97.11 \text{ kPa}$ (28.70 inches of Hg) to $p_2 = 100.50 \text{ kPa}$ (29.70 inches of Hg) in June at Peoria. Given the same data as used above, $m = 0.0317$ at noon and $m = 4.509$ at an hour close to sunset or sunrise. Then from Eq. 2.4, $T_R T_{g1} = 1.00625$ and $T_R T_{g2} = 1.00601$ around solar noon; and $T_R T_{g1} = 0.84509$ and $T_R T_{g2} = 0.84220$ at an hour close to sunset/sunrise. Therefore, the attenuation by Rayleigh scattering and permanent gas absorption changes by 0.02% to 0.34% of the average $T_R T_g$ as the surface pressure changes from one extreme to another. Clearly, substituting an average pressure, whether it is an average of the available hours of a day, or a monthly climatological average, for missing pressure data would result in non-detectable biases in the SR data and therefore was done.

B. Validation of Model

In order to validate the model, its output was compared with four sets of daily SR measurements. Two sets of those measurements were taken at the Illinois Climate Network (ICN) site at Peoria (PIA), one from May 30 to November 1, 1987, and the other from January 6 to December 31, 1988. The two other SR data sets used were for: 1) Chetek, Wisconsin, approximately 96 km north of Eau Claire (EAU), from January 1 to May 13, 1986; and 2) Delaware, Ohio, approximately 38 km north of Columbus (OSU), from January 1 to December 31, 1987. The SR measurements at Chetek were compared with the modeled SR output for Eau Claire, and the Delaware measurements were compared with Columbus model results. The measurements at Peoria were taken on the Illinois Central College campus, and the data used in the model were observed at the Peoria airport, about 15 kilometers across town. Both Chetek and Delaware are part of state-wide networks of Campbell Scientific Weather Stations located at Agricultural Experiment Stations, where LI-COR LI200S silicon pyranometers are used in obtaining SR measurements. The ICN site at Peoria uses an Eppley black and white pyranometer. These data sets comprised the only available measurements at these stations.

All modeled data for these comparisons, except the Peoria 1988 data, were the result of NCDC (archived) hourly data being input to the model. However, since the data received from NCDC only included hourly observations through 1987, the 1988 Peoria observations were retrieved from the University of Illinois Department of Atmospheric Sciences' archive of FAA-604 Data. Unfortunately, these data were received by satellite communication which occasionally caused characters to be dropped or extraneous characters to overwrite the data during transmission, with the result that some hours were unreadable. Therefore, many days were missing in the modeled Peoria SR data for 1988, since it was required that no more than 2 consecutive daylight hours be missing for interpolation purposes.

Scatter plots of each data set are shown in Figs. 2.2-2.5. The fitted regression of observed on modeled SR for the complete years yielded the results in Table 2.5. Figures 2.2-2.5 display different symbols for each season, as well as a seasonal breakdown of the r^2 values. While the seasonal r^2 values are with respect to their own regression lines, they give an indication of the predictive consistency of the model. The period October-December appears to have the least variation, as shown by the largest r^2 values of the four (or available) seasons. The remaining seasons follow closely, but lack a clear ordering.

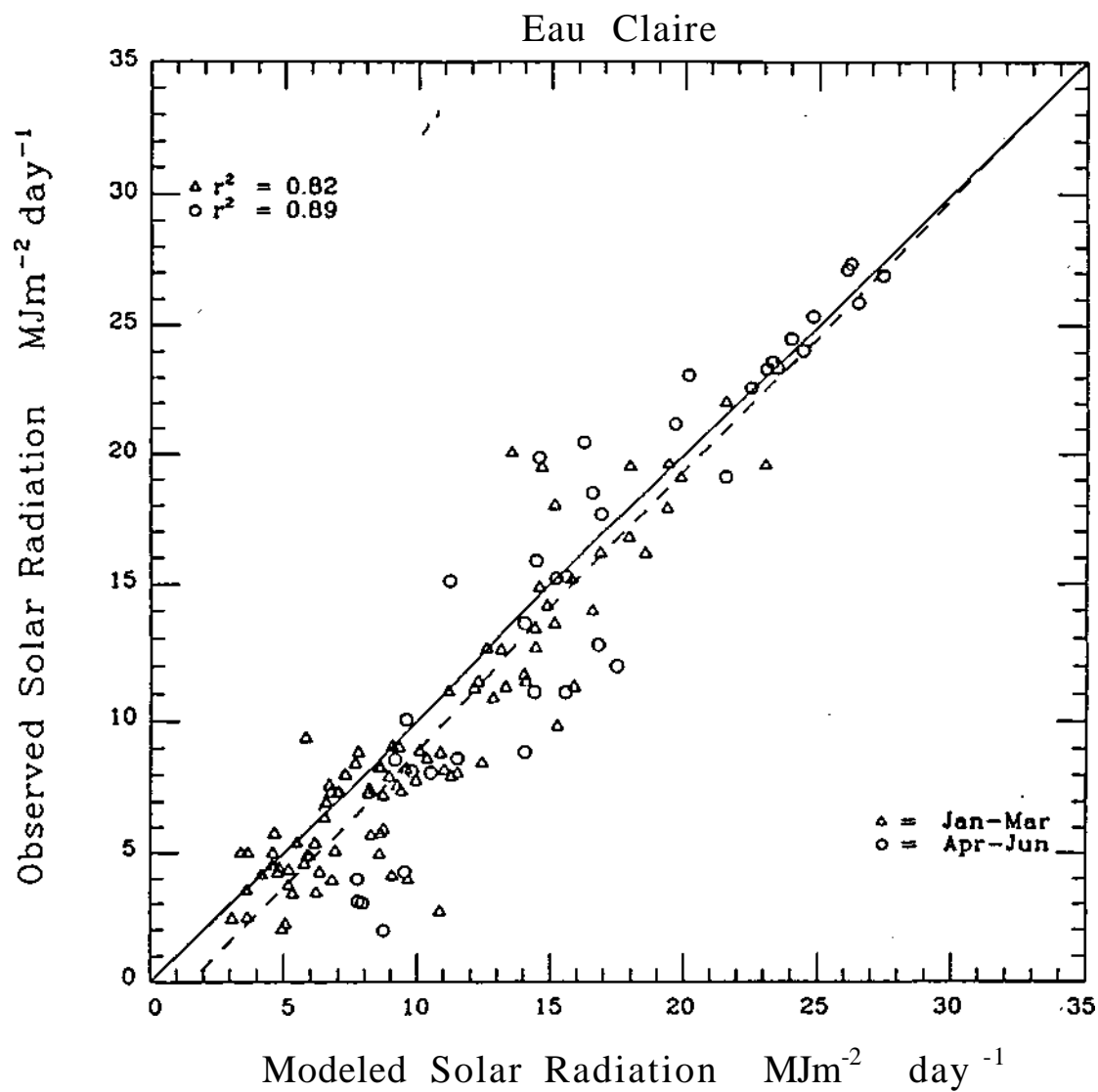


Fig. 2.2. Scatter plot of modeled versus observed daily SR for 130 days in 1986 at Eau Claire (and Chetek), WI. Regression line of all days is dashed (see Table 2.5); the 1:1 line is solid.

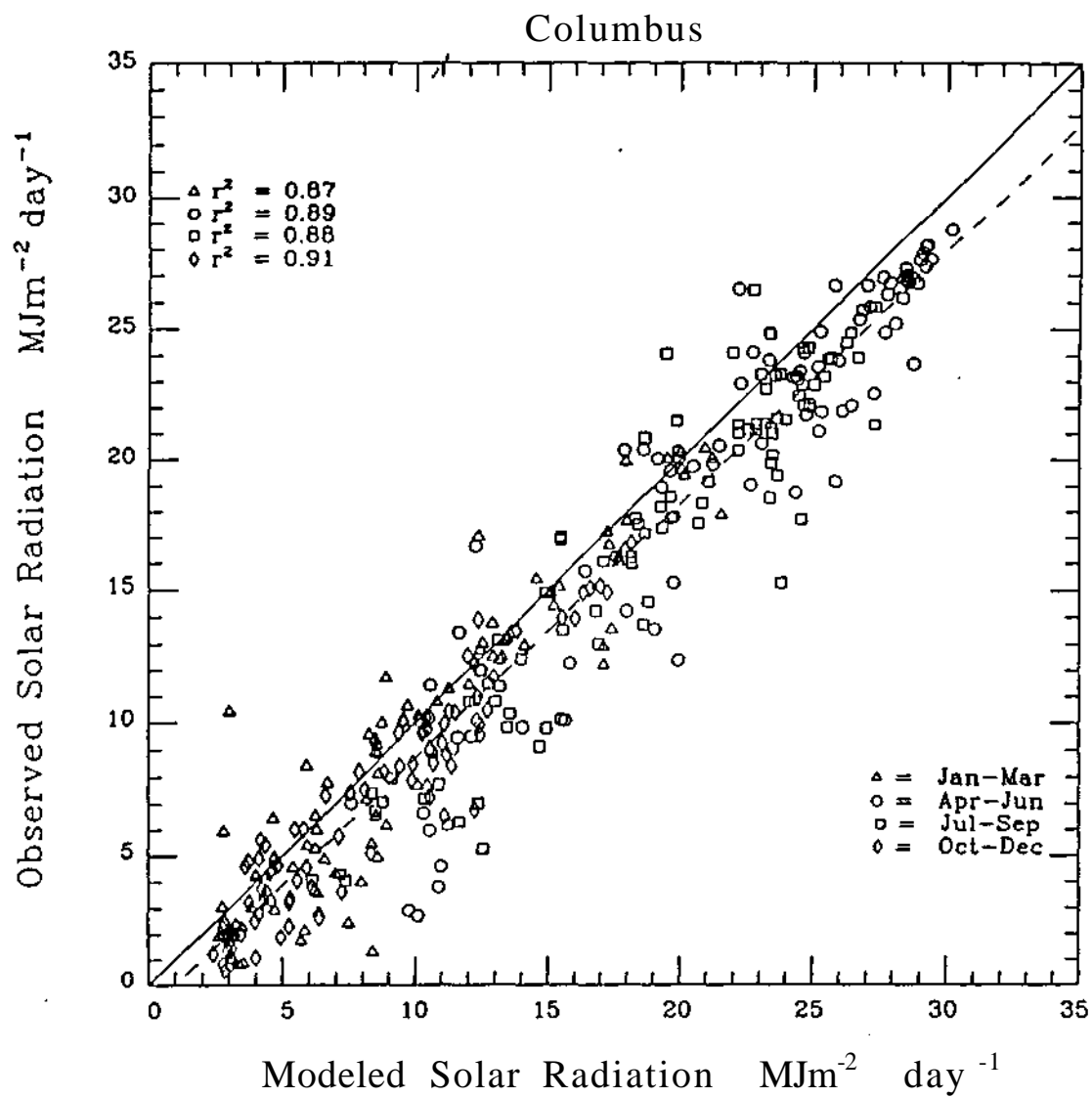


Fig. 2.3. As in Fig. 2.2, but for 361 days in 1987 at Columbus (and Delaware), OH.

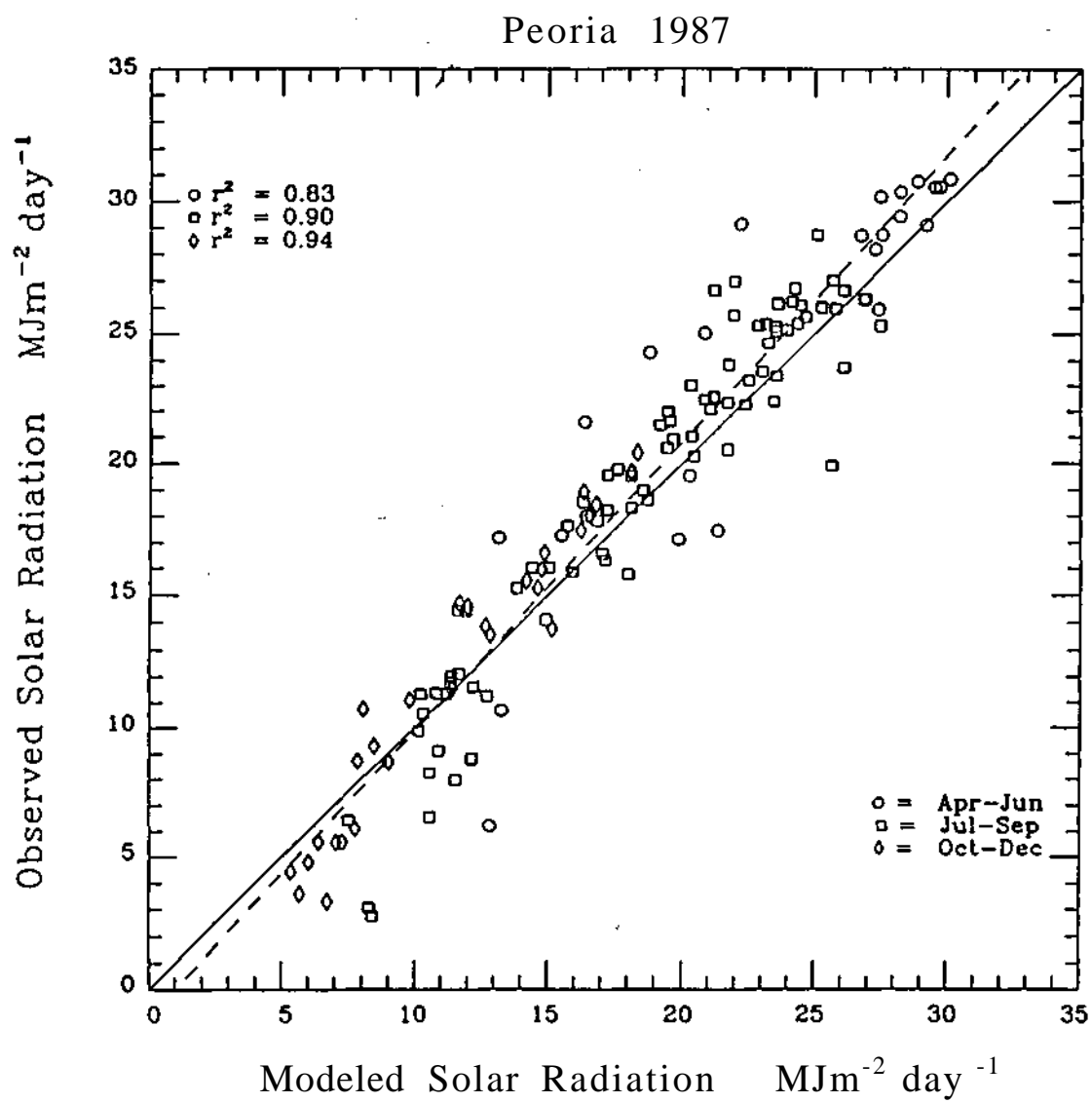


Fig. 2.4. As in Fig. 2.3, but for 136 days in 1987 at Peoria, IL

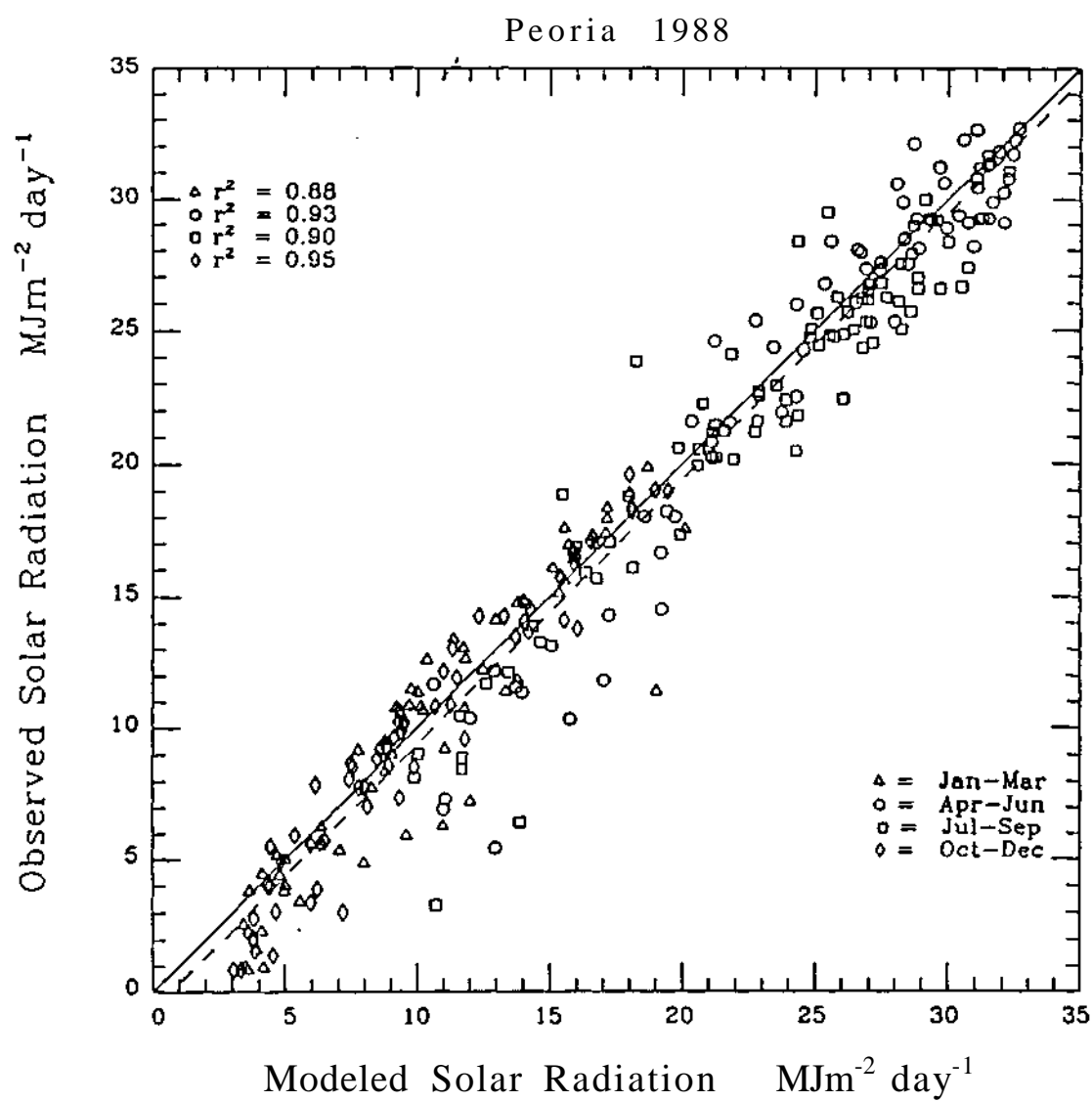


Fig. 2.5. As in Fig. 2.4, but for 286 days in 1988.

Table 2.5. Regression results of observed versus modeled SR for each of the four stations compared. All r^2 results were found to be significant at the greater than 99.9% confidence level.			
	r^2	slope	y-intercept (MJ m ⁻² day ⁻¹)
Eau Claire	0.88	1.05	-1.59
Columbus	0.93	0.96	-0.92
Peoria 1987	0.92	1.10	-1.12
Peoria 1988	0.96	1.01	-0.69

The regression lines (for all days) in Figs. 2.2-2.5 all lie fairly close to the 1:1 line. The Peoria 1987 and Eau Claire data regression lines cross the 1:1 line indicating that the model has a slight bias towards underestimating (overestimating) SR on days when that flux is high (low). However, both of these station's data sets used only the part of the year available for comparison. The Eau Claire comparison included only 130 evaluated days (between January 1 and May 12) in 1986, and the Peoria 1987 comparison included only 136 days (between June 5 and October 31). The Eau Claire data are somewhat clustered at the lower range of SR values, as one would expect according to the time of year used. The Columbus and Peoria 1988 regression lines appear more parallel to the 1:1 line, though they are both shifted downward. This would indicate that the model systematically overestimates SR by a small amount (typically less than 1 MJ m⁻² day⁻¹, as suggested by the regression line). The 1988 Peoria comparison included 286 days (between January 6 and December 31), and the Columbus comparison included 361 days (between January 1 and December 31) in 1987. Thus, one may conclude that the results from the Columbus and Peoria 1988 data comparisons may be more reliable since their sample sizes are at least twice that of the Eau Claire and Peoria 1987 comparisons and cover the entire year.

Figures 2.2-2.5 suggest that there may be a lower limit to SR values given by the model. This is particularly apparent for Peoria 1988 and Columbus, and suggests that the model overestimates very low SR values, which is also seen in the seasonal breakdown of the r^2 values. This may be due to the fact that most of the Eqs. 2.1-2.10 were empirically developed using data which may not have included very low SR

conditions. However, very low SR values are indicative of substantial cloudiness and are thus affected most by the transmission after cloud attenuation, T_c . The individual layer/cloud transmissivities, t_i , were developed using data when only a single cloud layer was observed (Meyers and Dale, 1983). Thus, perhaps the t_i values are not low enough, when multiple layers are present, in order to reflect very low SR values. Additionally, the presence of clouds above an overcast layer (i.e., not able to be seen by the observer) may attenuate SR more than if they were not present; however, the current method is unable to take this into account. Nonetheless, it is important to keep this lower-limit bias in mind when considering needs and uses of this model.

The mean error, mean absolute error, and rms error were computed for each comparison set as follows:

$$\left. \begin{aligned} \text{mean error} &= \sum_{i=1}^n (SR_{mod} - SR_{obs}) / n \\ \text{mean absolute error} &= \sum_{i=1}^n |SR_{mod} - SR_{obs}| / n \\ \text{rms error} &= \left[\sum_{i=1}^n (SR_{mod} - SR_{obs})^2 / n \right]^{1/2} \end{aligned} \right\} \quad (2.11)$$

where n is the number of days that both modeled and observed data were available. Not only were the errors calculated for the available data during each comparison period as a whole, but counterpart values were also obtained for each season and for clear days. These results are presented in Tables 2.6-2.9.

The mean error for the year ranges from -0.59 to 1.49 MJ m⁻² day⁻¹ between the stations, while the mean absolute error ranges from 1.40 to 1.97 MJ m⁻² day⁻¹ and the rms error ranges from 1.93 to 2.55 MJ m⁻² day⁻¹. For all 4 stations combined, the mean error is 0.83 MJ m⁻² day⁻¹, the mean absolute error is 1.75 MJ m⁻² day⁻¹, and the rms error is 2.33 MJ m⁻² day⁻¹.

These validation results compare favorably with those of Meyers and Dale (1983), who found an overall mean error of -0.12 MJ m⁻² day⁻¹, a mean absolute error of 1.28 MJ m⁻² day⁻¹, and an overall rms error of 1.69 MJ m⁻² day⁻¹. They used 5 days from each month in 1980 (60 days total) at each of the 12 stations equally scattered throughout the U.S. for comparisons. Because of the small sample size and some seasonal bias in the data sets, particularly in the Eau Claire and Peoria 1987 data, where there were only winter-spring and mainly summer data available, respectively, it is more useful to inspect the errors as a percentage of the mean daily SR measurement. In this light, the mean

Table 2.6. Mean error, mean absolute error, and root mean square (rms) error for modeled solar radiation at Eau Claire (EAU) in 1986. Units are MJ m⁻² day⁻¹, and percent of measured average.

	Mean Error	%	Mean Abs. Error	%	rms Error	%	Measured Average	No. of days
Year	1.02	9.2	1.89	17.0	2.55	23.0	11.09	130
Jan - Mar	1.09	12.2	1.74	19.5	2.34	26.2	8.95	91
Apr - May 12	0.85	5.3	2.23	13.9	2.97	18.5	16.10	39
Jul - Sep	—		—		—		—	—
Oct - Dec	—		—		—		—	—
Clear Days	-0.16	-1.0	0.21	1.4	0.24	1.5	15.38	6

Table 2.7a. As in Table 2.6, but for Columbus (OSU) in 1987.

	Mean Error	%	Mean Abs. Error	%	rms Error	%	Measured Average	No. of days
Year	1.49	11.4	1.97	15.0	2.55	19.5	13.10	361
Jan - Mar	0.97	8.4	1.59	16.8	2.21	23.4	9.45	91
Apr - Jun	1.98	10.2	2.43	12.5	3.08	15.9	19.43	90
Jul - Sep	1.99	11.7	2.42	14.2	2.93	17.2	17.04	89
Oct - Dec	1.21	18.3	1.45	21.9	1.78	26.9	6.62	91
Clear Days	1.39	6.3	1.39	6.3	1.49	6.8	22.00	11

Table 2.7b. As in Table 2.7a, but measured data were increased by 5%.								
	Mean Error %		Mean Abs. Error %		rms Error %		Measured Average	No. of days
Year	0.83	6.1	1.67	12.2	2.31	16.8	13.75	361
Jan - Mar	0.32	3.2	1.59	16.0	2.20	22.2	9.93	91
Apr - Jun	1.00	4.9	1.91	9.4	2.72	13.3	20.40	90
Jul - Sep	1.14	6.4	1.92	10.7	2.57	14.4	17.89	89
Oct - Dec	0.88	12.7	1.28	18.5	1.06	23.1	6.95	91
Clear Days	0.29	1.2	0.42	1.8	0.55	2.4	23.10	11

Table 2.8. As in Table 2.7a, but for Peoria in 1987.								
	Mean Error %		Mean Abs. Error %		rms Error %		Measured Average	No. of days
Year	-0.59	-3.2	1.79	9.7	2.28	12.3	18.47	136
Jan - Mar	—		—		—		—	—
Apr - Jun	-1.04	-4.4	2.49	10.6	3.14	13.3	23.52	25
Jul - Sep	-0.50	-2.6	1.67	8.7	2.14	11.1	19.25	82
Oct - Dec	-0.46	-3.9	1.51	12.7	1.70	14.2	11.91	29
Clear Days	-1.58	-7.5	1.58	7.5	1.65	7.9	21.00	7

Table 2.9. As in Table 2.8, but for all of 1988 at Peoria.								
	Mean Error %		Mean Abs. Error %		rms Error %		Measured Average	No. of days
Year	0.59	3.6	1.40	8.4	1.93	11.6	16.73	286
Jan - Mar	0.40	3.6	1.39	12.4	1.92	17.2	11.17	62
Apr - Jun	0.69	2.8	1.57	6.4	2.13	8.7	24.60	73
Jul - Sep	0.94	4.4	1.59	7.4	2.18	10.1	21.50	83
Oct - Dec	0.24	2.6	1.00	10.6	1.30	13.9	9.39	68
Clear Days	-0.12	-0.5	.065	3.1	0.78	3.7	21.38	13

error, mean absolute error, and the rms error for all stations are 5.6%, 11.7%, and 15.7%, respectively, whereas Meyers and Dale (1983) found -0.8%, 8.7% and 11.5%. In examining each station's individual error values and percentages for the year, for the seasonal averages, and for the clear days, these biases, due to the incomplete years of data used in validation, will become more evident as described below.

The Eau Claire data indicate very good agreement between the modeled and the observed data for clear sky days, well within the 5% uncertainty range common for most other SR models (see Meyers and Dale, 1983). While the lower percentages for the April-May 12 comparisons and the higher percentage error for January-March might indicate a possible seasonal bias in the model at Eau Claire, that is somewhat difficult to prove without the data for other seasons available. Nevertheless, if a whole year of data were compared, the overall errors for the year may decrease to a more reasonable level with the increase in sample size.

The errors shown for Columbus clearly demonstrate a potential overall bias in the modeled data for all seasons, the year as a whole, and clear sky days. The model may not predict SR as well here, or this may indicate a possible instrumental bias in the pyranometer which was used at Delaware. The errors show over-prediction of the model by about 5%. Since the model overestimates by about 5% for clear skies as well, this could be due to a dirty pyranometer or possibly one which was not optimally placed such

that, during some part of the day, the instrument was shaded and therefore caused less radiation to be detected than was actually incoming. If this were the case, this evidence clearly depicts the importance of site location, orientation and regular maintenance/instrumental upkeep not only for pyranometers, but all field equipment. Nevertheless, the Columbus comparison data appear more reasonable when the observed data are increased by 5%, as shown in the Table 2.7b.

The ICN SR measurements made in 1987 at Peoria are slightly questionable because positive hourly values of 0.01 to 0.13 MJ m⁻² were found to occur during night-time hours. However, an attempt was made to correct for this problem by averaging these night-time values and subtracting this average off each daylight hour before summing to get a daily total. In general, the model's performance was fairly good in predicting SR at Peoria in 1987, though it did miscalculate by an absolute average of about 1.7 MJ m⁻², with a slight bias to underpredict as indicated by the mean error of -0.59. This underprediction was clearly evident in the 7 clear days which occurred in September and October. Two of the 7 clear days were underestimated by over 2 MJ m⁻² day⁻¹. The large error shown for these clear days in 1987 at Peoria may have occurred due to 1) two of the seven days had very large errors, 2) there were only seven clear days (small sample size), and 3) the clear days only occurred during 2 months of the year.

The 1988 data for Peoria show by far the best comparison. This increases the confidence in the model because 1) the data are complete for 1988, and 2) the Illinois State Water Survey maintains the ICN automated weather station at Peoria, which assures the quality of the measurements. Additionally, Hollinger and Reitz (1990) suggest that, if all the measurement errors of the Eppley Black and White Pyranometer at this site were additive in the same direction, the accuracy would be approximately $\pm 1.4 \text{ MJ m}^{-2} \text{ day}^{-1}$. The mean absolute error of the Peoria comparisons for the year is 8.36% or 1.4 MJ m⁻², well within the expected 10% uncertainty range according to Meyers and Dale (1983), and in the realm of the measurement error, while the mean absolute error for clear days is well within the expected 5% uncertainty range (3.1%). It is evident, however, that there seems to be a seasonal bias in the model. The mean absolute error expressed as a percentage of the observed average is noticeably larger in January-March and October-December than in the other 2 mid-year seasons. But the percentage errors for all seasons are about $9 \pm 3\%$.

As explained previously, the 1988 Peoria model input data were from a different data source than for the other data sets used, which were from NCDC archives. It was found that the NCDC data sometimes only provided cloud heights every 3 hours, requiring interpolation of the values for the "off" hours, which may have introduced errors. Therefore, the different data source may have also contributed to the improved

comparisons in the 1988 Peoria data set over the results found in the other comparisons. In order to test this, the model was rerun using the 1988 Peoria data at 3 hour intervals, then re-compared with the observed data. These results are shown in Fig. 2.6 and Table 2.10. There were 47 more missing days due to the criterion of having no more than 2 consecutive daylight hours to interpolate. The (mean absolute) percentage errors changed by a negligible amount, and were about $10 \pm 3\%$. Thus, the interpolation scheme does not appear to introduce significant error and is judged to be adequate.

Table 2.10. As in Table 2.9, except cloud heights were only available every 3 hours as model input (i.e., modeled data are a test of the interpolation scheme).

	Mean Error %		Mean Abs. Error %		rms Error %		Measured Average	No. of days
Year	0.55	3.3	1.48	8.9	2.01	12.0	16.73	239
Jan - Mar	0.16	1.4	1.53	13.7	1.98	17.8	11.17	49
Apr - Jun	0.49	2.0	1.54	6.3	2.12	8.6	24.60	58
Jul - Sep	1.09	5.1	1.73	8.1	2.31	10.8	21.50	76
Oct - Dec	0.19	2.1	1.05	11.2	1.38	14.7	9.39	56
Clear Days	-0.12	-0.5	0.65	3.1	0.78	3.7	21.38	13

Meyers and Dale (1983) considered that their 8.7% mean absolute error for all stations shows excellent agreement between modeled and observed SR values. The results shown above from this study found the mean absolute error for all comparisons to be 11.7%, which shows very good agreement between modeled and observed SR, bearing in mind only parts of the year were used for comparison at some stations, and some of the observed data may contain errors/biases.

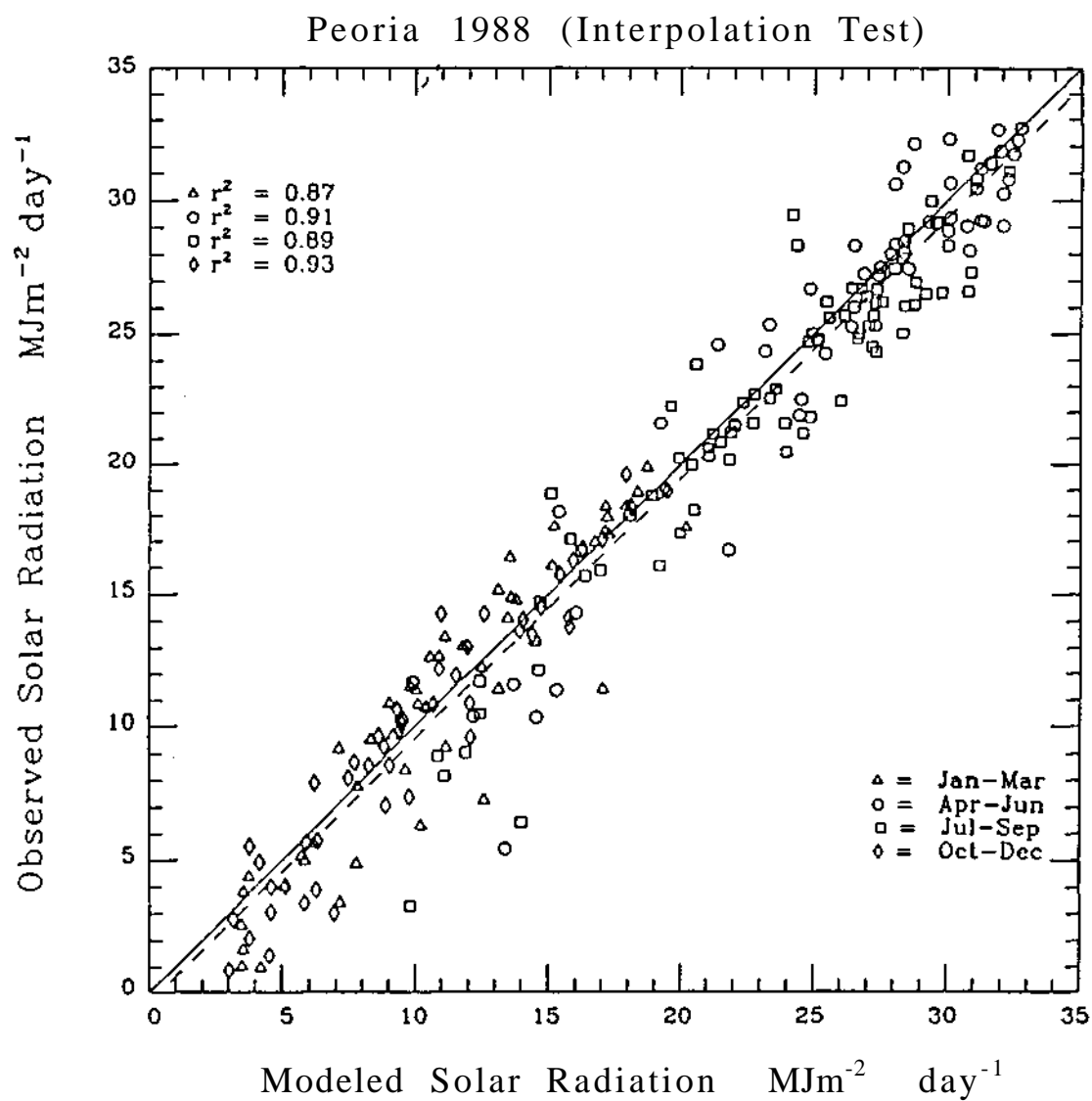


Fig. 2.6. Same as in Fig. 2.5, except cloud heights were only available every 3 hours as model input (i.e., modeled data are a test of the interpolation scheme).

CHAPTER III

COMPARISON WITH CORRECTED SOLAR RADIATION FROM SOLMET

The rehabilitated SOLMET (SOLar METeorological) SR data were released in 1977, and since that time have been used extensively in SR research. Because the data were corrected and published and are the primary source of SR data for the United States, many studies used the data to study the climatology of SR in the United States (Enmap Corp, 1980; Solar Energy Research Institute, 1981, 1990a; Balling, 1983; and many others). However, the accuracy of the SOLMET data is somewhat uncertain, since the data contain adjusted observations. Although the SR model used in this research was successfully validated using actual SR measurements as described in Chapter II, a comparison between the SOLMET data and the modeled SR was considered useful from the standpoints of further verifying the present model and/or providing new information on the accuracy of the SOLMET data.

This comparison, which is summarized below, indicates that the daily modeled SR values and daily SOLMET SR data are within about 10% of each other, with the tendency for modeled SR values to be higher than the SOLMET values. The r^2 values are around 0.94 for all periods compared. Seasonal comparisons show more overprediction of SR by the model as compared to the SOLMET data in the cooler months of October through March, and less overprediction in the warmer months (April-September).

A. Background to SOLMET Data

In 1972, the Atmospheric Radiation Working Group (ARWG) (chaired by Zdenek Sekera) reported that the SR network of the National Weather Service was marginal in spatial coverage, data quality, and instrument maintenance (ARWG, 1972). There was inadequate routine maintenance and station inspection, limited data monitoring and quality control, and field equipment deterioration. As a result, Working Group 1 from the Solar Energy Data Workshop held in November 1973 recommended that some (federal) agency: 1) rehabilitate the existing pyranometer data for the United States station network to at least a 5% accuracy for all possible stations for a period of 10 years, or longer where possible; and 2) include other relevant meteorological data together with the radiation information to permit correlation studies, etc. (Turner, 1974). The reasons for this rehabilitation included that fact that, over the years, a myriad of errors had found their way into the data due to the nature of the instrumentation and the data collection, and presentation procedures. The SR data were also referenced to

two different international scales: the Smithsonian Scale of 1913 and the International Scale of 1956. A detailed list of the reasons may be found in SOLMET, Volume II - Final Report (National Climatic Center, 1979).

The pyranometer network had grown from 83 stations in 1951 to 90 in 1973, with about 60 being National Weather Service sites. However, the National Climatic Center (NCC, now the National Climatic Data Center, NCDC) selected prime stations for the data rehabilitation on the basis of the most complete and correctable records (auxiliary recorder charts and nearby collateral hourly meteorological data available). Eventually, the 26 stations shown in Fig. 1.1 were chosen for the rehabilitation process and are known as the SOLMET (SOLar METeorological) stations.

The SOLMET data includes 3 sets of SR (direct and diffuse radiant energy) on a horizontal surface: observed (OBS), engineering corrected (ENG), and standard year corrected (STD) for the period 1952-1975. The OBS data are the original hourly values only corrected for the temperature response of the sensor. The ENG data are the observed data with additional corrections applied as suggested by the sensor, station, and recorder histories. These corrections include 1) calibration changes, 2) solar radiation scale differences, 3) midscale recorder chart setting, 4) Parson's black paint degradation, and 5) so-called "cross match" problem. The STD data are the observed data adjusted such that observed, clear, solar-noon irradiance values agree with theoretical clear, solar-noon irradiance values. In other words, one year of daily clear-sky, solar-noon irradiance values were calculated for each of the 26 stations, which then comprised the "standard" year of data that were used in adjusting the station's entire original data set. Of course, this approach ruled out any determination of long-term trends in the data due to aerosol turbidity, but it had already been determined at that time that the data were too erroneous/unreliable to see such a trend (NCC, 1979). A detailed description of the methods and techniques used in correcting and creating the SOLMET data now available may be found in SOLMET Volume II - Final Report (NCC, 1979).

B. Statistical Results

The present model was run with NCDC input data for the following four midwestern stations that are also SOLMET stations: Madison, Wisconsin (MSN); Omaha, Nebraska (OMA); Columbia, Missouri (COU); and Nashville, Tennessee (BNA). Daily totals of modeled SR were compared with the SOLMET data sets for the period of 1952-1975. Equation 2.11 was used, where SR_{obs} was either SOLMET SR_{OBS} , SR_{ENG} , or SR_{STD} . The results are summarized in Tables 3.1-3.4.

Table 3.1. Mean error, mean absolute error, and root mean square (rms) error of modeled solar radiation versus SOLMET a) OBS, b) ENG, and c) STD data for Madison. Units are MJ m⁻² day⁻¹, and percent of SOLMET average.

	Mean Error	%	Mean Abs. Error	%	rms Error	%	SOLMET Average	No. of days
a) OBS								
Year	-0.20	-1.4	1.88	13.1	2.46	17.2	14.32	7355
Jan - Mar	-0.44	-4.2	1.75	16.8	2.17	20.8	10.44	1815
Apr - Jun	-0.14	-0.7	2.55	12.6	3.20	15.8	20.29	1801
Jul - Sep	-0.27	-1.4	2.05	10.5	2.68	13.7	19.52	1849
Oct - Dec	0.06	0.8	1.20	16.5	1.48	20.3	7.27	1890
b) ENG								
Year	0.20	1.4	1.67	12.0	2.23	16.0	13.97	7346
Jan - Mar	0.13	1.3	1.48	15.0	1.91	19.2	9.90	1806
Apr - Jun	0.33	1.7	2.27	11.5	2.94	14.8	19.82	1801
Jul - Sep	0.00	0.0	1.85	9.6	2.43	12.6	19.26	1849
Oct - Dec	0.33	4.8	1.10	15.8	1.39	19.8	7.00	1890
c) STD								
Year	0.65	4.8	1.48	10.9	2.07	15.3	13.57	8945
Jan - Mar	0.79	8.5	1.36	14.6	1.91	20.6	9.30	2183
Apr - Jun	0.81	4.2.	1.99	10.3	2.70	13.9	19.44	2183
Jul - Sep	0.48	2.5	1.59	8.5	2.16	11.5	18.75	2297
Oct - Dec	0.54	7.9	0.98	14.3	1.31	19.2	6.83	2282

Table 3.2. As in Table 3.1, but for Omaha.								
	Mean Error	%	Mean Abs. Error	%	rms Error	%	SOLMET Average	No. of days
a) OBS								
Year	-0.71	-4.5	2.02	12.8	2.55	16.2	15.74	6456
Jan - Mar	-0.95	-8.2	2.04	17.5	2.47	21.2	11.66	1604
Apr - Jun	-0.77	-3.6	2.56	11.9	3.21	14.8	21.65	1609
Jul - Sep	-0.61	-3.0	2.05	10.1	2.59	12.7	20.36	1650
Oct - Dec	-0.52	-0.58	1.40	15.5	1.67	18.4	9.07	1593
b) ENG								
Year	-0.37	-2.4	1.76	11.4	2.30	15.0	15.40	6450
Jan - Mar	-0.41	-3.7	1.67	15.0	2.11	18.9	11.13	1598
Apr - Jun	-0.42	-2.0	2.30	10.8	2.95	13.9	21.30	1609
Jul - Sep	-0.43	-2.1	1.87	9.3	2.42	12.0	20.18	1650
Oct - Dec	-0.23	-2.6	1.20	13.6	1.46	16.7	8.78	1593
c) STD								
Year	-0.05	-0.3	1.52	10.1	2.11	14.0	15.05	7154
Jan - Mar	0.34	3.2	1.38	13.2	1.90	18.2	10.44	1729
Apr - Jun	-0.23	-1.1	2.06	9.7	2.72	12.9	21.17	1760
Jul - Sep	-0.36	-1.8	1.70	8.4	2.27	11.3	20.15	1840
Oct - Dec	0.08	0.9	0.98	11.7	1.28	15.4	8.35	1825

Table 3.3. As in Table 3.1, but for Columbia.								
	Mean Error %		Mean Abs. Error %		rms Error %		SOLMET Average	No. of days
a) OBS								
Year	-0.51	-3.2	1.89	11.8	2.39	15.0	15.95	8713
Jan - Mar	-0.35	-3.1	1.89	16.8	2.32	20.6	11.24	2113
Apr - Jun	-0.63	-2.9	2.35	10.8	2.94	13.5	21.79	2114
Jul - Sep	-0.74	-3.5	1.95	9.2	2.48	11.7	21.27	2242
Oct - Dec	-0.33	-3.5	1.39	14.6	1.68	17.6	9.56	2244
b) ENG								
Year	0.03	0.2	1.64	10.6	2.18	14.2	15.42	8701
Jan - Mar	0.32	3.0	1.55	14.6	2.02	19.1	10.59	2101
Apr - Jun	-0.03	-0.1	2.14	10.1	2.78	13.1	21.19	2114
Jul - Sep	-0.28	-1.4	1.75	8.4	2.29	11.0	20.81	2242
Oct - Dec	0.12	1.4	1.14	12.5	1.46	16.1	9.11	2244
c) STD								
Year	0.33	2.2	1.52	10.1	2.12	14.0	15.12	8946
Jan - Mar	0.73	7.2	1.45	14.2	1.99	19.6	10.18	2183
Apr - Jun	0.22	1.0	1.97	9.4	2.68	12.8	20.92	2183
Jul - Sep	-0.06	-0.3	1.66	8.0	2.25	10.9	20.59	2299
Oct - Dec	0.43	4.9	1.03	11.7	1.39	15.8	8.79	2281

Table 3.4. As in Table 3.1, but for Nashville, TN.								
	Mean Error %		Mean Abs. Error %		rms Error %		SOLMET Average	No. of days
a) OBS								
Year	0.36	2.4	1.92	12.6	2.46	16.1	15.25	8419
Jan - Mar	0.50	4.7	1.85	17.4	2.31	21.8	10.58	2058
Apr - Jun	0.27	1.3	2.29	10.8	2.89	13.6	21.18	2048
Jul - Sep	0.42	2.1	2.18	11.0	2.77	14.0	19.80	2135
Oct - Dec	0.27	2.8	1.38	14.3	1.72	17.9	9.65	2178
b) ENG								
Year	0.63	4.2	1.79	11.9	2.35	15.7	15.00	8410
Jan - Mar	0.83	8.1	1.69	16.5	2.22	21.6	10.27	2049
Apr - Jun	0.51	2.4	2.16	10.3	2.80	13.4	20.93	2048
Jul - Sep	0.65	3.3	2.07	10.6	2.61	13.4	19.57	2135
Oct - Dec	0.52	5.6	1.25	13.3	1.63	17.3	9.40	2178
c) STD								
Year	1.20	8.3	1.74	12.1	2.32	16.1	14.41	8901
Jan - Mar	1.37	14.2	1.69	17.5	2.26	23.3	9.69	2184
Apr - Jun	1.25	6.2	2.10	10.4	2.75	13.6	20.19	2140
Jul - Sep	1.24	6.5	1.98	10.4	2.51	13.2	18.99	2295
Oct - Dec	0.96	10.8	1.22	13.8	1.62	18.2	8.88	2282

It is evident from the SOLMET averages in Tables 3.1-3.4 that the SOLMET SR data at these stations were all decreased, on average, by about $0.8 \text{ MJ m}^{-2} \text{ day}^{-1}$ during the correction process from OBS to STD data. For example, at Columbia, the SOLMET means (in $\text{MJ m}^{-2} \text{ day}^{-1}$) over the period are: 1) OBS = 15.95; 2) ENG = 15.42; and 3) STD = 15.12, which decrease quite consistently by a total of $0.83 \text{ MJ m}^{-2} \text{ day}^{-1}$ from OBS to STD.

The modeled-versus-SOLMET mean error percentages are fairly small (around $0 \pm 4\%$) throughout all data sets at all stations, except for Nashville, where the comparisons deviate from each other by about $5 \pm 3\%$. The mean absolute error percentages, as well as the rms error percentages, consistently decrease from OBS to ENG to STD data set comparisons with modeled values for all stations with one exception. Those error percentages *increase* rather than decrease for the Nashville comparisons from ENG to STD data sets. The mean absolute deviations of modeled and STD values are all around 10% for each station's comparison, except at Nashville, where the error is about 12%. Note, however, that if the SOLMET data sets for Nashville were consistently decreased rather than increased (from OBS to ENG to STD data), as occurred for the other three stations, the error percentages would have been closer to 10% than the 12% found for the Nashville STD data comparisons with the model output.

The seasonal breakdown of the comparisons of modeled and SOLMET values indicates a possible bias. The differences tend to be greater in the cool months of October through March for all data set comparisons, with smallest differences occurring during the mid-year months of April through September.

Tables 3.1-3.4 indicate the modeled data and SOLMET data are with about 10% of each other. The tables show that the modeled values compare closest to the SOLMET STD data except for Nashville; they also suggest a possible bias in the model of overestimating SR in the cooler months when SR is low.

Figures 3.1-3.4 contain scatter diagrams of approximately 8 years worth of randomly chosen (using a random number generator) daily SR comparisons, so as to represent the 24 years of daily comparisons of SOLMET versus modeled data, for each of the 4 stations. These plots confirm that there is a lower bound to the daily SR values that the model will produce, as was suggested by Figs. 2.2-2.5. This further confirms that the model tends to overestimate when incoming radiation is low. The fitted regression results of SOLMET on modeled data for all days for each data set at each station are shown in Table 3.5, with the regression lines shown on the scatter plots. All regression lines except for the STD data at Nashville cross the 1:1 line at a slight angle, indicating

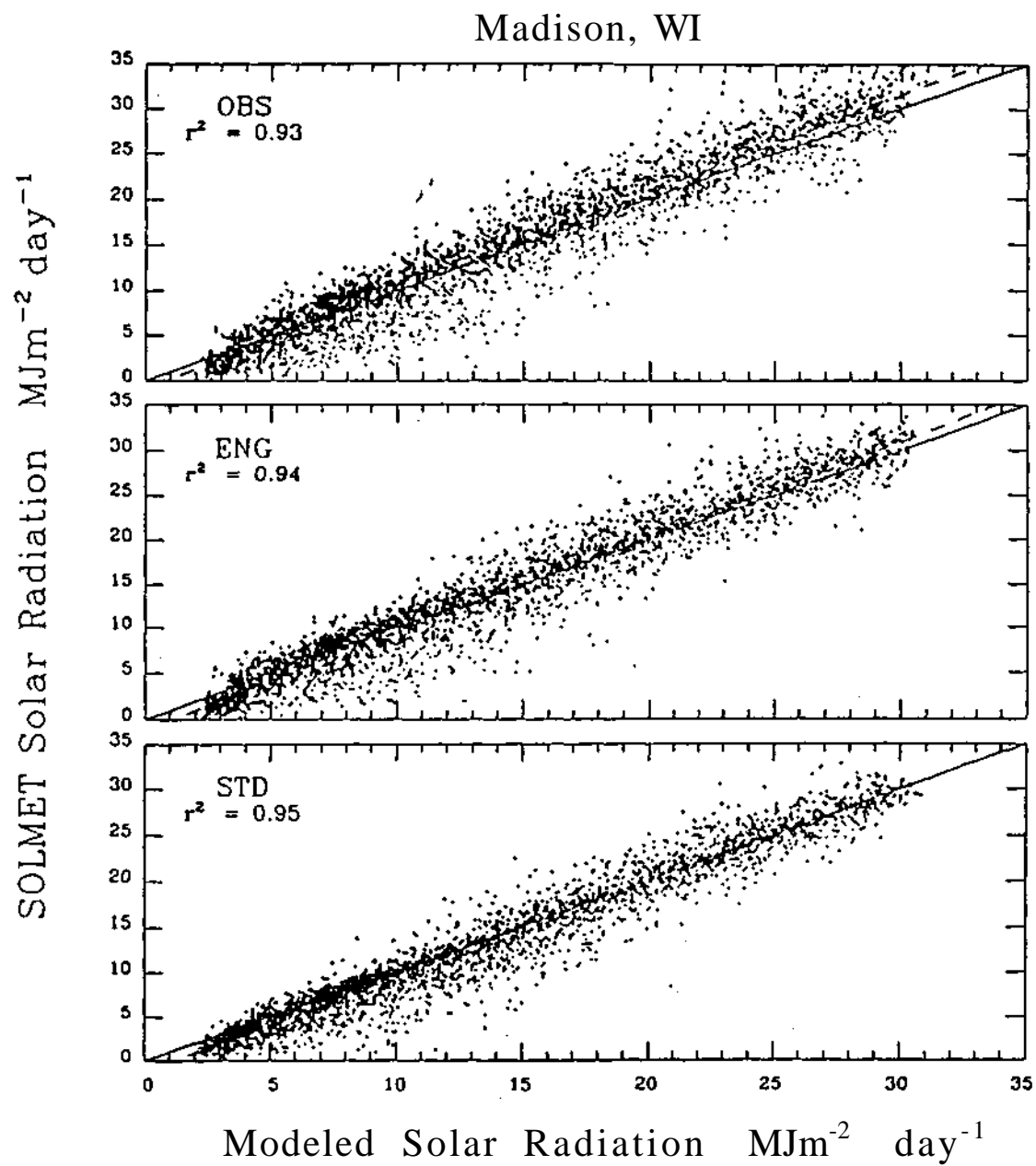


Fig. 3.1. Scatter diagram of 3000 randomly selected pairs of modeled versus SOLMET daily data for Madison. Solid line is 1:1 line; regression line is dashed.

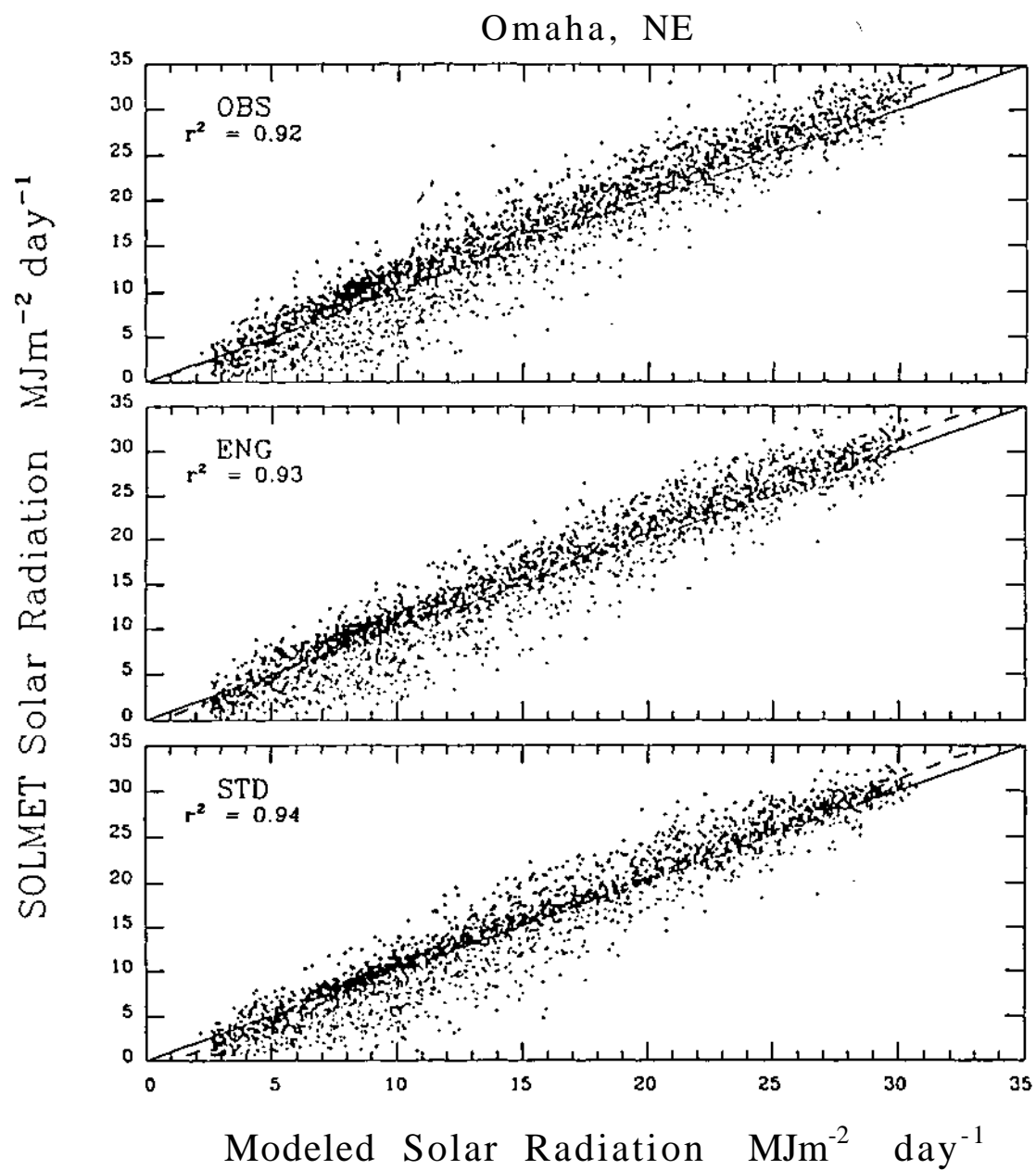


Fig. 3.2. Scatter diagram of 3000 randomly selected pairs of modeled versus SOLMET daily data for Omaha. Solid line is 1:1 line; regression line is dashed.

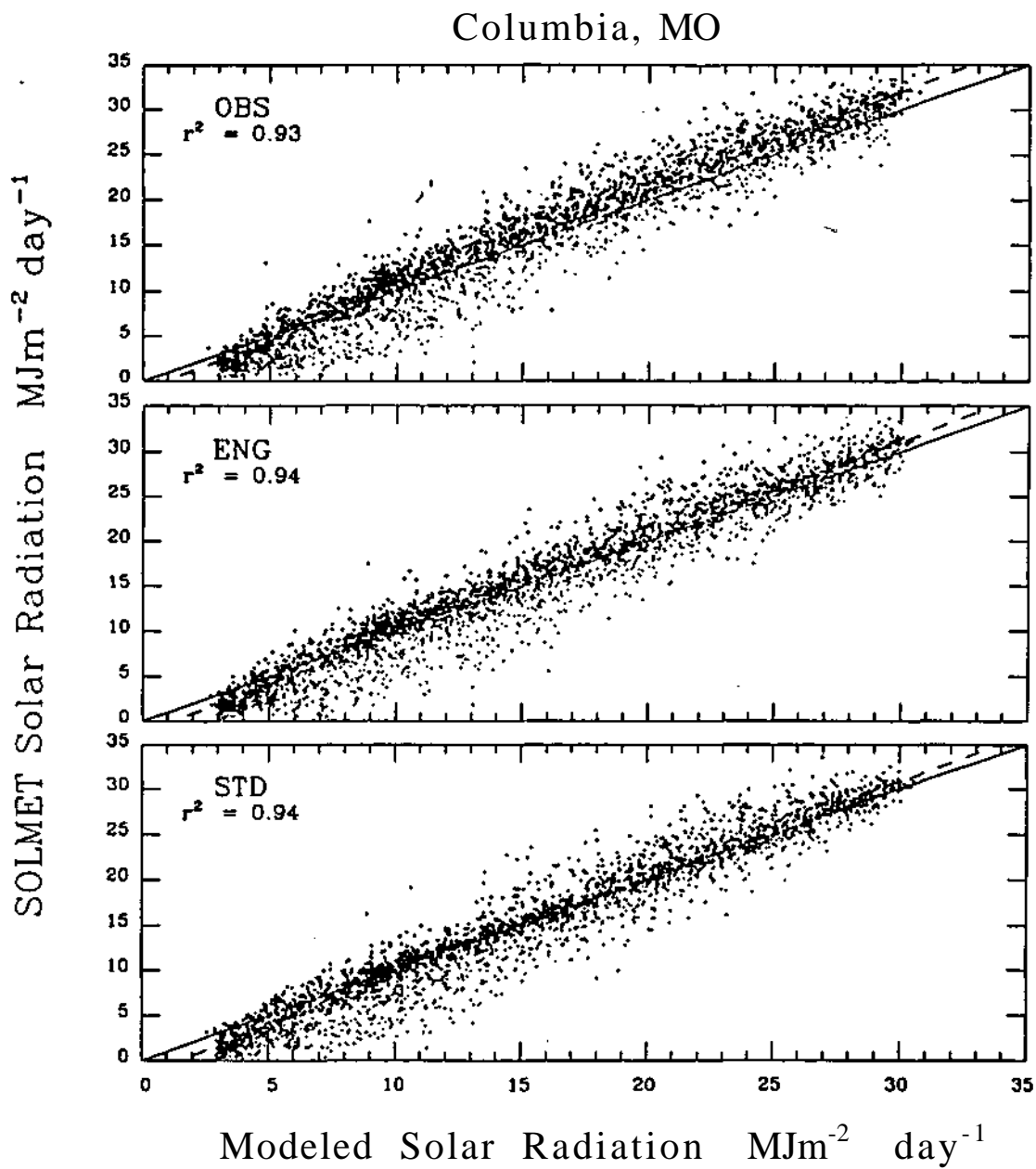


Fig. 3.3. Scatter diagram of 3000 randomly selected pairs of modeled versus SOLMET daily data for Columbia. Solid line is 1:1 line; regression line is dashed.

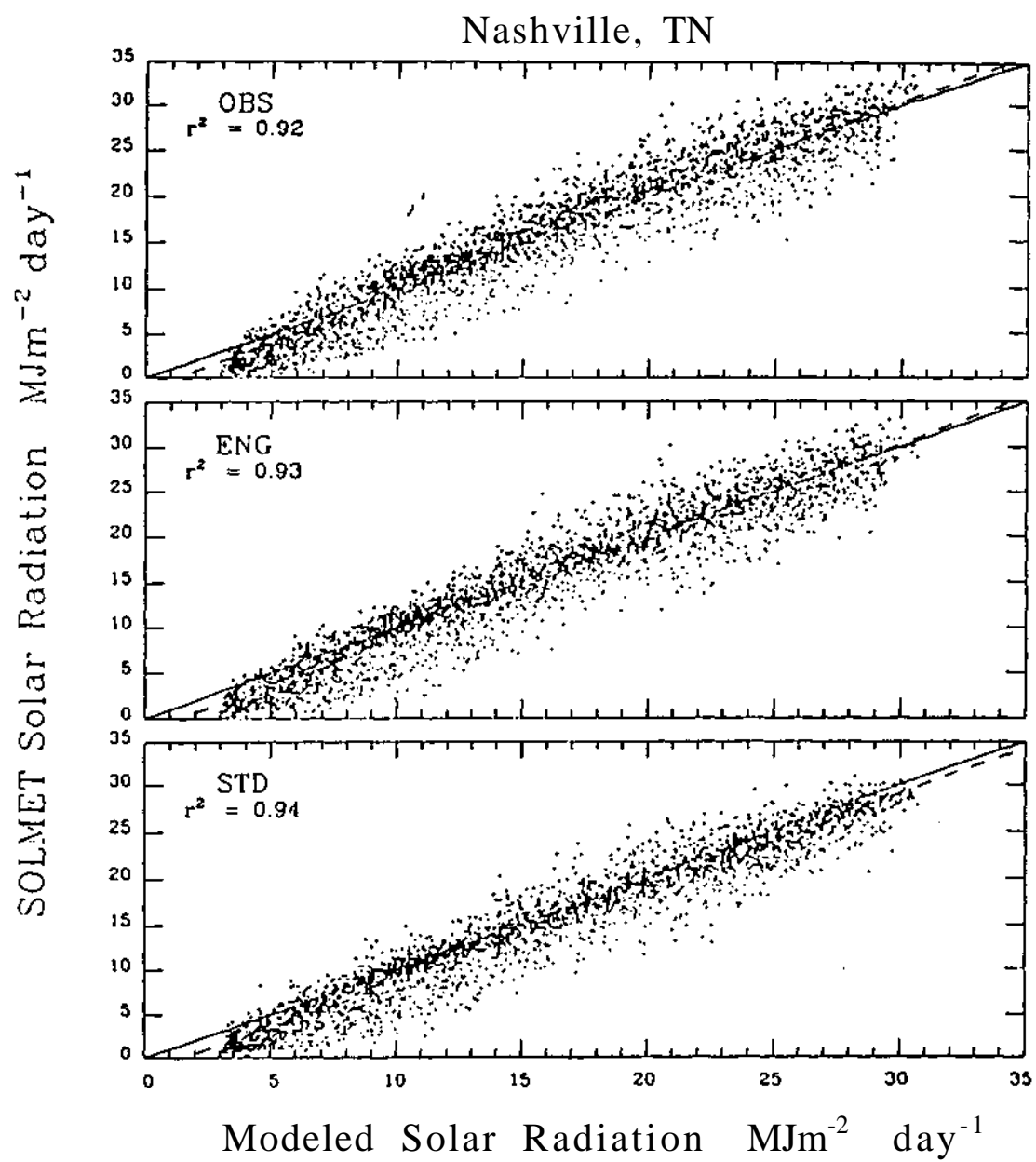


Fig. 3.4. Scatter diagram of 3000 randomly selected pairs of modeled versus SOLMET daily data for Nashville. Solid line is 1:1 line; regression line is dashed.

Table 3.5. Coefficient of determination (r^2), slope (m), and intercept (b) for regression of SOLMET on modeled daily solar radiation (SR), for indicated SOLMET data sets and stations.

SOLMET Station and Data	r^2	m	b
Madison (MSN)			
OBS	0.93	1.08	-0.90
ENG	0.94	1.07	-1.16
STD	0.95	1.04	-1.22
Omaha (OMA)			
OBS	0.92	1.07	-0.33
ENG	0.93	1.07	-0.64
STD	0.94	1.08	-1.14
Columbia (COU)			
OBS	0.93	1.10	-1.01
ENG	0.94	1.08	-1.32
STD	0.94	1.08	-1.60
Nashville (BNA)			
OBS	0.92	1.06	-1.33
ENG	0.93	1.06	-1.50
STD	0.94	1.02	-1.57

a small bias in the model towards overestimating for very low SR and underestimating for high values. This is consistent with the seasonal variations of mean error percentages shown in Tables 3.1-3.4, and with the above observation that the model overestimates when radiation is low. As the SOLMET data get "better corrected" at each station, the regression results improve from OBS to ENG to STD data sets, showing increasing r^2 values between the data. The slopes decrease toward 1.0, and the y-intercepts decrease away from zero as the data become better corrected. The STD r^2 results are 0.945 ± 0.008 for all stations, which indicates the model does a very good job in predicting the SOLMET STD values for all stations.

C. Comparing with Baker and Klink's Data

At approximately the time NCC was in the process of rehabilitating the SOLMET data, Baker and Klink (1975) (henceforth referred to as B&K) attempted to analyze the SR climate of the North Central Region using unrehabilitated SR records for the period 1952-1970. They made an effort to correct the data, but the tests were not as rigorous as those described in SOLMET - Volume II (NCC, 1979), and histories of the instruments used were not available to permit evaluation of that instrumentation. Apparently, the only adjustments made by B&K to data from all stations used were 1) daily totals that exceeded 90% of their extraterrestrial counterparts were removed from the record, and 2) all daily totals previous to July 1, 1957 were reduced by 2% to conform to the International Pyroheliometric Scale of 1956.

The time unit used in the B&K study was the climatological week, where week 1 is the week of March 1-7, and week 52 is February 21-27. They omitted week 53 from consideration, which includes February 28 and 29. Tables 25, 21, and 19 in B&K's bulletin included mean SR for each climatological week at 3 of the 4 SOLMET stations discussed in Section IIIB above: Madison, Omaha, and Columbia. B&K's published weekly means were therefore compared with the present model output averaged for each climatological week for the same time period at these stations. These comparisons are shown graphically in Fig. 3.5. The values that B&K used compare very well with the modeled values at these three stations. The data set comparisons for Columbia seem to be very close, while the data for Omaha appear to differ the most from each other. Baker & Klink's data for Madison show a large amount of variability in the weekly means from about week 5 to week 25; however, B&K's bulletin does not discuss or explain the reasons for this variability.

Because B&K used unrehabilitated SOLMET data for their study of SR, the data published in their bulletin for these three stations were also here compared with the three sets of SOLMET data for each station. These results are shown in Figs. 3.6-3.8.

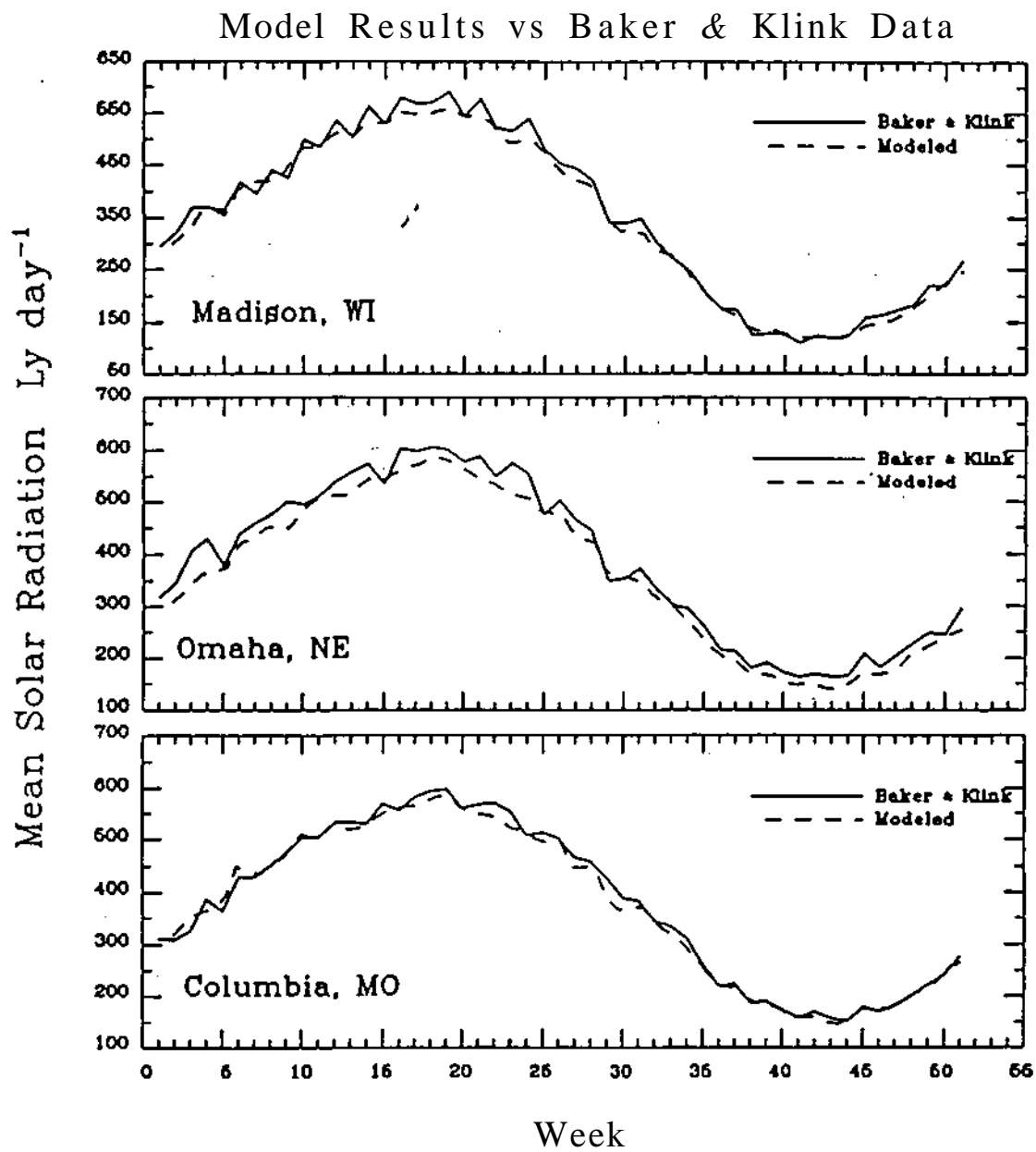


Fig. 3.5. Comparison of the climatological weekly averages of Baker & Klink's data (solid line) versus modeled output (dashed) for Madison, Omaha, and Columbia.

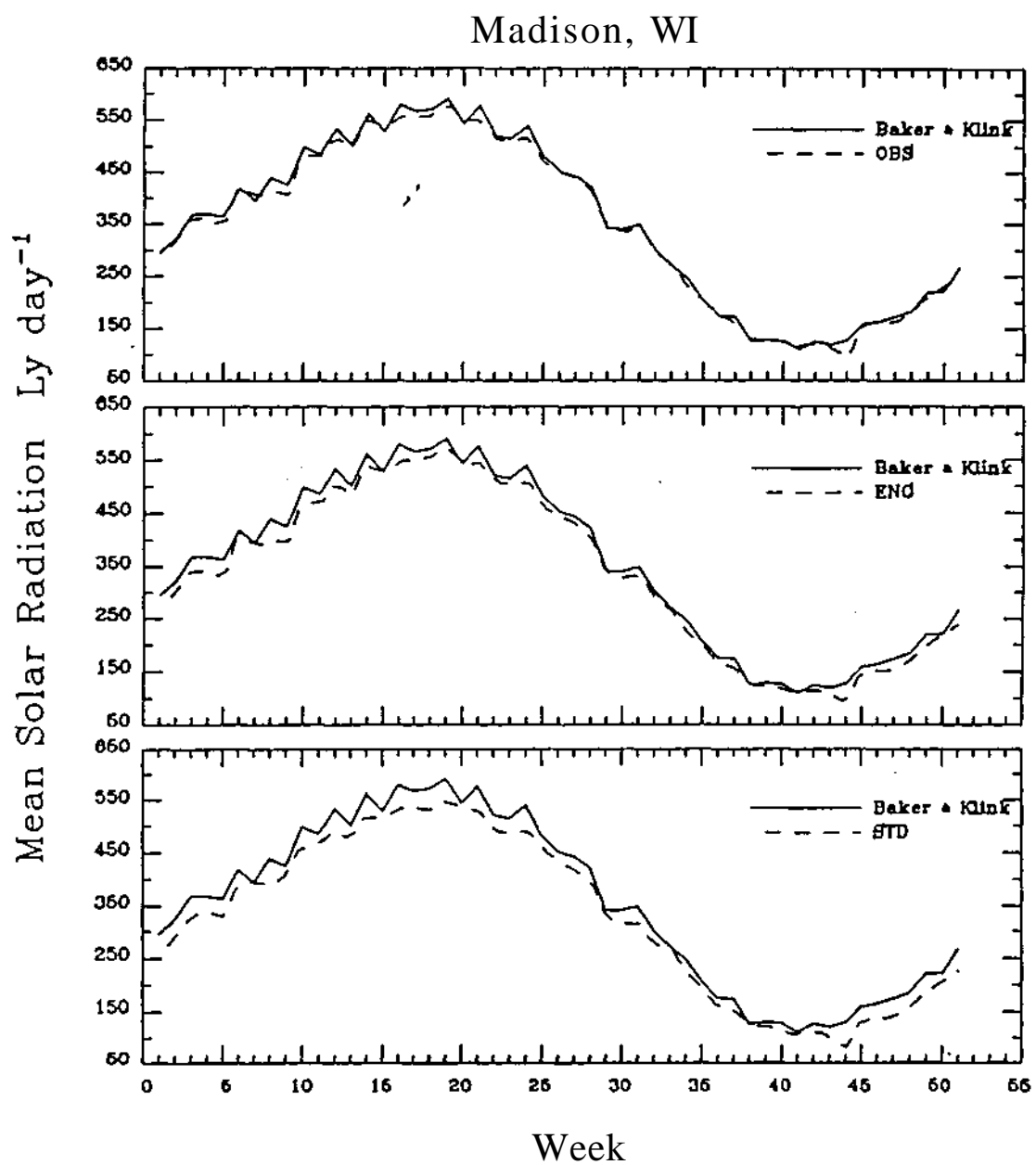


Fig. 3.6. Comparison of the climatological weekly averages of Baker & Klink's data (solid line) versus the SOLMET data sets (dashed) for Madison.

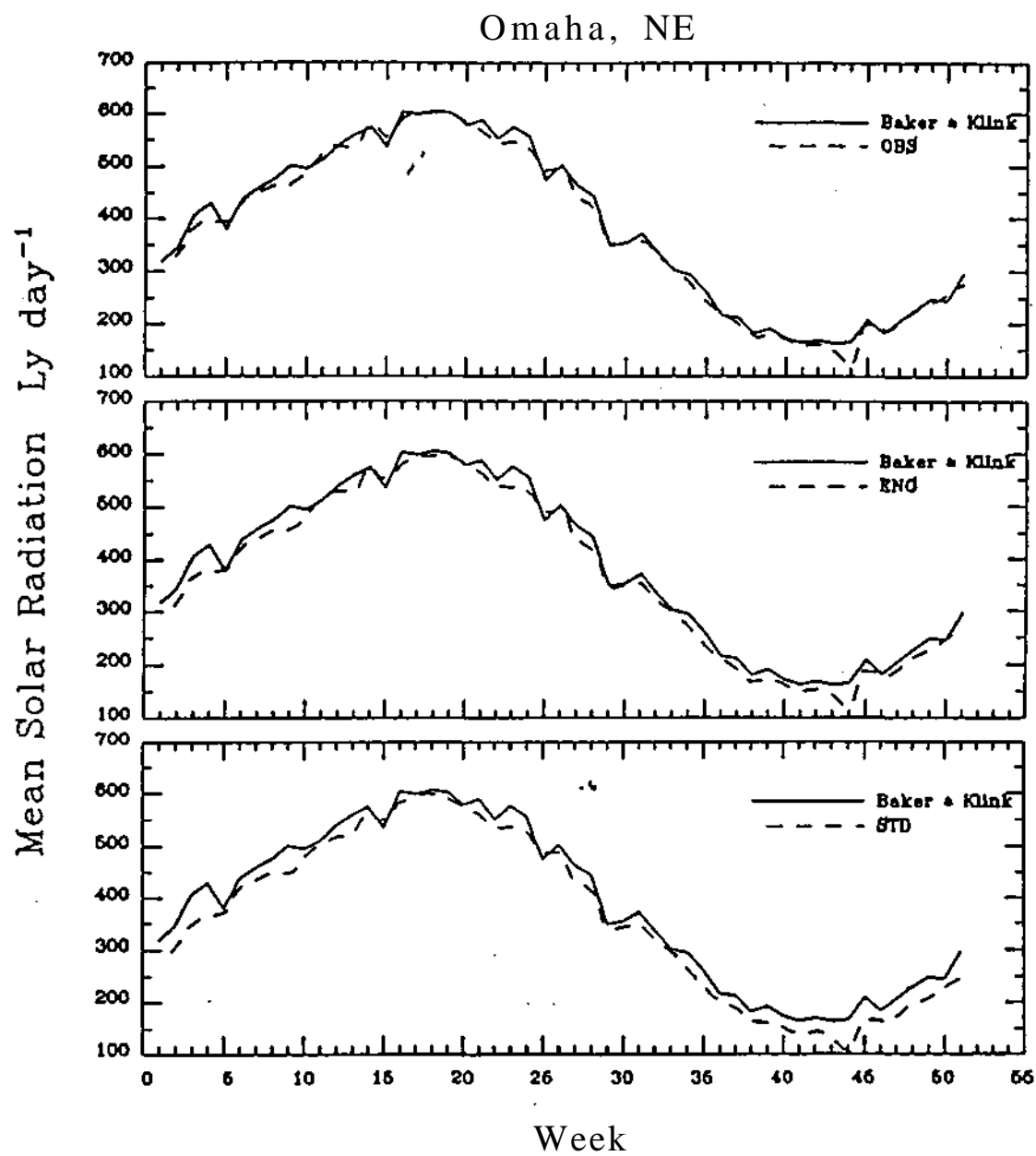


Fig. 3.7. Comparison of the climatological weekly averages of Baker & Klink's data (solid line) versus the SOLMET data sets (dashed) for Omaha.

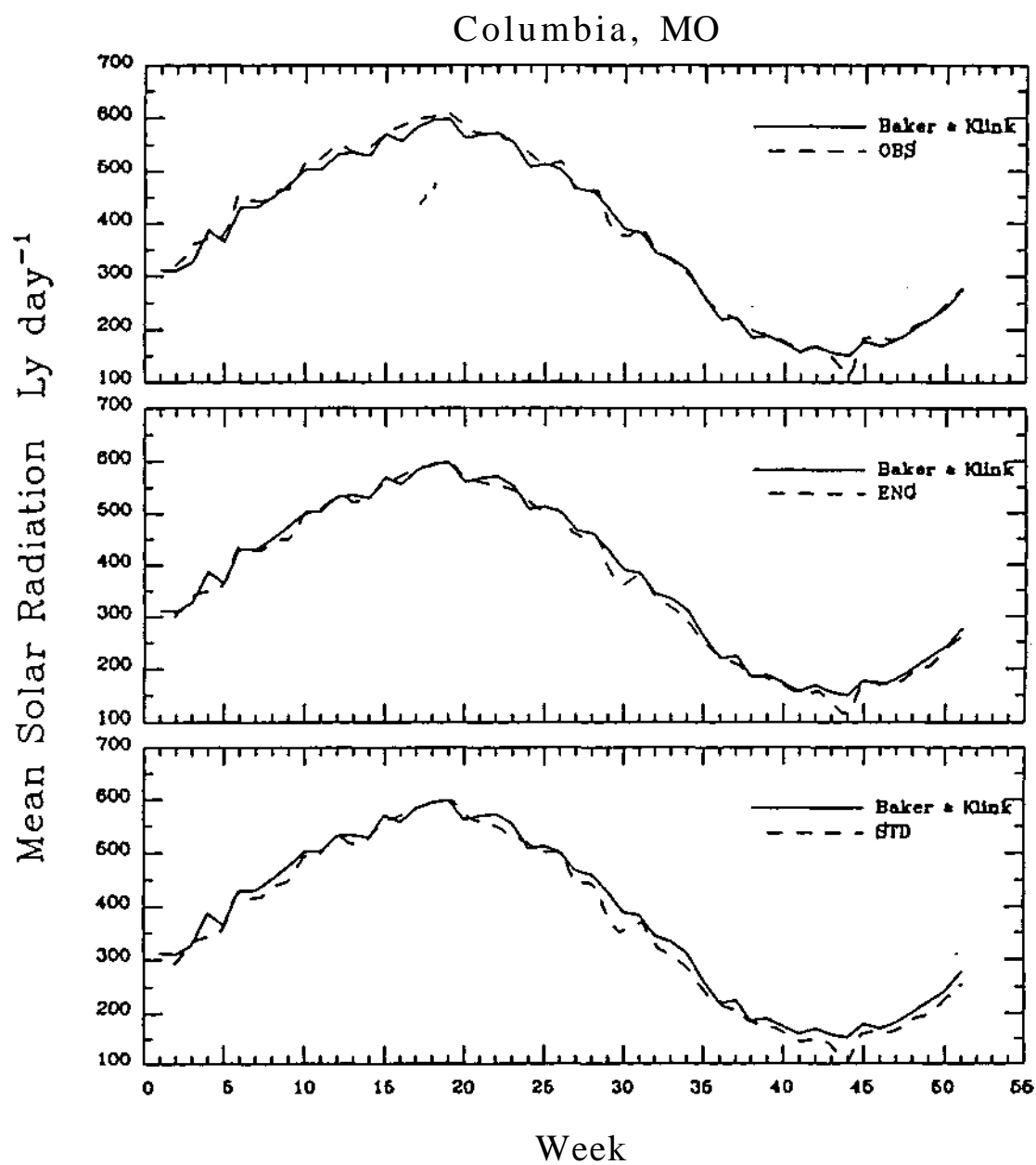


Fig. 3.8. Comparison of the climatological weekly averages of Baker & Klink's data (solid line) versus the SOLMET data sets (dashed) for Columbia.

As one would expect, the best comparison for each station is that of B&K's data versus the SOLMET OBS data, since B&K used unrehabilitated (or observed) SR data in their study.

Closer examination of each station's three comparisons indicates that the deviation in B&K's versus SOLMET STD data is very similar to the deviations of their data versus the OBS and ENG data comparisons for Columbia, while the results for Omaha and Madison show a larger increase in differences between B&K's data and SOLMET OBS to ENG to STD data sets. This would suggest that the changes in the SOLMET data due to the successive corrections from OBS to ENG to STD data are largest for Madison and smallest for Columbia. Subsequently, the climatological weekly means of the model results (for the SOLMET period-of-record) were compared with the three SOLMET data sets' weekly means, and are shown in Figs. 3.9-3.11. All comparisons show smaller deviations in SOLMET versus modeled weekly means than for SOLMET versus B&K's data. This would indicate that the modeled SR very closely resembles the SOLMET data when averaged over weeks.

The modeled versus SOLMET climatological weekly mean values for the three stations are shown in scatter diagram form in Figs. 3.12-3.14. These depictions more clearly show which SOLMET data set gives closest to a 1 to 1 correspondence with the modeled SR. For Columbia, the SOLMET ENG data are closest to the modeled values when averaged over the weeks, since most values lie above the 1:1 line for OBS data and below the 1:1 line for STD data. The STD data set can be ruled out as closest to the modeled values for Madison since nearly all points fall below the 1:1 line; similarly, the SOLMET OBS data can be ruled out for Omaha since most values are above the 1:1 line. Therefore, for Madison, the OBS and ENG data sets compare very well with the modeled results when averaged, and for Omaha, the SOLMET ENG and STD data sets both compare well with modeled SR when averaged over the climatological weeks.

D. Extension of SOLMET using Regression Estimates

One of the goals of the overall SOLMET rehabilitation effort was to generate estimated SR data for 75 to 200 sites, as an interim step until a new National Weather Service SR network could accumulate a sufficiently large data base (NCC, 1979). Linear regression equations relating measured hourly SR to commonly reported weather elements were derived for the 26 SOLMET stations and used by the NCC 1) when standard year corrected (STD) data were missing or when their value exceeded the corresponding hourly extraterrestrial radiation value; and 2) to extend the SOLMET-based network to 222 additional locations. The equations used were linear regressions of hourly global SR on: 1) the solar Zenith angle, 2) the amount of opaque cloudiness

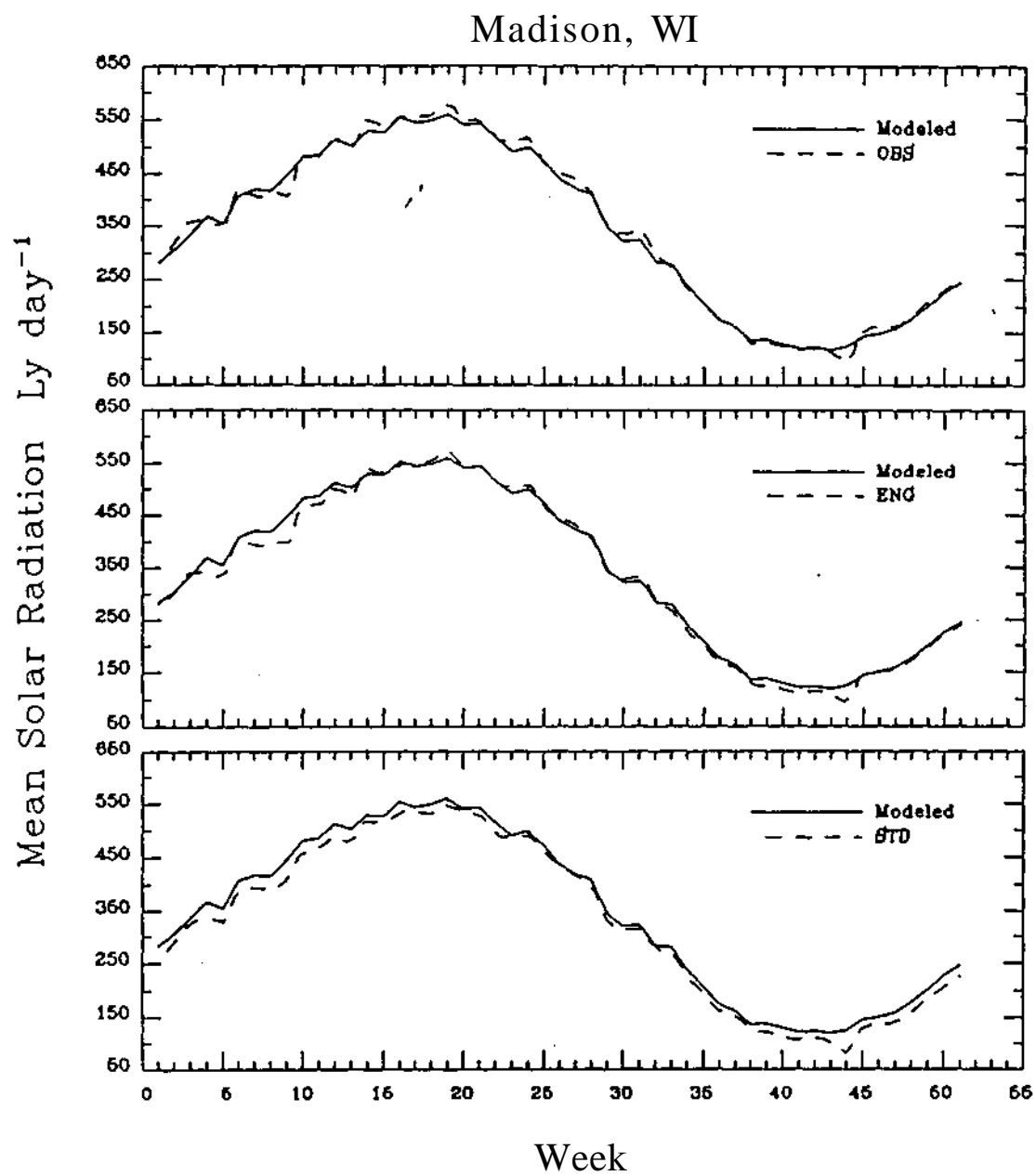


Fig. 3.9. Comparison of the climatological weekly averages of the modeled output (solid line) versus the SOLMET data sets (dashed) for Madison.

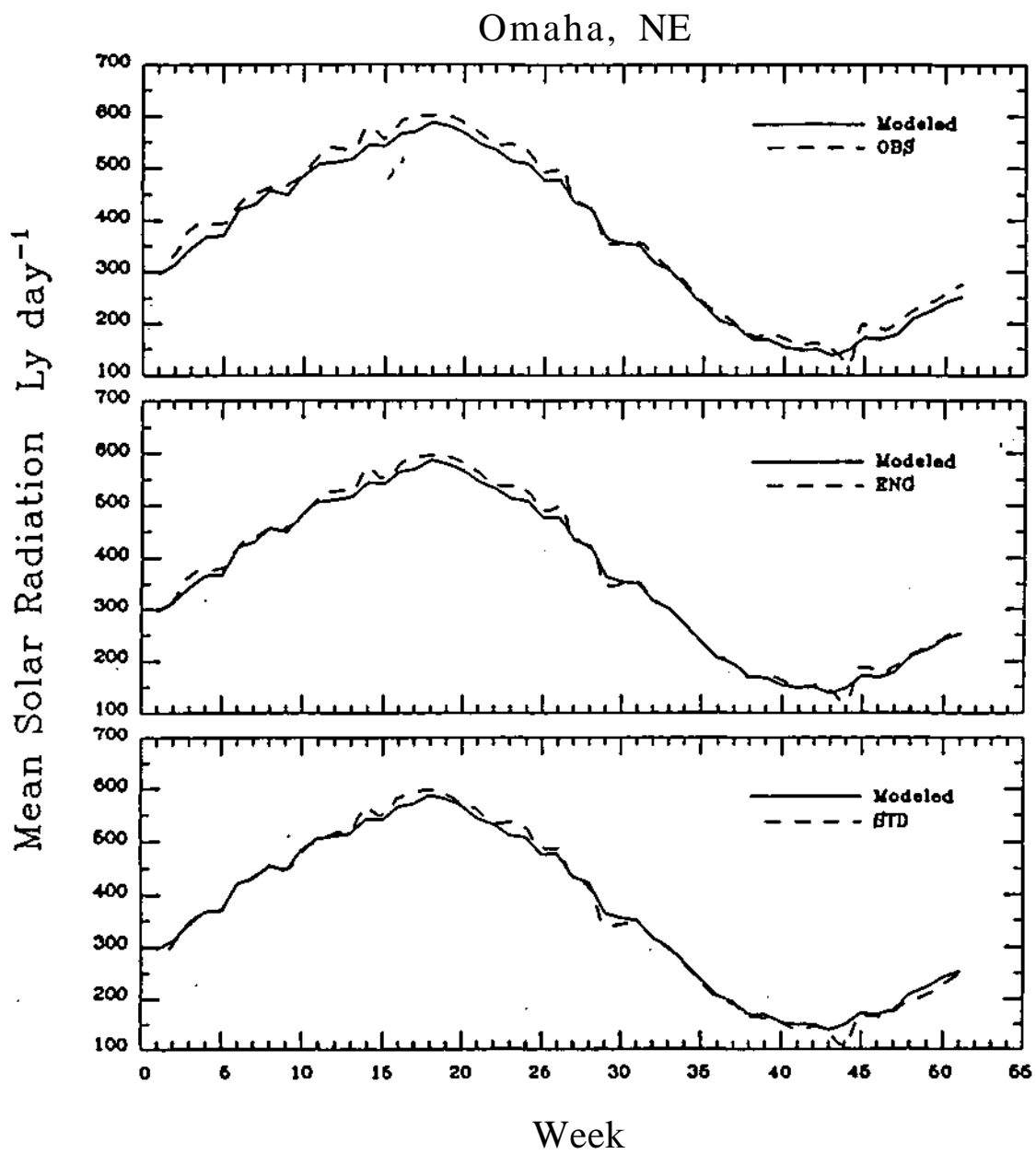


Fig. 3.10. Comparison of the climatological weekly averages of the modeled output (solid line) versus the SOLMET data sets (dashed) for Omaha.

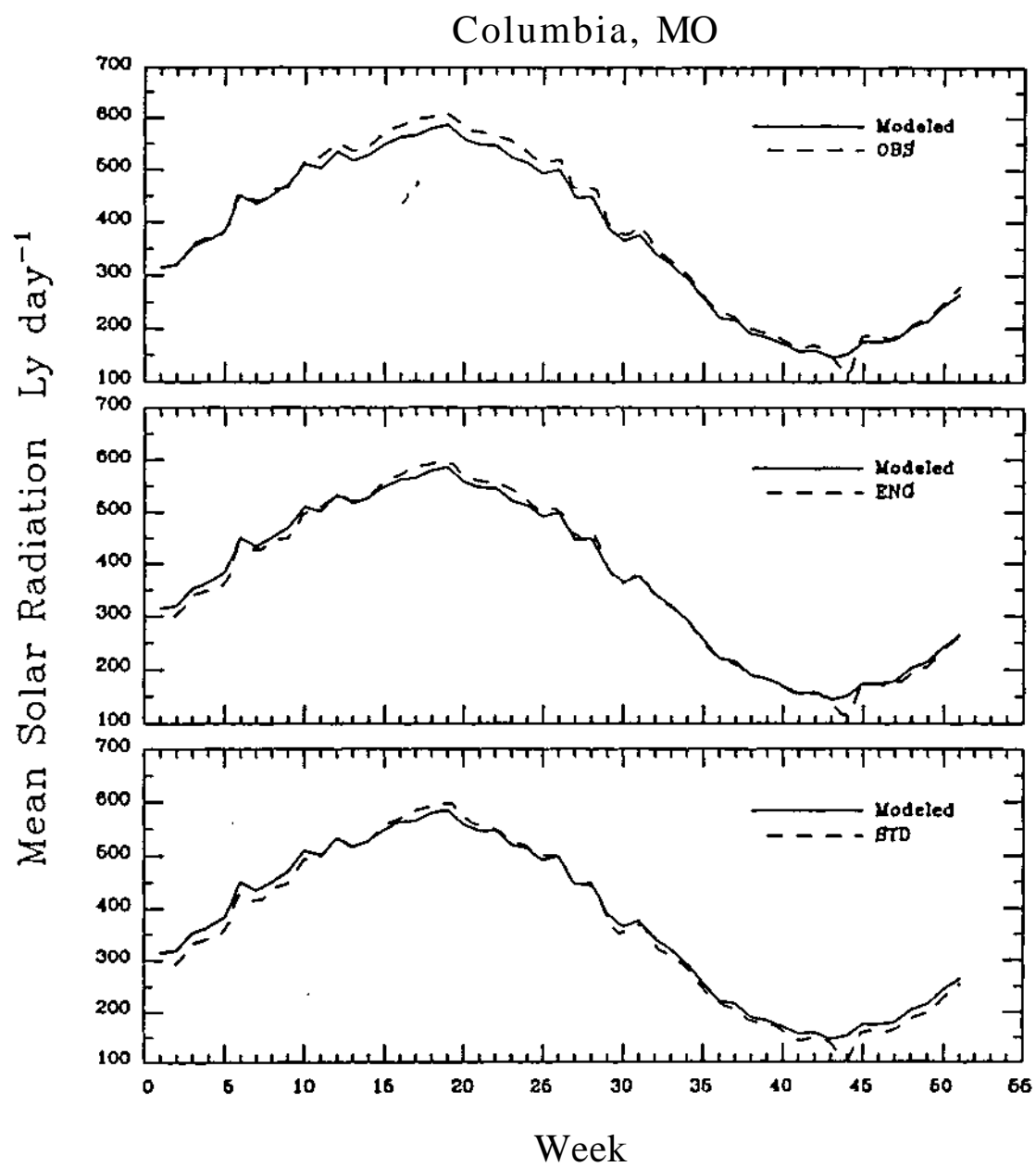


Fig. 3.11. Comparison of the climatological weekly averages of the modeled output (solid line) versus the SOLMET data sets (dashed) for Columbia.

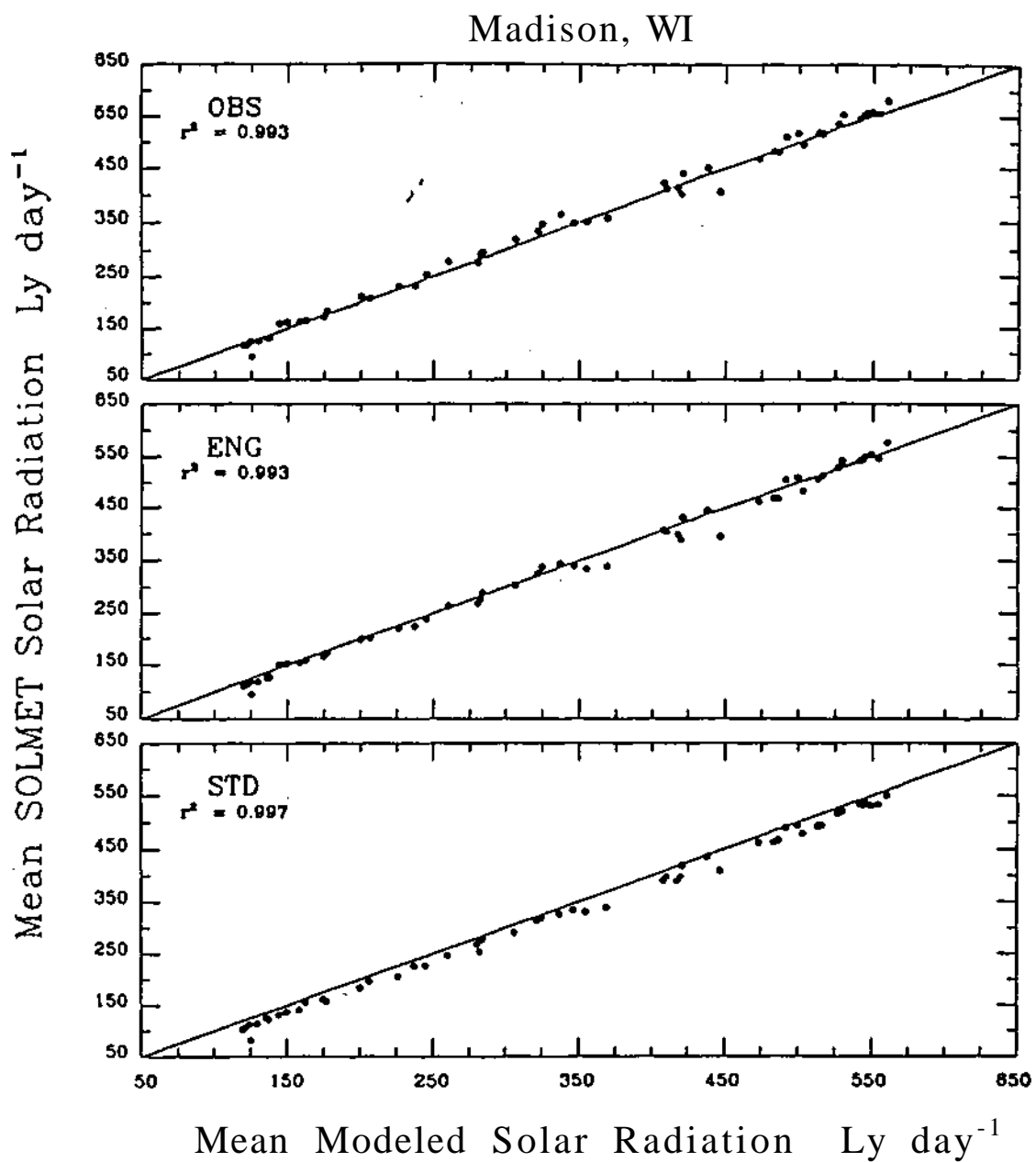


Fig. 3.12. Scatter diagram comparing the climatological weekly averages of the modeled output versus the SOLMET data sets for Madison.

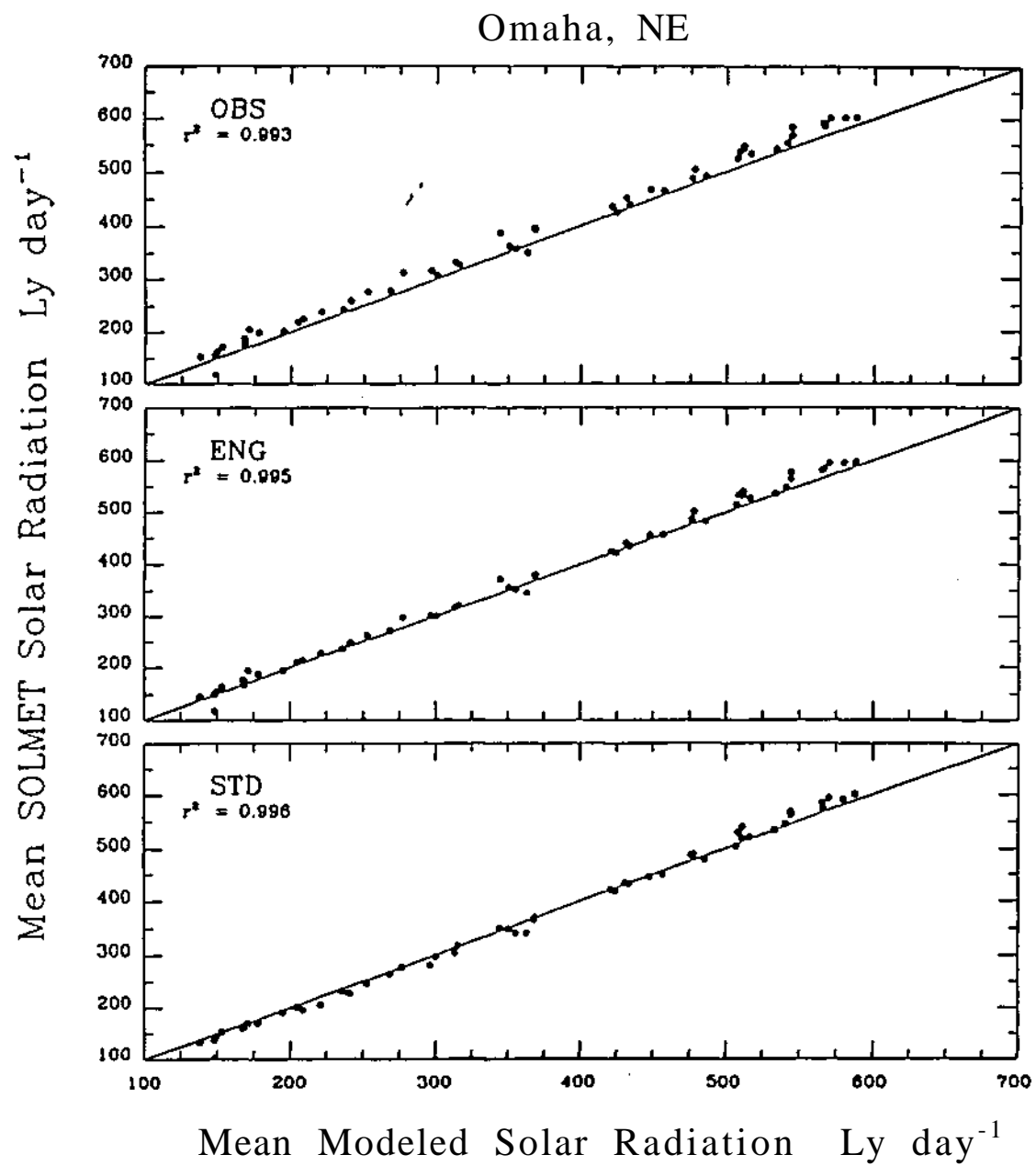


Fig. 3.13. Scatter diagram comparing the climatological weekly averages of the modeled output versus the SOLMET data sets for Omaha.

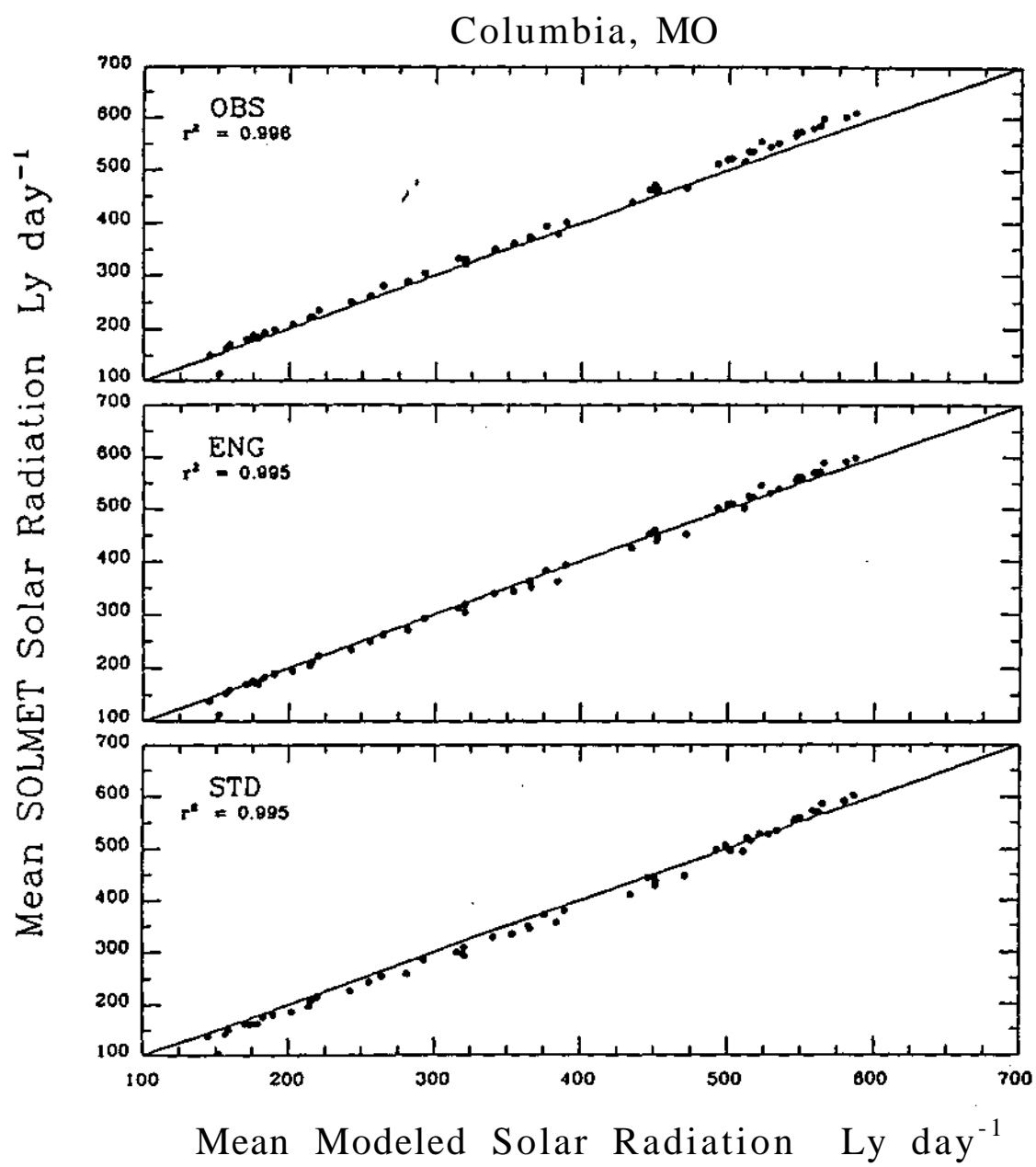


Fig. 3.14. Scatter diagram comparing the climatological weekly averages of the modeled output versus the SOLMET data sets for Columbia.

if available; if not, on the sky cover, 3) the minutes of sunshine where available, and 4) a yes-no precipitation indicator (NCC, 1979). It is important to note that the cloudiness was accounted for only in an average sense. Cloud types, heights, and amounts of various reported layers were ignored. The estimates of variability resulting from the regressions, expressed as the ratio of standard error of estimate to mean value, ranged from 10 to 30% for hourly values, 5 to 18% for daily values, less than 7% for monthly values, and 1 to 4% for annual estimates. These percent errors for the 4 SOLMET stations in/near the Midwest and for Washington, DC (which was used for the extension to Indianapolis) are shown in Table 3.6.

Table 3.6. Percent error of daily, monthly, and annual totals computed from fitted SOLMET hourly SR values. Mean daily totals are in $\text{KJ m}^{-2} \text{ day}^{-1}$.					
Station	Percent Error			Mean Daily Total	No. of Years
	Daily	Monthly	Annual		
Madison	13.7	5.1	3.0	13243	21
Omaha	12.3	4.1	1.8	14767	19
Columbia	11.1	4.0	1.9	16646	24
Nashville	12.2	5.9	4.1	13914	24
Washington, DC	12.8	4.0	2.8	13361	24

The extension of the regression estimates to the additional derived SR data stations was done in the following matter. The contiguous United States was divided into 25 climatologically similar regions such that each region was represented by one of the rehabilitated SOLMET data stations. New York City (Central Park) was not used since this site was thought to be representative of only a special central urban area. A total of 222 additional stations were selected based on the completeness of their meteorological records and the uniform distribution across the United States. The regression equations derived for the rehabilitated SOLMET data stations were then used to generate hourly SR values for these additional stations in each of the 25 regions.

The above mentioned regression equations for the SOLMET station Washington, DC were used to generate SR data for Indianapolis, Indiana (IND), one of the 222 extended stations. These Indianapolis data were here compared with the daily totals generated by the SR model described in Chapter II. The results are summarized in Table 3.7 and presented in Fig. 3.15. The modeled SR values differ only slightly more from the regression-extended SOLMET data for Indianapolis than for the 4 SOLMET station comparisons discussed in Section IIIB. The mean absolute error is 11.5%; although the rms error is nearly 15%, this is only about 2% higher than the daily total error at Washington, DC shown in Table 3.6. Again there is evidence that the model over predicts in winter compared to summer. The fitted regression results of SOLMET on modeled at Indianapolis are: slope of 0.98, y-intercept of 0.96, and r^2 of 0.96. These values are comparable to those listed in Table 3.5 for the 4 "original" SOLMET stations in the Midwest. According to the regression line shown in Fig. 3.15, it appears the model consistently overestimated the regression-extended SOLMET SR values by an average of $1 \text{ MJ m}^{-2} \text{ day}^{-1}$.

B&K also published the climatological weekly means for Indianapolis that were used in their study. These data were here compared with the model results and are shown in Fig. 3.16a. This shows that the modeled output and the data used by B&K are in good agreement. Subsequently, the climatological weekly means of the regression-estimated SOLMET data for Indianapolis were compared with B&K's data and are illustrated in Fig. 3.16b. It is apparent that B&K did not use the regression-extended data for Indianapolis in their study, since Fig. 3.16b shows the SOLMET values to be much smaller than B&K's values. Additionally, Fig 3.16c illustrates approximately the same amount of discrepancy between the modeled SR and the regression-estimated SOLMET SR at Indianapolis. Thus, even though B&K admit that the quality of the data used in their research is questionable, these results seem to indicate that the SOLMET data, particularly the data derived using regression equations, should be viewed with even more caution. This is in agreement with what the Solar Energy Research Institute (1990b) found. They used data collected by the upgraded NOAA (National Oceanographic and Atmospheric Administration) SOLRAD (SOLar RADiation) network from 1977-1980 to evaluate the quality of the SOLMET and the regression-extended SOLMET data bases. They concluded that "significant shortcomings were discovered, particularly in the modeled [regression-extended] data" (Solar Energy Research Institute, 1990b).

E. Summary

The results presented in this chapter suggest that the model described in Chapter II is in very good agreement with the SOLMET data. Although the SOLMET data have

Table 3.7. Mean error, mean absolute error, and root mean square (rms) error of modeled versus regression-extended SOLMET SR for Indianapolis. Units are MJ m⁻² day⁻¹, and percent of SOLMET average.

	Mean Error	%	Mean Abs. Error	%	rms Error	%	SOLMET Average	No. of days
Year	1.33	10.0	1.52	11.5	1.98	15.0	13.24	9128
Jan - Mar	1.37	15.8	1.54	17.8	2.18	25.2	8.66	2273
Apr - Jun	1.49	7.9	1.79	9.5	2.25	11.9	18.83	2275
Jul - Sep	1.53	8.5	1.74	9.6	2.07	11.5	18.01	2298
Oct - Dec	0.93	12.5	1.02	13.7	1.28	17.3	7.43	2282

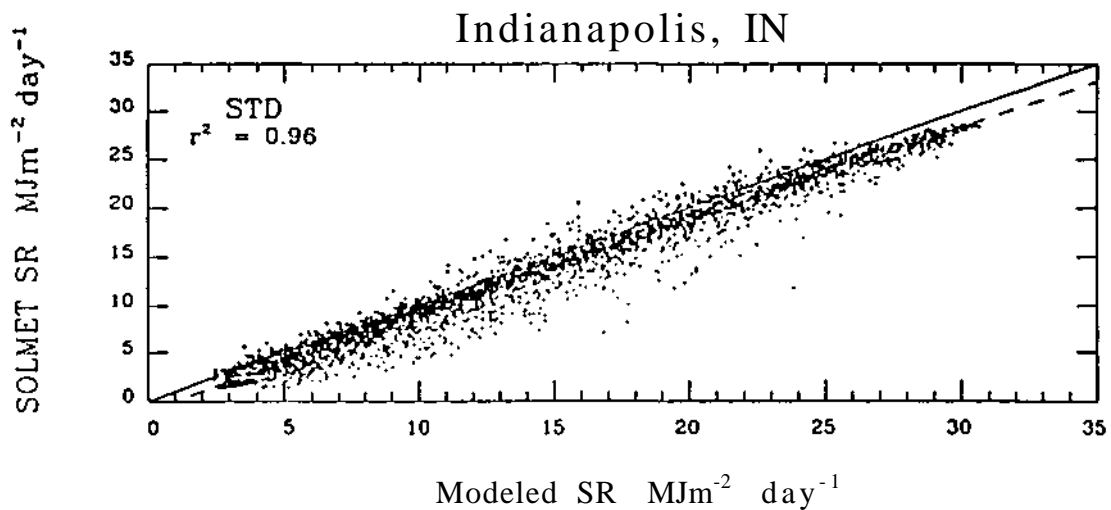


Fig. 3.15. Scatter diagram of 3000 randomly selected pairs of modeled versus SOLMET daily data for Indianapolis. Solid line is 1:1 line; regression line is dashed.

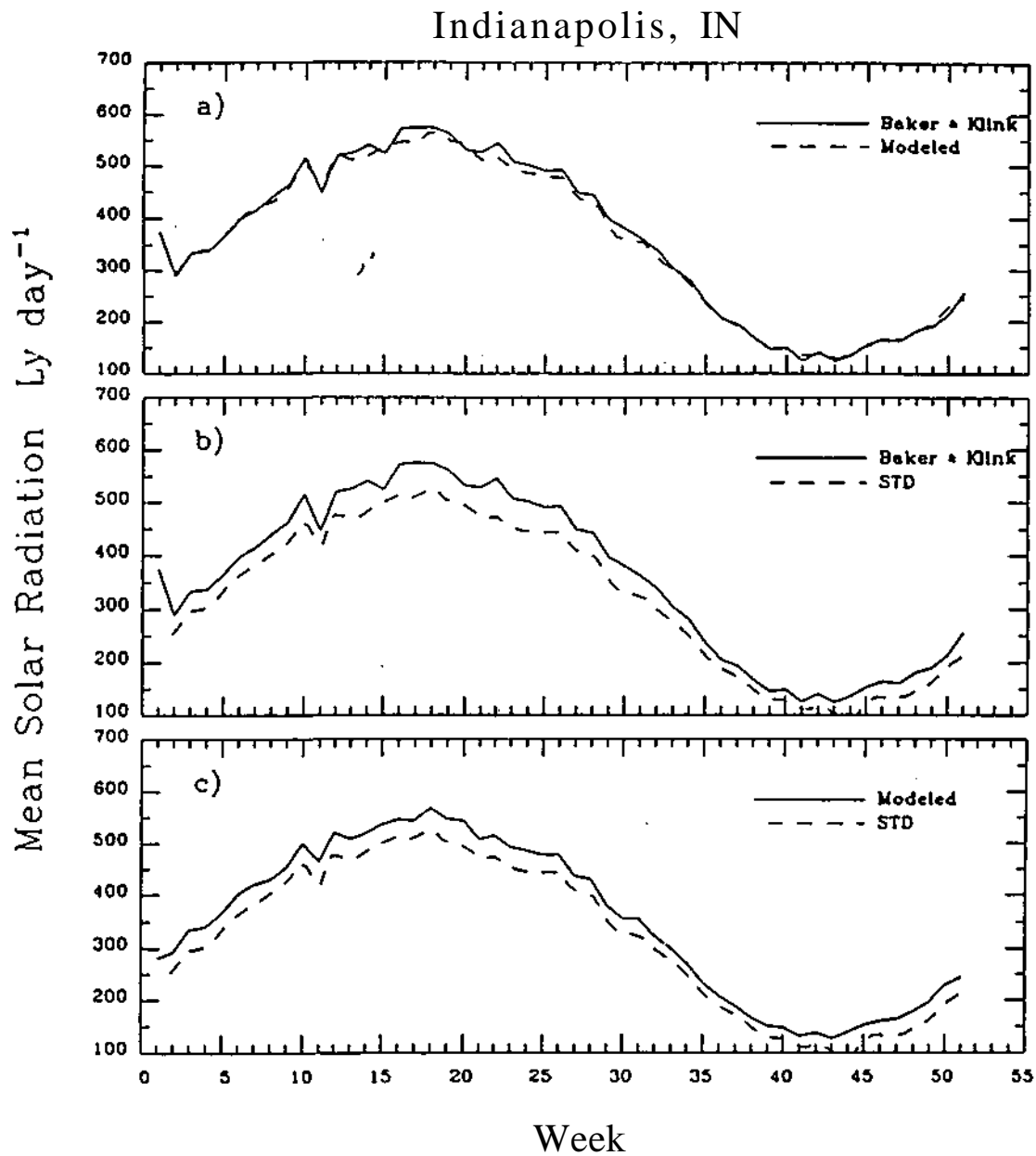


Fig. 3.16. Comparison of the climatological weekly averages of a) Baker & Klink's data (solid) versus the modeled output (dashed); b) Baker & Klink's data (solid) versus the SOLMET data (dashed); and c) modeled output (solid) versus the SOLMET data (dashed) for Indianapolis.

traditionally been questioned, since they are rehabilitated values, they have been used extensively during the last two decades in SR research of both spatial and temporal variability in the United States. However, the semi-physical SR model used in this research has been shown to be valid and adequate in producing daily SR values at stations where standard meteorological data (surface hourly observations) are available. Thus, with this model, there exists the potential to create daily SR values (even hourly values if needed) for as dense a network as is the network of surface hourly observations, and for as long a time period as the surface observations have been taken. The SOLMET data are useful since they are complete and available for stations which are widely separated in the United States. The model-generated SR data offer two advantages: 1) the ability to detect smaller scale variability throughout an increased-density network; and 2) the possibility of including (20) more years of data in order to examine the history or trends of SR. The following chapter capitalizes on these advantages to investigate some aspects of the spatial and temporal variability of solar radiation in the Midwest. First, detailed monthly mean spatial patterns of SR for the Midwest are presented. The 40-year time series of individual monthly mean SR values for 7 highly reliable stations are then analyzed in some detail. Similar time series for the remaining stations are also used to establish the spatial coherency of the overall secular SR trend for the region.

CHAPTER IV

ASPECTS OF THE SPATIAL AND TEMPORAL VARIABILITY OF SOLAR RADIATION IN THE MIDWEST

Chapter II described the SR model used to create a 40 year SR database of daily totals for 53 stations in the Midwest. In general, the time period treated was 1948-1987. However, for some stations, the necessary surface observational data were available from 1945, and their SR data sets thus included 3 more years. Conversely, a few stations, such as Chicago O'Hare, did not start collecting the needed surface data until several years after 1948 (for example, 1958 at O'Hare). The latest starting year of the 53 Midwest stations used here was for Kansas City International Airport, which started in 1972. Additionally, some stations had data interruptions lasting anywhere from 1 to 20 years during the 40 year period. Summaries of the stations used and their SR data bases generated can be found in Appendices A and B. Appendix B gives an indication of the quality of the data for each station, indicating the number of days in the 40-year period that were missing and the number of days for which cloud height was estimated using Table 2.3. The SR model was validated using 4 years of measurements at 3 stations, as shown in Chapter II, and was further tested in Chapter III using rehabilitated and unrehabilitated SOLMET SR data, as well as regression-extended SOLMET data.

This chapter presents some preliminary analyses of the above SR data base. The spatial patterns of mean monthly SR over the Midwest are shown and discussed; time series analyses for each station, including the statistical significance and spatial coherency of the trends identified, are also reported and discussed.

A. Spatial Variability

Calendar monthly means were calculated for each of the 53 stations for its period-of-record. Analyses of the resulting spatial patterns are presented in Figs. 4.1-4.3.

The most basic feature of these SR fields is a northward decrease in SR, as one would expect, with the strongest gradient in October and weakest in March. In fall, the increased frequency of cyclones in the Great Lakes area acts to increase cloudiness there, while the southern portion of the region generally remains cloud-free under the influence of high pressure (Parker *et al*, 1989). Thus, the result is a large gradient in mean cloudiness and SR (e.g., the October mean transmission after cloud attenuation, T_c , is 63.5% for Sault Ste Marie and 81.3% for Memphis). In spring, however, somewhat the opposite is true. The frequency of cyclones is higher in the southern part of the region

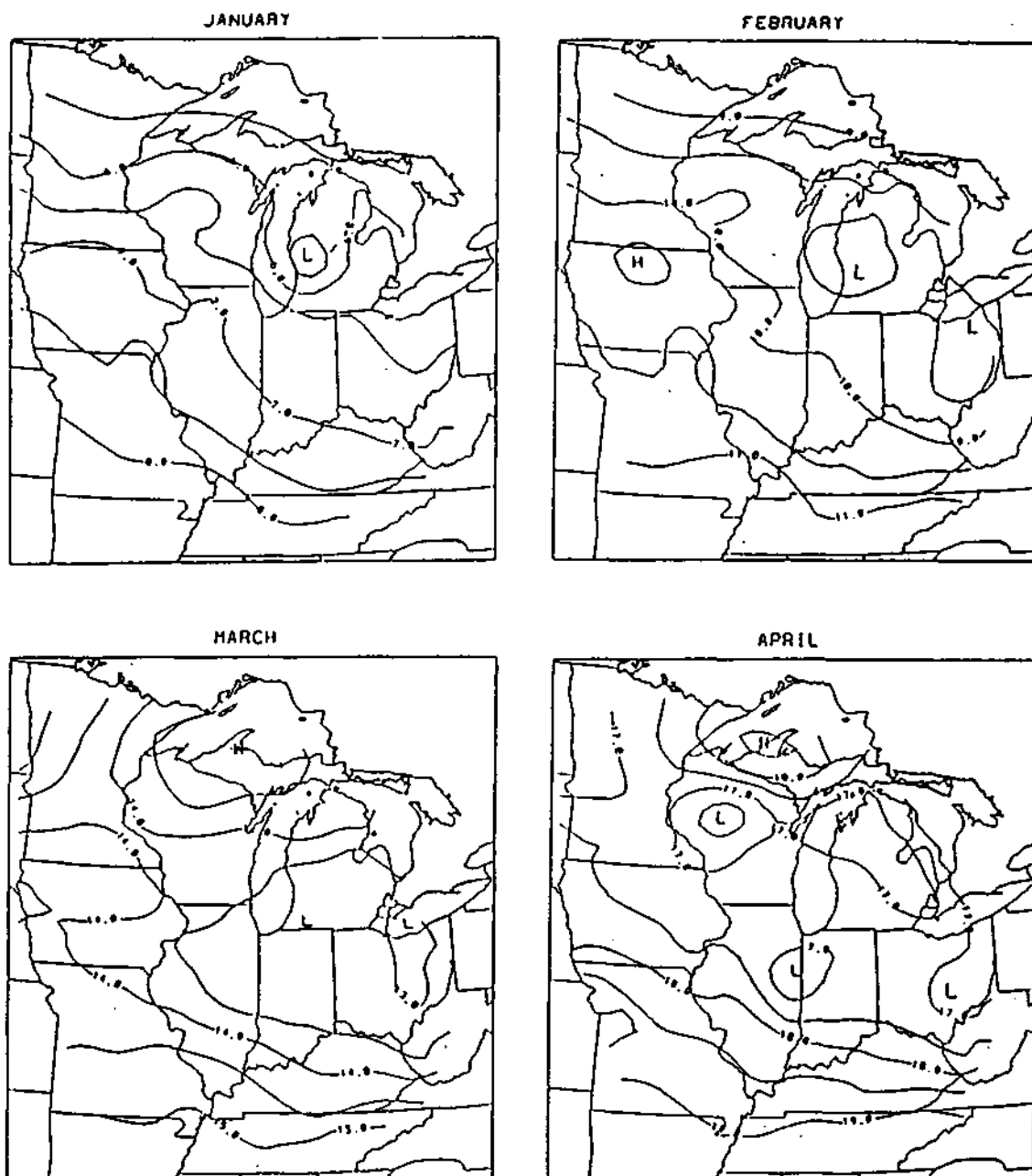


Fig. 4.1. Spatial variations in mean daily totals of SR for January, February, March, and April over the midwest region. Contour interval is 0.5 MJ m⁻² day⁻¹.

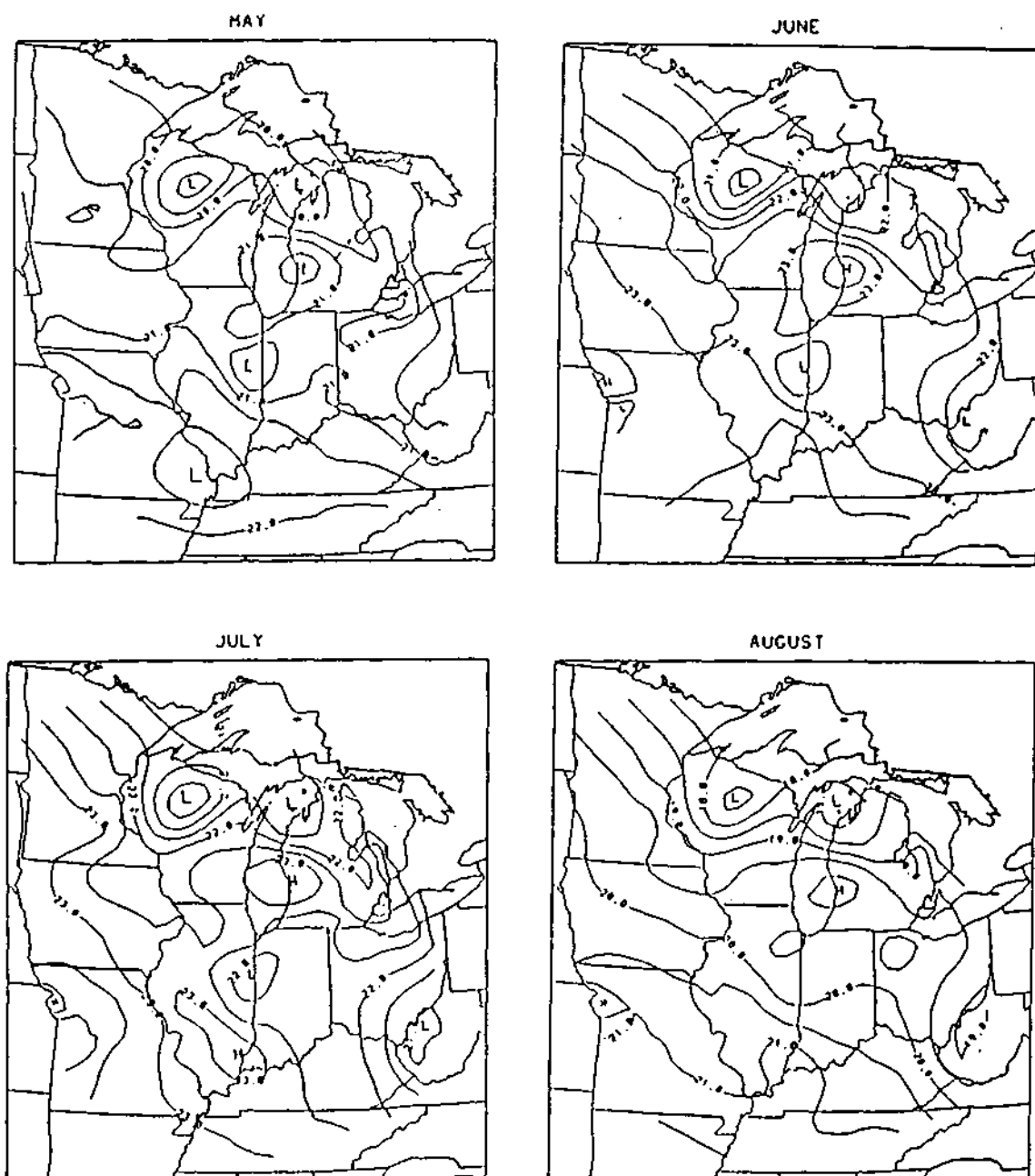


Fig. 4.2. As in Fig. 4.1, but for May, June, July, and August.

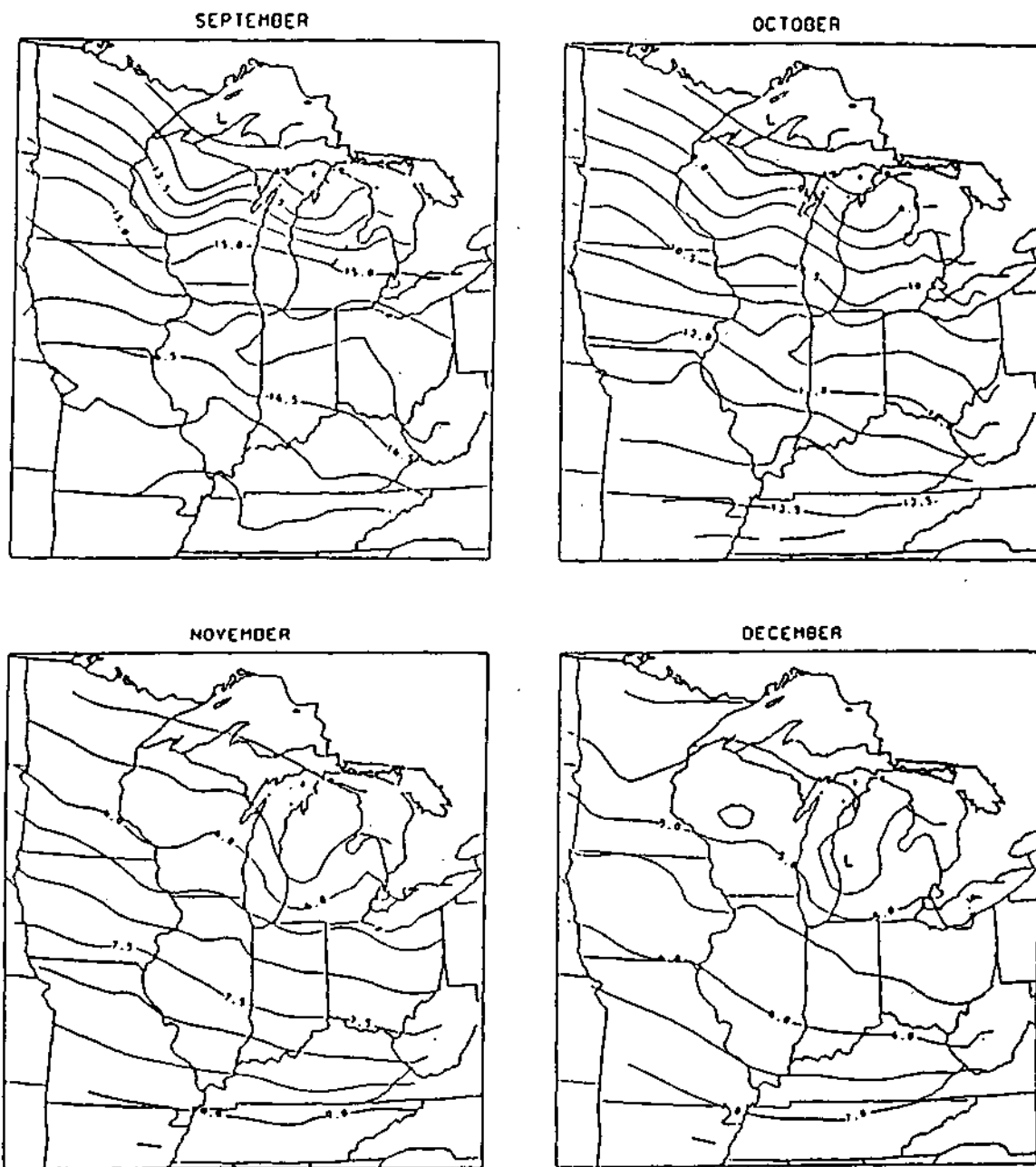


Fig. 4.3. As in Fig. 4.1, but for September, October, November, and December.

than to the north, which is generally under the influence of Arctic high pressure (Parker *et al.*, 1989). The mean T_c for March is 80.7% for International Falls and 66.7% for Indianapolis. Therefore, one might expect to find the weakest SR gradient in this season, as was found here.

For most months, however, the SR isopleths cross the latitude lines at a slight angle rather than running parallel to them. This northwest to southeast orientation might be due to a number of factors, as was suggested by Baker and Klink (1975): 1) the increasing altitude towards the west, which results in a shorter air mass path length for the sun's rays; 2) population and industrialization; and 3) atmospheric humidity. The latter two factors increase in a generally northwest to southeast direction and presumably act to decrease radiation in that direction. The above isopleth pattern is also apparent in Reitan's (1960) precipitable water fields for the United States, particularly for the summer months, and in the map of July average dew points for the United States in Volume 11 (Climates of North America) of the World Survey of Climatology (Bryson and Hare, 1974, Fig. 3.10). That Volume additionally reveals 1) a similar orientation of SR isopleths on the Canadian side of the Great Lakes (Fig. 2.23), and 2) a westward increase in the average annual evaporation from Midwestern lakes (Fig. 3.30). Since drier air would enhance evaporation, the latter implies less atmospheric humidity from the southeast to the northwest in the Midwest as well.

The northwest to southeast orientation of SR isopleths is also seen in the monthly maps of mean daily SR in Bennett (1965) and in the SR percentile maps for the Midwest of Baker and Klink (1975). However, neither of those studies 1) used data from as dense a network as the 53 stations employed here; 2) used as many years of data as was studied in this research; and 3) produced an analysis with the spatial detail of Figs. 4.1-4.3. For comparative purposes, the United States patterns obtained by Bennett (1965) and Baker and Klink (1975) are reproduced in Appendices C and D, respectively. The contours over the Midwest region in Bennett's Figures (Appendix C) have no detail; generally one, or at most two, contours pass through the region. While the Figures of Baker and Klink (Appendix D) have detailed contours, they may be somewhat uncertain since the data were from only 10 stations in the region, whereas 53 were used here.

As can be seen from Figs. 4.1-4.3, the SR pattern for the Midwest is less smooth and more mesoscale in character from the late spring into the summer months. One prominent feature evident during these months (April -August) is an area of low SR over northern Wisconsin extending into the Upper Peninsula of Michigan and over northern Lake Michigan into northern Lower Michigan. The stations in this area are Eau Claire and Green Bay (Wisconsin) and Gwinn and Traverse City (Michigan). The quality of the data at Green Bay is believed to be very good (see Appendix B). Although the data

quality for the other three stations is less certain, the pattern is believed to be correct. Gwinn's data set contains only about 30% of the number of days included in the Green Bay set, and over 50% of Gwinn's surface observations did not include cloud heights and thus were estimated using ceiling heights as shown in Table 2.3. Data from Eau Claire and Traverse City are both complete for the 40 years, with very few missing days, but cloud heights at every layer for their entire period-of-analysis were unknown and therefore also estimated using the method shown in Table 2.3. Thus, this area of low SR, particularly over Eau Claire, Wisconsin where the "Low" is centered, was first believed to be unrealistic. However, total sky cover statistics for the period-of-analysis at Eau Claire show a lower percentage of clear sky hours by 2 to 5% than at either Minneapolis or Green Bay. Eau Claire also shows a higher percentage of overcast hours by as much as 5% compared to these other 2 stations. Additionally, this area of low SR over northern Wisconsin in spring and summer is evident in Figs. C.5-C.7 (from Bennett, 1965) and Fig. D.2 (from Baker and Klink, 1975), although indicated with fewer contours.

Some additional mesoscale features also occur in the spring and summer months. For example, Rantoul (Illinois) and Charleston (West Virginia) have consistently low values during these months; Kansas City's Downtown Airport (lower SR) and more-removed International Airport (higher SR) differ in their June and July means; and lows or highs appear over Paducah (Kentucky), depending on the month (May versus June and July).

A possible explanation for the discrepancy between the two Kansas City airports might be an urban/industrialization effect; the International Airport is located just outside the metropolitan area to the north and would thus be less affected by the (industrial and population) pollution to which the downtown airport would be subjected.

The quality of the Rantoul and Paducah data sets may not be as good as those for other stations. Surface hourly observations started in 1949 at Rantoul, but ended in 1970. Thus, Rantoul's period-of-analysis is about 45% shorter than those of most other stations. Additionally, 30% of Rantoul's surface observations did not include cloud heights, which were then estimated using the method of Table 2.3. Similarly, Paducah started taking surface observations in 1949, but operations ceased between 1965 and 1985. Thus, their data set also includes only about half the number of days as those for the apparently most reliable stations. Approximately 75% of Paducah's data also did not include cloud heights, which had to be estimated using ceiling heights (Table 2.3). Therefore, these station's means may be viewed with some caution due to the estimation of cloud heights; yet the mesoscale features resulting from these data disappear in the cooler months of September-March. Additionally, when comparing year to year values for any month (time series discussed in detail in Section B of this chapter and shown in

Appendix E for all stations) for a station for which cloud heights have been estimated with a station that had cloud heights given, the data do not seem out of line. For example, the yearly values for July at Rantoul appear to be quite consistent with the July yearly values for Indianapolis and for Peoria. Thus, it appears as if estimating cloud heights did not introduce any significant/noticeable biases into the data, and consequently confirms the mesoscale features.

All months show the thermal effect of the Great Lakes. In summer, the predominantly southwesterly winds (Eichenlaub *et al.*, 1990) blowing across the relatively cool water will suppress convection and cloud formation over and along the eastern shore of Lake Michigan, for example, as is evident by the SR maxima over the Muskegan (Michigan) vicinity during these months. This finding is consistent with summertime satellite imagery for this area (e.g., Scott and Grosh, 1979; Changnon, 1980).

During September/October through March/April, the Great Lakes are warmer than the surrounding air or land (Eichenlaub *et al.*, 1990). The predominantly westerly winds over the Lakes carry warm, moist air across to the eastern side, causing clouds to form there, as shown by the progressive appearance of low SR over Lower Michigan from October through January and February. A further characteristic of the fall SR pattern is the return to the smooth northwest-southeast oriented isopleth pattern in September from the primarily mesoscale character of July and August. This smooth pattern continues into October, November, and December with the large gradient of October continuously weakening into November and December.

B. Secular Variation

Time series of mid-season (January, April, July, and October) individual monthly mean SR values for 1948-1987 were examined in detail for 7 selected stations and are displayed in Figs. 4.4-4.7. The stations chosen were International Falls (Minnesota), Sault Ste Marie (Michigan), Sioux City (Iowa), Madison (Wisconsin), Cleveland (Ohio), Evansville (Indiana), and Springfield (Missouri). They were selected because of the high quality of their SR data sets (i.e., 40 years complete and non-estimated cloud heights), and their relatively even spatial distribution in the region (cf. Fig 2.1).

A linear regression line was fitted to each time series plot as shown in Figs. 4.4-4.7. Additionally, the slopes of the regression lines were subjected to the Students *t* test to determine their statistical significance.

The time series (Figs. 4.4-4.7) show considerable interannual variability, as is expected, with southern stations often displaying more variability than their northern

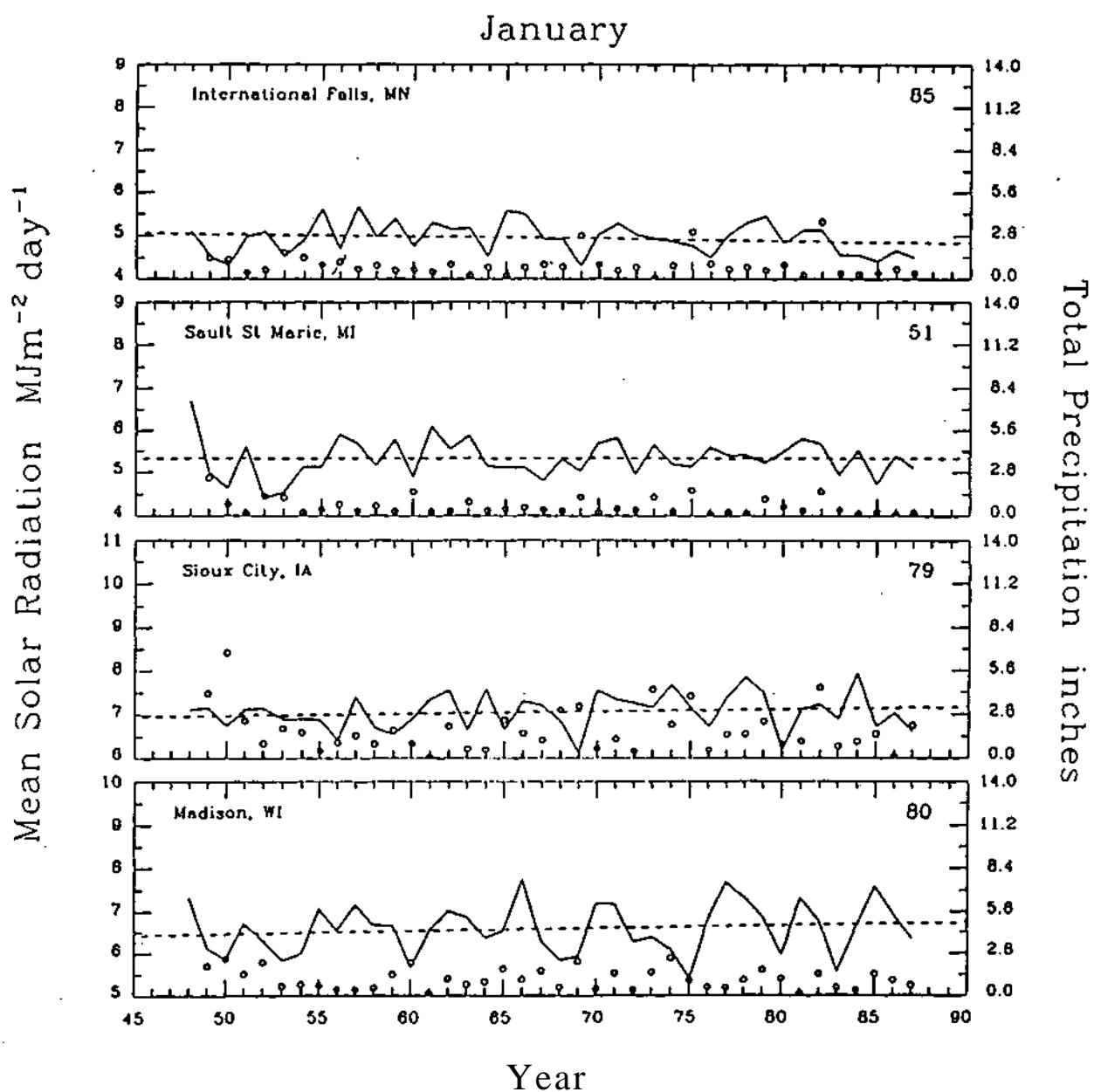


Fig. 4.4a. Solid line is time series of monthly mean SR values for January at International Falls, Sault Ste Marie, Sioux City, and Madison. Dashed line is regression line; open circles are total precipitation. The number in the upper right-hand corner of each graph is the level of statistical significance of the SR time series.

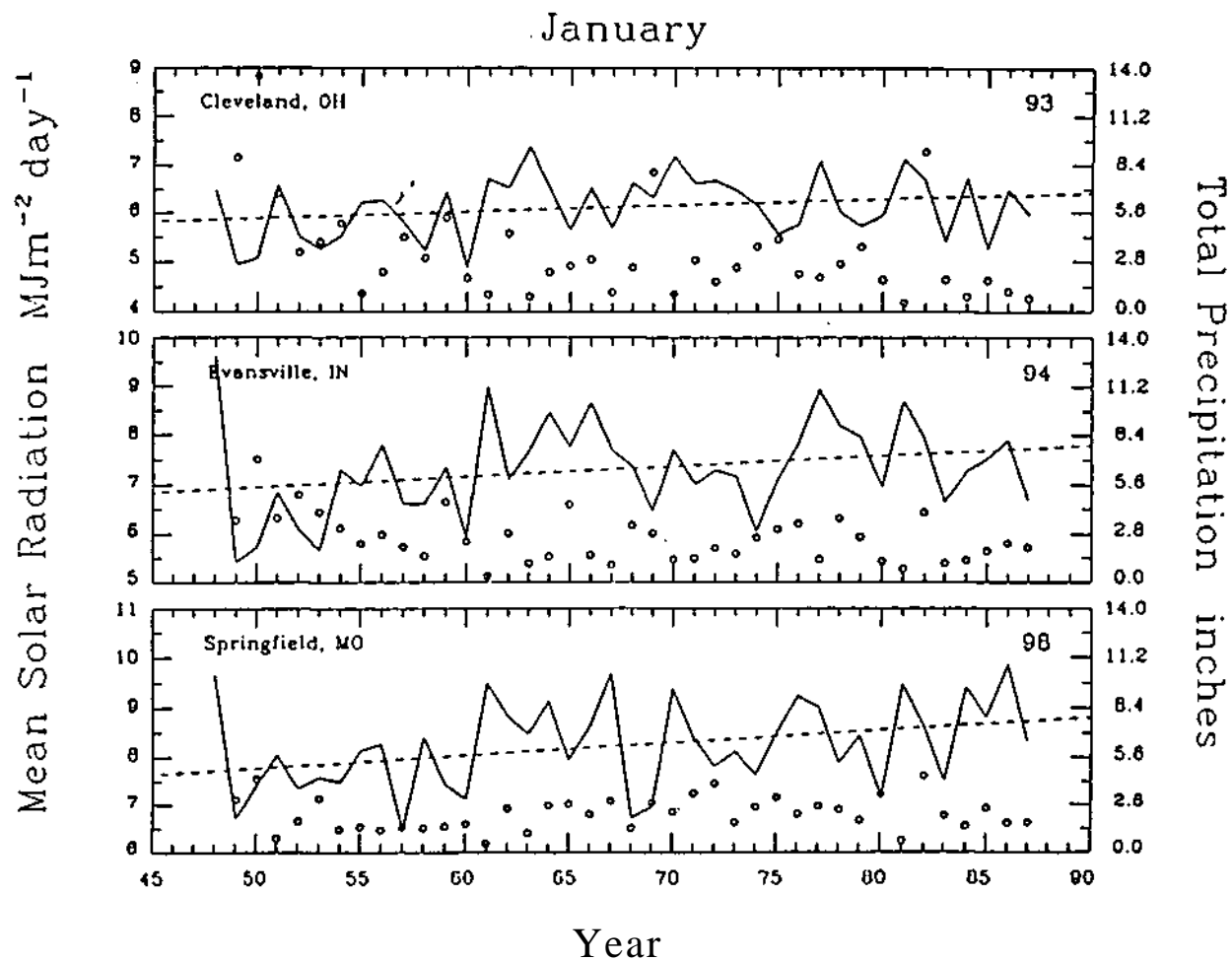


Fig. 4.4b. Solid line is time series of monthly mean SR values for January at Cleveland, Evansville, and Springfield. Dashed line is regression line; open circles are total precipitation. The number in the upper right-hand corner of each graph is the level of statistical significance of the SR time series.

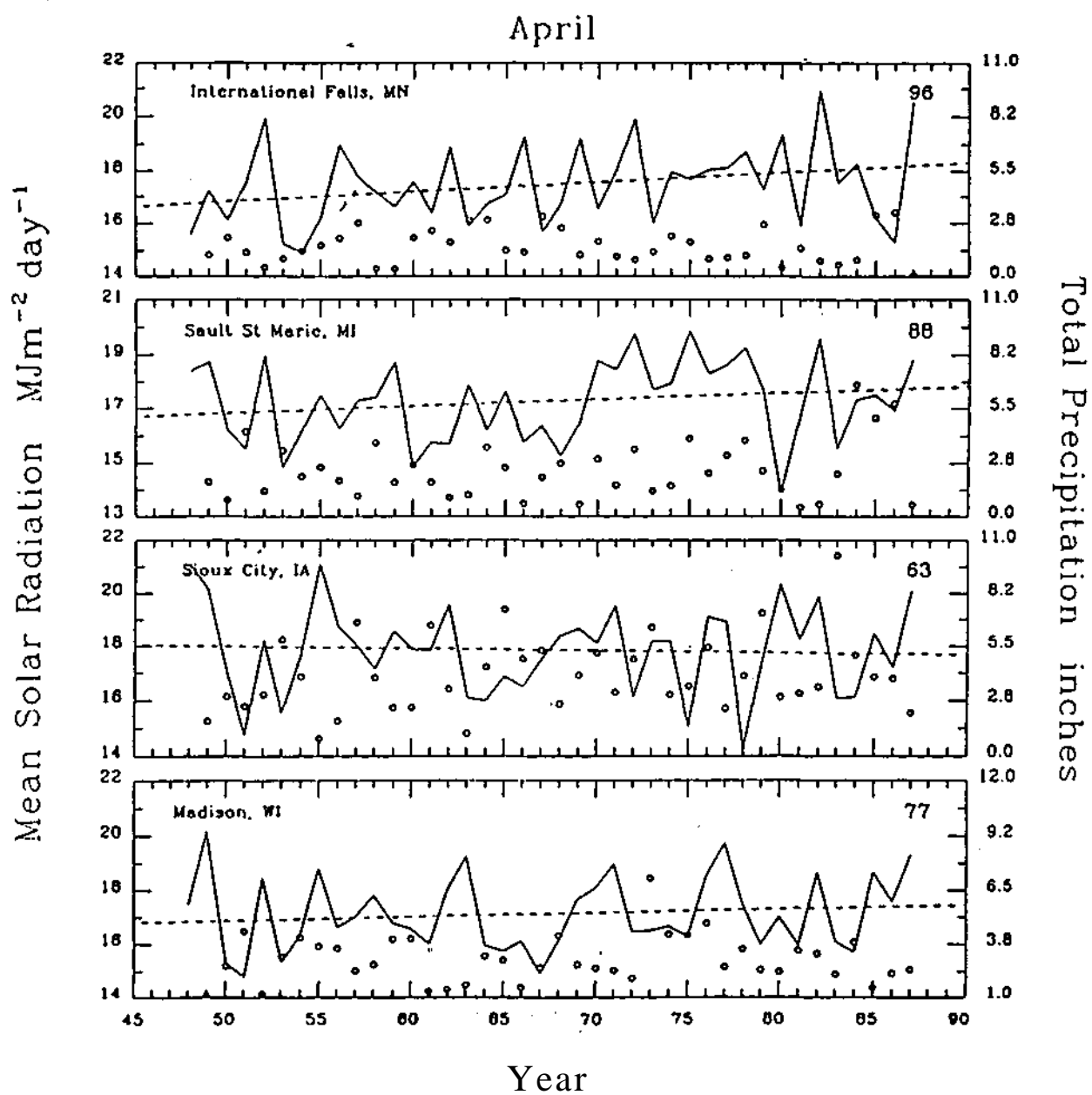


Fig. 4.5a. As in Fig. 4.4a, but for April.

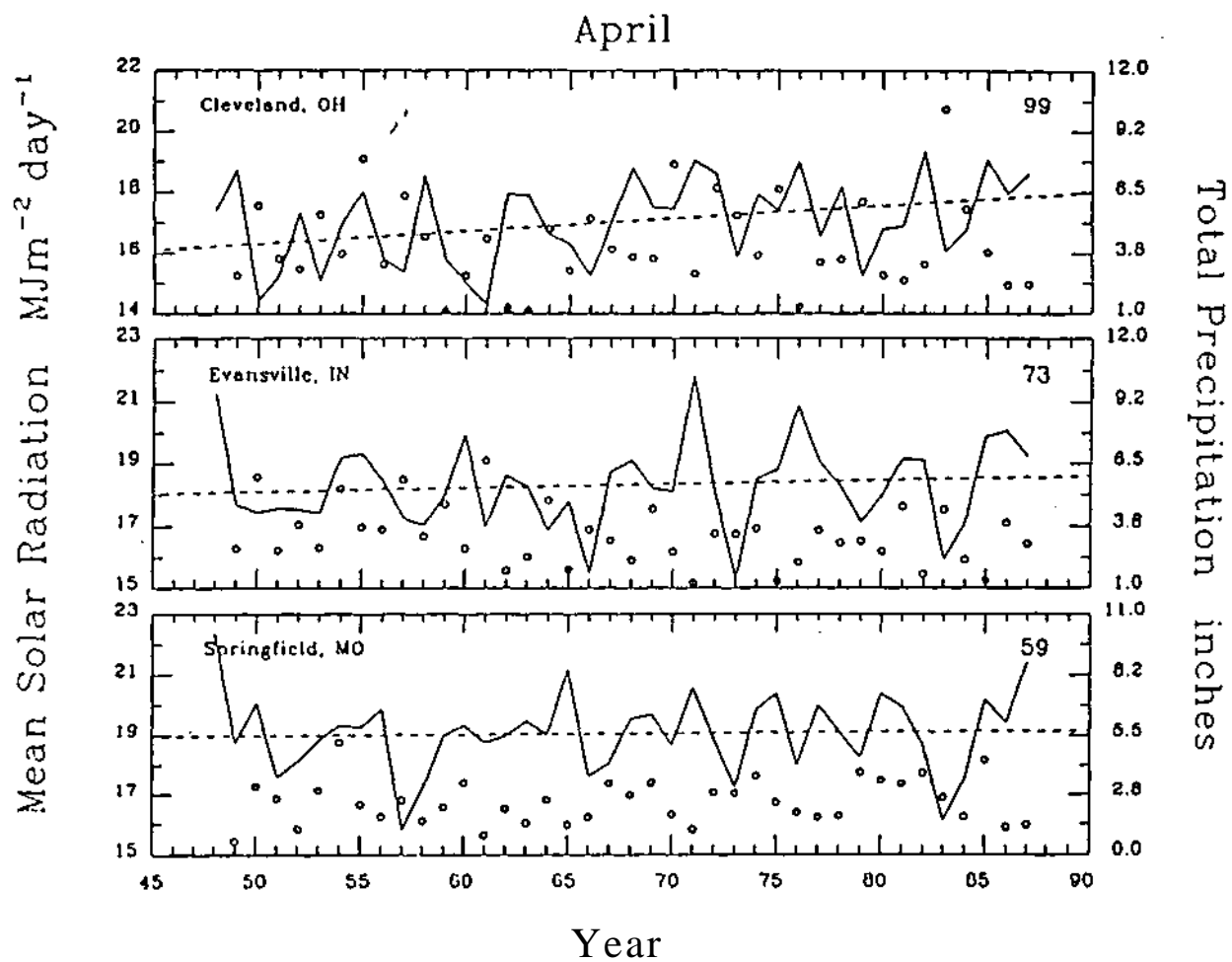


Fig. 4.5b. As in Fig. 4.4b, but for April.

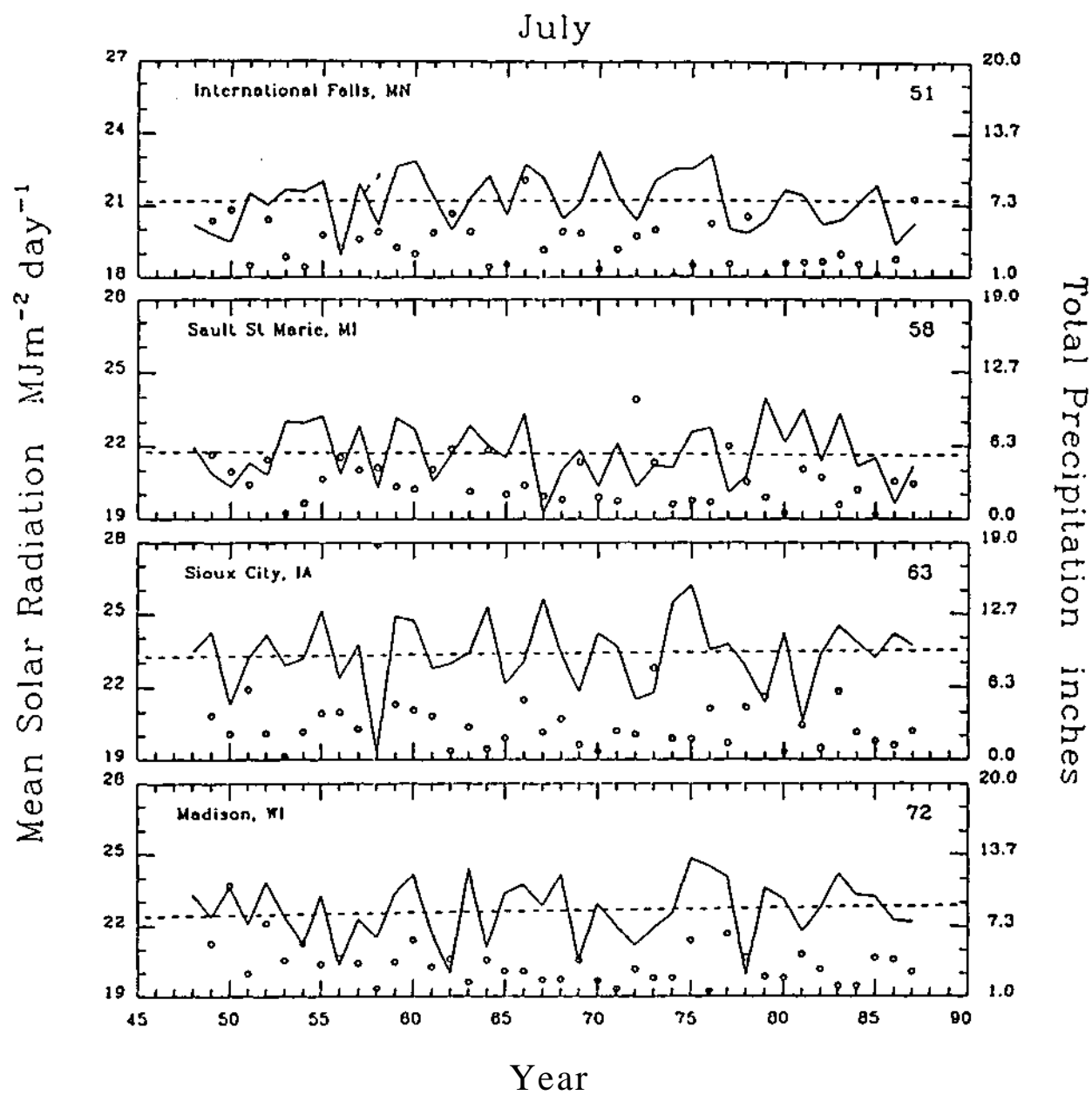


Fig. 4.6a. As in Fig. 4.4a, but for July.

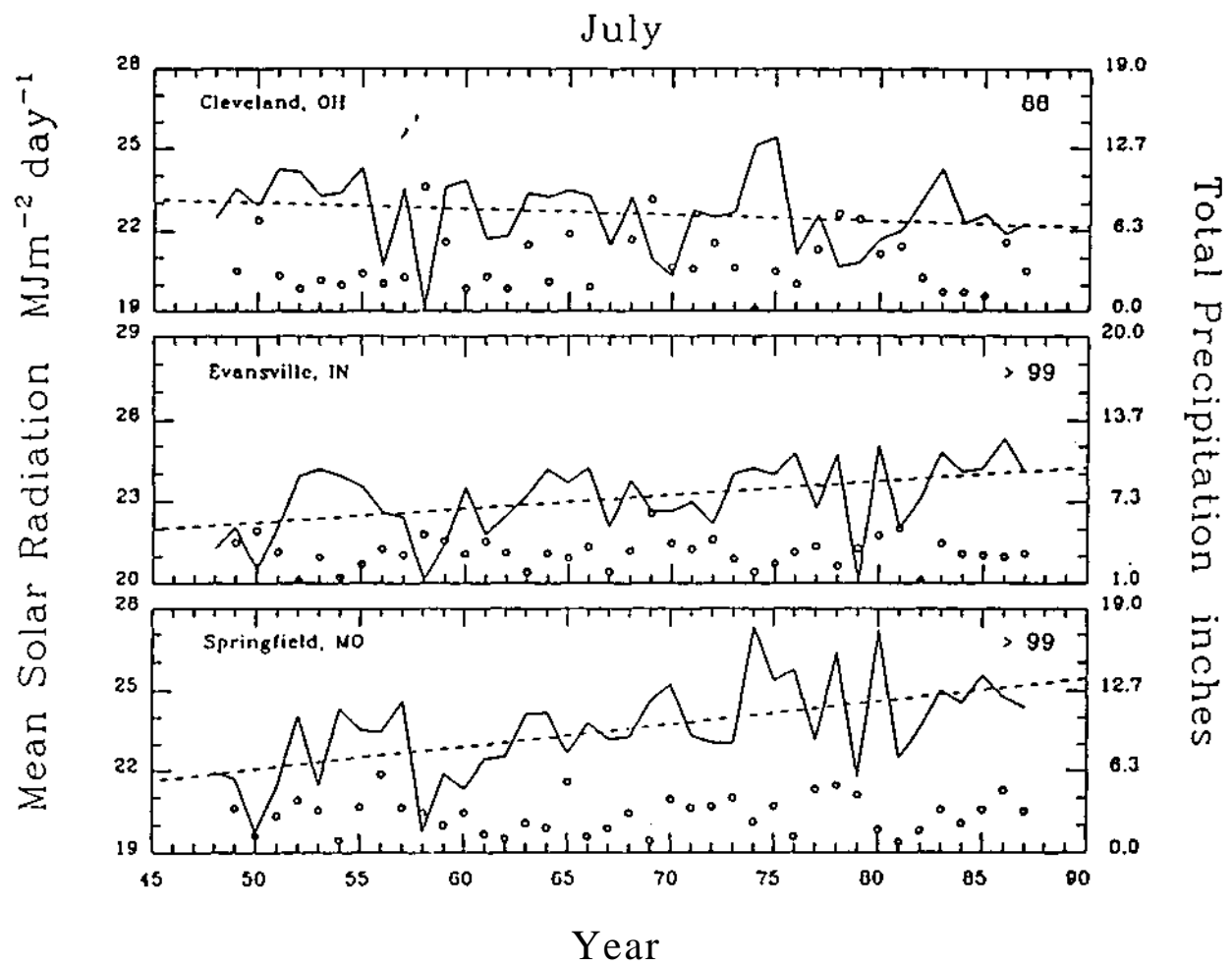


Fig. 4.6b. As in Fig. 4.4b, but for July.

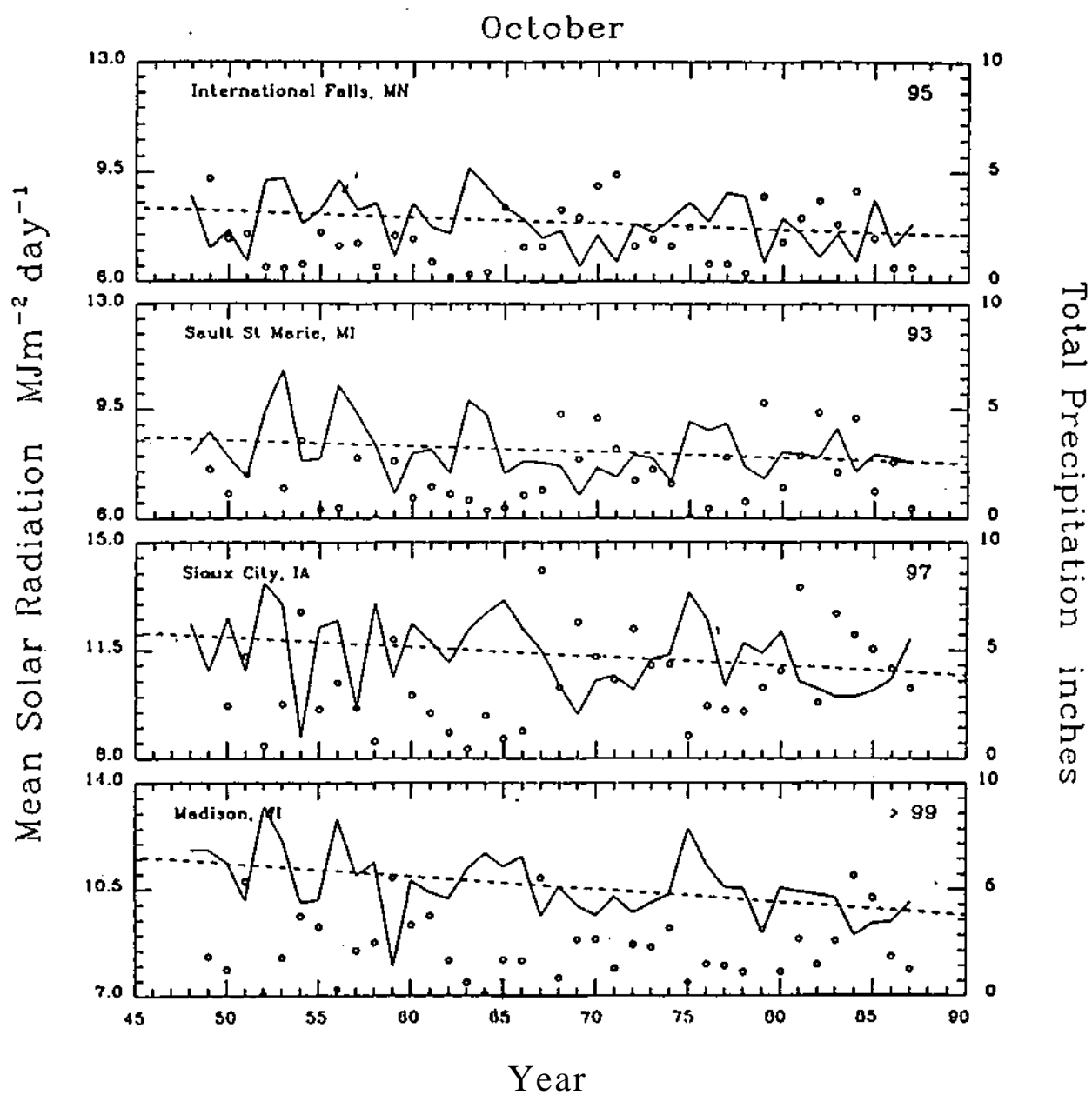


Fig. 4.7a. As in Fig. 4.4a, but for October.

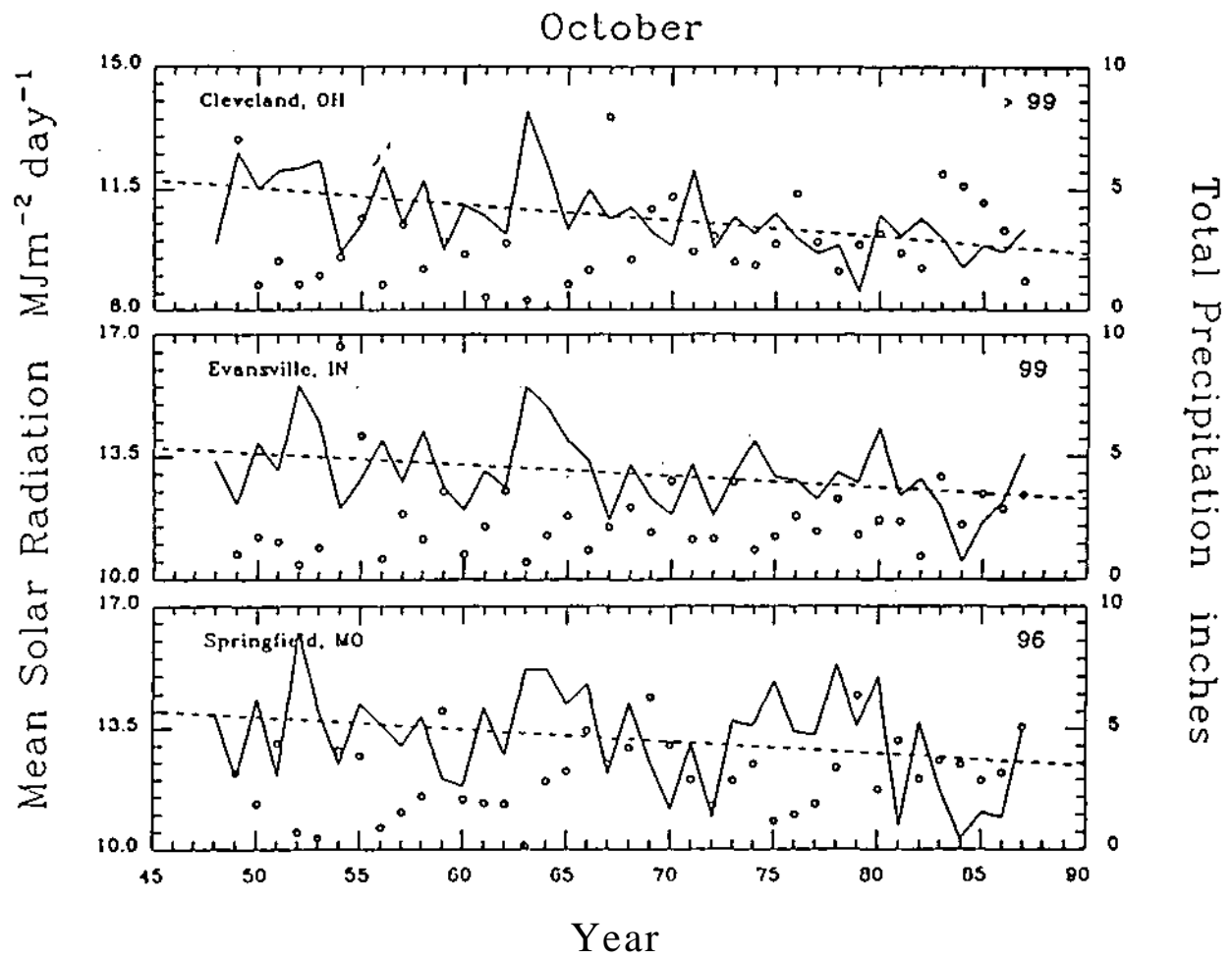


Fig. 4.7b. As in Fig. 4.4b, but for October.

counterparts. However, all stations indicate considerable interannual variability in the spring (April) and fall (October) when day-lengths are rapidly changing, and presumably there is greater interannual variability in storm systems and cloud cover. In general, the interannual variability shows station-to-station consistency. For example, Fig. 4.4b shows that SR at Cleveland, Evansville, and Springfield all have January local minima in 1960 and then increase in 1961. Similarly, these three stations all show minima in the early mid-1970s, maxima in the late mid-1970s, and minima in the late 1970s to around 1980. International Falls, Sault Ste Marie, Sioux City, and Madison also display consistent trends for these years in January, as well as other months and years (e.g., local minima in October 1959 followed by one or two year increases, then moderate decreases (1962), and then strong increases in 1963-1964).

In examining the long-term trends and their significance for each of the 4 months at these 7 stations (Table 4.1 and Figs. 4.4-4.7), some interesting results emerge. The most obvious is that all stations show a downward trend for October for the 40 year period; at 5 of the 7 stations, the trend exceeds $30 \text{ KJ m}^{-2} \text{ year}^{-1}$, which is highly significant (>95% confidence level). The two stations with the smallest and least significant October decreases are the farthest north stations: International Falls and Sault Ste Marie. Note, however, that these northern stations were additionally significant at the 90-95% confidence level. The July results (Fig. 4.6) largely show increases over the 40 years, with the exception of Sault Ste Marie and Cleveland which show small and somewhat insignificant decreases and International Falls which shows virtually no change. The largest trend for all stations and months presented here is the $84.6 \text{ KJ m}^{-2} \text{ year}^{-1}$ increase at Springfield for July, which is highly significant, as is the nearly $50 \text{ KJ m}^{-2} \text{ year}^{-1}$ increase for July at Evansville.

The April and January time series (Figs. 4.5 and 4.4, respectively) also show mostly positive, but less significant, tendencies at these 7 stations. International Falls and Cleveland show highly significant increases in April means, around $40 \text{ KJ m}^{-2} \text{ year}^{-1}$, while Sioux City shows an insignificant negative trend for that month. Sault Ste Marie shows virtually no trend for January, while International Falls has experienced a slight negative trend.

In order to set the trends for the 7 chosen reliable stations in the wider spatial context of the region, trends for the other 46 Midwest stations were additionally found for the mid-season months and were tested for statistical significance. These results for all stations are given in Appendix E. Figure 4.8 portrays the spatial coherency of these trends for the Midwest.

Figure 4.8 shows a strikingly coherent temporal trend pattern for October. That is, the October trends for all stations are negative, and most are highly or extremely (>99%) significant. The October trends significant at the >99% level are generally located at stations in the central part of the region. Thus, the spatial coherency of these trends is extremely high, and confirms the results identified from the 7 chosen reliable stations discussed previously. Only 16 October trends are not significant at the >95% level. Half (or 8) of these stations have shorter than 40 year periods-of-analysis, ranging from 14 years at Gwinn (Michigan) to 33 years at St. Cloud (Minnesota). These shorter periods result in smaller degrees of freedom which, in turn, are reflected in the significance value (i.e., the smaller the degrees of freedom, the larger the *t* value must

Table 4.1. Slopes of regressions multiplied by 1000 for SR (i.e., KJ m ⁻² year ⁻¹) and 100 for precipitation (i.e., hundredths of inches year ⁻¹) for the indicated stations and months. Numbers below slopes indicate level of statistical significance of the trend based on the Student's <i>t</i> test. Highly significant trends (>95% confidence level) are in bold.								
Station	January		April		July		October	
	SR	Precip	SR	Precip	SR	Precip	SR	Precip
International Falls	-5.2	-0.25	37.6	-0.14	0.4	-4.50	-18.7	1.55
	85	59	96	54	51	94	95	80
Sault Ste Marie	0.2	1.11	24.7	1.14	-3.3	0.85	-18.8	3.54
	51	78	88	78	84	67	93	95
Sioux City	4.7	-1.25	-7.9	2.80	6.4	-3.82	-30.6	3.66
	79	95	63	91	63	91	97	96
Madison	6.9	-1.18	14.2	0.64	10.7	-6.25	-42.4	0.11
	80	89	77	64	72	99	> 99	52
Cleveland	13.1	-5.24	41.5	-3.71	-22.3	0.27	-46.9	0.46
	93	> 99	99	98	88	57	> 99	58
Evansville	20.9	-10.06	12.2	0.43	49.6	0.02	-32.8	2.99
	94	> 99	73	56	> 99	50	99	88
Springfield	25.6	-1.82	4.4	4.09	84.6	-4.76	-35.5	3.09
	98	81	59	93	> 99	86	96	83

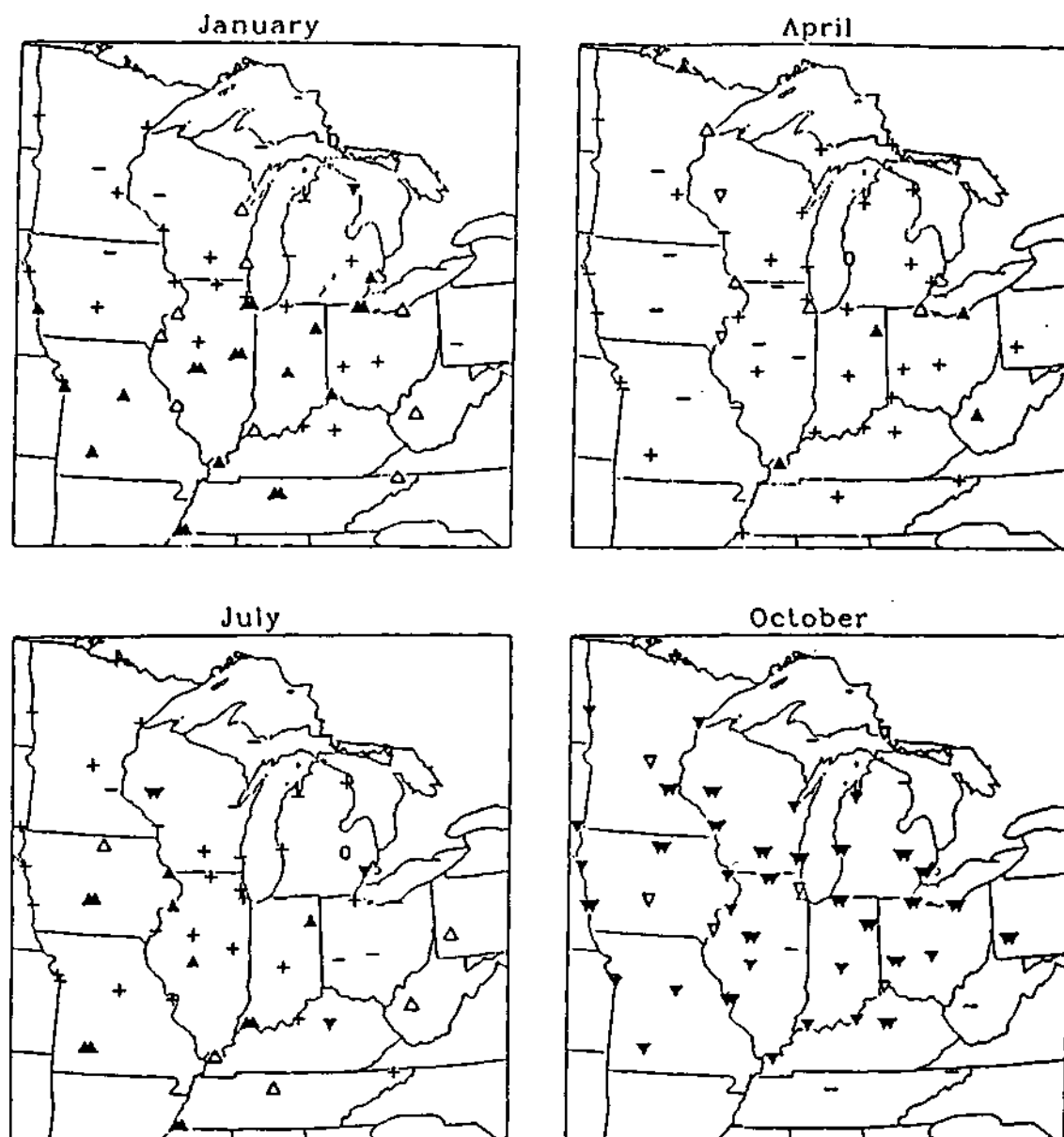


Fig. 4.8. Spatial coherency of SR trends for 1948-1987 for January, April, July, and October months. Relatively insignificant (<90%) positive and negative trends are shown with a + and -, respectively; significant (90-95%) positive and negative trends display a Δ and ▽, respectively; and highly significant (>95%) positive and negative trends are shown as Δ and ▽, respectively. Double solid triangles indicate significance at the >99% confidence level. No trend is signified by a 0.

be in order to be significant). The other 8 stations with <95% significant October trends have anywhere from 39 to 43 years of data for each station. Four of these stations (International Falls, Des Moines, Sault Ste Marie, and Covington/Cincinnati) are significant between the 90-95% level. The other 4 stations with about 40 years of data each are farther south and east, and have trends that are <90% significant.

The January results show a swath of significant (>90%) upward trends in the central Midwest, generally oriented in a south-southwest to north-northeast direction, with more than half of these trends highly significant (>95%). Additionally, six of these trends were found to be >99% significant and are spatially coherent in eastern Illinois and western Tennessee, with the exception of Toledo. This is consistent with the January results for the 7 stations shown in Table 4.1. The highly significant positive trend at Springfield (Missouri) is nearly surrounded by other stations with highly significant trends as well.

The stations with positive trends for April tend to be in the eastern portion of the Midwest, while those with negative trends for that month are largely in the western part of the region. Only a few (11) stations have significant trends, and only 5 of those are highly significant (>95%). There is little spatial coherency in the stations with highly significant trends, except for Fort Wayne and Cleveland which are near Toledo, whose tendency is 90-95% significant. Most April trends, however, are not (>90%) significant.

The July trends show less spatial coherence throughout the region than those for the other mid-season months. About two-thirds of the trends are positive, and not quite half of these trends are significant (>90%) or highly significant (>95%). The negative trends are found mostly around the Great Lakes and in Ohio, with a few exceptions (Alpena, Muskegan, and Toledo show positive trends). Positive trends prevail elsewhere. The most significant ones are located in the central part of the region, but they are interspersed with some insignificant positive and negative trends. These significant positive trends are somewhat coherent in the southwest quadrant of the Midwest, which supports the key result for Springfield (Missouri) previously discussed. Springfield, Evansville, and Memphis show the highest significance (>99%) of the positive trends in this area. Springfield and Memphis are surrounded by positive trends, though not all are highly significant. Evansville is mostly near stations with positive trends as well, except for Covington/Cincinnati and Lexington, which show negative and highly significant negative trends, respectively.

C. Comparison with Precipitation, Cloudiness, and Visibility

Time series of individual monthly precipitation totals for 1949-1987 were additionally examined for the 4 months and 7 stations previously discussed. A linear regression line was fit to the data for each month and station, as was done to find trends in SR, and subsequently, the slopes were tested for statistical significance. These results are also shown in Table 4.1. Figures 4.4-4.7 also have monthly totals of precipitation for indicated mid-season months and years, but do not show the precipitation regression lines.

Most of the precipitation trends for each calendar month and station show results that are physically consistent with the SR trends obtained (Table 4.1). That is, when the trend of SR is increasing (decreasing) during the 40 year period, the tendency is for precipitation to decrease (increase). The exceptions are found generally when the trends in either SR or precipitation or both are small and statistically insignificant (e.g., January at International Falls, and April at Madison, Evansville, and Springfield). The SR trend for July at Evansville is a highly significant positive trend, while the precipitation trend indicates no clear 40 year trend there.

Of the 28 precipitation trend lines produced, only five were found to be highly significant (>95% confidence level). Of these five, two showed corresponding highly significant SR trends (April at Cleveland and October at Sioux City), and two showed corresponding significant (90-95%) SR trends (January at Cleveland and Evansville). An additional 6 precipitation trends were found to be significant at the 90-95% confidence level. However, only the October significant precipitation trend at Sault Ste Marie corresponds to a significant SR trend.

When comparing the SR and precipitation time series in detail, one might expect to find SR maxima and precipitation minima to coincide and vice versa. The October data for Madison show good examples of this negative relation. The years 1951, 1959, 1967, and 1984 had large precipitation during October, while these months are minima in mean SR. Likewise, the Octobers of 1952, 1956, 1964, and 1975 show very little precipitation at Madison, while these months show peaks in SR. However, it is interesting to note that even though 1959 clearly shows the lowest daily SR mean for October, precipitation for that month totaled no more than for 1951, 1967, or 1984. Similarly, precipitation in October 1964 was nearly the same as in 1952, yet the 1964 SR averaged over $1.5 \text{ MJ m}^{-2} \text{ day}^{-1}$ less than the mean for 1952. A further example is that the mean daily October SR totals in 1979 and 1984 are nearly equal, yet 1979 received about 50% the precipitation total of 1984. Most other stations and months (e.g., January and April at Cleveland and January at Evansville) show similar negative relations

between SR and precipitation, but they are generally not as outstanding as the above October results for Madison.

If one considers that insolation is mostly dependent on cloud cover, these examples illustrate that (total) precipitation and (mean) cloudiness (i.e., mean SR) do not perfectly correlate all the time. This is not surprising since precipitation can come from different types of clouds and, of course, not all clouds bear precipitation. That is to say that precipitation amounts vary considerably, depending on the synoptic situation. One may hypothesize that 5 occurrences of convective thunderstorms during a month could produce equal or more precipitation over an area than a mid-latitude cyclone which has stalled out over the same area for a week, or even a mid-latitude cyclone passing over the area every few days during the month. Yet a cyclone periodically passing (or stalled) over the area could yield more cloudiness during the month than a few thunderstorms, even though the thunderstorms could produce a greater amount of precipitation. In addition, it is not uncommon for traveling mid-latitude cyclones to yield cloudiness for several days, with little to no precipitation in some locations. Preliminary tests also compared time series of the number of precipitation days per month with monthly mean SR, but this approach shed no more light on the SR-precipitation relationship.

The seasonal SR trends identified and discussed above are consistent with previous results on the secular variation of Midwestern cloudiness (e.g., Changnon, 1981; Angell *et al.*, 1984). Changnon (1981) found that the greatest percentage increase in cloudy days for the Midwest from 1901-1977 occurred in the fall season, which agrees very well with the October results in Fig. 4.8. Summer followed closely, with much lesser increases in spring and winter. While Changnon's summer and winter results are less consistent with the results shown here (Fig. 4.8), the spring analyses agree well. Angell *et al.* (1984) found a similar significant increase in cloudiness for the United States from 1950-1982, dominated by the greatest change in autumn and least in spring, both of which agree with Fig. 4.8. Both of these studies identified similar trends in percent possible sunshine data. Angell *et al.* (1984) point out that no distinction was made in their study (as was also the case for Changnon, 1981) between low, middle, and high (cirrus) clouds. Thus, the same amount of indicated cloudiness could have a quite different effect on the radiation balance at the earth's surface, depending on the type, thickness and height of the clouds; this is a drawback of these types of studies. The model used in this research does make use of cloud heights (from which cloud types can be inferred) in better determining SR attenuation due to cloud cover (cf. Table 2.2). Furthermore, since cloudiness trends may be inferred from the SR trends presented here (Fig. 4.8), these implicit new cloudiness trends reinforce the previous cloud-based work.

Some scientists (e.g., Reinking, 1968; Kuhn, 1970; Changnon, 1981; Angell *et al.*, 1984) have postulated that contrail-induced cirrus clouds have increased dramatically since the mid-1960s. The transmissivity of cirrus (i.e., high) clouds (Table 2.2) is 0.87-0.95, depending on sky condition (i.e., scattered, broken, or overcast). Thus, increased amounts of contrail-induced cirrus clouds may indeed be reflected in increased cloudiness trends, but may not be noticeable in monthly means of surface SR trends, such as those shown for particularly January and July in Fig 4.8, which exhibit the most discrepancy with the seasonal cloudiness trends.

Vinzani and Lamb (1985) studied the 1949-1980 visibility variations in the Illinois vicinity. They found overall decreasing trends in summer, spring, and autumn, with the most pronounced decrease in summer and least in autumn, and no marked decline in winter. According to Fig. 4.8, these visibility decreases are mostly associated with increasing SR, except in October when SR trends are also downward. Note that visibility is not a direct input to the semi-physical model used here (cf. Chapter II). However, due to the very good agreement between the modeled and measured SR values presented earlier, it appears that either surface visibility has a small influence on SR, or the other variables, such as T_a , T_R , or T_g may adequately portray visibility's contribution.

CHAPTER V

CONCLUSION

A. Summary

This study arose from the need for a detailed documentation of the solar radiation (SR) climate of the Midwest region. The Midwest Climate Center (MCC) required an historical SR data base in order to generate historical data bases for other variables (e.g., soil moisture), and to provide its clients with timely crop yield assessments, in addition to other SR-related climate information. Furthermore, previous SR climate studies have been contradictory in establishing the SR climate of the Midwest region, partly due to the lack of available data. Because the network of SR measurements for this region is either sparse or lacking in longevity, a semi-physical SR model based on Meyers and Dale (1983) was implemented and used to create a 40-year (1948-1987) data base of daily SR values for 53 stations in the Midwest.

The advantages of the model used include: 1) its dependence on standard hourly meteorological data (surface pressure, dew point temperature, and cloud height and fractional sky cover) as input; 2) its accommodations of the effects of Rayleigh scattering, absorption by water vapor and permanent gases, absorption and scattering by aerosols and clouds, and the contribution from ground-to-cloud-to-ground reflectance; and 3) the fact that it is both computationally efficient and was previously found, as well as proven here to be very accurate. Techniques employed to insure the most complete possible SR data base for each station included: 1) using ceiling height to estimate various cloud layer heights when cloud heights were missing; 2) interpolation of modeled parameters over one or two consecutive hours with no data; 3) substituting climatological values of dew point temperatures and surface pressure when one of those elements was missing for all hours of a day; and 4) using nearby stations with snow cover or a climatology of snow cover when a particular station's daily snow cover value was missing. As a result, the daily SR data set generated is 93% complete for the 53 stations for 1948-1987.

The model-generated SR values were compared and validated against several sets of measured SR data. The first validation involved comparison with 4 samples of high quality SR data comprising the available measurements from Chetek (near Eau Claire, Wisconsin), Delaware (near Columbus, Ohio), and two different years of data from Peoria (Illinois). Seasonal r^2 values displaying model consistency indicate least variation in October-December, closely followed by the remaining seasons. However, scatter diagrams suggest that there may be a lower limit to SR values given by the model,

implying that the model overestimates very low SR values. These results were seen in the mean errors, mean absolute errors, and rms errors. Additionally, the errors indicate that the model generally tends to overpredict daily totals of SR on average, but more so (by approximately 4%) in the cooler months of October-March than the warmer months of April-September. The mean absolute error for all stations was $1.75 \text{ MJ m}^{-2} \text{ day}^{-1}$, which translates to 11.7% of the mean daily SR measurement. Meyers and Dale (1983) obtained a mean absolute error of 8.7% in their more limited validation of the same model against 5 days of SR observations from each month in 1980 at each of 12 stations equally scattered throughout the United States. Thus, the model exhibits very good agreement with observed SR, and proves comparable to previous validations.

The rehabilitated SOLMET (SOLar METeorological) SR data for a sparse network of United States stations have been used extensively in SR research, even though their accuracy is somewhat uncertain because they contain adjusted observations. In order to further verify the model used in this research, and to provide new information on the accuracy of the SOLMET data, a comparison was made between 5 sets of SOLMET data (including one regression-extended set) and the model-generated SR. The comparisons indicated that the daily modeled SR values and daily SOLMET SR data are within about 10% of each other, with the tendency for modeled SR values to be higher than SOLMET values. Seasonal comparisons demonstrated more overprediction of SR by the model as compared to the SOLMET data in the cooler months of October through March, and less overprediction in the warmer months (April-September), as was seen in the previous comparisons discussed above. Comparisons of modeled data with regression-extended SOLMET data revealed slightly larger discrepancies, suggesting that the regression-extended SOLMET data should be viewed with caution. This is in agreement with the findings of the Solar Energy Research Institute (1990b).

The quality and density of the modeled SR data offer the following advantages over the SOLMET data: 1) the ability to detect smaller scale spatial variability throughout an increased-density network; and 2) the ability to incorporate an additional 20 years of data (or more, based on availability), in order to facilitate analysis of historical trends.

Accordingly, the model-generated daily SR data for 53 Midwestern stations for 1948-1987 were then used to document aspects of the spatial and temporal variability of SR for the region. These analyses used station SR averages for individual months. The monthly mean spatial patterns obtained exhibited some pronounced characteristics. The most dominant feature is a northward decrease in SR, with the strongest gradient being in October and the weakest in March. For most months, however, the SR isopleths have

a slight northwest-southeast orientation rather than running parallel to the latitude circles. This suggests the influence on SR of altitude (which decreases the air mass path length), population / industrialization, and atmospheric humidity, all of which act to decrease SR in an eastward direction. This near-zonal SR pattern is most pronounced during the fall and winter months. However, the pattern becomes more mesoscale in character from the late spring into the summer months. The apparently most substantive mesoscale features evident during these months include: 1) low SR over northern Wisconsin extending into the Upper Peninsula of Michigan and over northern Lake Michigan into northern Lower Michigan; 2) lower SR for Kansas-City's Downtown Airport than for its more-rural International Airport; and 3) SR maxima along the eastern shore of Lake Michigan. The thermal effect of the Great Lakes is additionally seen in the cooler months (September-April), as shown by the progressive appearance of low SR over Lower Michigan from October through February. The fall season also sees the return of the aforementioned near-zonal SR pattern from the primarily mesoscale character of summer.

Investigation of the temporal SR variability during 1948-1987 involved both detailed analyses of time series for 7 especially reliable stations, and identification of overall trends for all 53 stations. The time series showed considerable interannual variability, with southern stations often displaying more variability than their northern counterparts. A key result was that long term (40-year) trends for the Midwest region show a strikingly coherent pattern for October: all 53 stations have downward trends and most are highly (>95%) or extremely (>99%) statistically significant based on the Student's *t* test. The (19) October trends significant at the >99% level are generally located at stations in the central part of the region. January shows a swath of significant (>90%) upward trends in the central Midwest, generally oriented in a south-southwest to north-northeast direction. Another key result is that more than half of these trends are highly significant (>95%), with six of these significant at the >99% level.

The stations with positive trends for April were found to be in the eastern portion of the Midwest, while those with negative trends were largely in the western part of the region. However, only a few of those trends were found to be statistically significant. July trends showed less spatial coherence throughout the region than those for the other mid-season months. The negative July trends were found predominantly around the Great Lakes and in Ohio, and the positive trends prevailed mostly in the central part of the region.

The final analysis undertaken involved a comparison of monthly precipitation totals with monthly mean SR. Most precipitation trends identified for 1949-1987 were physically consistent with the SR trends obtained: when SR increased (decreased) during

the 40 year period, the tendency was for precipitation to have decreased (increased). However, statistical significance tests on the precipitation regression lines produced mostly insignificant results, with only a few precipitation trends being highly (>95%) significant. When the SR and precipitation time series were examined in detail, SR maxima and precipitation minima and vice versa were found to coincide in some but not all cases.

The seasonal SR trends identified in this research were noted to be consistent with one of the principal results of previous investigations into the secular variation of Midwestern cloudiness: the pronounced SR decrease over the region in fall coincided with substantial percentage increases in the number of cloudy days. Much smaller increases in cloudiness were previously found to have occurred in spring, for which the present SR results displayed no significant trend. Visibility trends previously studied were decreasing in summer, spring, and autumn, with the most pronounced decline in summer and least in autumn, and no marked decrease in winter. This declining visibility was mostly associated with increasing SR, except in October when SR trends were also downward.

B. Future Research

The quality of the data set developed here could be further improved by decreasing the number of missing values and increasing the quality of the heuristically determined parameters. Additional work would increase the completeness of the daily records. Missing values of daily SR at each station could be estimated using nearby stations. Investigation of the heuristic employed to determine cloud heights is warranted due to the sensitivity of the model to this parameter. For example, if it is found that clouds occur more frequently at a particular height in a particular area of the Midwest, a weighting function could be added which would account for this bias at the appropriate level and station. The application of these enhancements would produce a more complete data set with improved confidence for use as the basis for further investigation.

The large data set developed during this research provides endless opportunities for investigations into the SR climate of the Midwest. Further spatial analyses might involve regionalization studies using the rotated Principal Component approach of Richman and Lamb (1985). The application of their technique to the present high density data set would likely yield SR-regionalizations of substantially greater reliability than the discrepancies observed in other climate-regions studies, such as those reproduced in Figs. 1.2 and 1.3 (Willmott and Vernon, 1980 and Balling and Vojtesak, 1983, respectively). Additional interstation correlation investigations may yield further into spatial SR patterns. Subsequent examinations of the SR time series may reveal sub-

seasonal scale variations in the data. Irregardless, inspection of the meteorological or synoptic conditions during October over the last 40 years is warranted in order to reveal the causes in the significant downward October SR trends.

For this period of record (1948-1987), other researchers have observed and tabulated physical and biological phenomena that may be related to SR variations (e.g., Kunkel, 1990b). For example, the correlation of agricultural yields with SR may provide insight into the long term adaptability of crops to their environment. Furthermore, ancillary data sets (e.g., detailed cloud information) obtained as input to the SR model are now available for study. Therefore, further investigation of cloudiness trends using the detailed cloud information utilized here (cloud type, height, and thickness) is warranted in order to determine the reason for the slightly inconsistent results with the SR trends.

Radiant heat energy is an important component of systems (e.g., photosynthesis, atmospheric circulation, and solar power) studied by many disciplines. The interdisciplinary transfer of information (i.e., this SR data set) resulting from this thesis can provide the basis for subsequent research into these systems, thereby furthering humanity's quest to unravel nature's complexities.

REFERENCES

- Aguado, E., 1986: Local-scale variability of daily solar radiation - San Diego County, California. *J. Clim. & Appl. Meteor.*, 25, 672-678.
- Angell, J. K. and J. Korshover, 1975: Variation in sunshine duration over the contiguous United States between 1950 and 1972. *J. Appl. Meteor.*, 14, 1174-1181.
- Angell, J. K. and J. Korshover, 1978: A recent increase in sunshine duration within the contiguous United States. *J. Appl. Meteor.*, 17, 819-824.
- Angell, J. K., J. Korshover, and G. F. Cotton, 1984: Variation in United States cloudiness and sunshine, 1950-82. *J. Clim. & Appl. Meteor.*, 23, 752-761.
- Atmospheric Radiation Working Group (ARWG), 1972: Major problems in atmospheric radiation: An evaluation and recommendations for future efforts. *Bull. Amer. Meteor. Soc.*, 53, 950-956.
- Atwater, M. A. and J. T. Ball, 1978: Intraregional variations of solar radiation in the eastern United States. *J. Appl. Meteor.*, 17, 1116-1125.
- Atwater, M. A. and J. T. Ball, 1981: A surface solar radiation model for cloudy atmospheres. *Mon. Wea. Rev.*, **109**, 878-888.
- Atwater, M. A. and P. S. Brown, Jr., 1974: Numerical computations of the latitudinal variation of solar radiation for an atmosphere of varying opacity. *J. Appl. Meteor.*, 13, 289-297.
- Baker, D. G. and J. C. Klink, 1975: *Solar Radiation Reception, Probabilities, and Areal Distribution in the North-Central Region*. University of Minnesota Agricultural Experiment Station Technical Bulletin 300, Minneapolis, Minnesota, 54 pp.
- Balling, R. C, Jr., 1983: Harmonic analysis of monthly insolation levels in the United States. *Solar Energy*, 31, 293-298.
- Balling, R. C, Jr. and R. S. Cervený, 1983: Spatial and temporal variations in long-term normal percent possible solar radiation levels in the United States. *J. Clim. & Appl. Meteor.*, 22, 1726-1732.
- Balling, R. C, Jr. and M. J. Vojtesak, 1983: Solar climates of the United States based on long-term monthly averaged daily insolation values. *Solar Energy*, 31, 283-291.
- Bennett, I., 1964: A method for preparing maps of mean daily global radiation. *Arch. Met. Geoph. Biokl. Ser. B.*, 13, 216-248.
- Bennett, I., 1965: Monthly maps of mean daily insolation for the United States. *Solar Energy*, 9, 145-158.
- Bennett, I., 1975: Variation of daily solar radiation in North America during extreme months. *Arch. Met. Geoph. Biokl. Ser. B.*, 23, 31-57.
- Biga, A. J. and R. Rosa, 1980: Estimating solar irradiation sums from sunshine and cloudiness observations. *Solar Energy*, 25, 265-272.

- Bristow, C. L. and G. S. Campbell, 1984: On the relationship between incoming solar radiation and daily maximum and minimum temperature. *Agric. & For. Meteor.*, 31, 159-166.
- Bryson, R. A. and F. K. Hare, (eds) 1974: *World Survey of Climate: The Climates of North America*, Vol. 11. Elsevier Scientific Publ. Co., New York, New York, 420 pp.
- Changnon, S. A., 1980: Evidence of urban and lake influences on precipitation in the Chicago area. *J. Appl. Meteor.*, 19, 1137-1159.
- Changnon, S. A., 1981: Midwestern cloud, sunshine and temperature trends since 1901: possible evidence of jet contrail effects. *J. Appl. Meteor.*, 20, 496-508.
- Changnon, S. A., P. J. Lamb, and K. G. Hubbard, 1990: Regional Climate Centers: New institutions for climate services and climate-impact research. *Bull. Amer. Meteor. Soc.*, 71, 527-537.
- Doehring, F. and T. Karl, 1981: *A History of Sunshine Data in the United States 1891-1980*. Historical Climatology Series No. 2-2, National Climate Center, Asheville, North Carolina, 40 pp.
- Eichenlaub, V. L., J. R. Harman, F. V. Nurnberger, and H. J. Stolle, 1990: *The Climatic Atlas of Michigan*. University of Notre Dame Press, Notre Dame, Indiana, 165 pp.
- Enmap Corporation, 1980: *Map of solar energy in the United States and southern Canada*. Boulder, Colorado, 1 pp.
- Glover, J. and J. S. G. McCulloch, 1958: The empirical relation between solar radiation and hours of bright sunshine in the high-altitude tropics. *Arch. Met. Geoph. Biokl. Ser. B.*, 8, 56-60.
- Granger, O. E., 1980: Climatology of global solar radiation in California and an interpolation technique based on orthogonal functions. *Solar Energy*, 24, 153-168.
- Hollinger, S. E. and R. R. Reitz, 1990: *Calibration and verification for the Illinois Climate Network*. Paper No. 904048 for presentation at the 1990 International Summer Meeting, The American Society of Agricultural Engineers, St. Joseph, Michigan, 12 pp.
- Kerr, J. P. and H. E. Rosendal, 1968a: Distribution of global radiation in Wisconsin December 1966 through June 1967. *Mon. Wea. Rev.*, 96, 232-236.
- Kerr, J. P., G. W. Thurtell, and C. B. Tanner, 1968b: Mesoscale sampling of global radiation - analysis of data from Wisconsin. *Mon. Wea. Rev.*, 96, 237-241.
- Kondratyev, K., 1969: *Radiation in the Atmosphere*. Academic Press, New York, New York, 912 pp.

- Kuhn, P. M, 1970: Airborne observations of contrail effects on the thermal radiation budget. *J. Atmos. Sci.*, 27, 937-942.
- Kunkel, K. E., 1990b: Operational soil moisture estimation for the midwestern United States. *J. Appl. Meteor.*, 29, 1158-1166.
- Kunkel, K. E., S. A. Changnon, C. G. Lonnquist, and J. R. Angel, 1990a: A real-time climate information system for the midwestern United States. *Bull. Amer. Meteor. Soc*, 71, 1601-1609.
- Martines-Lozano, J. A., F. Tena, J. E. Onrubia, and J. De La Rubia, 1984: The historical evolution of the Ångström formula and its modifications: Review and Bibliography. *Agric. Meteor.*, 33, 109-128.
- Meyers, T. P. and R. F. Dale, 1983: Predicting daily insolation with hourly cloud height and coverage. *J. Clim. & Appl. Meteor.*, 22, 537-545.
- Moss, D. N., 1967: Solar energy in photosynthesis. *Solar Energy*, 11, 173-179.
- National Climatic Center, 1978: *SOLMET Volume I - User's Manual TD-9724*. Ashville, North Carolina, 50 pp.
- National Climatic Center, 1979: *SOLMET Volume II - Final Report TD-9724*. Ashville, North Carolina, 184 pp.
- National Climatic Data Center, 1986: *Manual to Surface Airways Hourly TD-3280*. Ashville, North Carolina, 39 pp.
- Neild, R. E., M. W. Seeley, and N. H. Richman, 1978: The computation of agriculturally oriented normals from monthly climatic series. *Agric. Meteor.*, 19, 181-187.
- Northrup Services, Inc., 1979: *Solar-Climatic Statistical Study*. United States Department of Energy, Washington, DC, 48 pp.
- O'Brien, G., 1978: *Climatic Region Determination*. Appendix A of regional conceptual design for residential photovoltaic systems. Monthly Progress Report No. 3. Department of Energy, SAND 78-7013, Philadelphia, Pennsylvania, 29 pp.
- Parker, S. S., J. T. Hawes, S. J. Colucci, and B. P. Hayden, 1989: Climatology of 500 mb cyclones and anticyclones, 1950-85. *Mon. Wea. Rev.*, 117, 558-570.
- Pinker, R. T. and L. M. Militana, 1981: Small scale variability in the global solar radiation in the Washington, DC. area. *Solar Energy*, 26, 473-428.
- Rangarajan, S., M. S. Swaminathan, and A. Mani, 1984: Computation of solar radiation from observations of cloud cover. *Solar Energy*, 32, 553-556.
- Reddy, S. J., 1971: An empirical method for the estimation of total solar radiation. *Solar Energy*, 13, 289-290.
- Reddy, S. J., 1974: An empirical method for the estimating sunshine from total cloud amount. *Solar Energy*, 15, 281-285.
- Reddy, S. J., 1987: An estimation of global solar radiation and evaporation through precipitation - a note. *Solar Energy*, 38, 97-104.
- Reinking, R. G., 1968: Insolation reduction by contrails. *Weather*, 23, 171-173.

- Reitan, C. H., 1960: Mean monthly values of precipitable water over the United States, 1946-1956. *Mon. Wea. Rev.*, 88, 25-35.
- Richman, M. B. and P. J. Lamb, 1985: Climatic pattern analysis of three- and seven-day summer rainfall in the central United States: Some methodological considerations and a regionalization. *J. Clim. & Appl. Meteor.*, 24, 1325-1343.
- Rietfeld, M. R., 1978: A new method for estimation the regression coefficients in the formula relating solar radiation to sunshine. *Agric. Meteor.*, 19, 243-252.
- Rosenberg, N. J., B. L. Blad, and S. B. Verma, 1983: *Microclimate: The Biological Environment*. John Wiley & Sons, Inc., New York, New York, 495 pp.
- Schmetz, J. and E. Raschke, 1978: A method to parameterize the downward solar radiation. *Arch. Met. Geoph. Biokl. Ser. B.*, 26, 143-151.
- Scott, R. W. and R. C. Grosh, 1979: Chicago area cloud distributions from satellite photography. From *Studies of Urban and Lake Influences on Precipitation in the Chicago Area*. Vol. II of Final Report NSF Grant ENV77-15375, Illinois State Water Survey Contract Rep. 220, Champaign, Illinois, 44-52.
- Smith, W. L., 1966: Note on the relationship between total precipitable water and surface dewpoint. *J. Appl. Meteor.*, 5, 726-727.
- Schulze, R. E., 1976: A physically based method of estimating solar radiation from suncards. *Agric. Meteor.*, 16, 85-101.
- Sneath, P. H. A. and R. R. Sokal, 1973: *Numerical Taxonomy*. Freeman, San Francisco, California, 573 pp.
- Solar Energy Research Institute, 1981: *Solar Radiation Energy Resource Atlas of the United States*. SERI/SP-642-1037, Golden, Colorado, 142 pp.
- Solar Energy Research Institute, 1990a: *Insolation Data Manual*. SERI/TP-220-3880, Golden, Colorado, 281 pp.
- Solar Energy Research Institute, 1990b: *1961-1990 Solar Radiation Data Base*. SERI/TP-220-3632, Golden, Colorado, 4 pp.
- Suckling, P. W., 1983: Extrapolation of solar radiation measurements: Mesoscale analyses from Arizona and Tennessee Valley Authority regions. *J. Clim. & Appl. Meteor.*, 22, 488-494.
- Terjung, W. H., 1970: Global classification of solar radiation. *Solar Energy*, 13, 67-81.
- Thekarhara, M. P., 1976: Solar radiation measurement: Techniques and instrumentation. *Solar Energy*, 18, 309-325.
- Turner, C. (ed.), 1974: *Report and Recommendations of the Solar Energy Data Workshop*. Environmental Research Laboratories, Silver Spring, Maryland, 218 pp.
- United States Department of Interior, 1970: *The National Atlas of the United States of America*. Washington, DC, 417 pp.
- Vinzani, P. G. and P. J. Lamb, 1985: Temporal and spatial visibility variations in the Illinois vicinity during 1949-80. *J. Clim. & Appl. Meteor.*, 24, 435-451.
- Walraven, R., 1978: Calculating the position of the sun. *Solar Energy*, 20, 393-397.

- Ward, J. H., 1963: Hierarchical grouping to optimize an objective function. *J. Am. Statist. Ass.*, 58, 236-244.
- Willmott, C. J. and M. T. Vernon, 1980: Solar climates of the conterminous United States: A preliminary investigation. *Solar Energy*, 24, 295-303.

APPENDIX A

STATION NAMES AND IDENTIFIERS

The following is an alphabetical list by state of the stations, corresponding FAA identifiers, and dates for which hourly surface observational data (TD-3280) was used to calculate solar radiation (SR).

Illinois

Chicago (Midway)	MDW	01/48 - 12/79
Chicago (O'Hare)	ORD	11/58 - 12/87
Moline	MLI	02/48 - 12/87
Peoria	PIA	01/48 - 12/87
Rantoul	RTL	01/49 - 12/70
Rockford	RFD	12/48 - 02/51,03/51 - 12/54,11/58 - 12/87
Springfield	SPI	01/48 - 06/88

Indiana

Evansville	EVV	01/48 - 12/87
Fort Wayne	FWA	01/48 - 12/87
Indianapolis	IND	01/48 - 12/87
South Bend	SBN	01/48 - 12/87

Iowa

Burlington	BRL	01/48 - 01/80
Des Moines	DSM	01/45 - 12/87
Dubuque	DBQ	02/51 - 09/81,11/82 - 12/87
Mason City	MCW	01/48 - 12/87
Sioux City	SUX	01/48 - 12/87

Kentucky

Cincinnati (Covington)	CVG	01/48 - 12/87
Lexington	LEX	01/48 - 12/87
Louisville	SDF	01/48 - 12/87
Paducah	PAH	09/49 - 12/64,10/84 - 12/87

Michigan

Alpena	APN	09/59 - 12/87
Detroit	DET	01/48 - 12/87
Flint	FNT	12/48 - 12/87
Gwinn	SAW	10/56 - 12/57,04/58 - 10/58,09/59 - 12/70
Muskegon	MKG	01/48 - 12/87
Sault Ste Marie	SSM	01/48 - 12/87
Traverse City	TVC	12/48 - 12/87

Minnesota

Duluth	DLH	01/48 - 12/87
International Falls	INL	01/48 - 12/87
Minneapolis-St Paul	MSP	01/45 - 12/87
St Cloud	STC	01/48 - 12/87

Missouri

Columbia	COU	01/45 - 10/69,11/69 - 12/87
Kansas City (Downtown)	MKC	01/48 - 09/72,01/75 - 12/87
Kansas City (International)	MCI	10/72 - 12/87
Springfield	SGF	01/48 - 12/87
St. Louis	STL	01/45 - 12/87

Nebraska

Omaha	OMA	01/48 - 12/87
-------	-----	---------------

North Dakota

Fargo	FAR	01/48 - 12/87
-------	-----	---------------

Ohio

Cleveland	CLE	01/48 - 12/87
Columbus	OSU	01/48 - 12/87
Dayton	DAY	01/48 - 12/87
Toledo	TOL	01/46 - 01/55,02/55 - 12/87

Pennsylvania

Pittsburgh	PIT	01/45 - 09/52,07/82 - 06/83, 09/52 - 12/87
------------	-----	--

South Dakota

Sioux Falls	FSD	01/48 - 12/87
-------------	-----	---------------

Tennessee

Bristol	TRI	01/48 - 12/87
Memphis	MEM	01/48 - 12/87
Nashville	BNA	01/48 - 12/87

West Virginia

Charleston	CRW	02/49 - 12/87
------------	-----	---------------

Wisconsin

Eau Claire	EAU	10/49 - 12/87
Green Bay	GRB	09/49 - 12/87
La Crosse	LSE	01/48 - 12/87
Madison	MSN	01/48 - 12/87
Milwaukee	MKE	01/48 - 12/87

APPENDIX B

DATA BASE INFORMATION

<p>Table B.1. Summary of the modeled solar radiation data base produced for each station listed in Appendix A (listed alphabetically by station). Any day with Data, is listed either in Missing Data or Good Data. Good Data includes Flagged Data; days are flagged if no cloud heights were given during the day, and there was at least 1 hour with sky condition not clear (CLR). Stations for which there were separate data tapes (e.g., because of station moves, etc.) are listed separately and identified.</p>							
Station	Starting Date	Ending Date	Number of Days in Record with...				
			Data	Missing Data	Good Data	Flagged Data	No Data
APN	09-01-1959	12-31-1987	10349	2	10347	14	0
BNA	01-01-1948	12-31-1987	14610	9	14601	208	0
BRL	01-01-1948	01-01-1980	11689	2	11687	5478	0
CLE	01-01-1948	12-31-1987	14603	10	14593	2	7
COU1	01-01-1945	10-31-1969	9070	80	8990	372	0
COU2	11-01-1969	12-31-1987	6635	0	6635	15	0
CRW	02-01-1949	12-31-1987	14213	12	14201	703	0
CVG	01-01-1948	12-31-1987	14601	13	14588	214	9
DAY	01-01-1948	12-31-1987	14610	18	14592	192	0
DBQ	02-01-1951	12-31-1987	13054	1259	11795	27	429
DET	01-01-1948	12-31-1987	14607	76	14531	7659	3
DLH	01-01-1948	12-31-1987	14610	12	14598	4	0
DSM	01-01-1945	12-31-1987	15705	56	15649	373	0
EAU	10-01-1949	12-31-1987	13971	12	13701	13959	0

EVV	01-01-1948	12-31-1987	14610	7	14603	203	0
FAR	01-01-1948	12-31-1987	14602	5	14597	91	8
FNT	12-01-1948	12-31-1987	14275	16	14259	2556	0
FSD	01-01-1948	12-31-1987	14610	3	14607	192	0
FWA	01-01-1948	12-31-1987	14609	15	14594	41	1
GRB	09-01-1949	12-31-1987	14001	0	14001	14	0
IND	01-01-1948	12-31-1987	14608	9	14599	223	2
INL	01-01-1948	12-31-1987	14608	18	14590	20	2
LEX	01-01-1948	12-31-1987	14610	9	14601	16	0
LSE	01-01-1948	12-31-1987	14610	7	14603	7079	0
MCI	10-01-1972	12-31-1987	5564	2	5562	14	6
MCW	01-01-1948	12-31-1987	14609	106	14503	13660	1
MDW	01-01-1948	12-31-1979	11688	7	11681	21	0
MEM	01-01-1948	12-31-1987	14610	12	14598	873	0
MKC	01-01-1948	12-31-1987	13787	70	13717	3903	823
MKE	01-01-1948	12-31-1987	14610	4	14606	6	0
MKG	01-01-1948	12-31-1987	14609	2	14607	184	1
MLI	02-09-1948	12-31-1987	14571	7	14564	15	0
MSN	01-01-1948	12-31-1987	14610	13	14597	16	0
MSP	01-01-1945	12-31-1987	15705	84	15621	189	0
OMA	01-01-1948	12-31-1987	14610	33	14577	3378	0
ORD	11-01-1958	12-31-1987	10653	3	10650	11	0
OSU	01-01-1948	12-31-1987	14610	3	14607	189	0
PAH	01-01-1949	12-31-1987	7030	306	6724	5324	7214
PIA	01-01-1948	12-31-1987	14589	4	14585	193	21
PIT1	01-01-1945	05-31-1984	3546	133	3413	1067	10850

PIT2	09-16-1952	12-31-1987	12890	55	12835	13	0
RFD1	12-01-1948	02-28-1951	820	6	814	814	0
RFD2	03-01-1951	12-31-1987	12052	1	12051	1382	1403
RTL	01-01-1949	12-31-1970	8035	6	2474	8029	0
SAW	11-01-1956	12-31-1970	4713	21	4692	2544	461
SBN	01-01-1948	12-31-1987	14610	2	14608	186	0
SDF	01-01-1948	12-31-1987	14610	9	14601	195	0
SGF	01-01-1948	12-31-1987	14610	9	14601	193	0
SPI1	01-01-1948	12-31-1983	13146	7	13139	6	3
SPI2	01-01-1984	06-30-1988	1643	0	1643	11	0
SSM	01-01-1948	12-31-1987	14610	2	14608	188	0
STC	01-01-1948	12-31-1987	14610	1733	12877	115	0
STL	01-01-1945	12-31-1987	15705	69	15636	372	0
SUX	01-01-1948	12-31-1987	14610	3	14607	194	0
TOL1	01-01-1946	01-12-1955	3299	68	3231	0	0
TOL2	02-01-1955	12-31-1987	12022	3	12019	3	0
TRI	01-01-1948	12-31-1987	14610	9	14601	190	0
TVC	12-01-1948	12-31-1987	14275	45	14230	14065	0

APPENDIX C

FIGURES FROM BENNETT (1965)

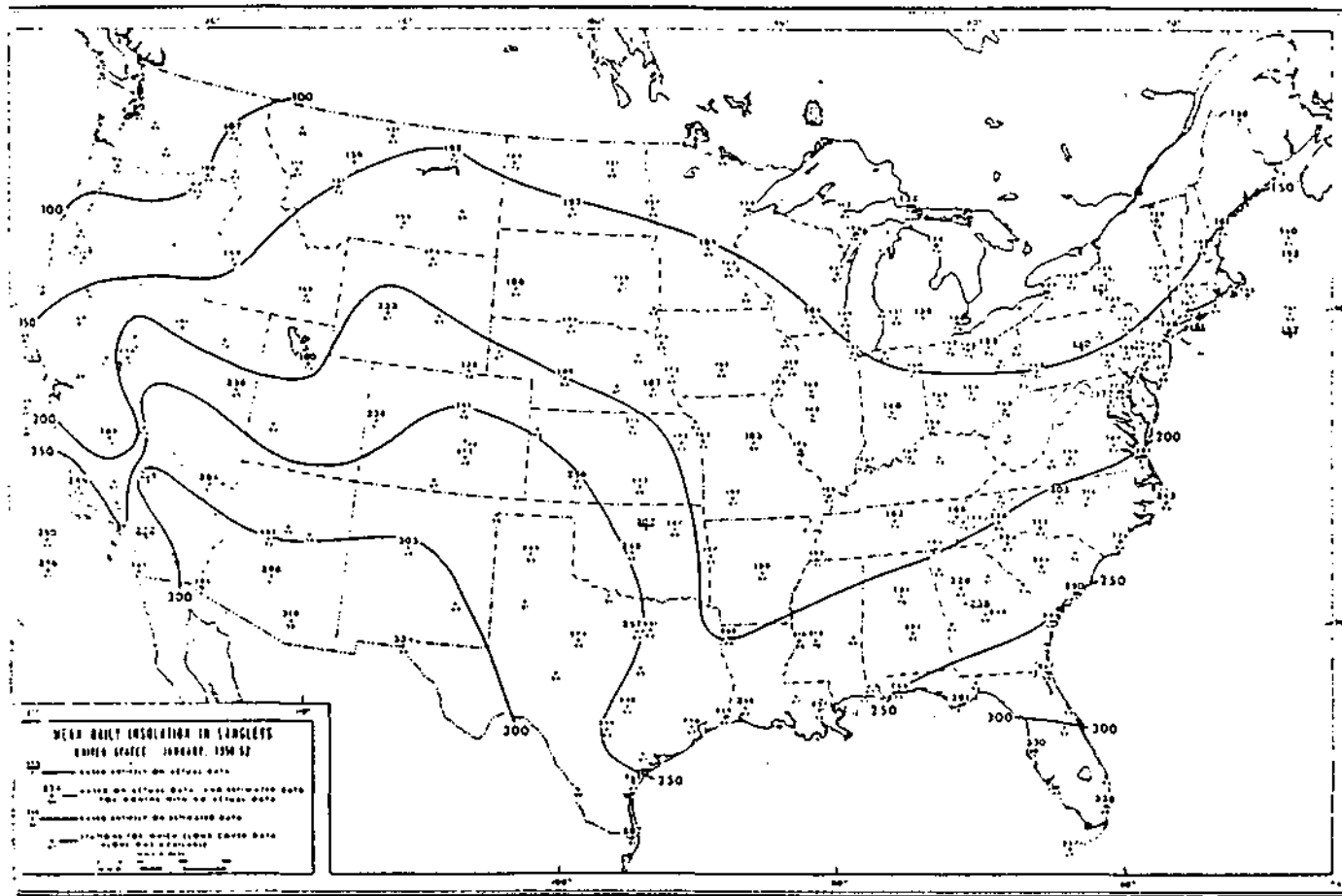


Fig. C.1. Mean daily insolation in langley units from 1950-1962 during January (from Bennett, 1965).

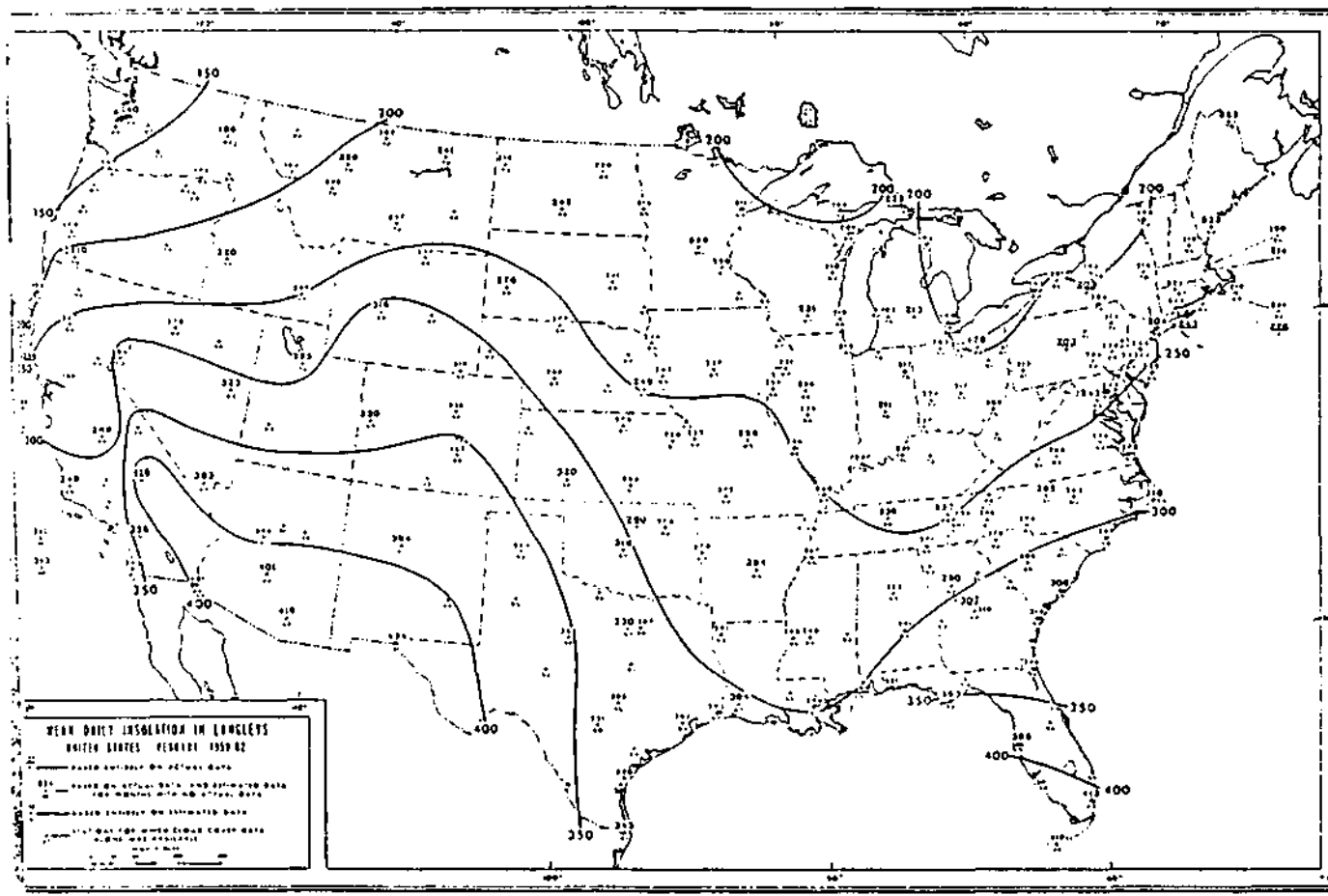


Fig. C.2. As in Fig. C.1, but for February.

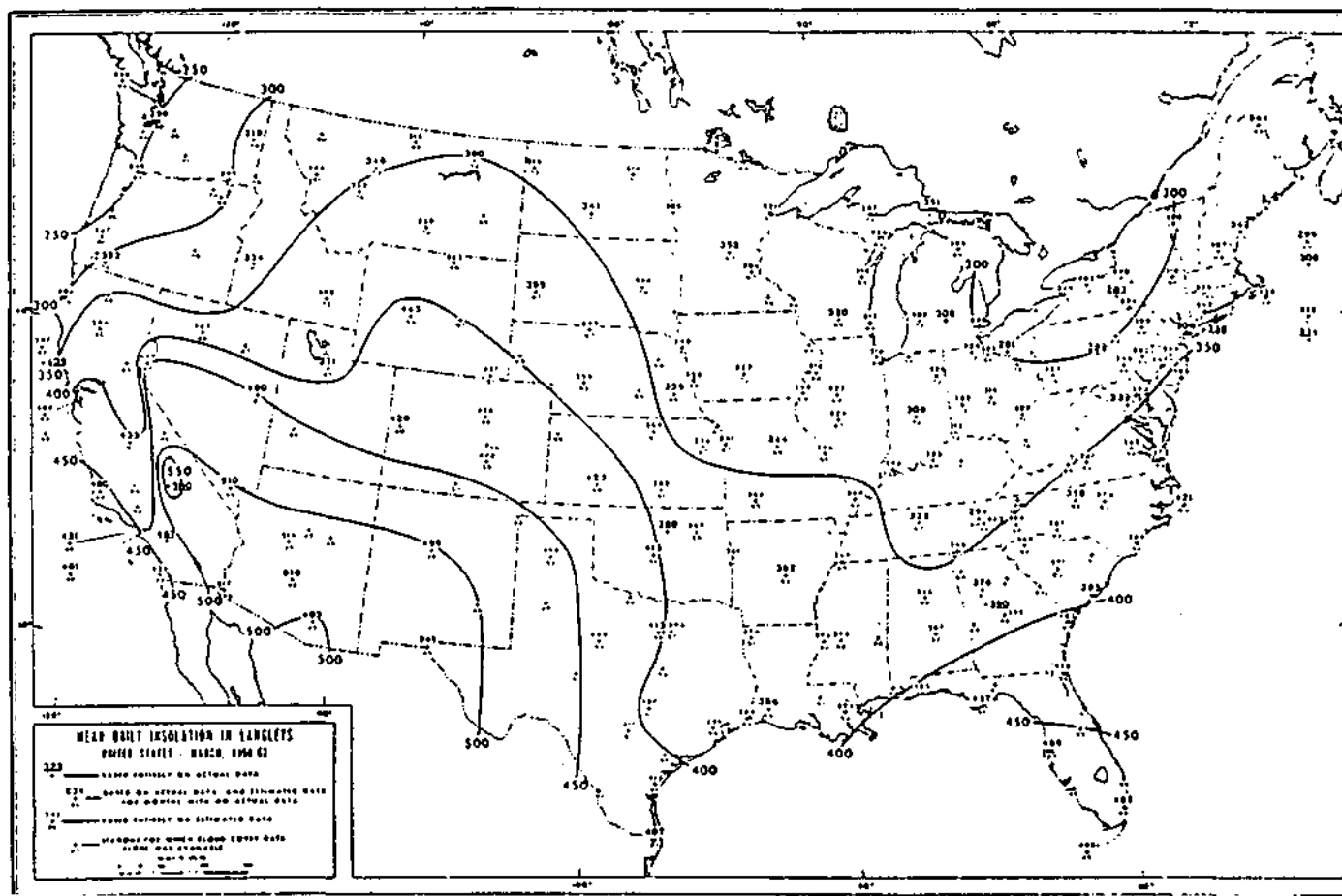


Fig. C.3. As in Fig. C.1, but for March.

Fig. C.4. As in Fig. C.1, but for April.

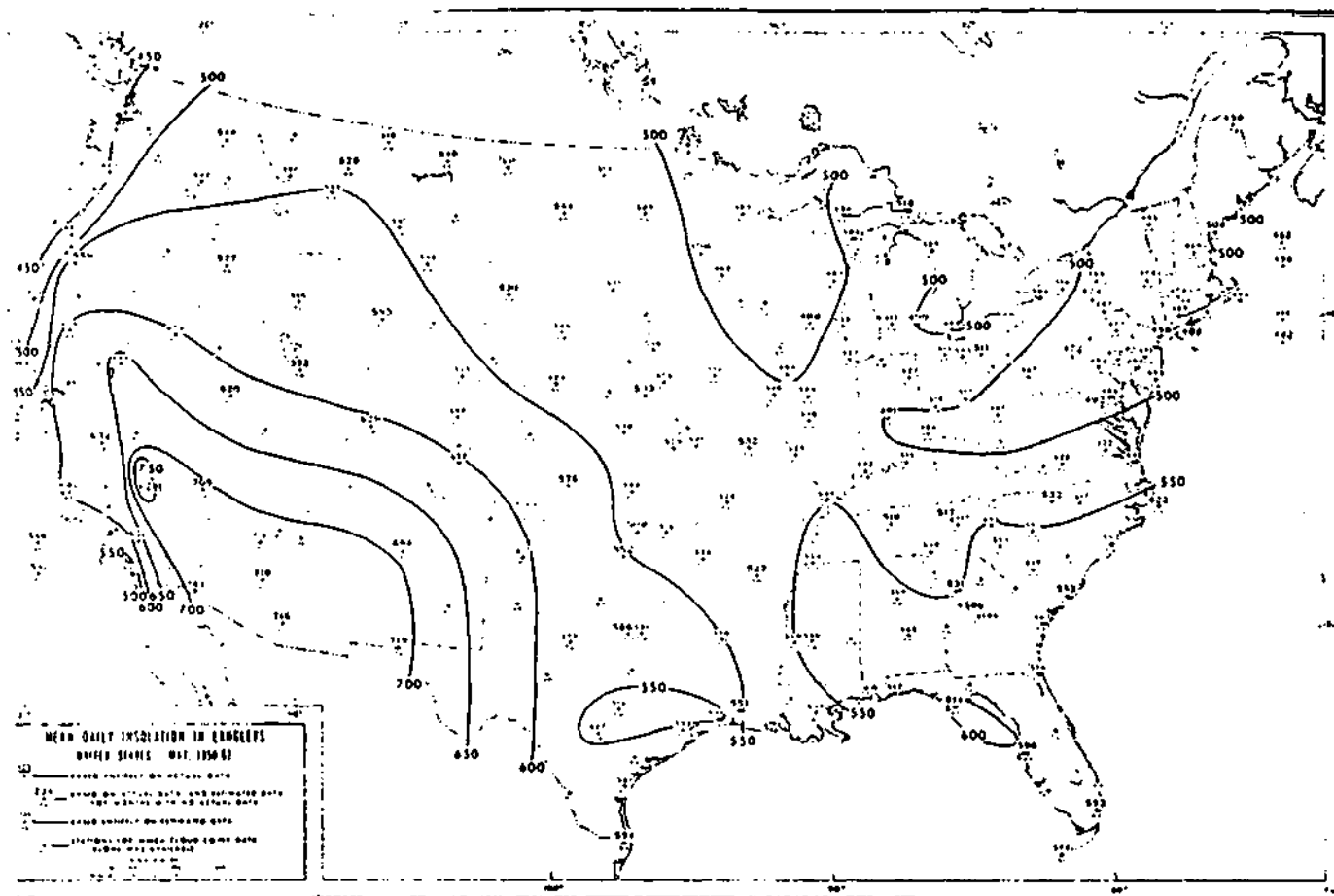


Fig. C.5. As in Fig. C.1, but for May.

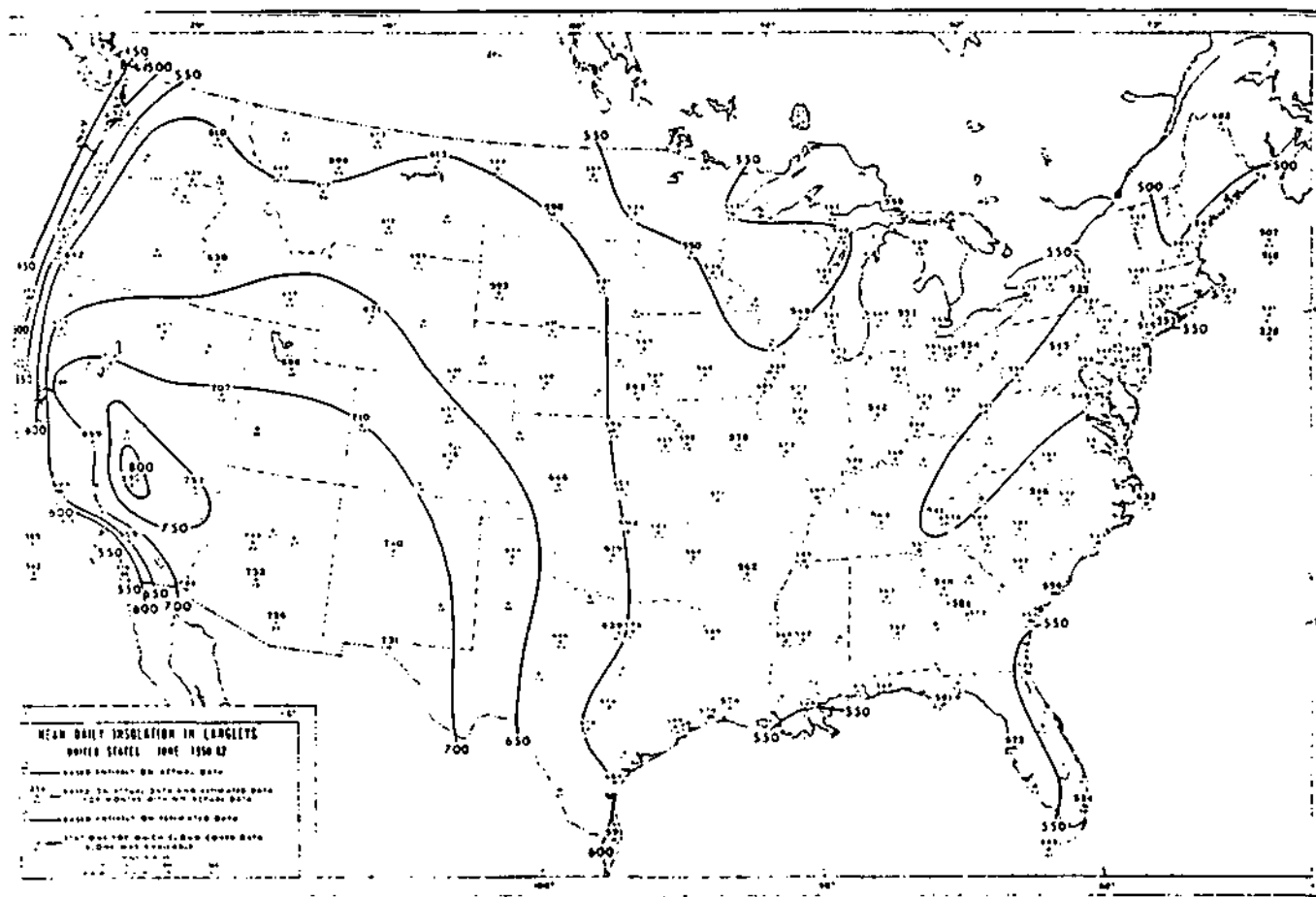


Fig. C.6. As in Fig. C.1, but for June.

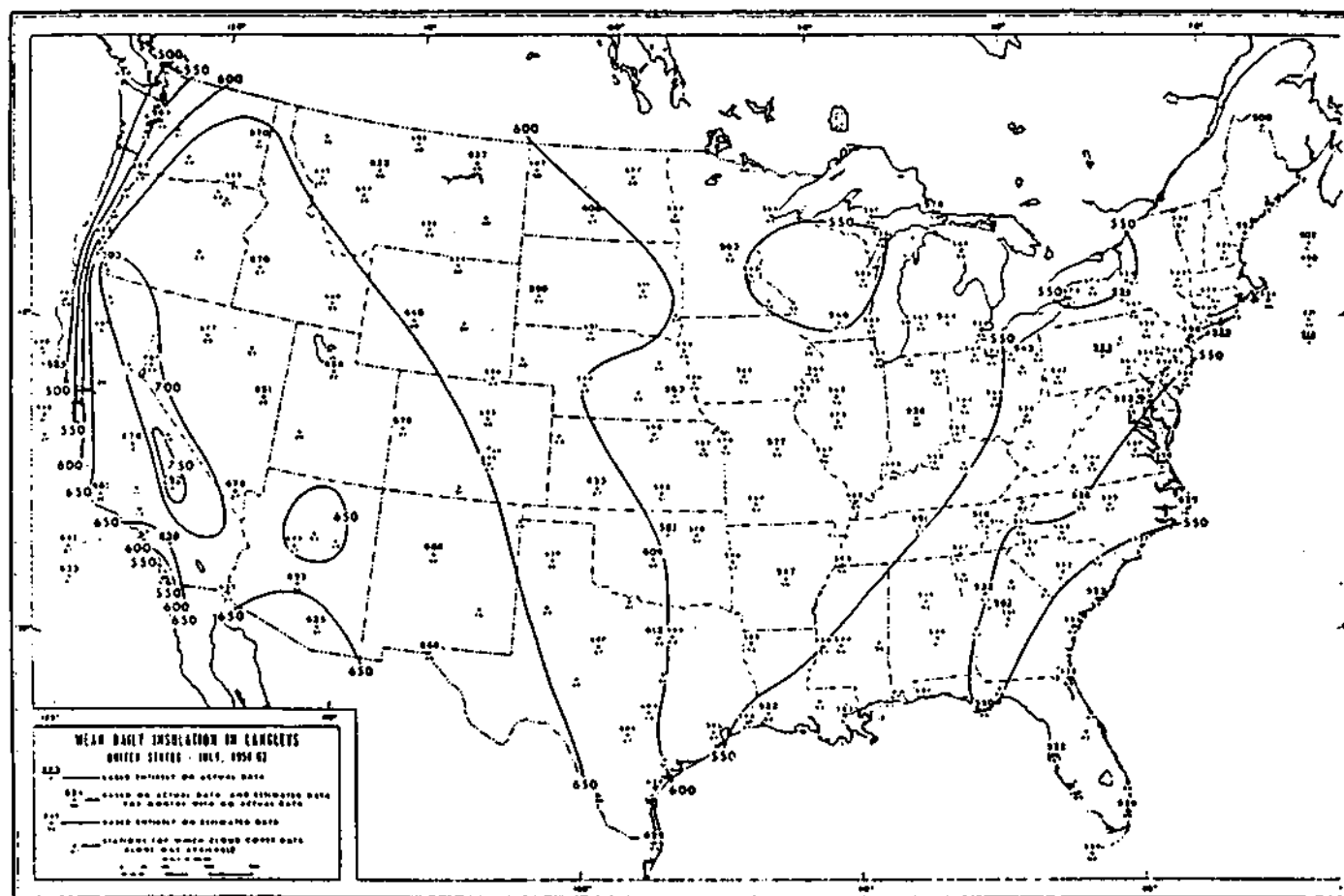


Fig. C.7. As in Fig. C.1, but for July.

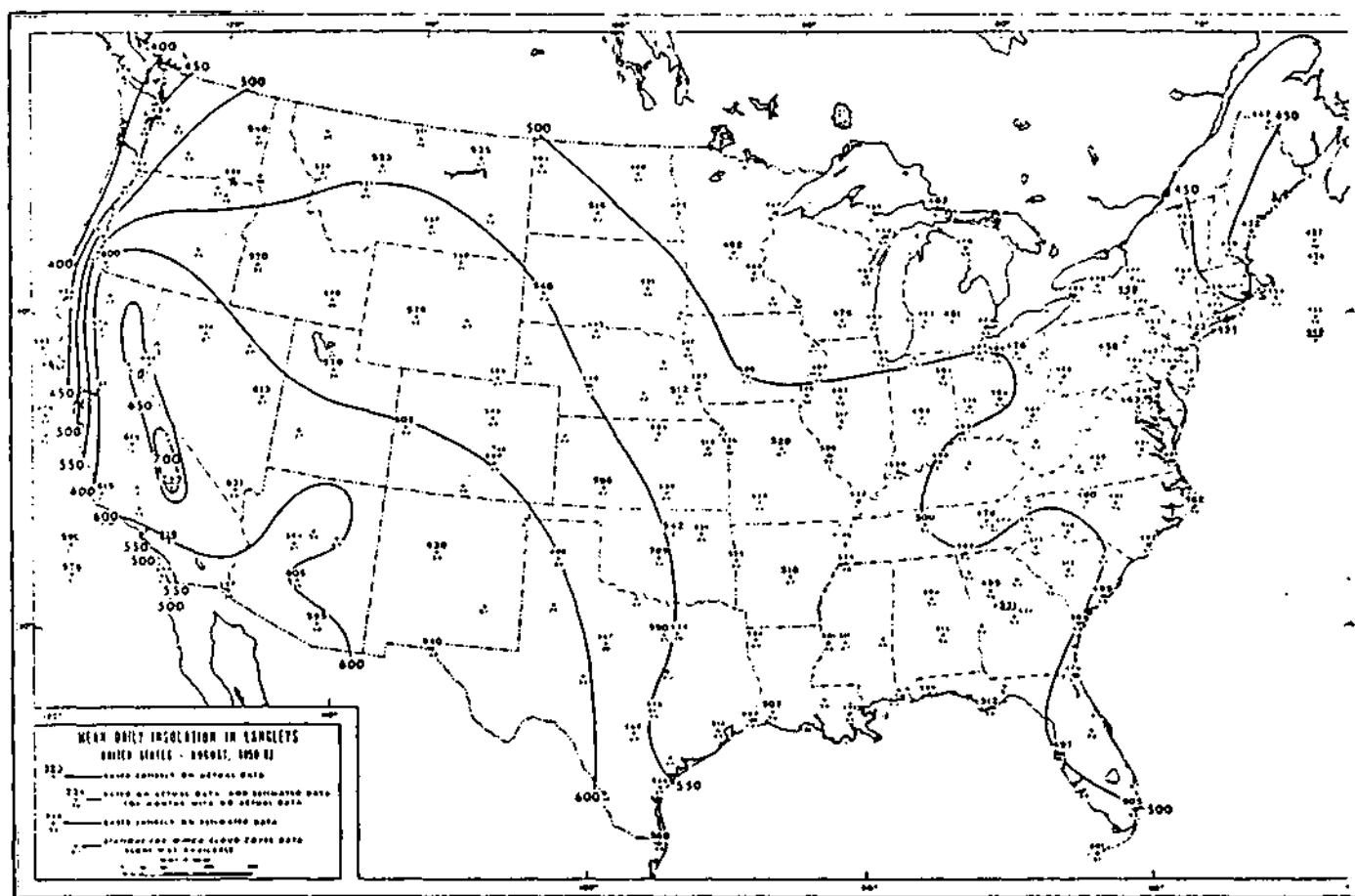


Fig. C.8. As in Fig. C.1, but for August.

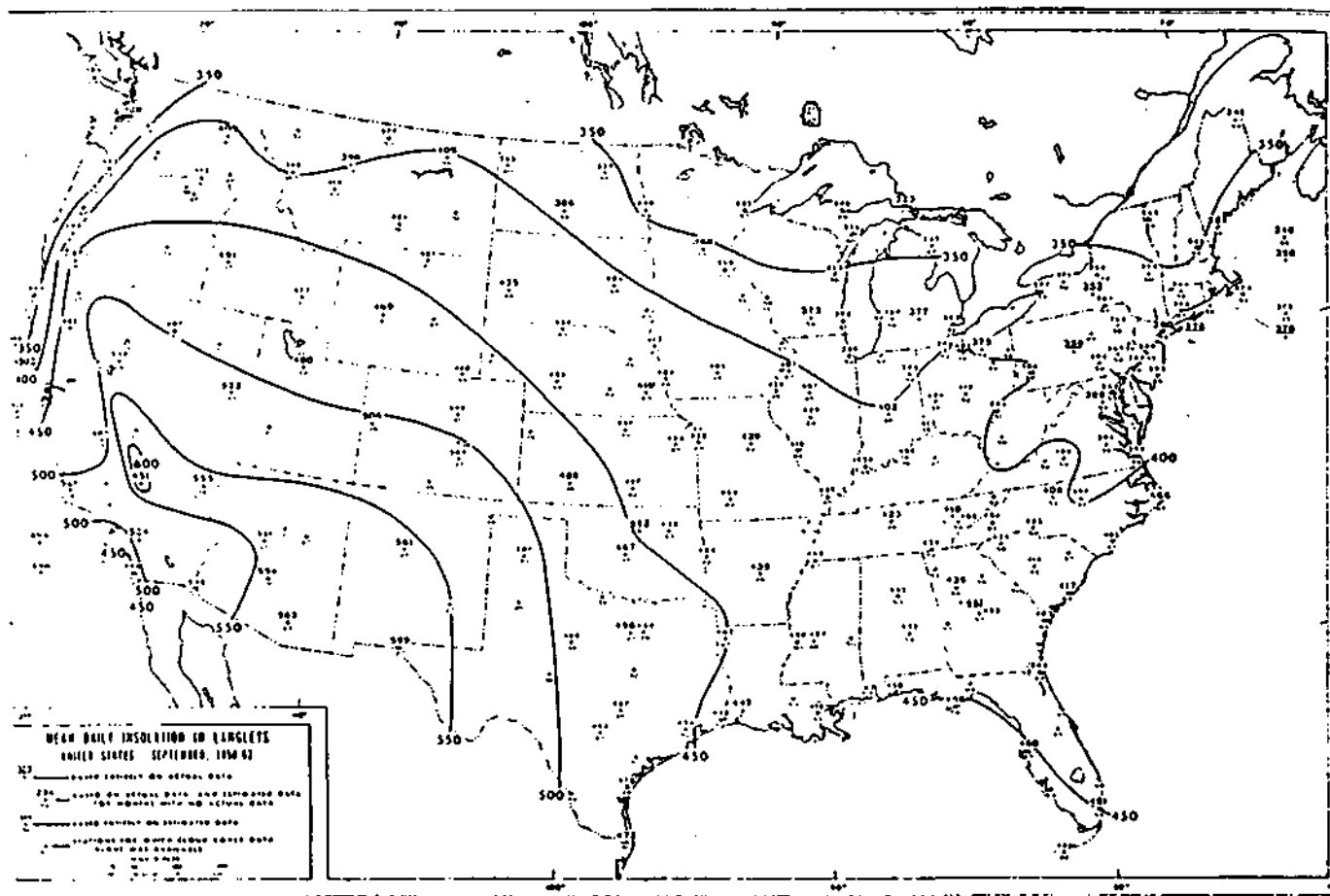


Fig. C.9. As in Fig. C.1, but for September.

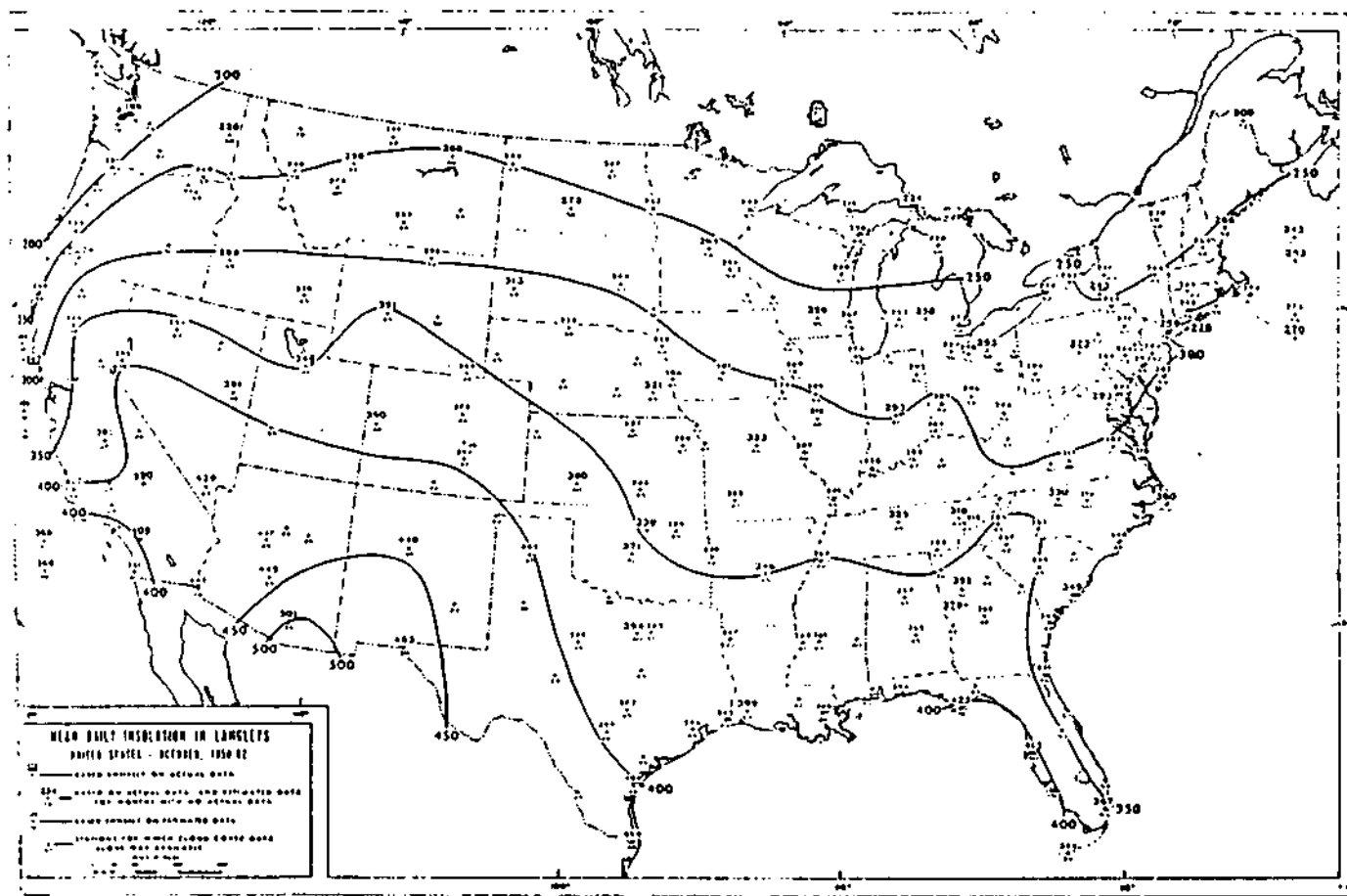


Fig. C.10. As in Fig. C.1, but for October.

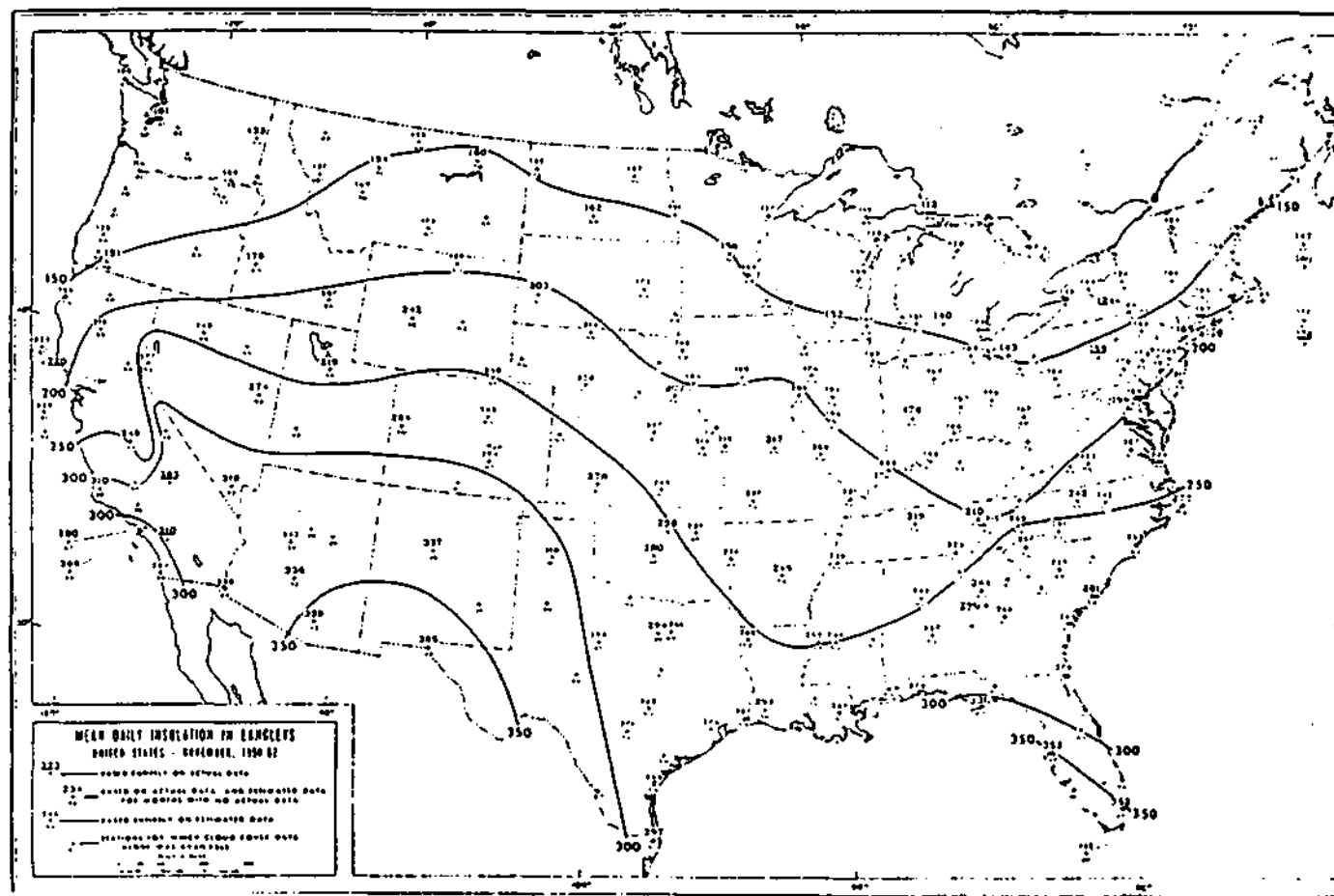


Fig. C.11. As in Fig. C.1, but for November.

Fig. C.12. As in Fig. C.1, but for December.

APPENDIX D

FIGURES FROM BAKER AND KLINK (1975)

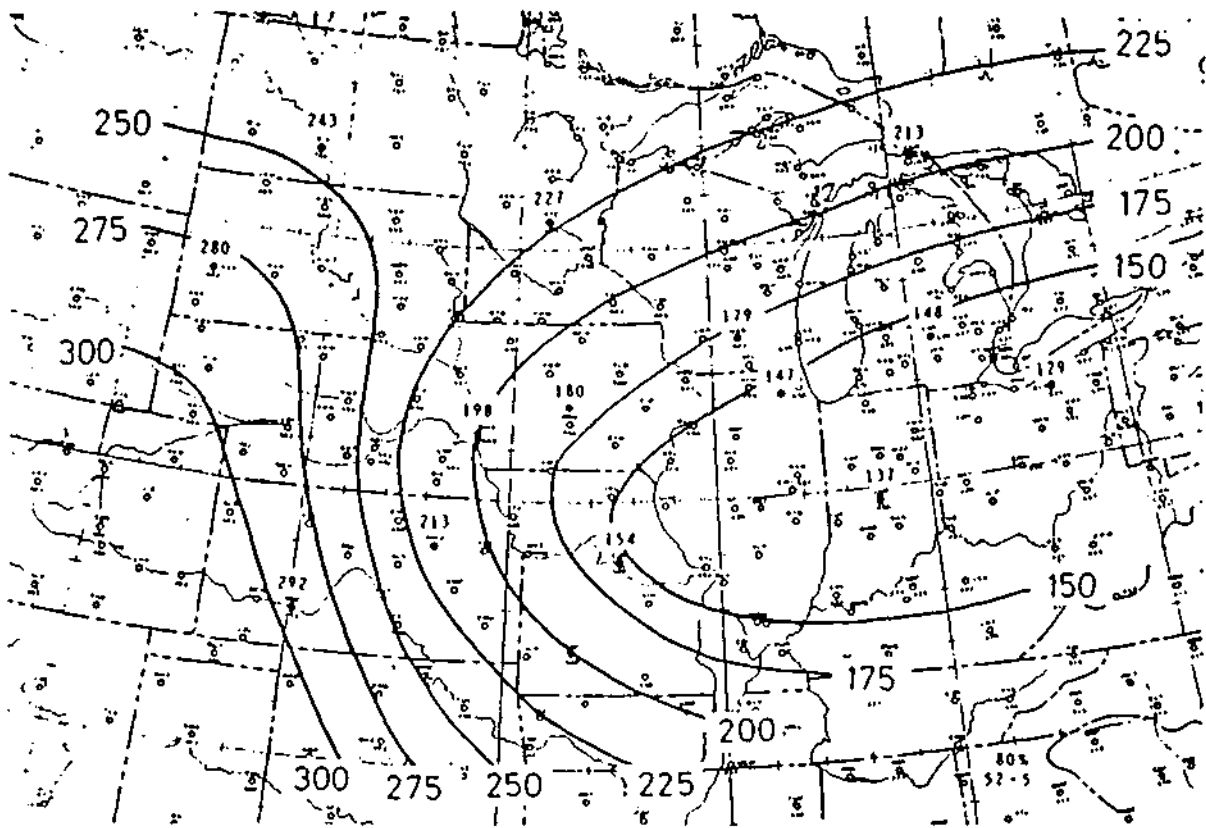


Fig. D.1. Average daily radiation received at the 80-percent level of probability during a period of similar radiation pattern that lasts from February 21 - April 4 (from Baker and Klink, 1975).

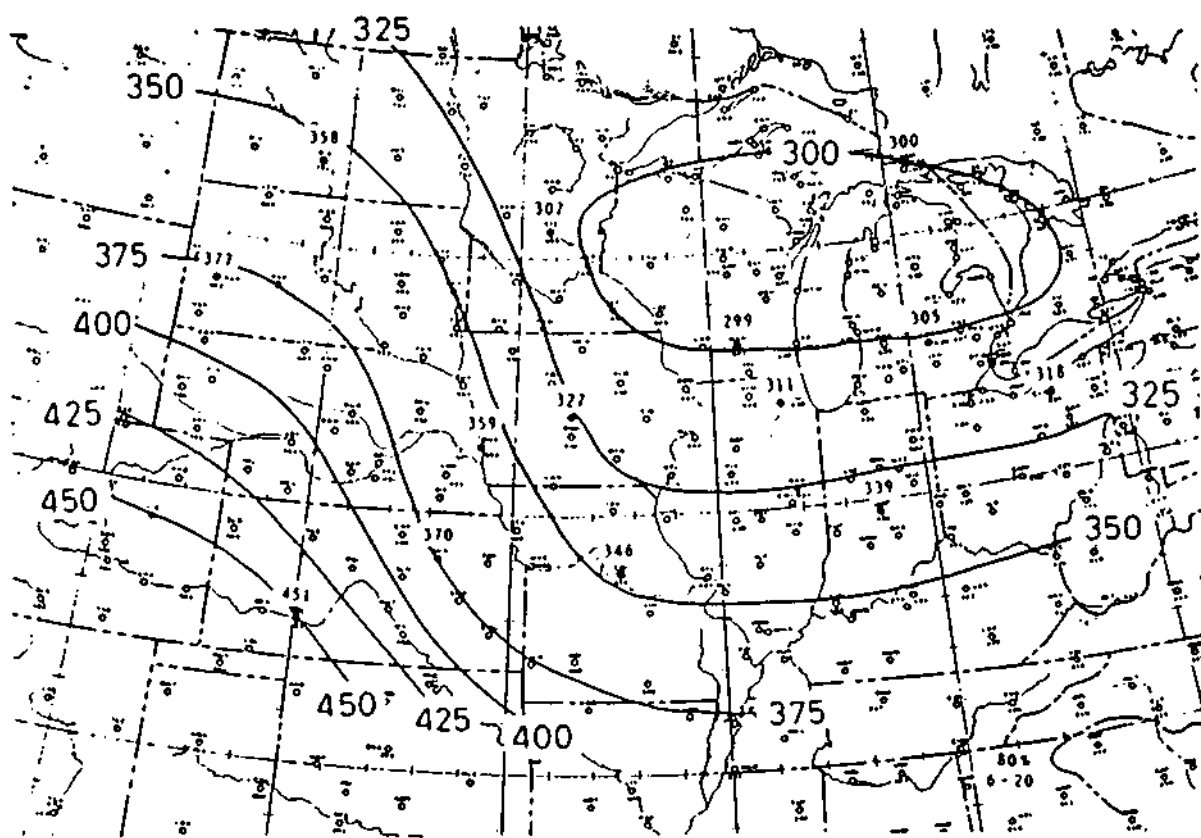


Fig. D.2. Same as in Fig. D.1, except from April 5 - July 18.

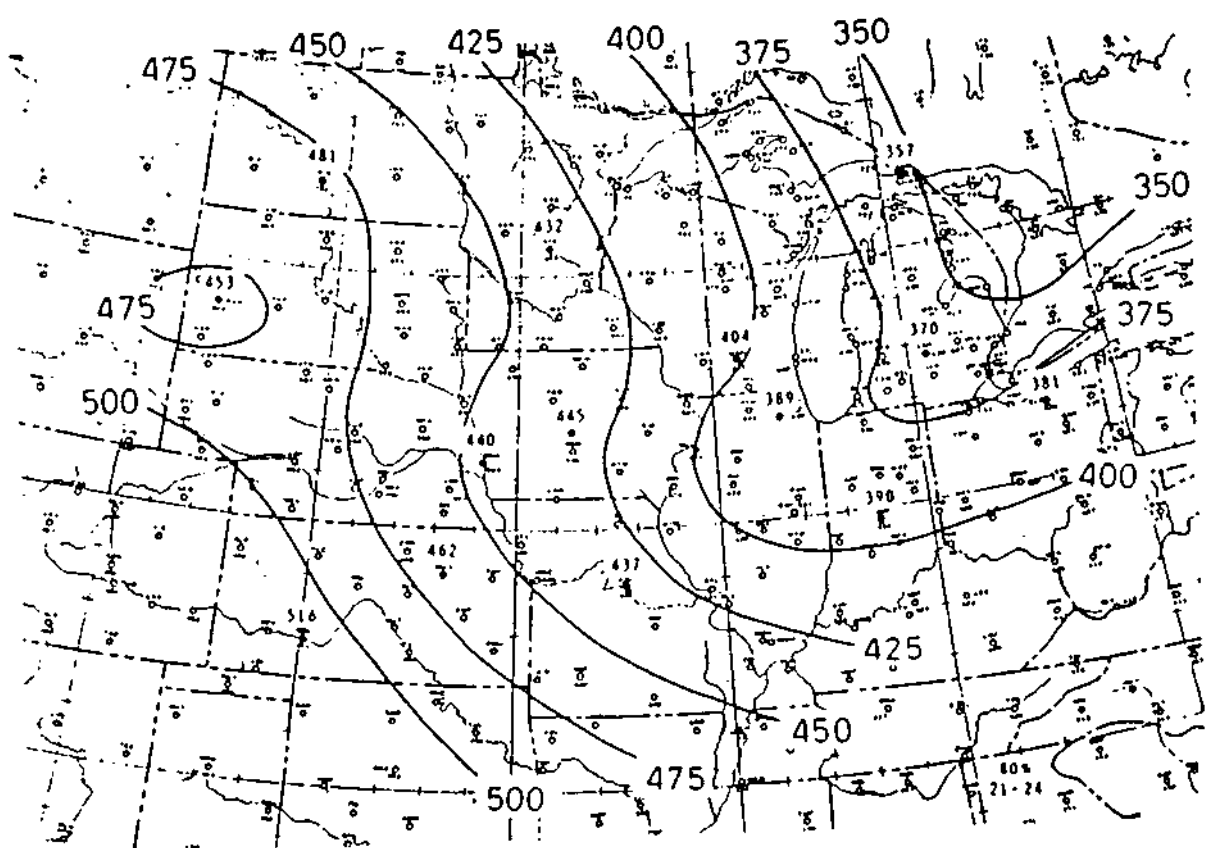


Fig. D.3. Same as in Fig. D.1, except from July 19 - August 15.

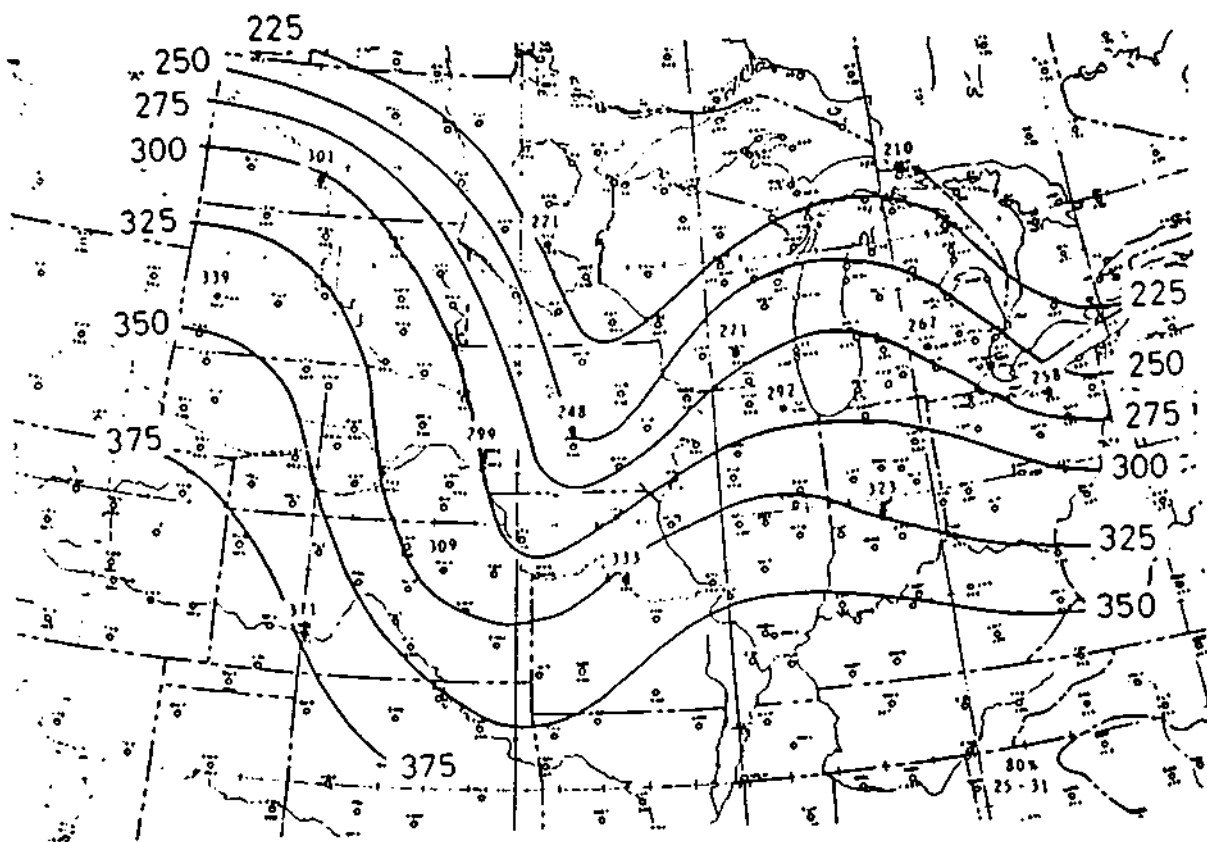


Fig. D.4. Same as in Fig. D.1, except from August 16 - October 3.

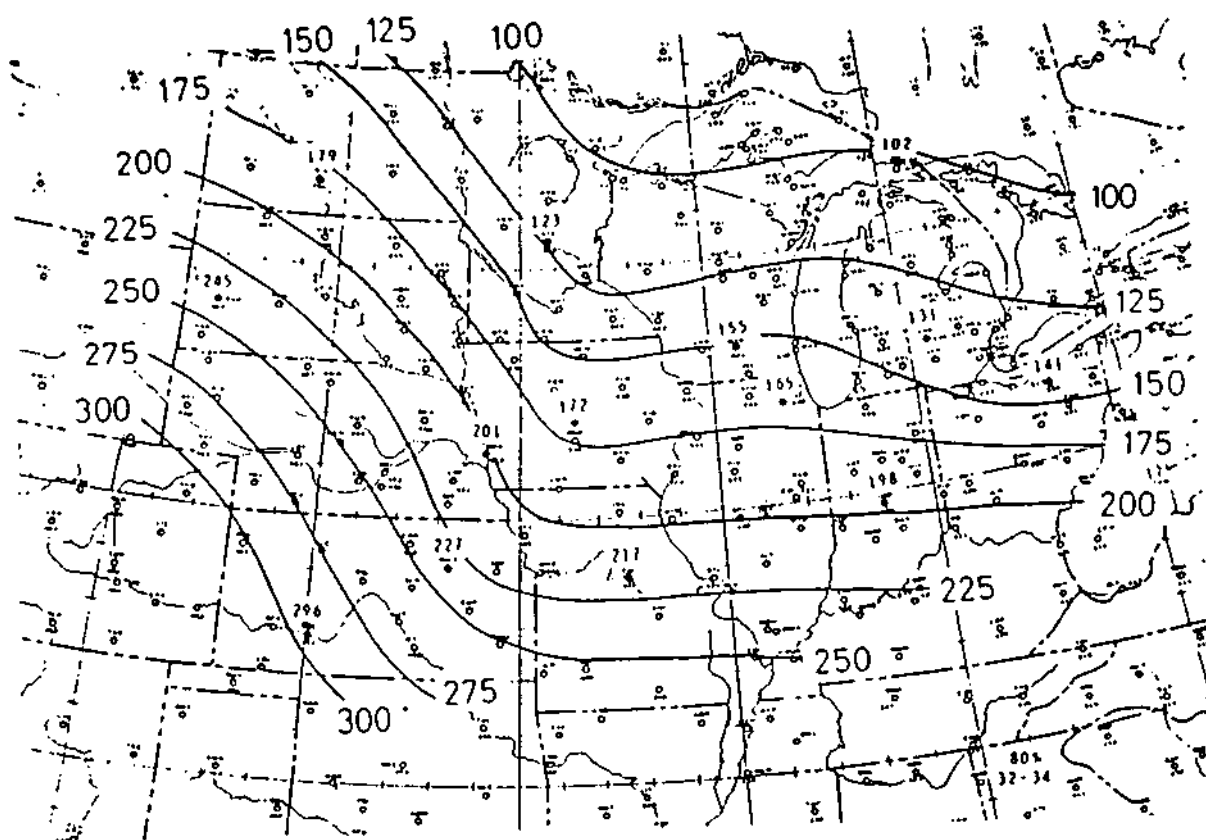


Fig. D.5. Same as in Fig. D.1, except from October 4 - October 24.

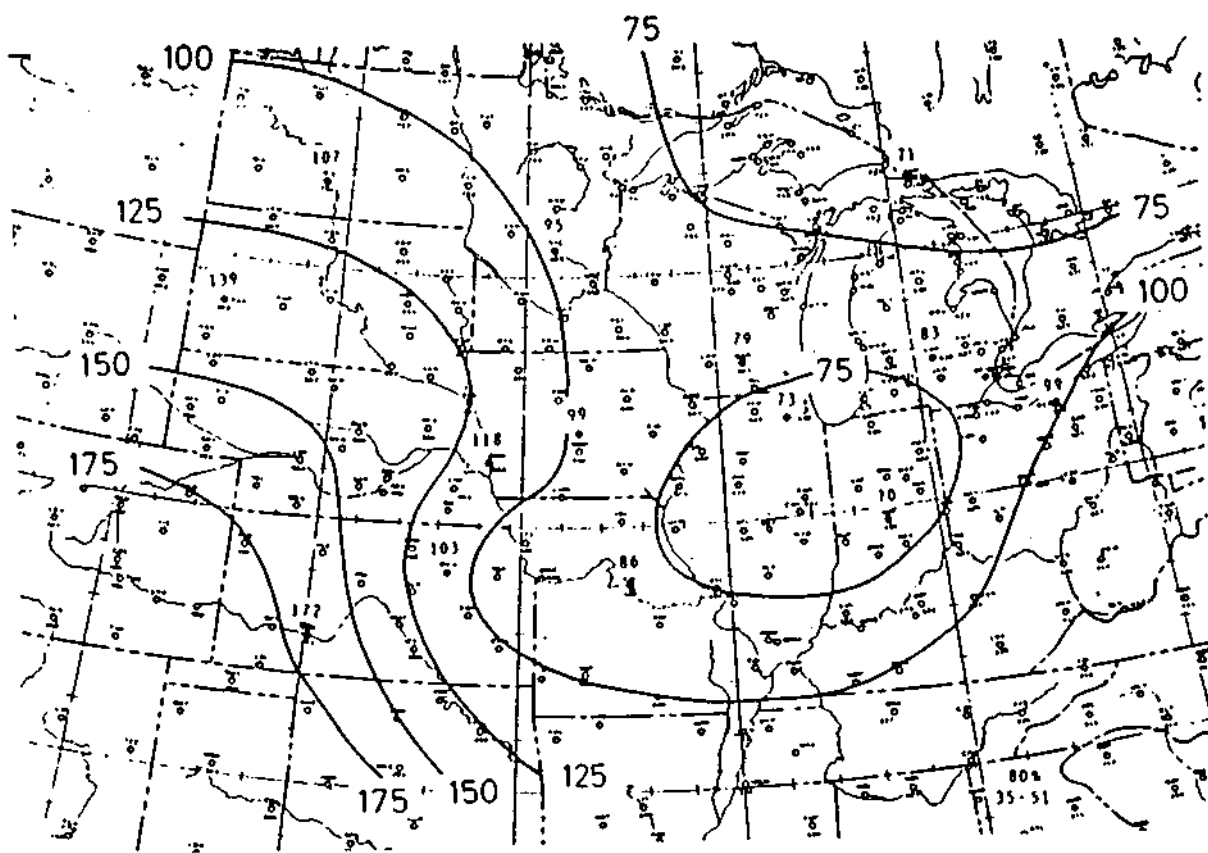


Fig. D.6. Same as in Fig. D.1, except from October 25 - February 20.

APPENDIX E

MID-SEASON TIME SERIES

Time series plots for all stations for the mid-season months January, April, July, and October. Number in upper right-hand corner indicates the statistical significance of the trend (slope), based on the Student's t test.

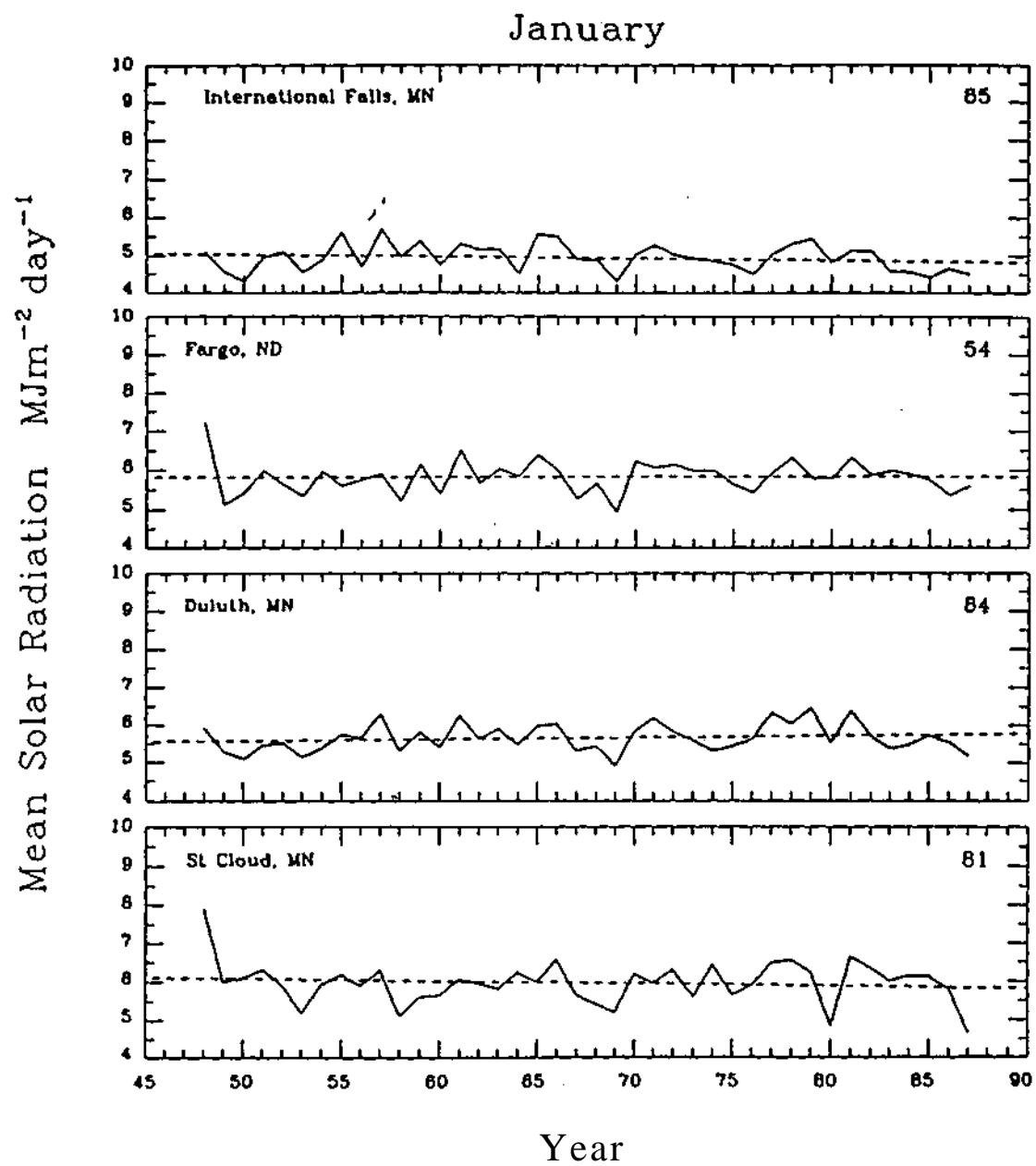


Fig. E.1. Solid line is SR time series for indicated month and stations; dashed line is regression line. Number in upper right-hand corner indicates statistical significance of the regression line slope.

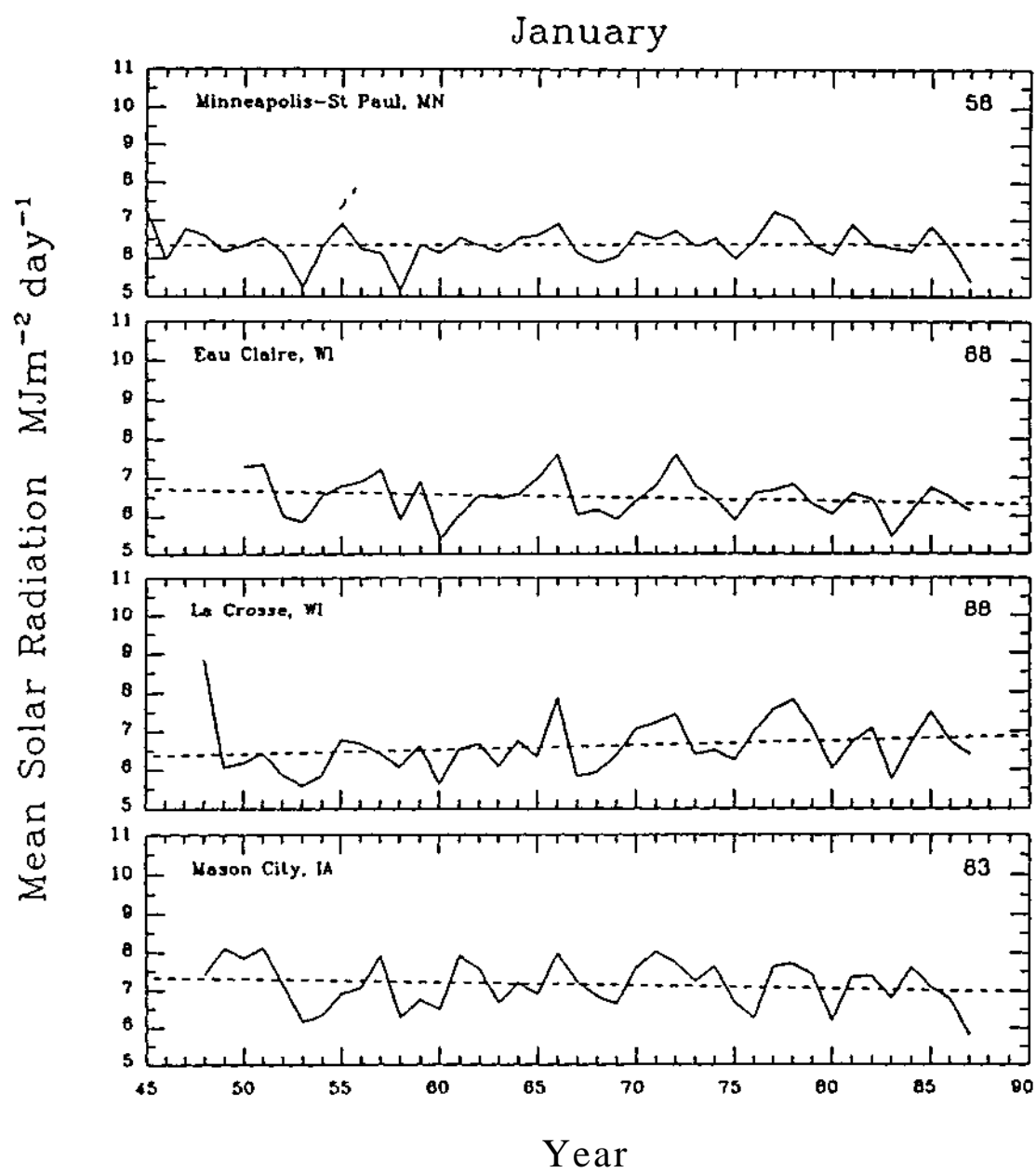


Fig. E.2. As in Fig. E.1.

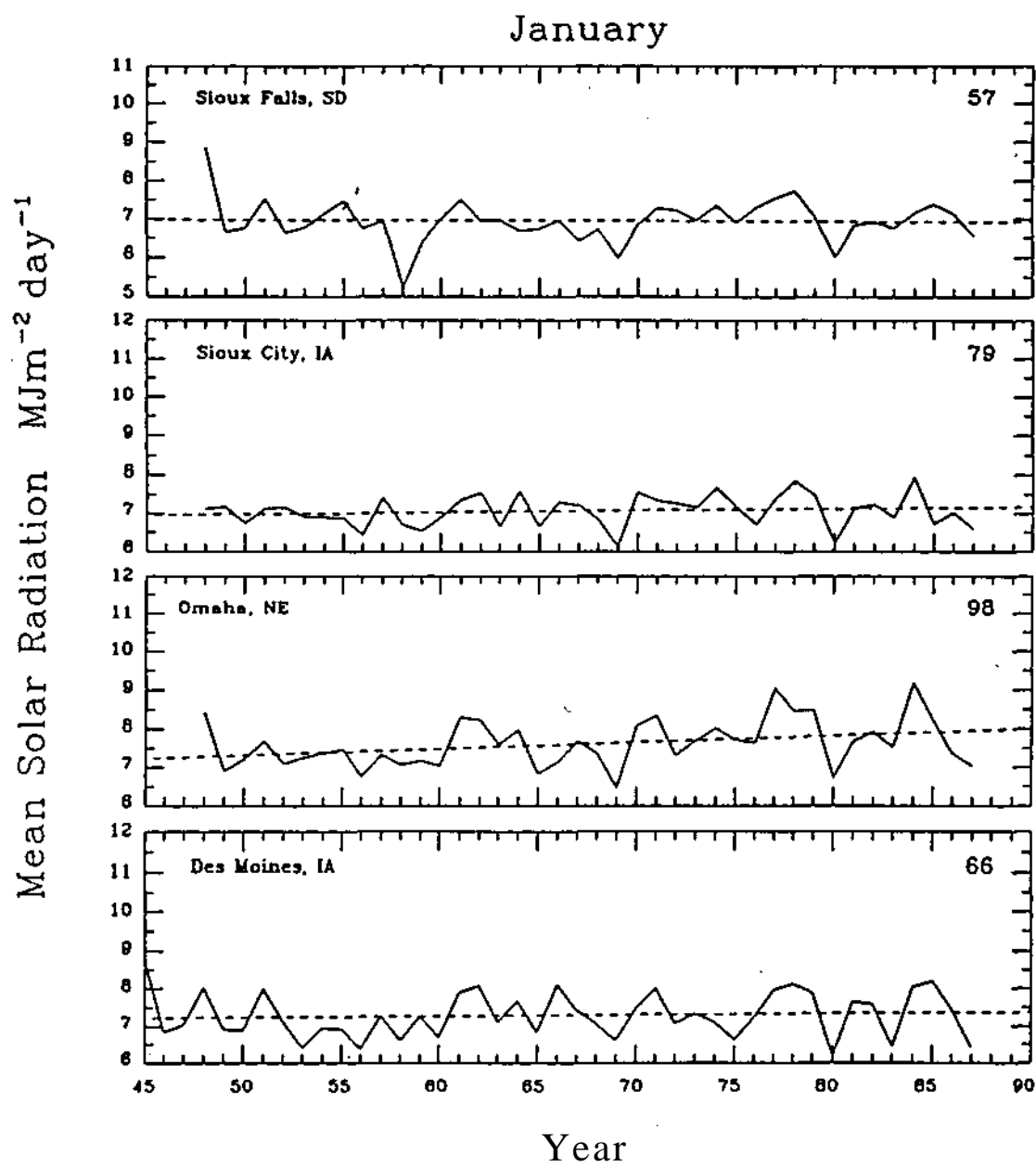


Fig. E.3. As in Fig. E.1.

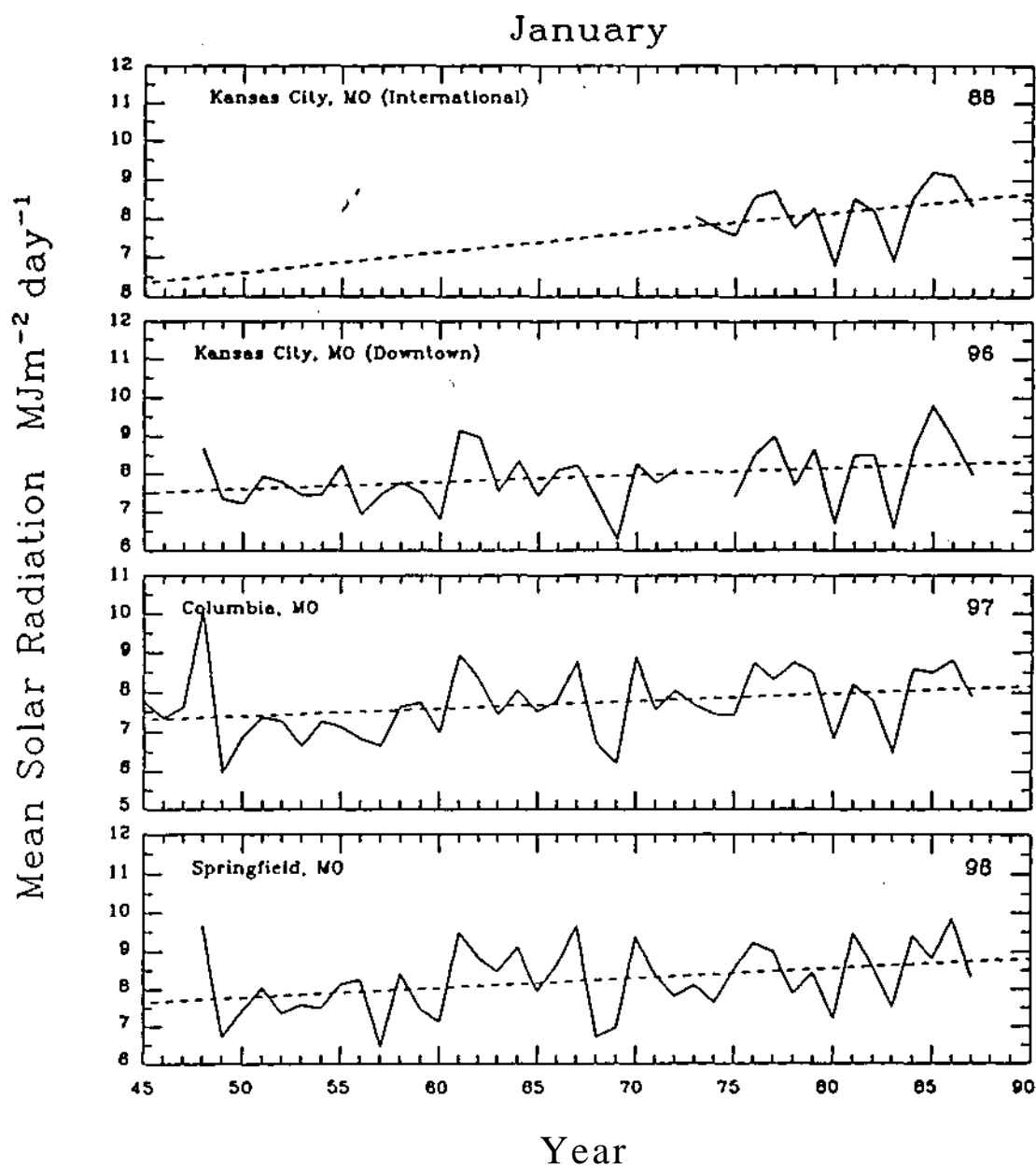


Fig. E.4. As in Fig. E.1.

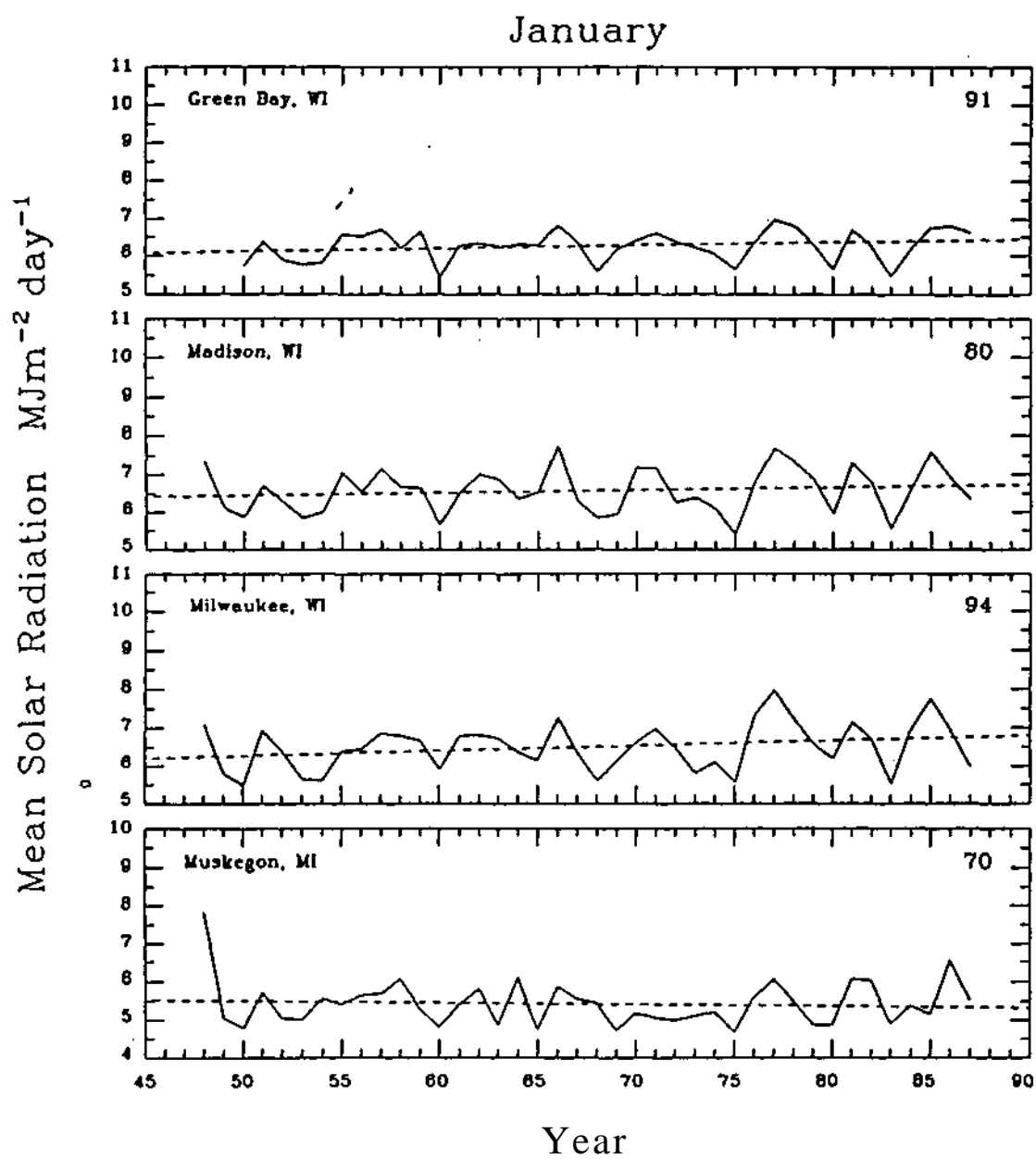


Fig. E.5. As in Fig. E.1.

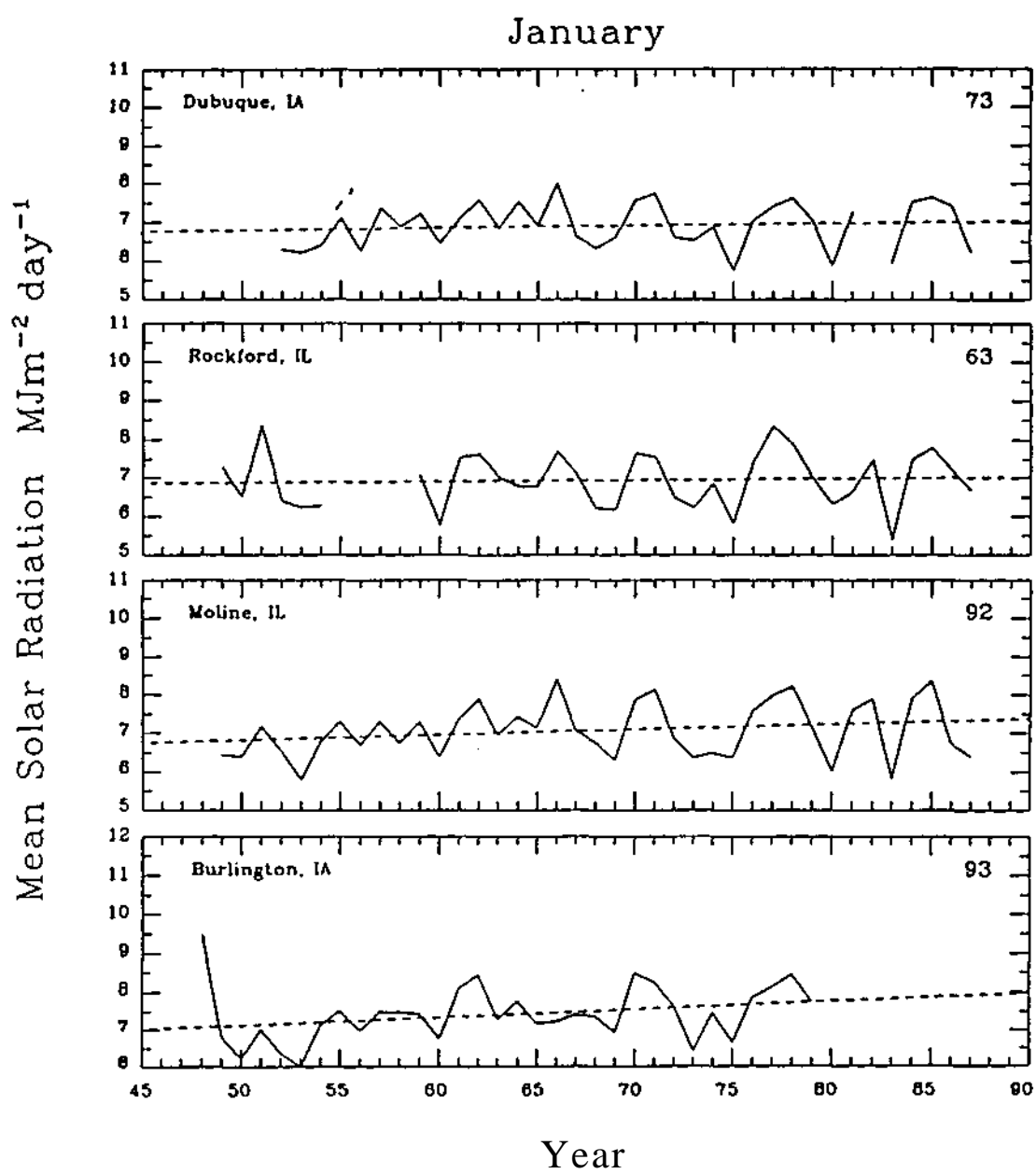


Fig. E.6. As in Fig. E.1.

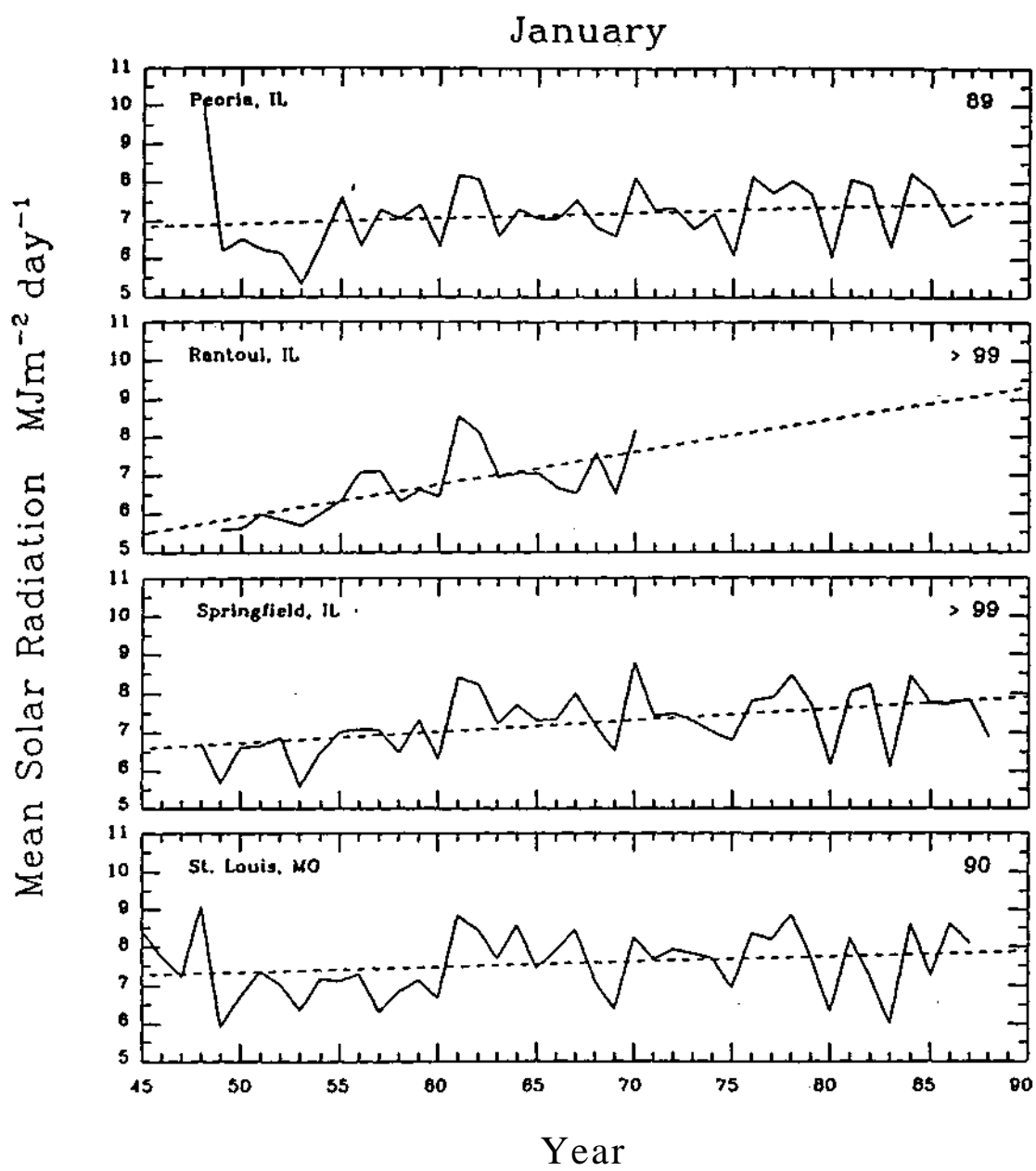


Fig. E.7. As in Fig. E.1.

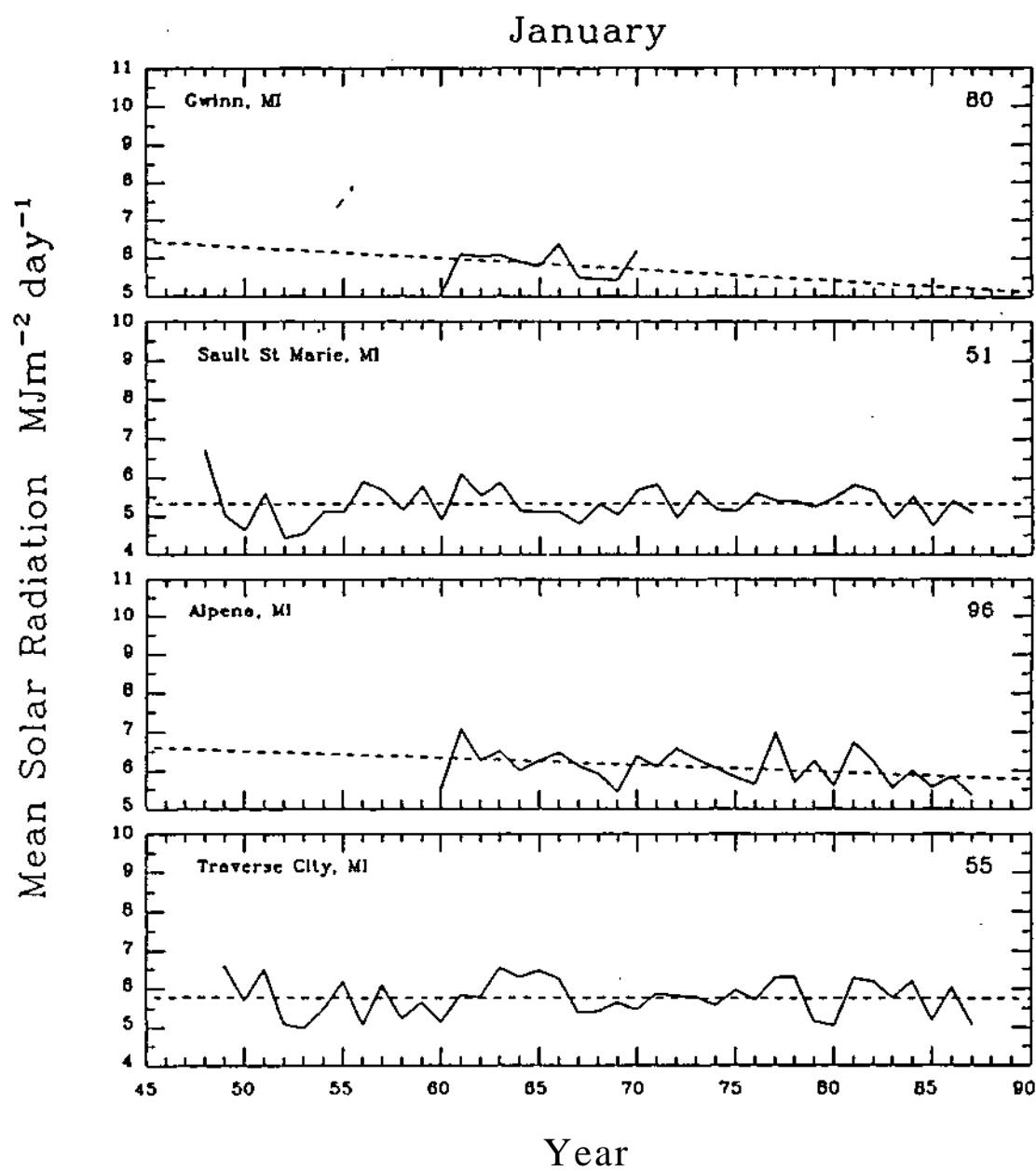


Fig. E.8. As in Fig. E.1.

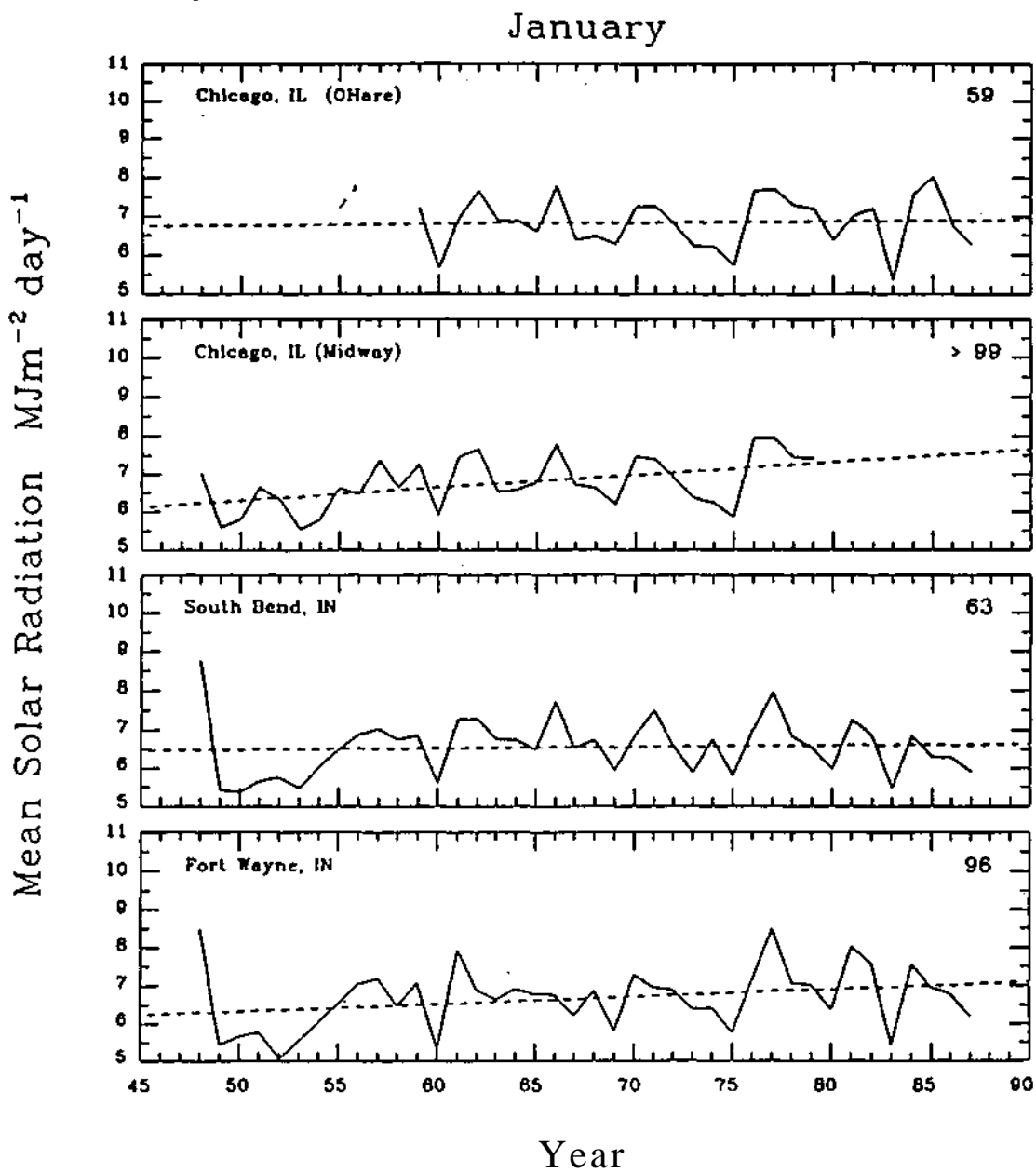


Fig. E.9. As in Fig. E.1.

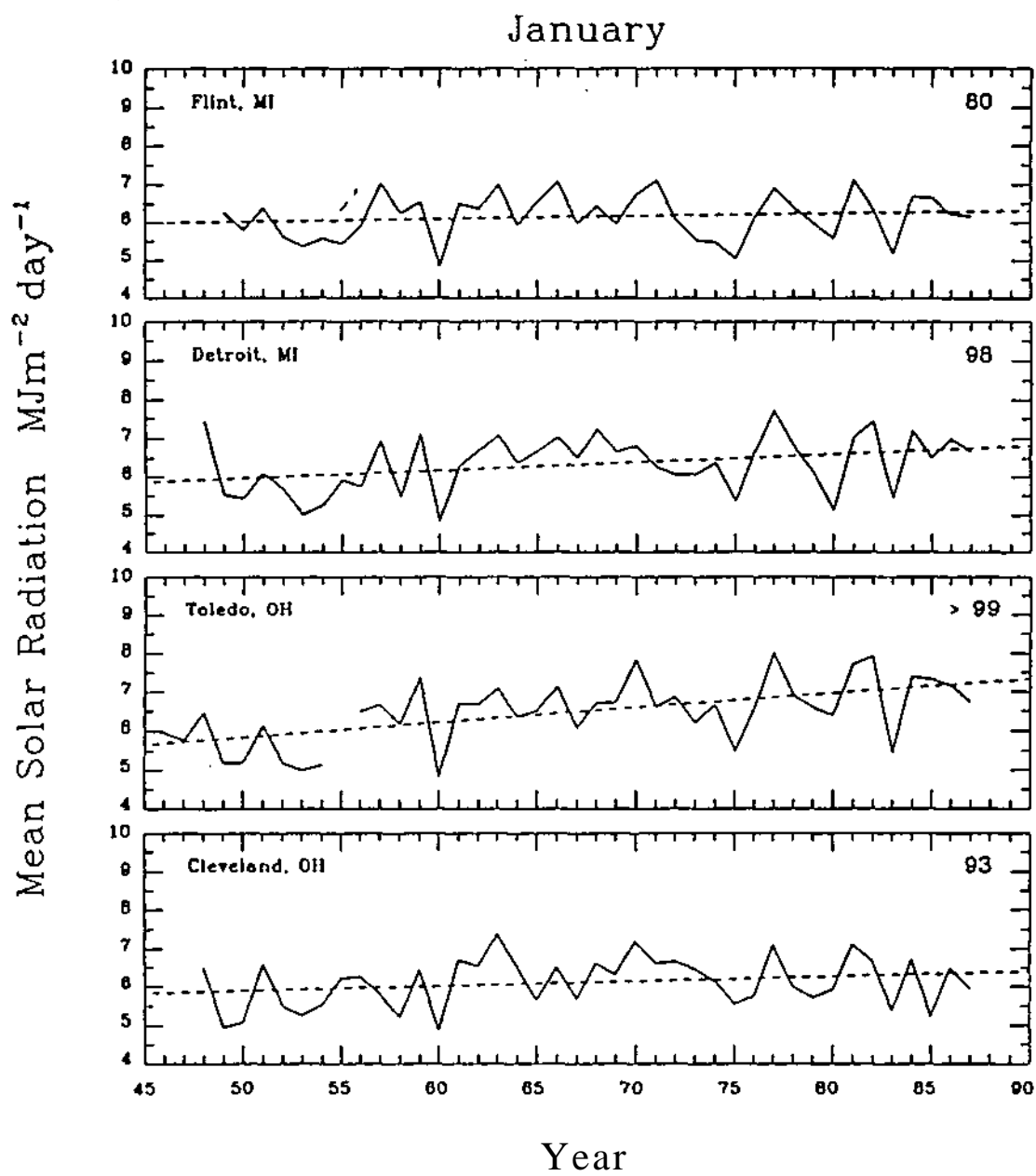


Fig. E.10. As in Fig. E.1.

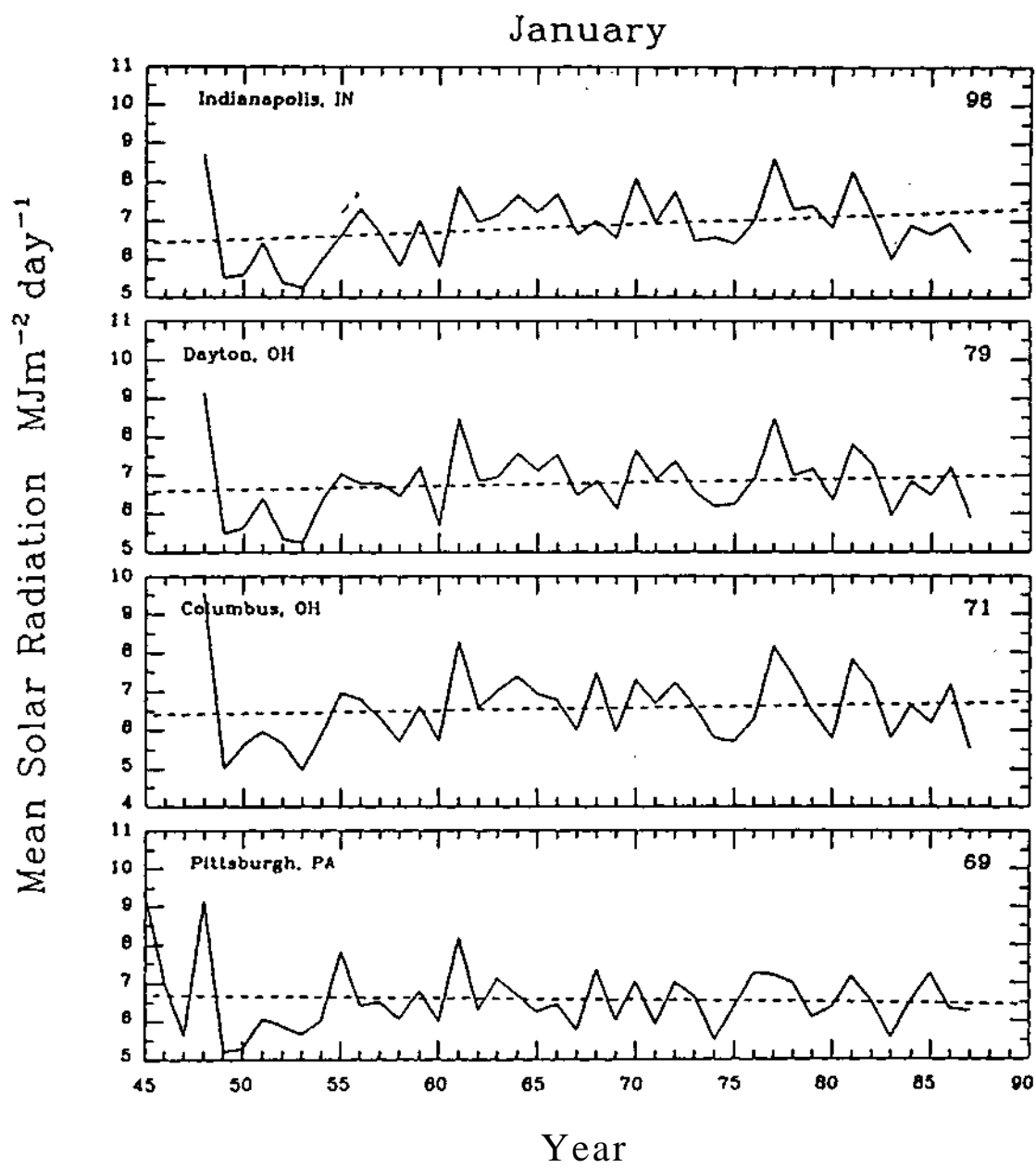


Fig. E.11. As in Fig. E.1.

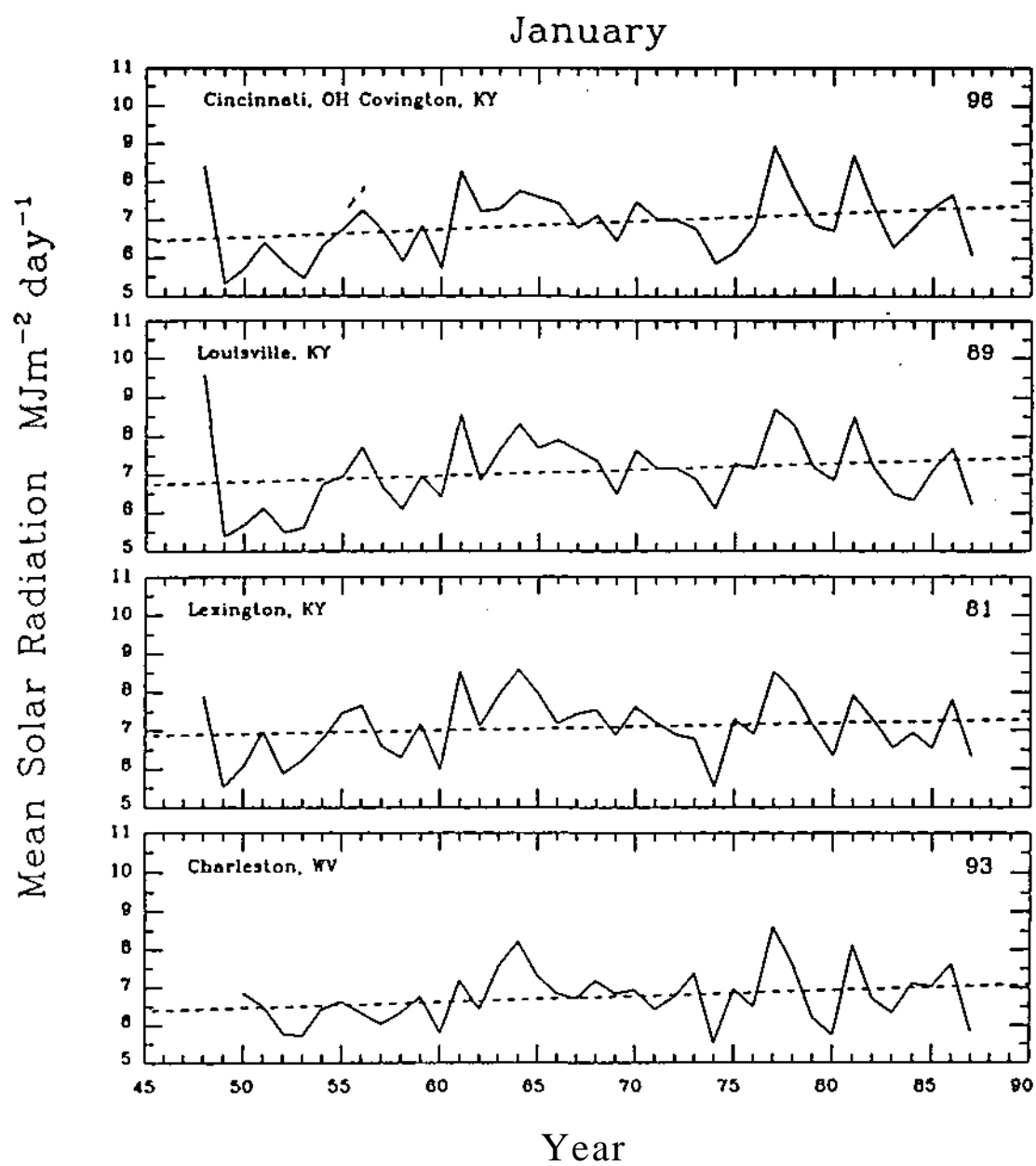


Fig. E.12. As in Fig. E.1.

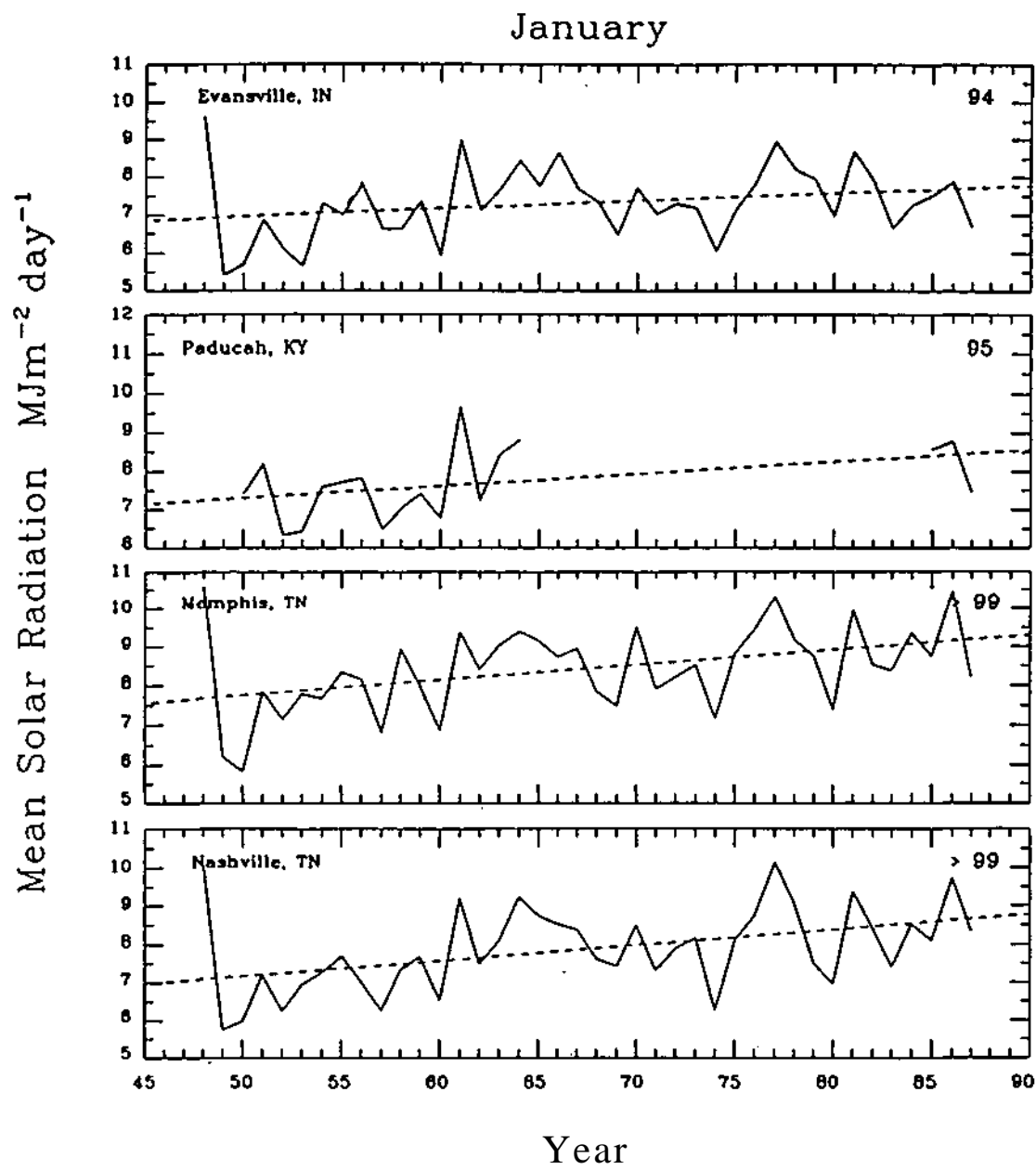


Fig. E.13. As in Fig. E.1.

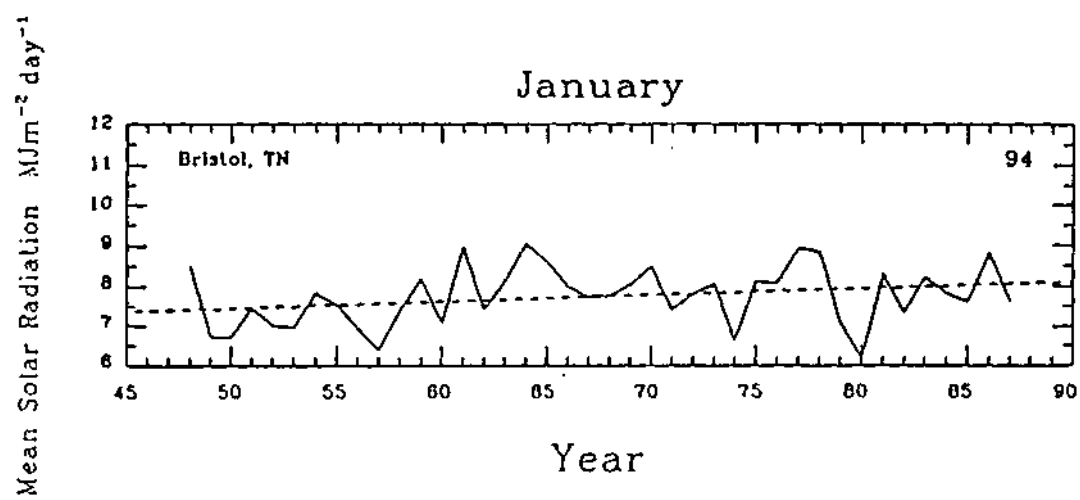


Fig. E.14. As in Fig. E.1.

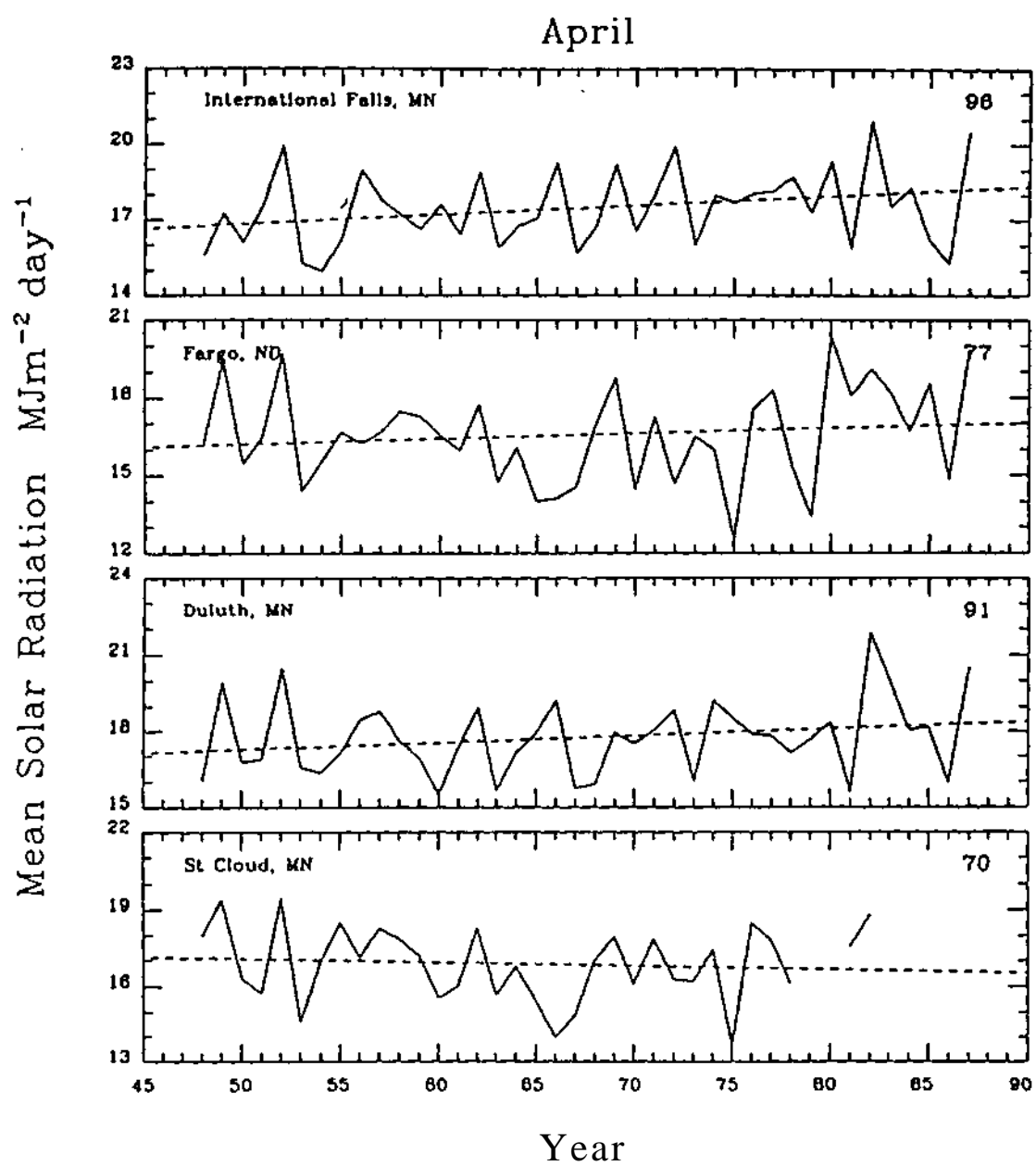


Fig. E.15. As in Fig. E.1.

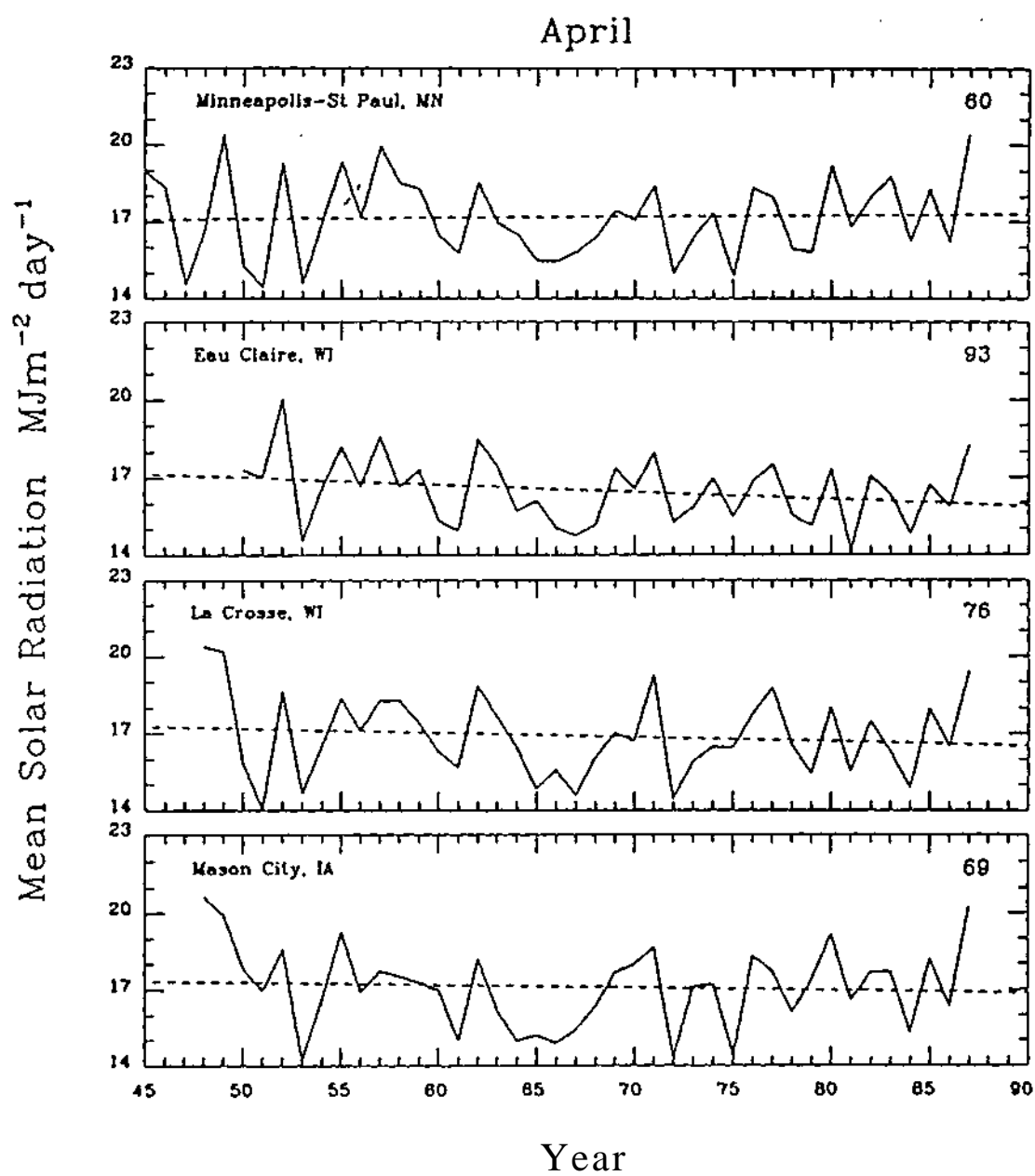


Fig. E.16. As in Fig. E.1.

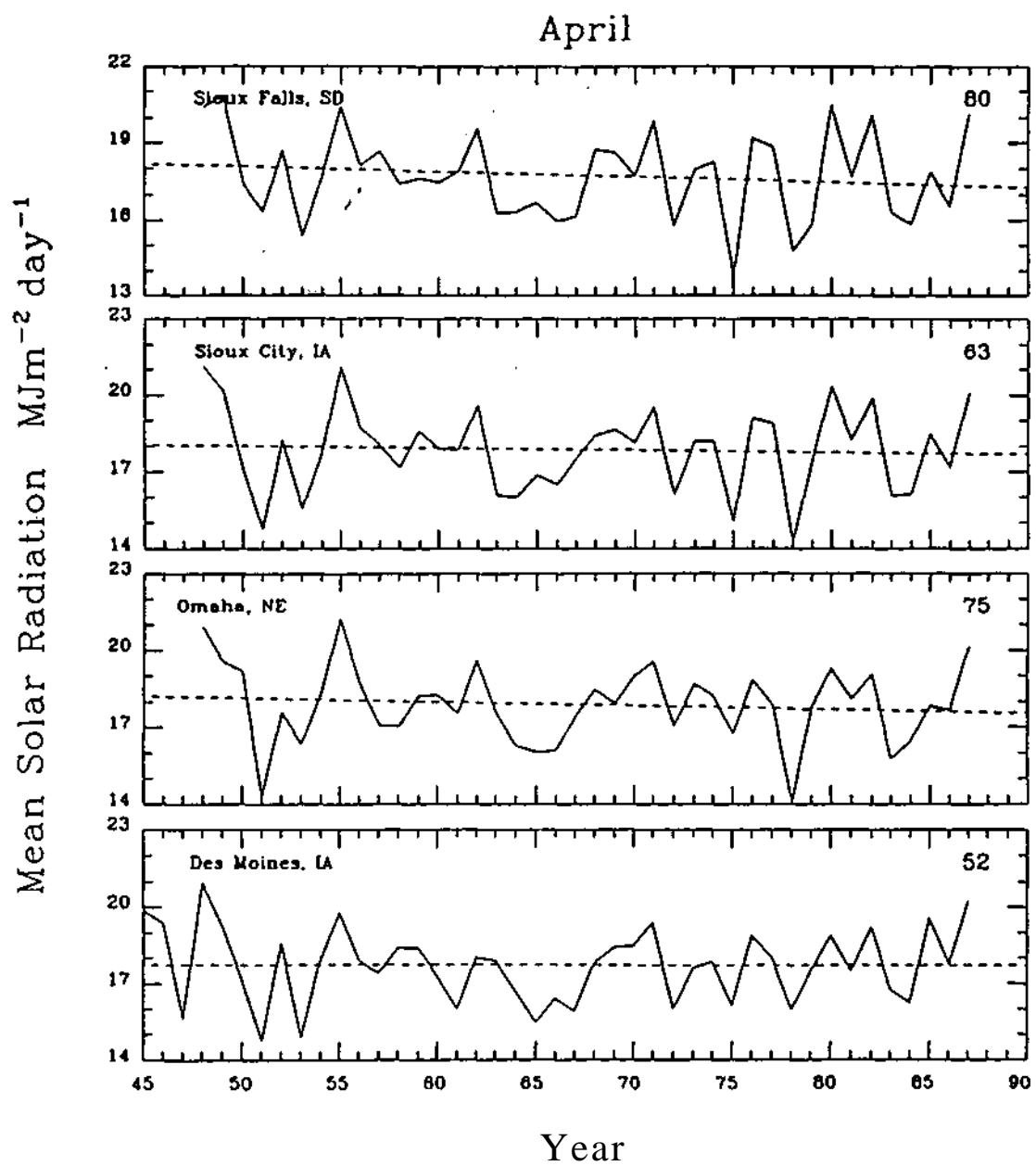


Fig. E.17. As in Fig. E.1.

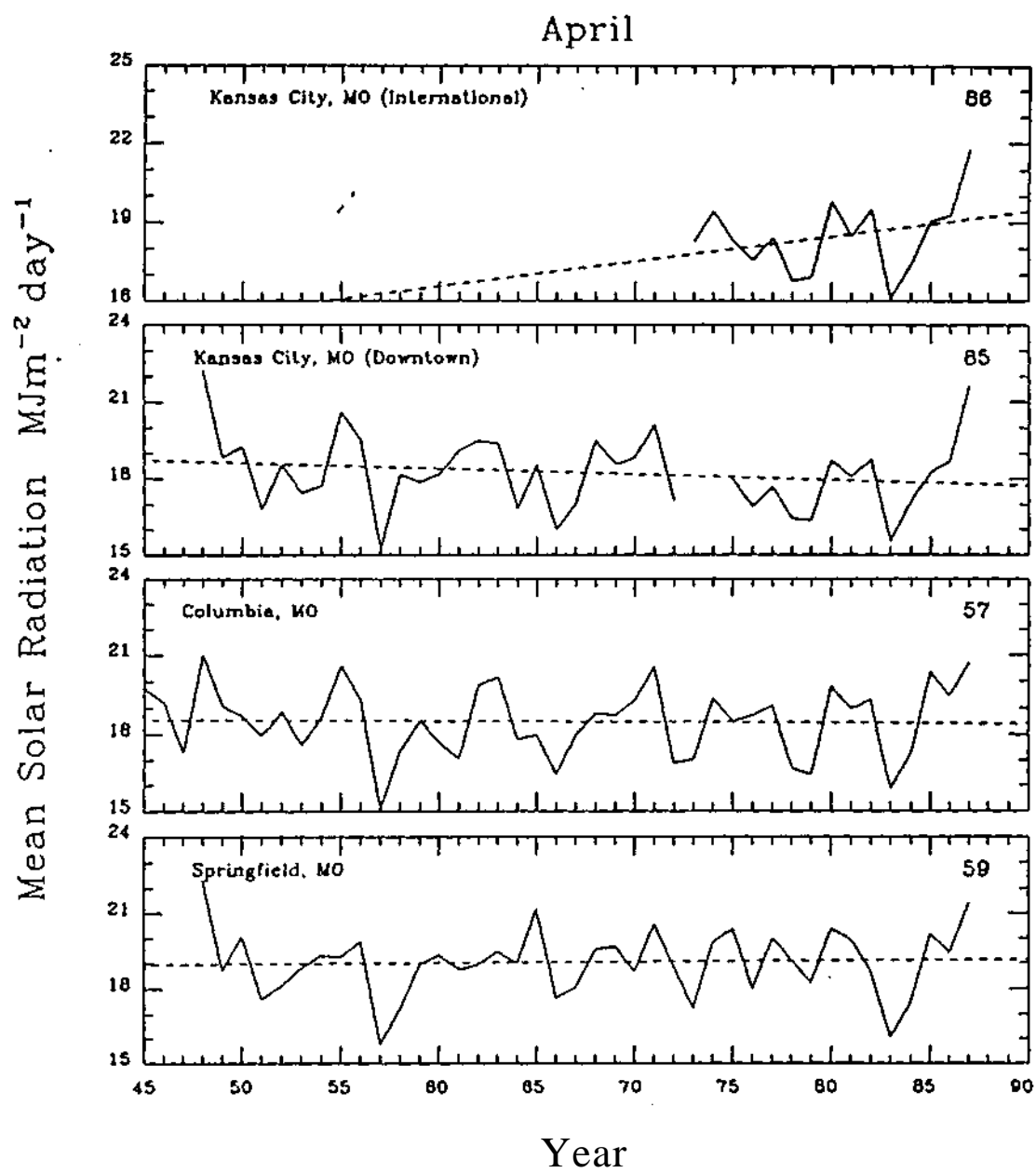


Fig. E.18. As in Fig. E.1.

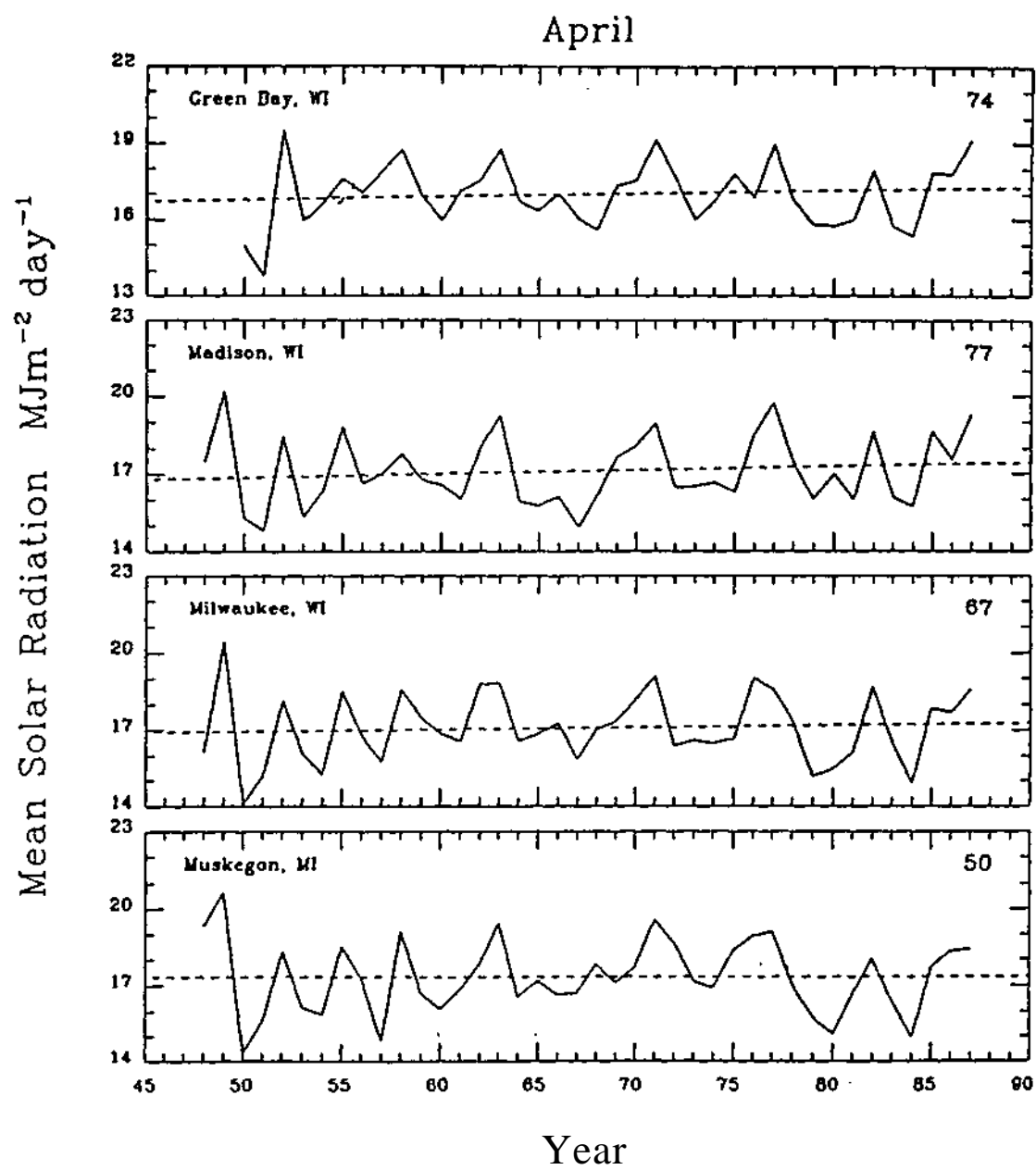


Fig. E.19. As in Fig. E.1.

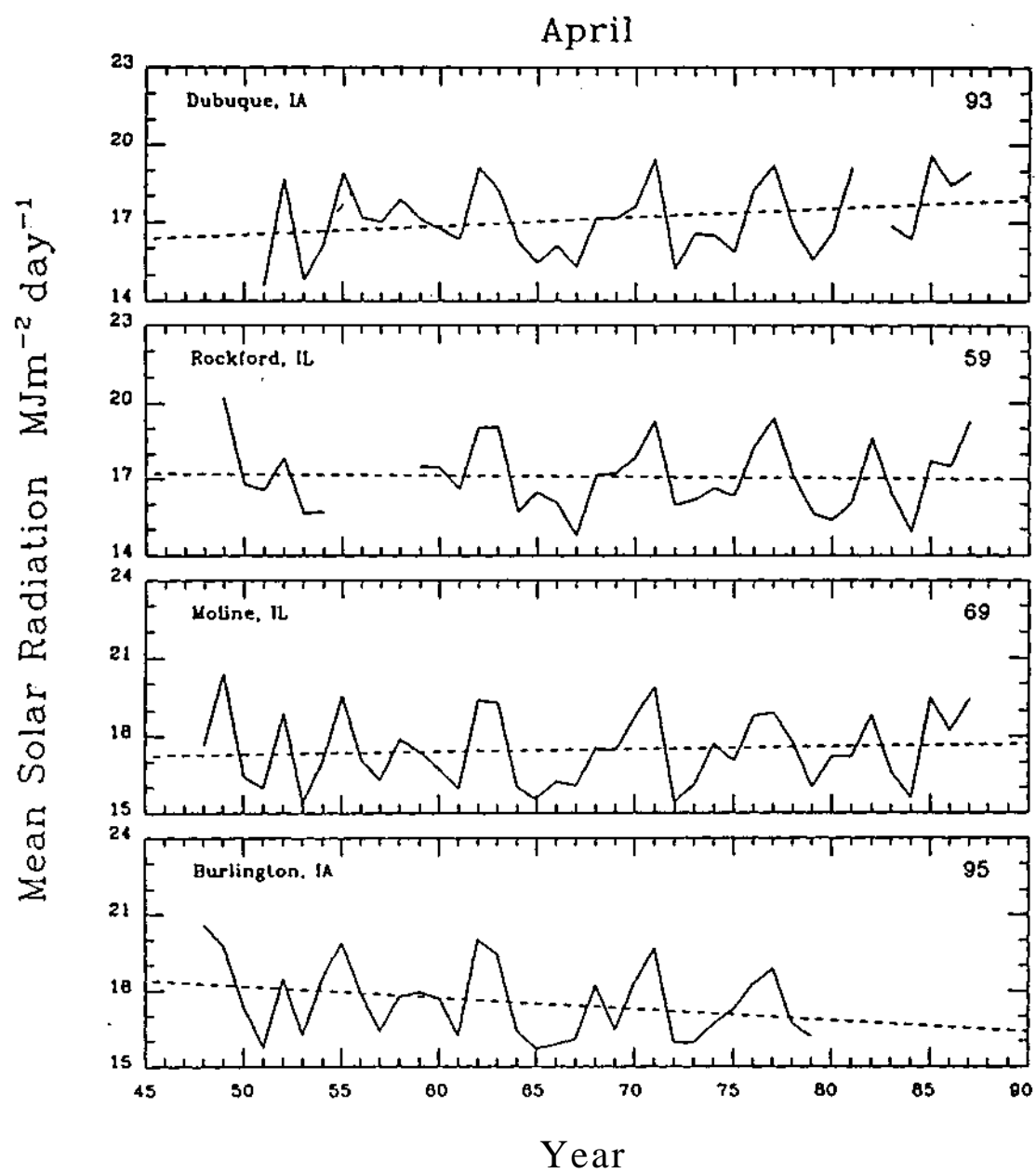


Fig. E.20. As in Fig. E.1.

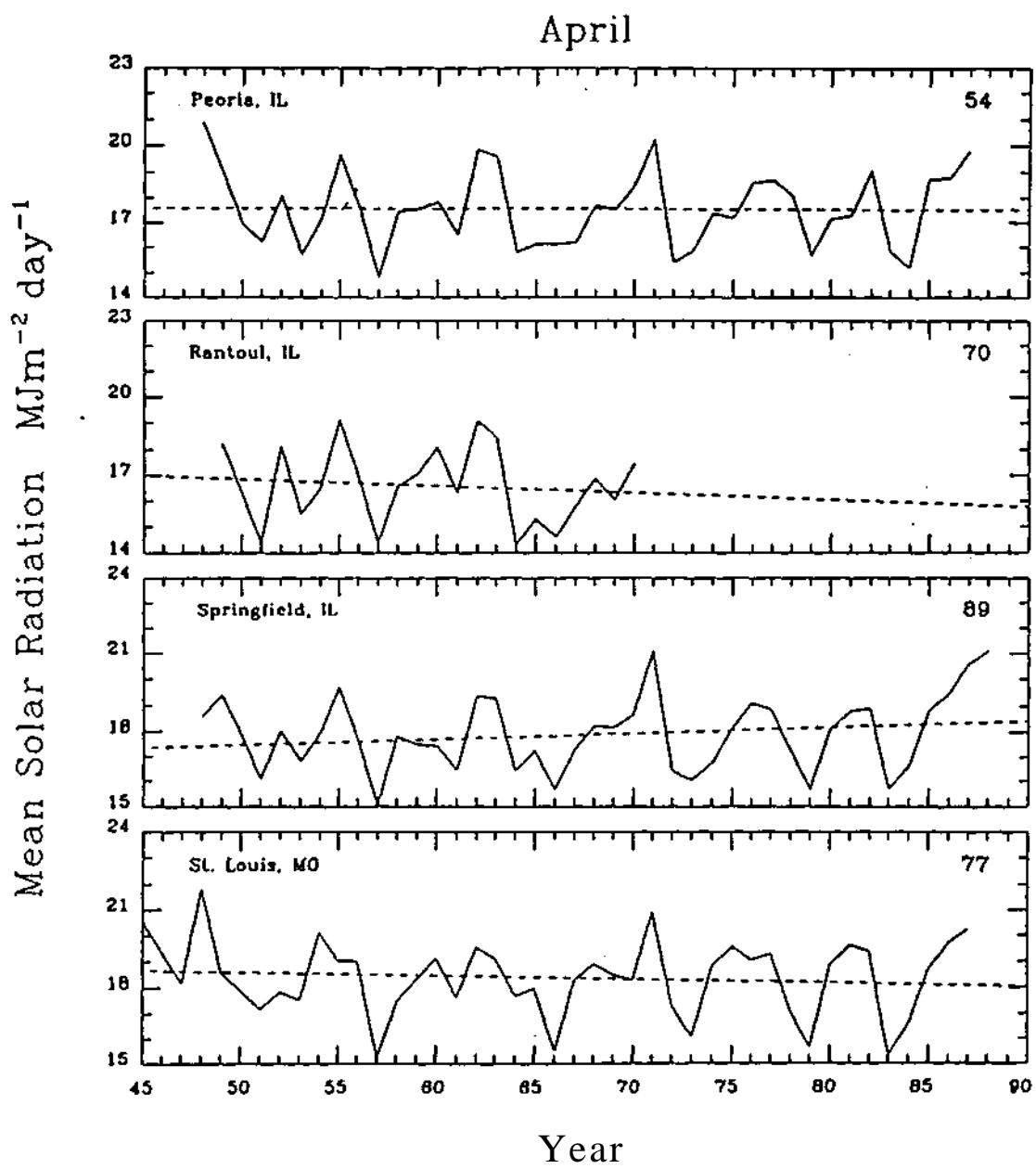


Fig. E.21. As in Fig. E.1.

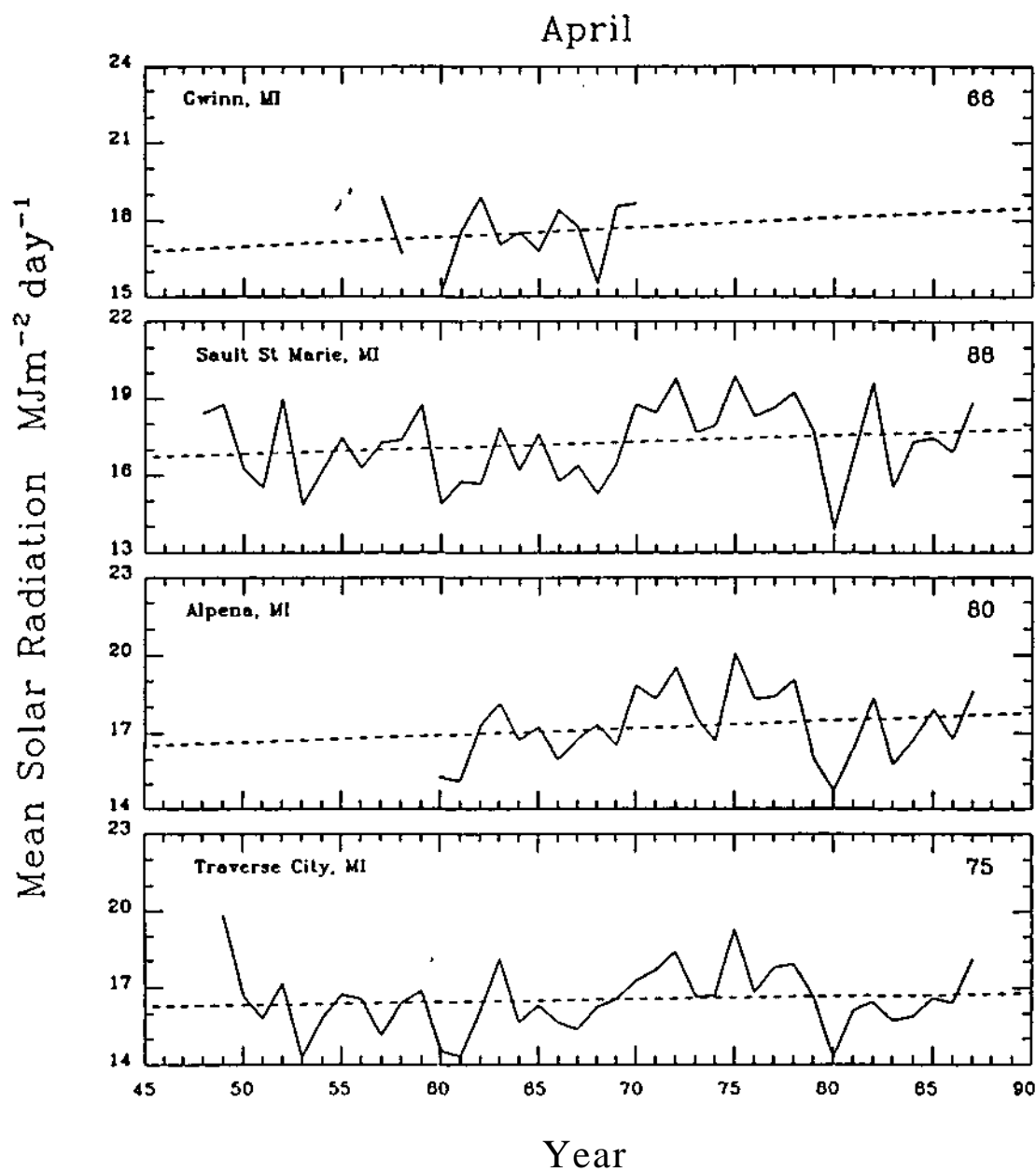


Fig. E.22. As in Fig. E.1.

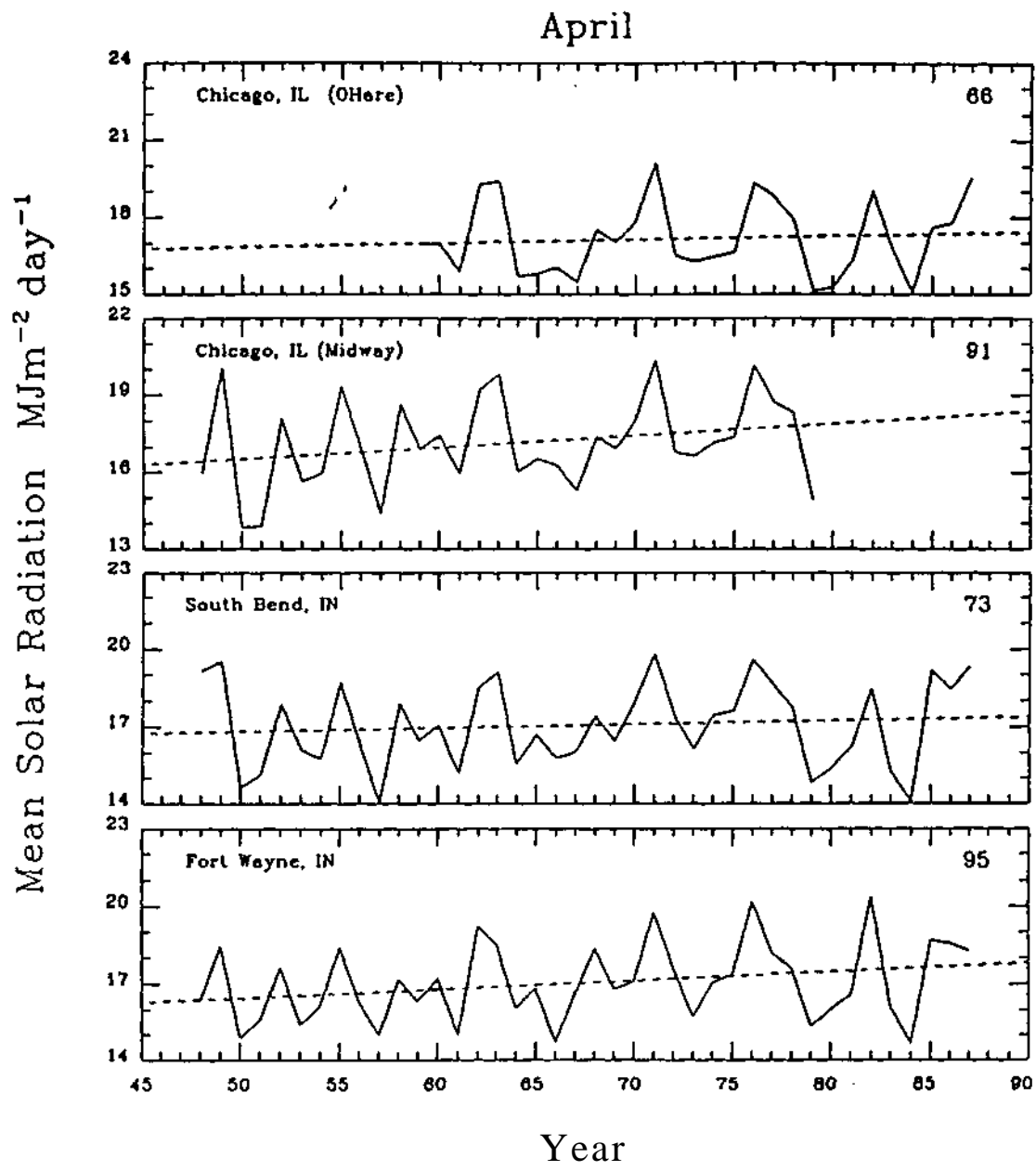


Fig. E.23. As in Fig. E.1.

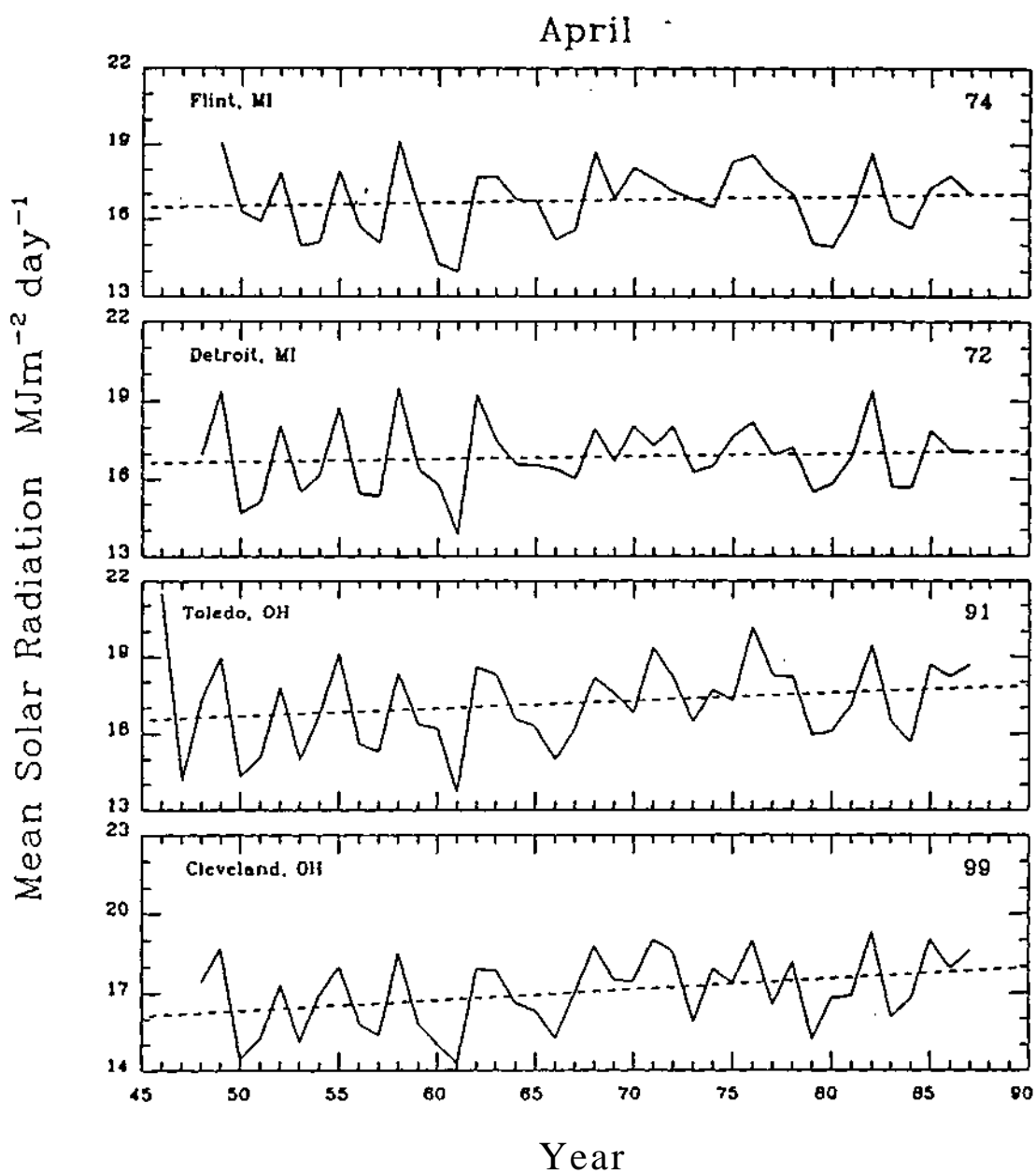


Fig. E.24. As in Fig. E.1.

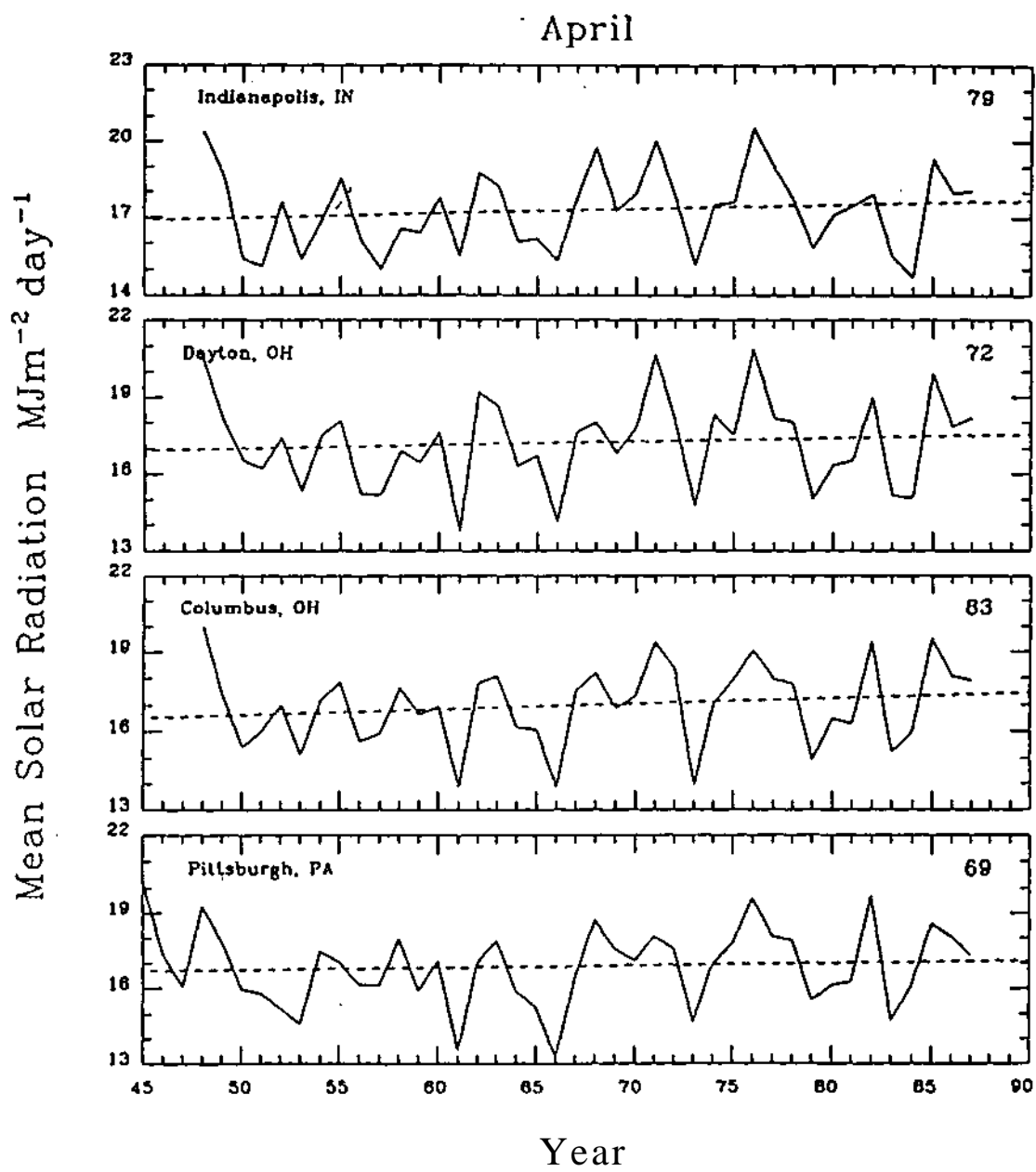


Fig. E.25. As in Fig. E.1.

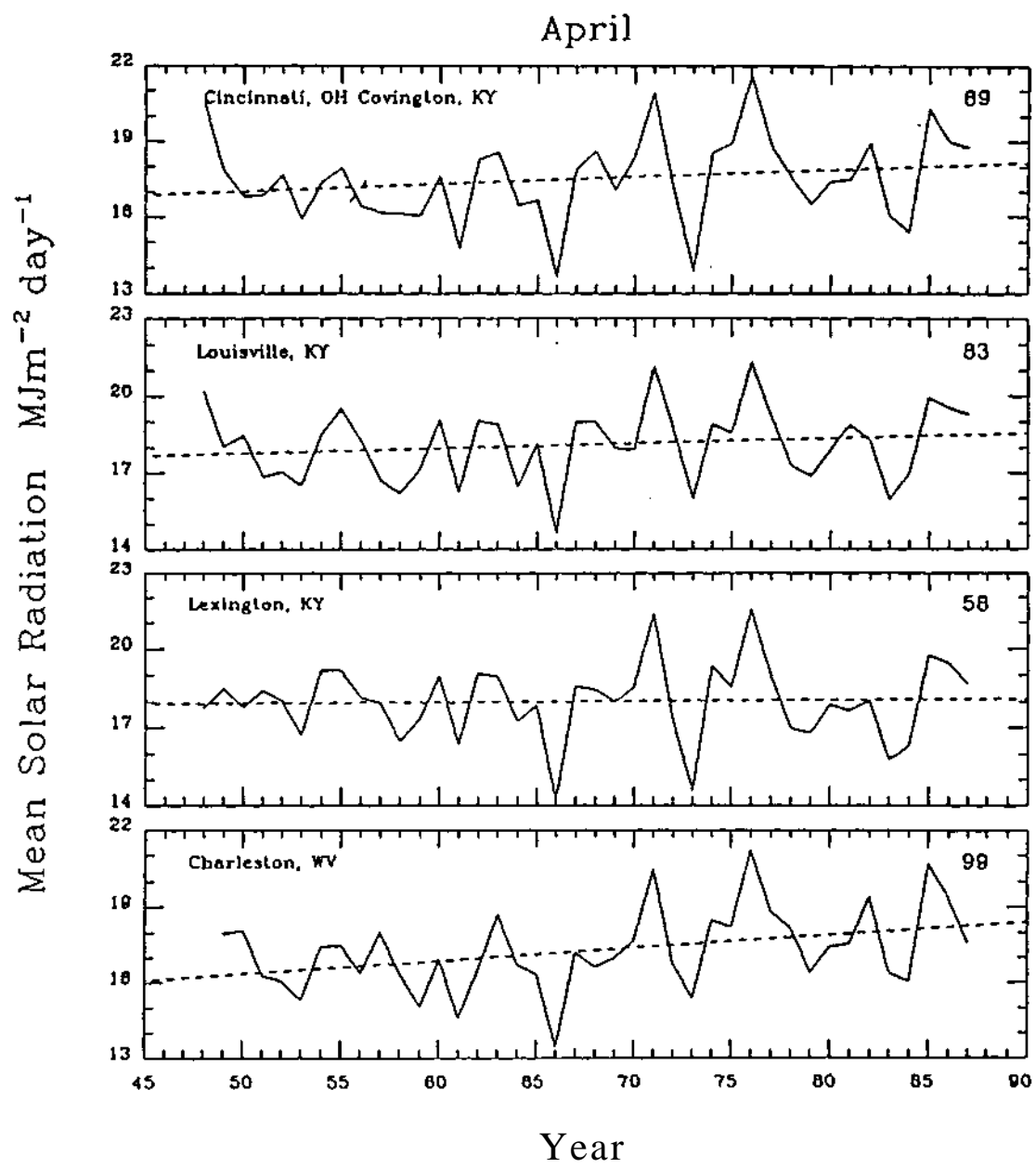


Fig. E.26. As in Fig. E.1.

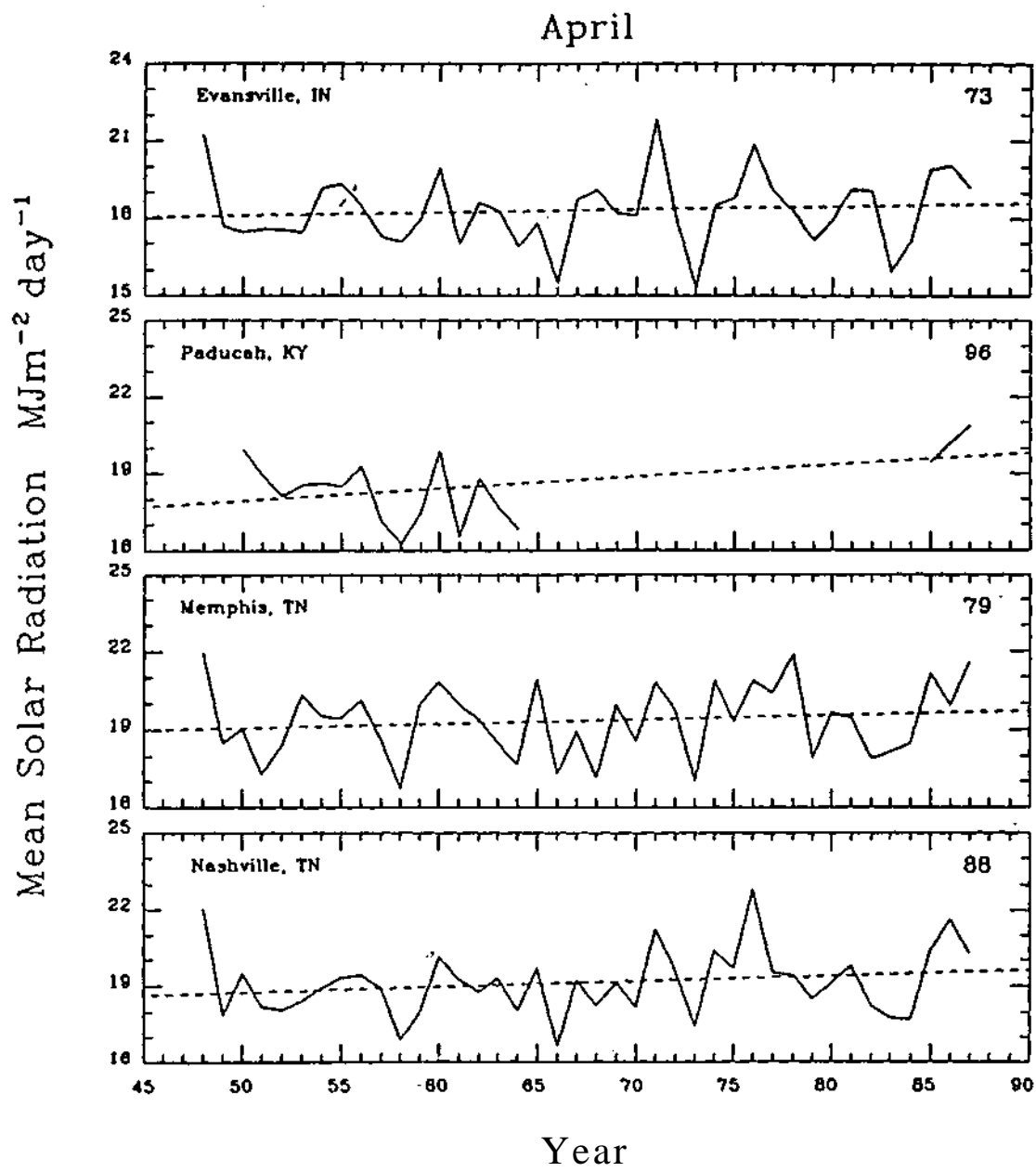


Fig. E.27. As in Fig. E.1.

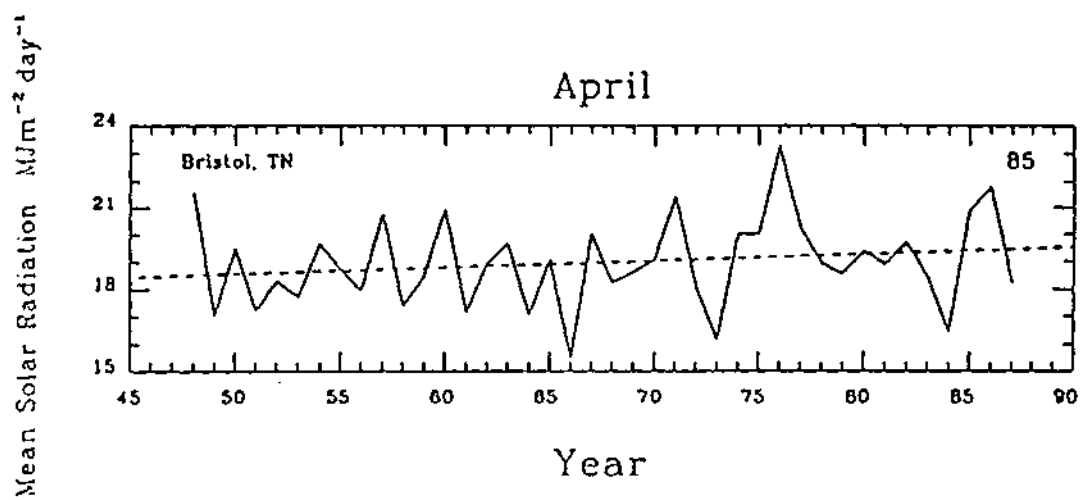


Fig. E.28. As in Fig. E.1.

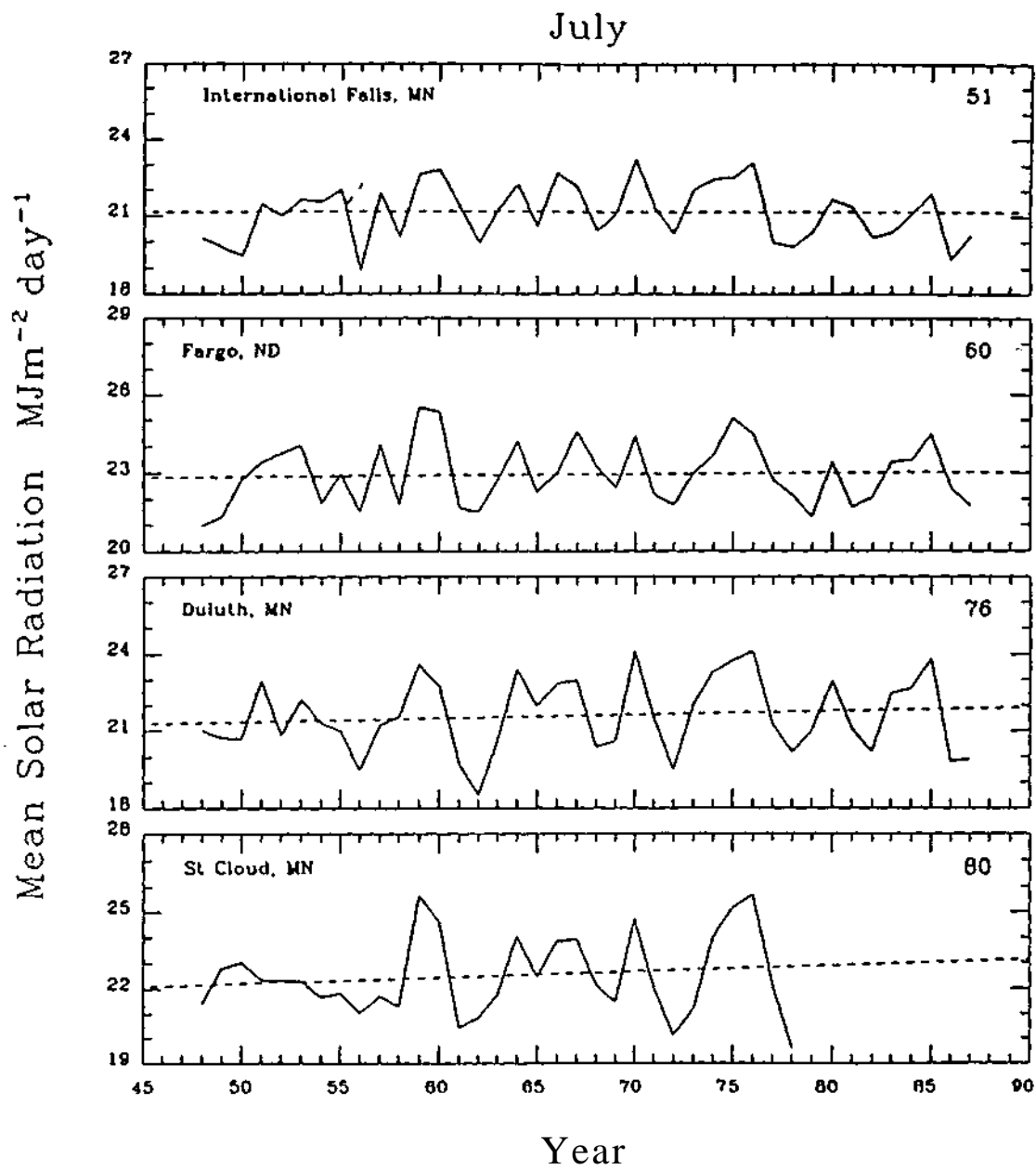


Fig. E.29. As in Fig. E.1.

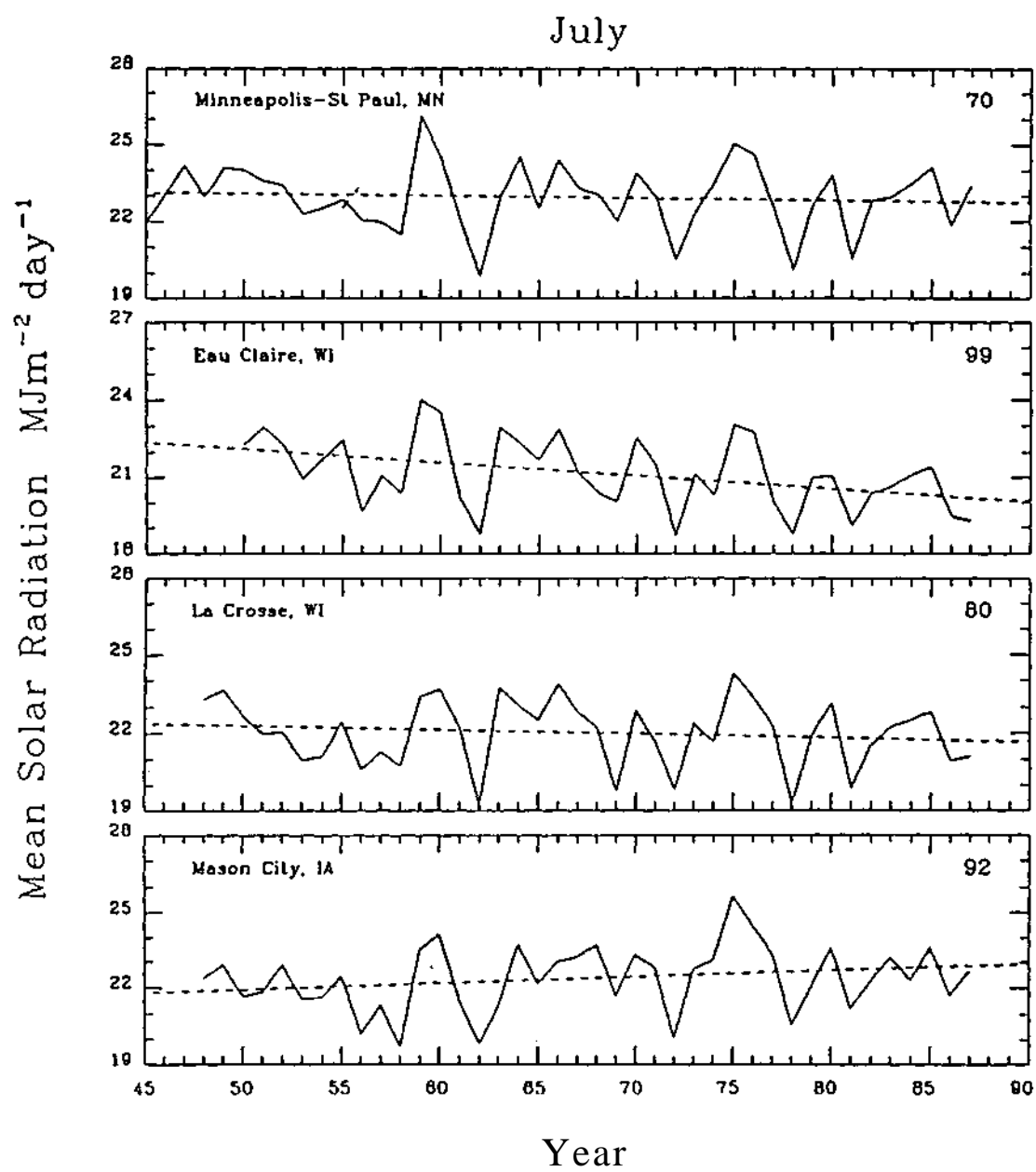


Fig. E.30. As in Fig. E.1.

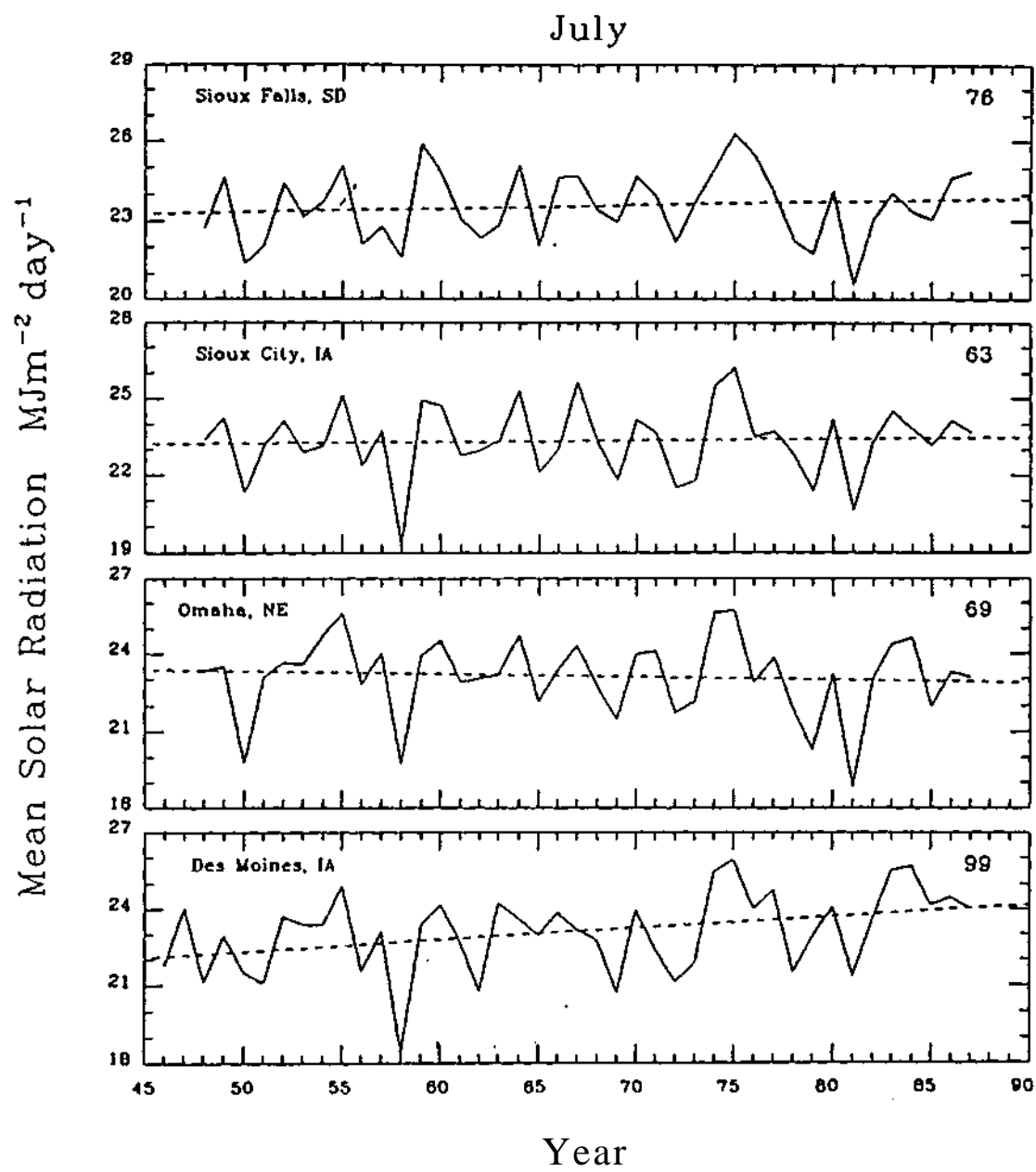


Fig. E.31. As in Fig. E.1.

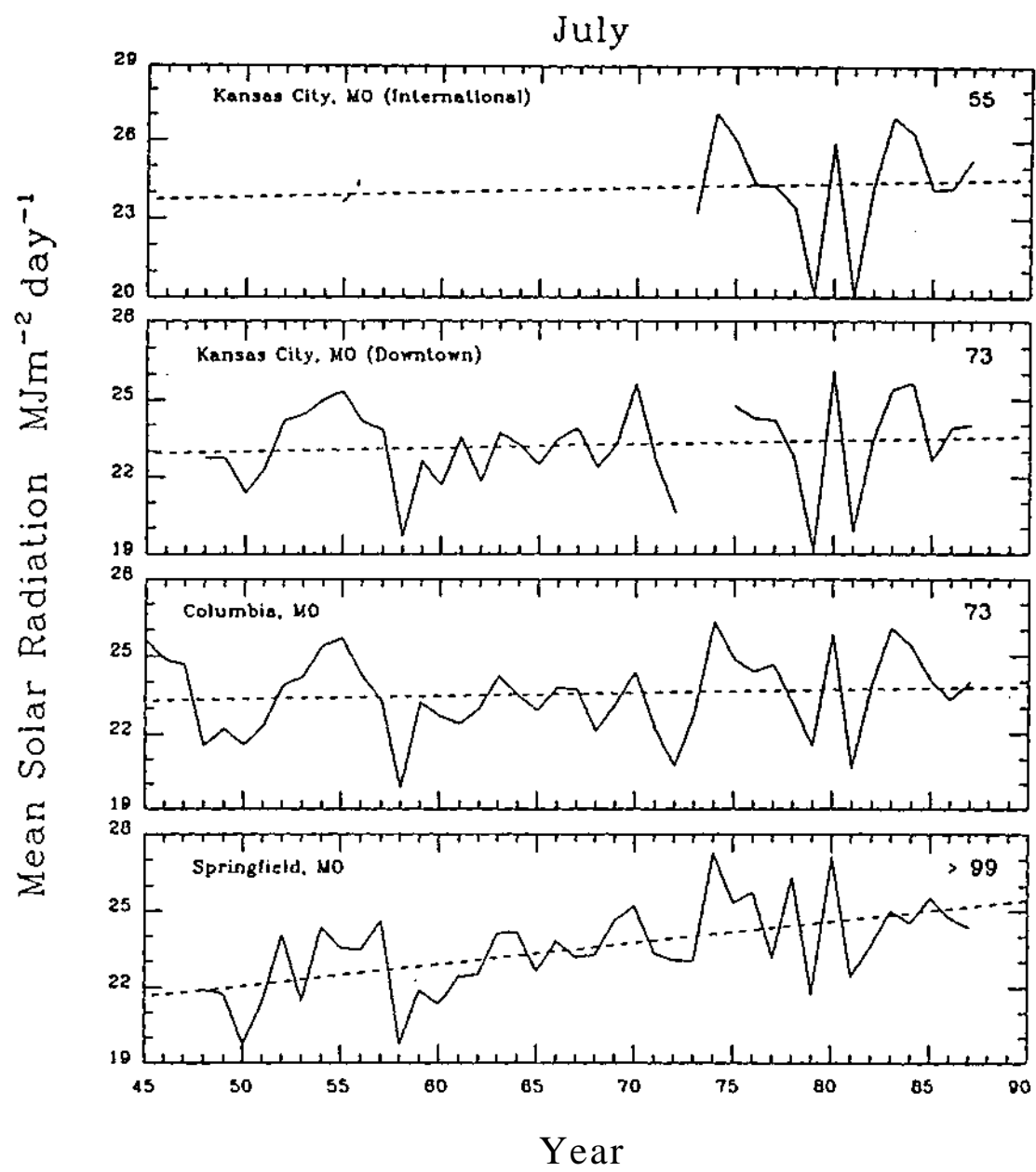


Fig. E.32. As in Fig. E.1.

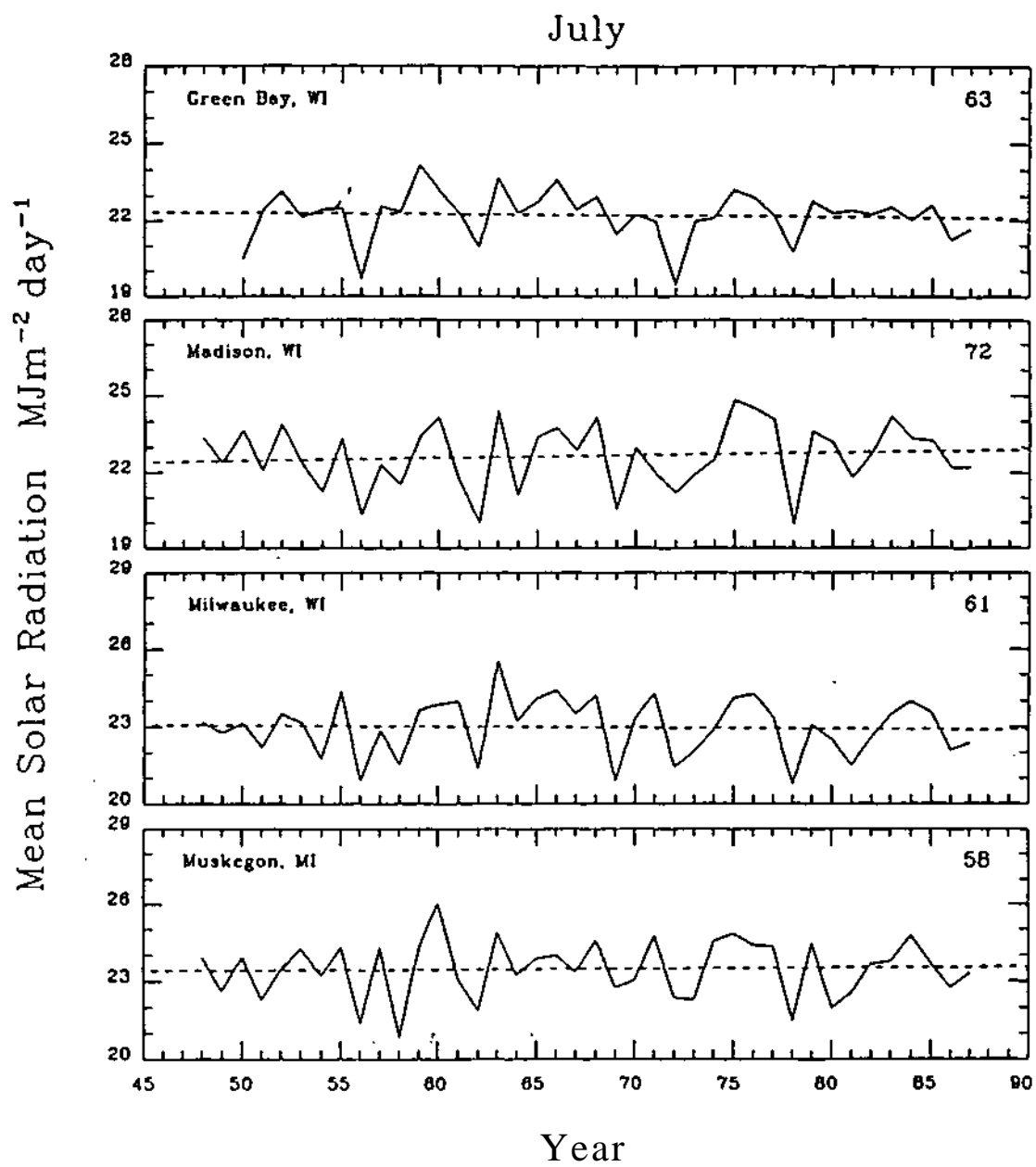


Fig. E.33. As in Fig. E.1.

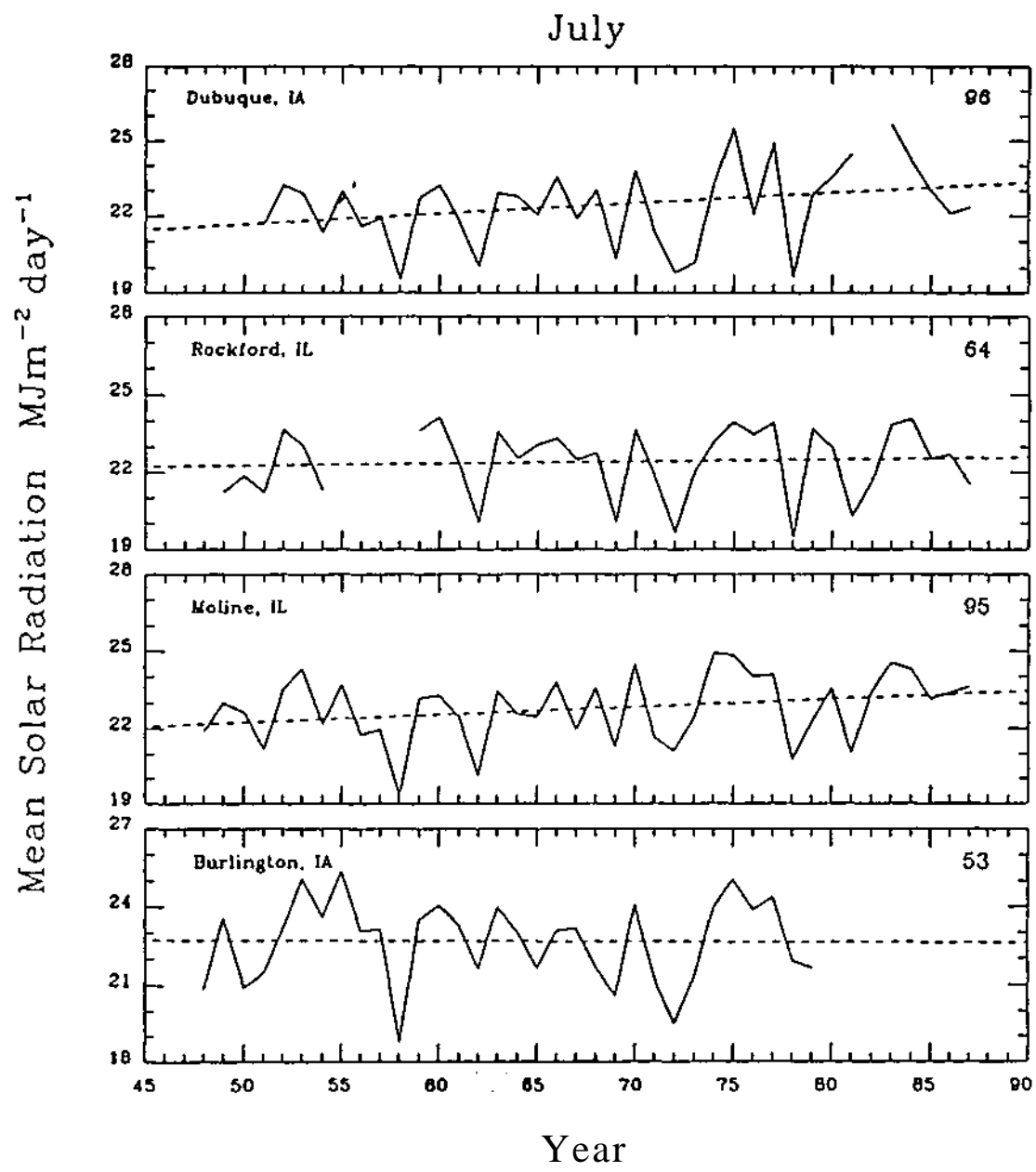


Fig. E.34. As in Fig. E.1.

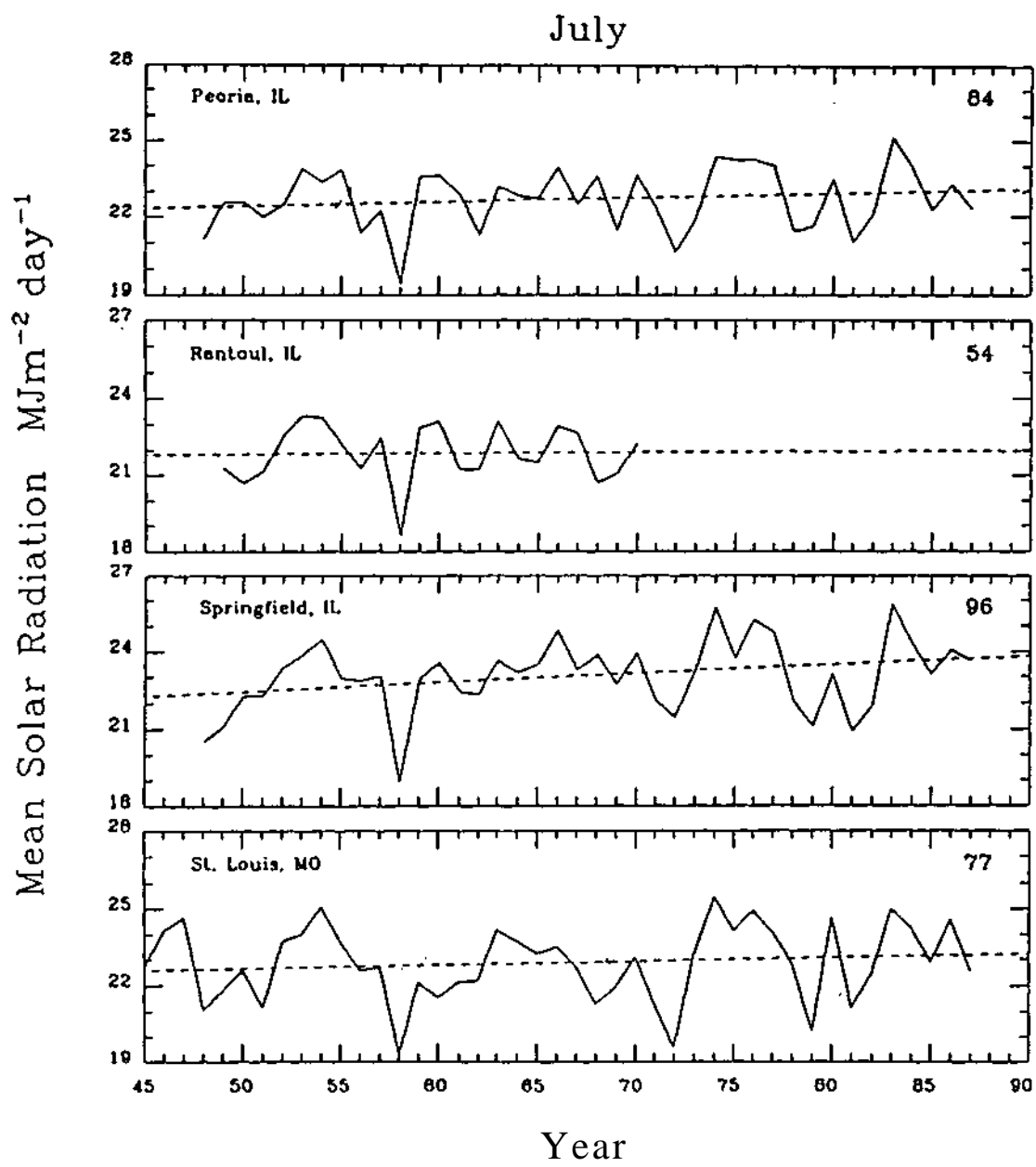


Fig. E.35. As in Fig. E.1.

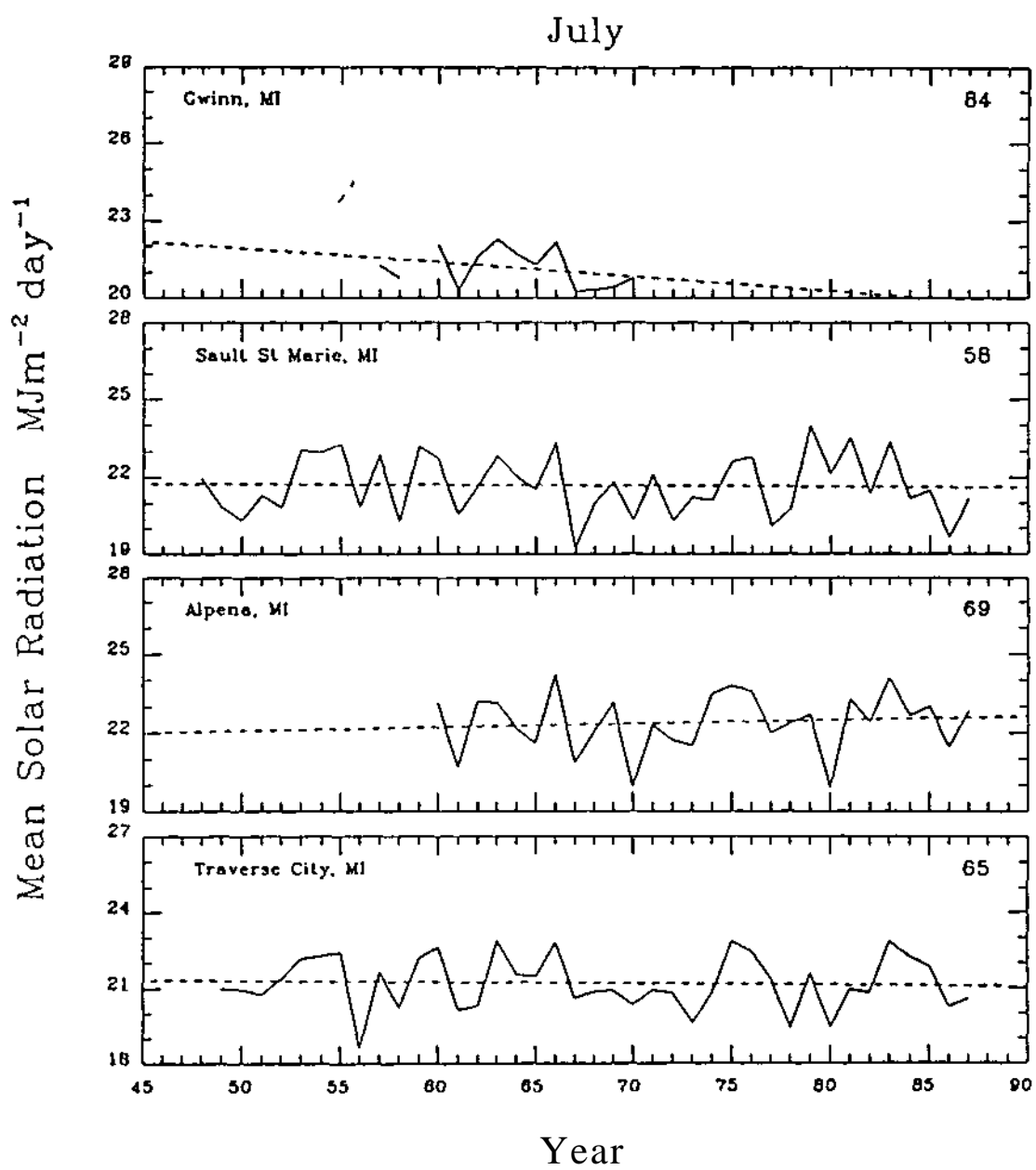


Fig. E.36. As in Fig. E.1.

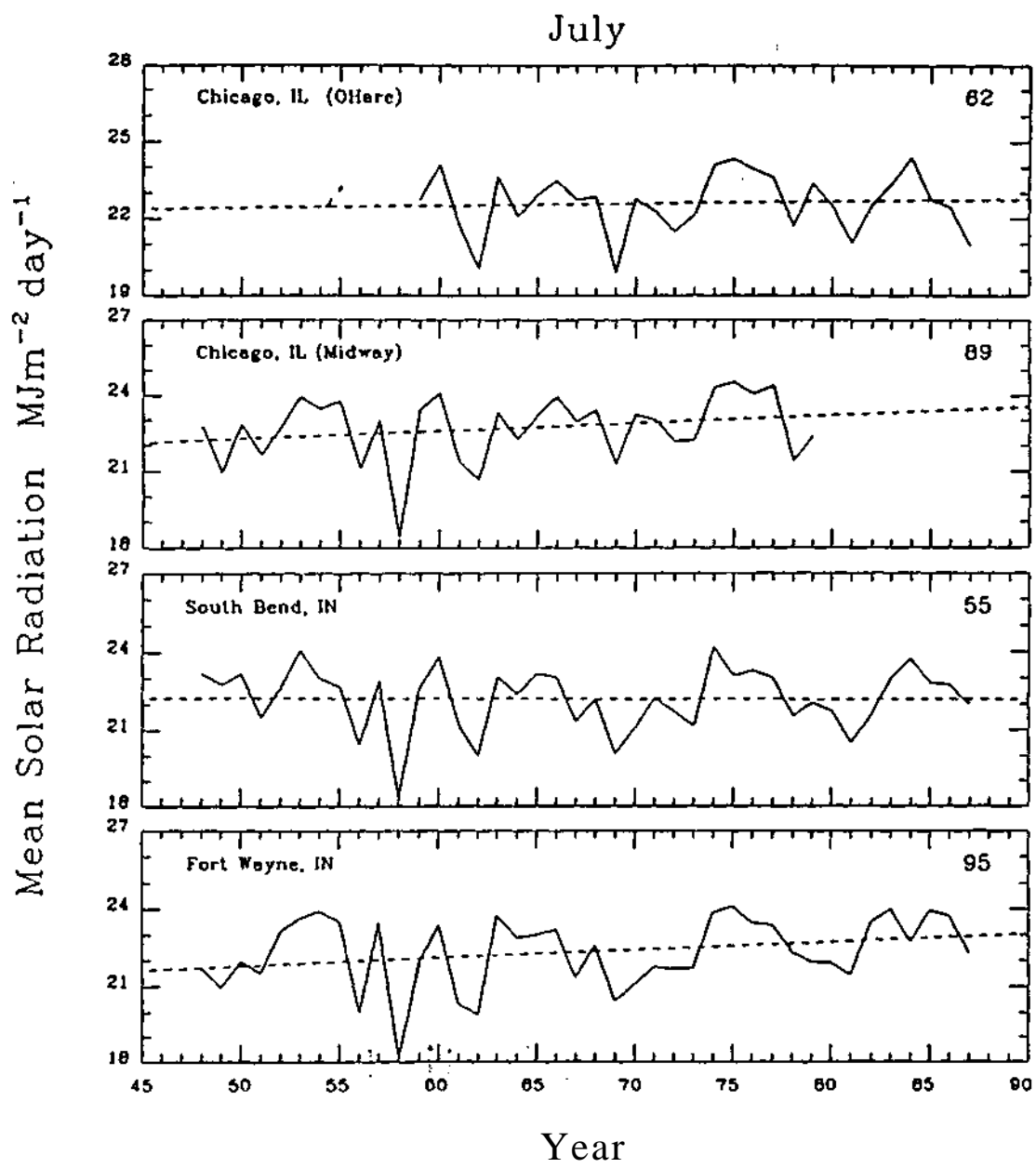


Fig. E.37. As in Fig. E.1.

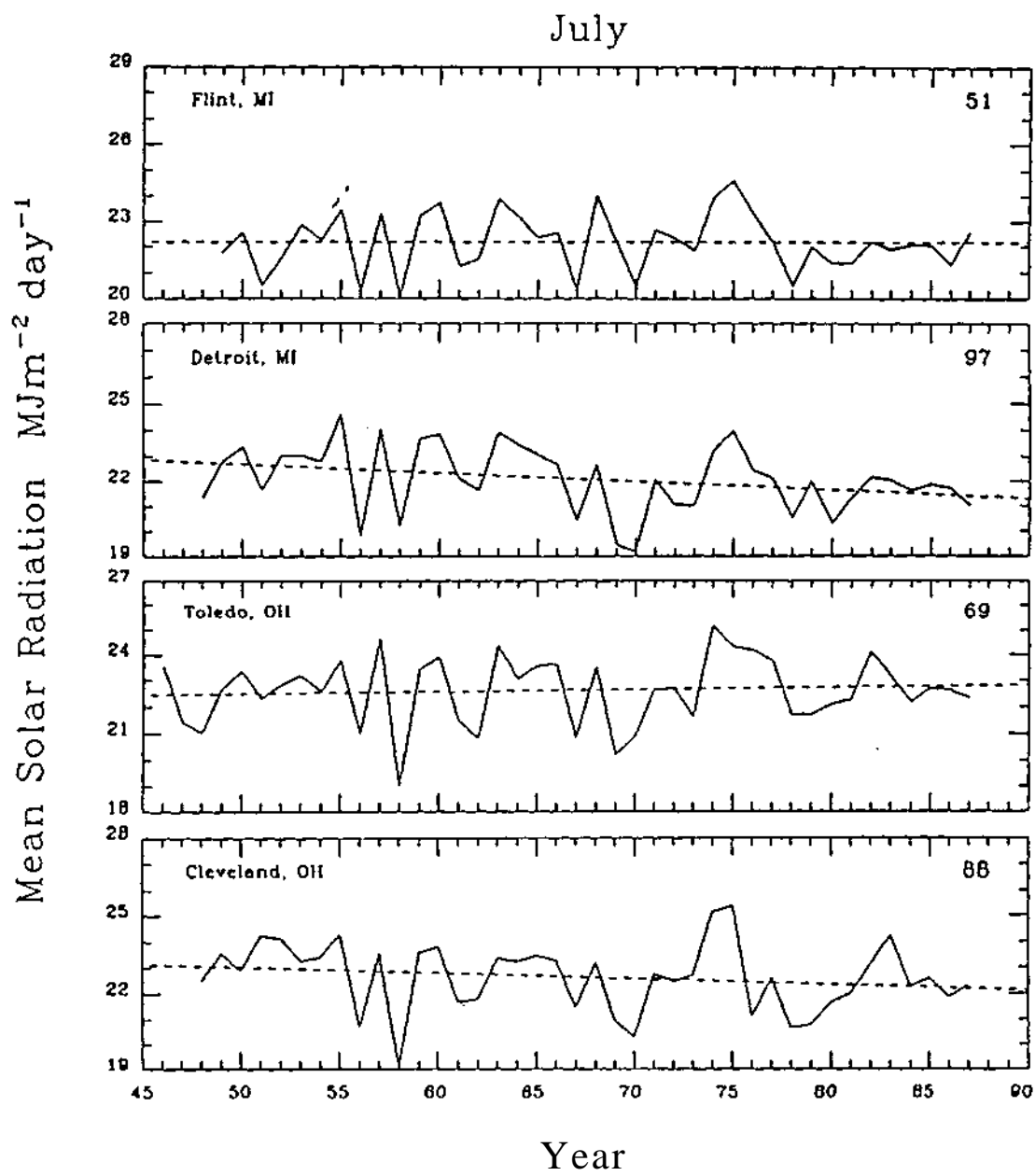


Fig. E.38. As in Fig. E.1.

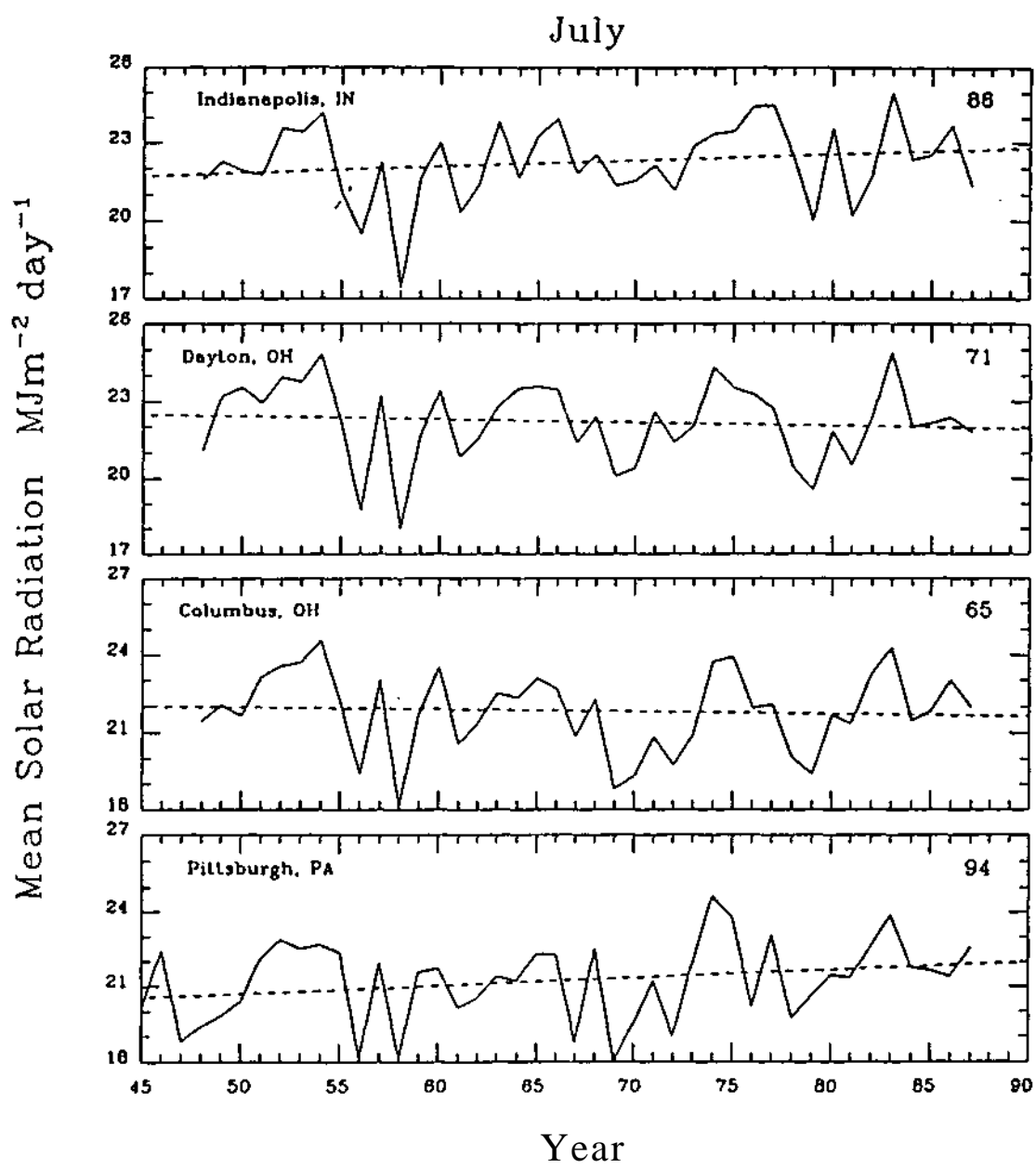


Fig. E.39. As in Fig. E.1.

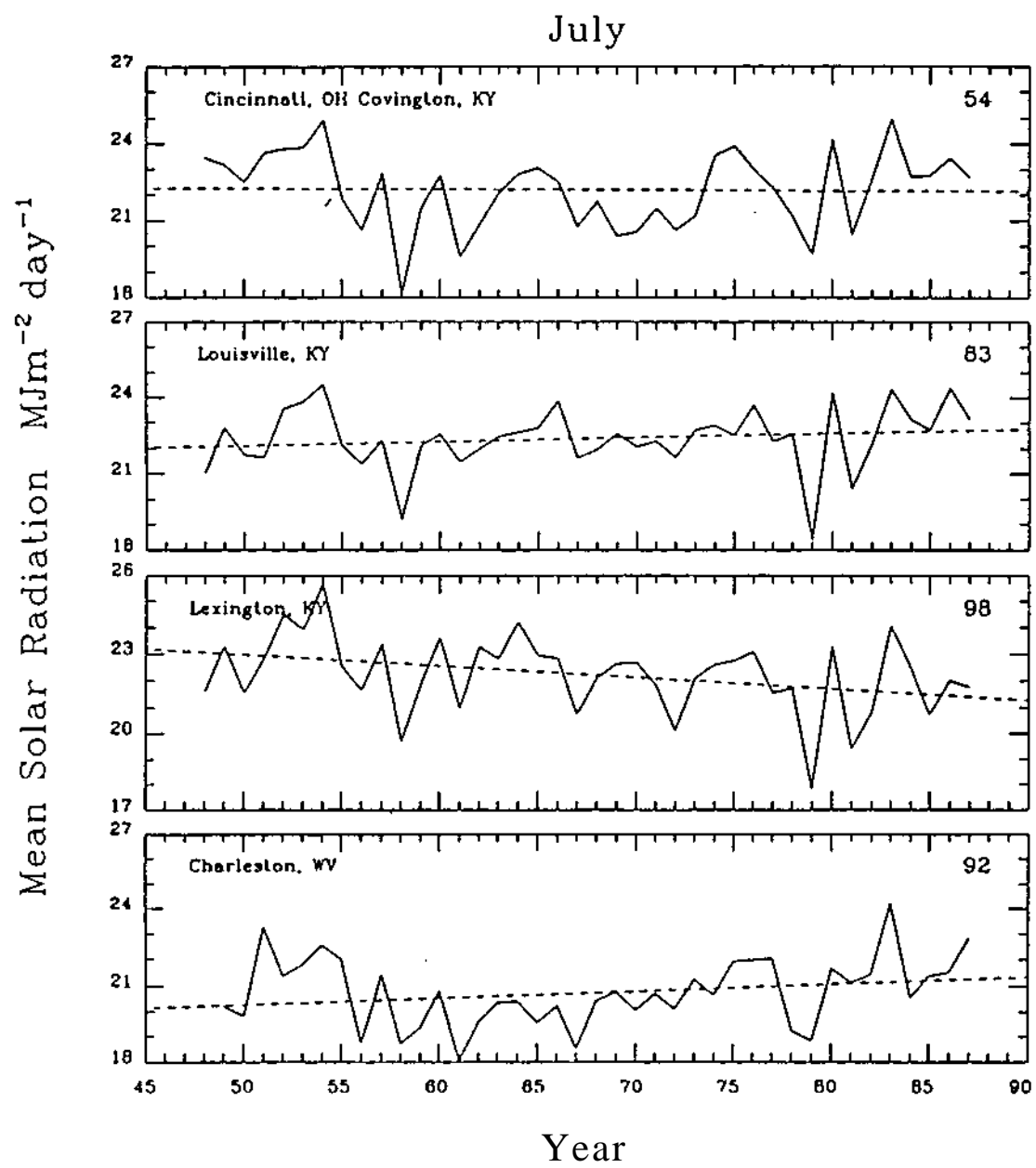


Fig. E.40. As in Fig. E.1.

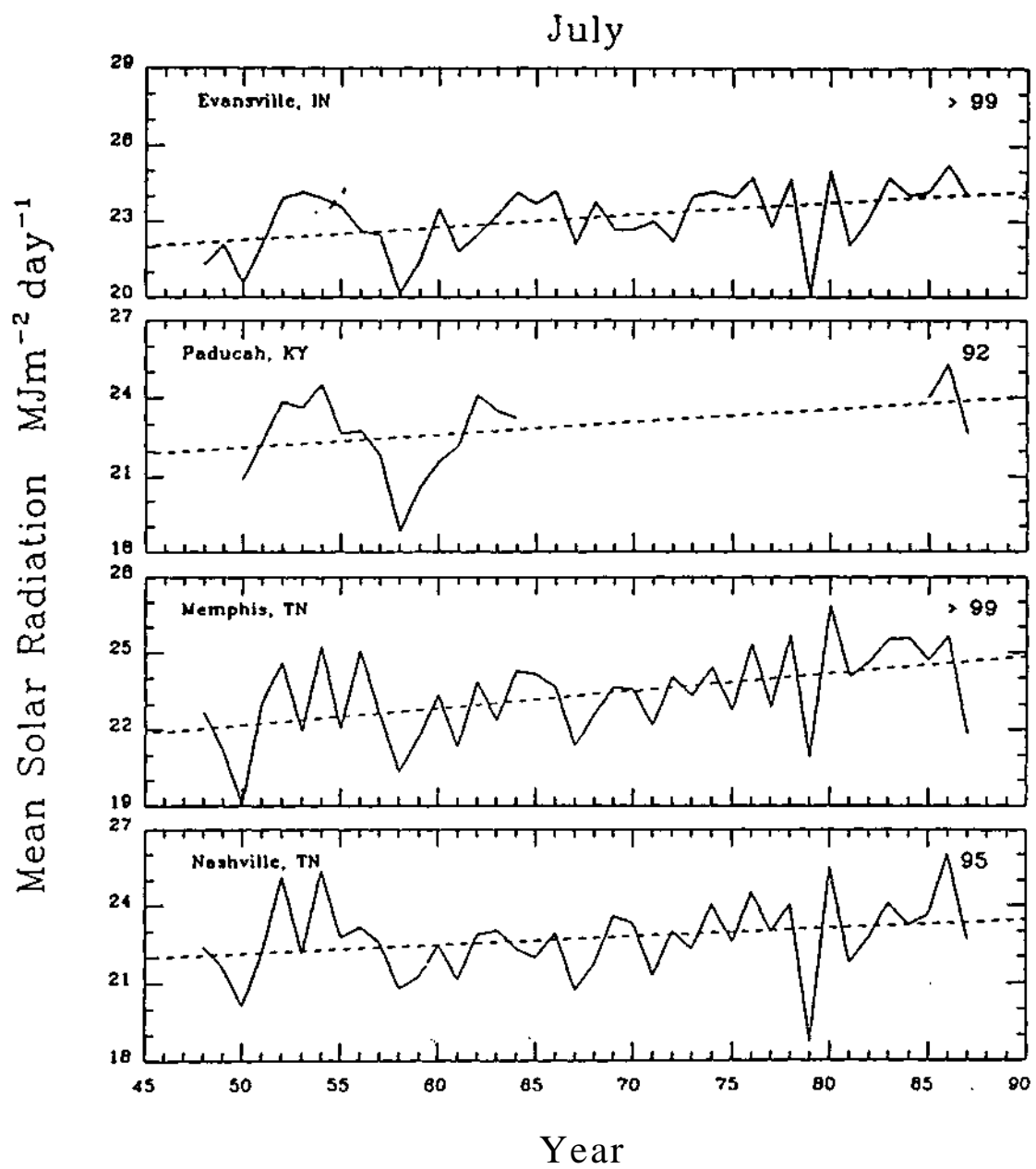


Fig. E.41. As in Fig. E.1.

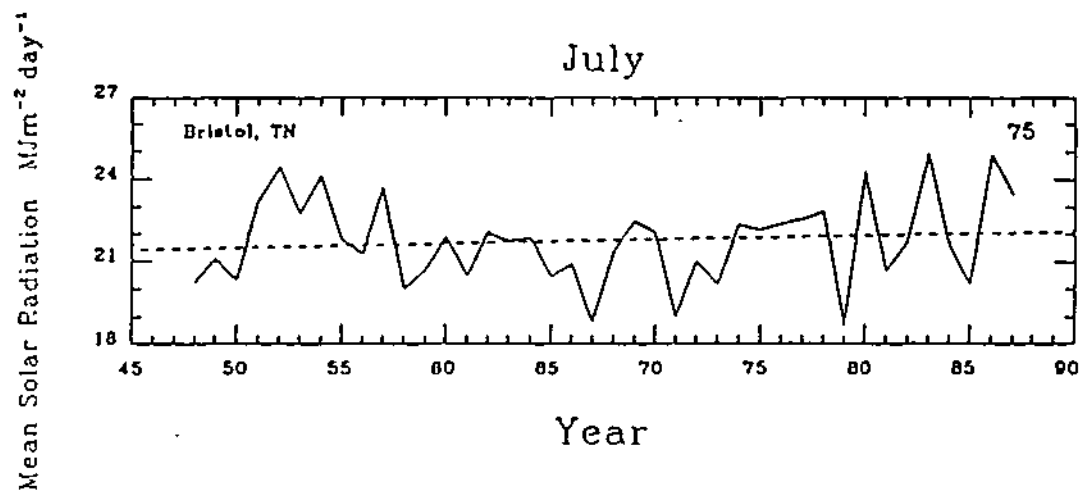


Fig. E.42. As in Fig. E.1.

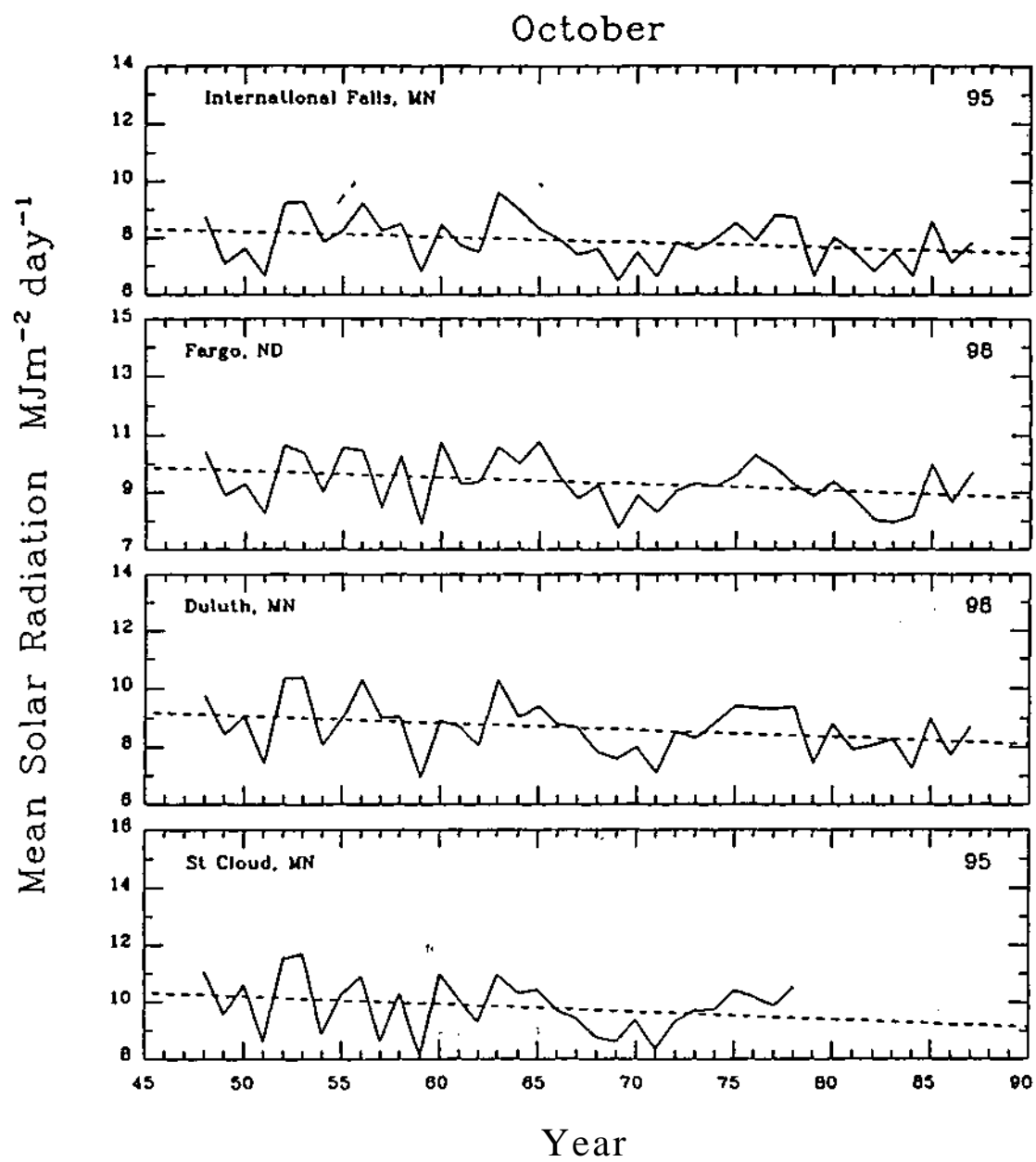


Fig. E.43. As in Fig. E.1.

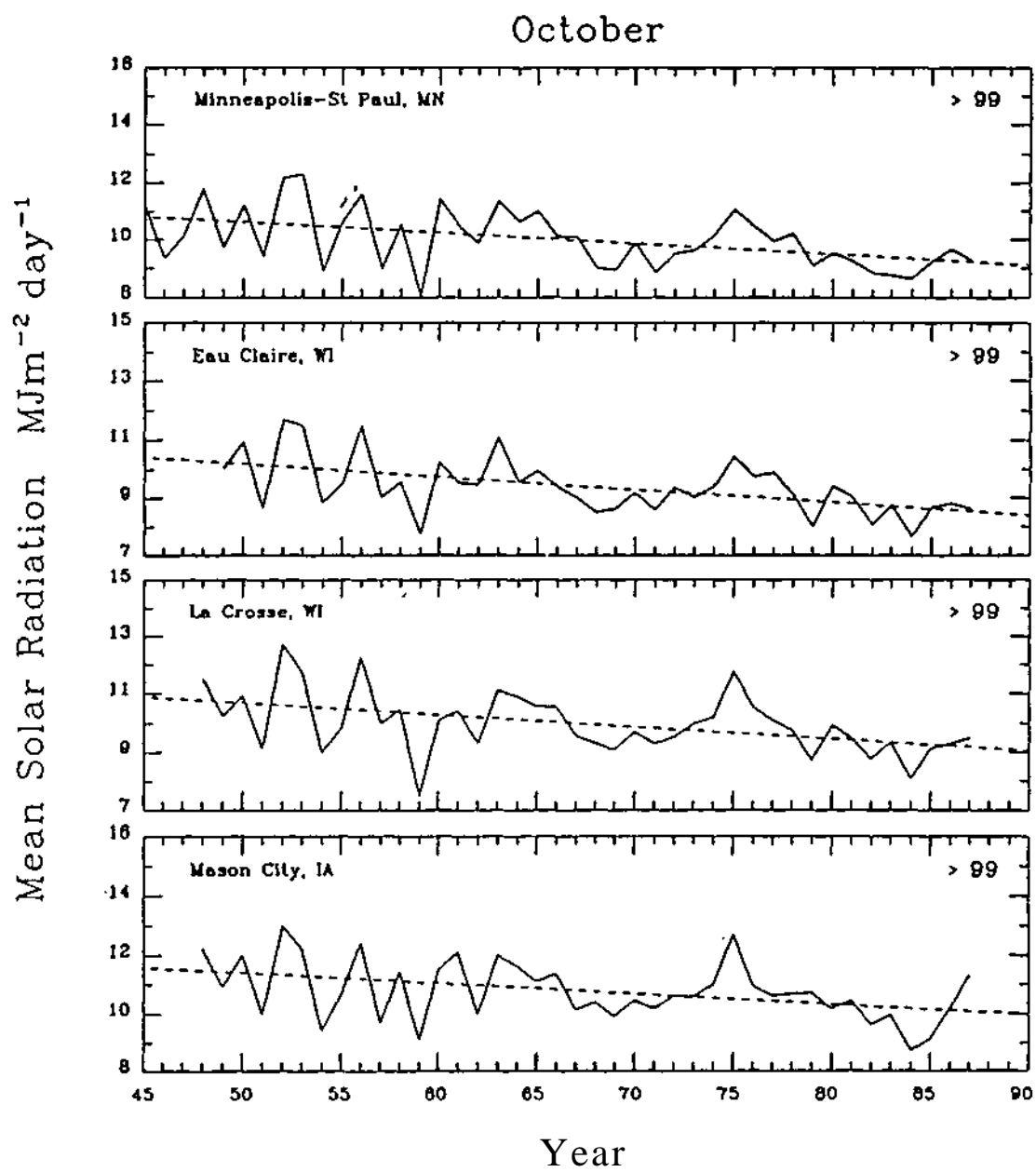


Fig. E.44. As in Fig. E.1.

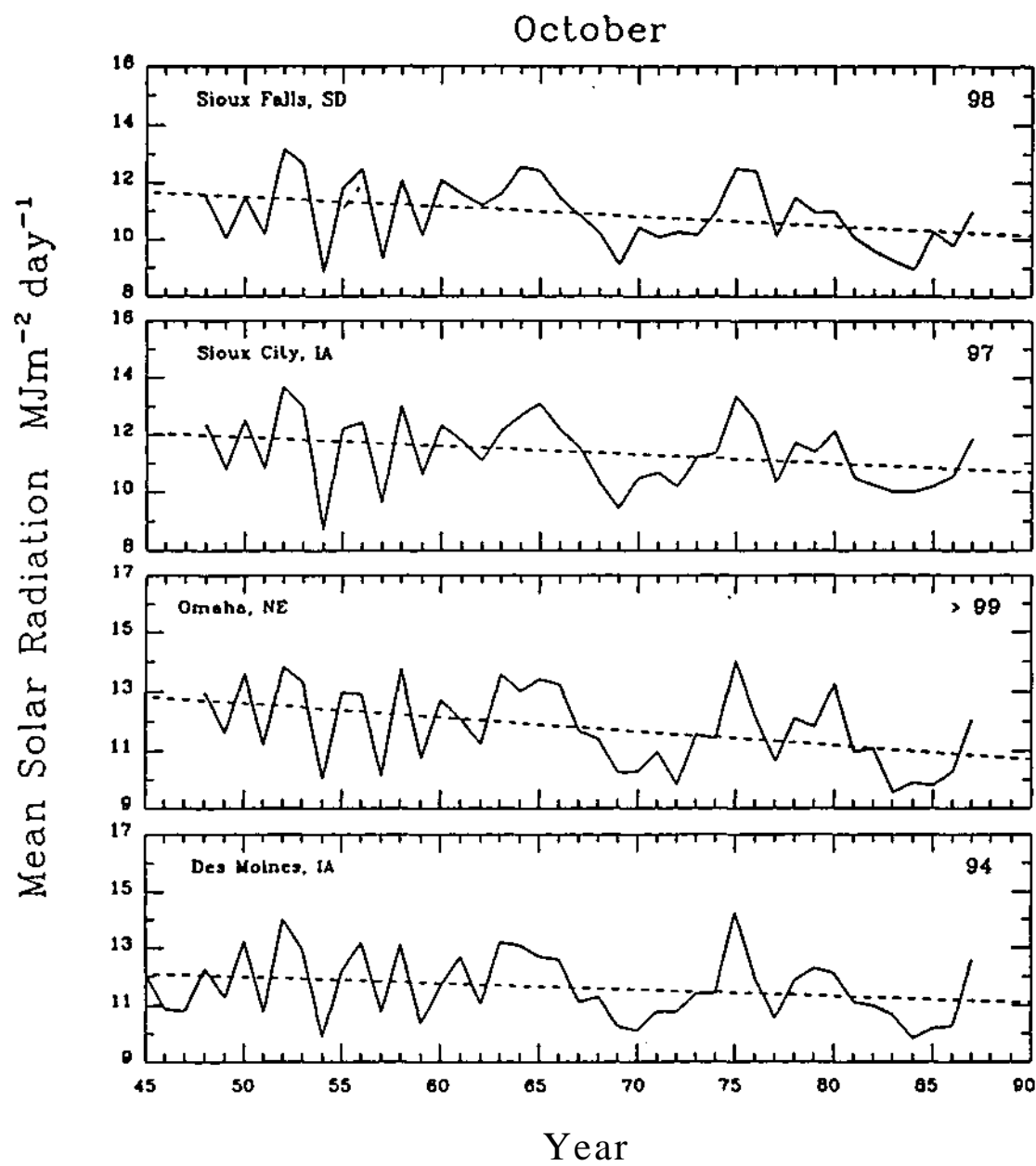


Fig. E.45. As in Fig. E.1.

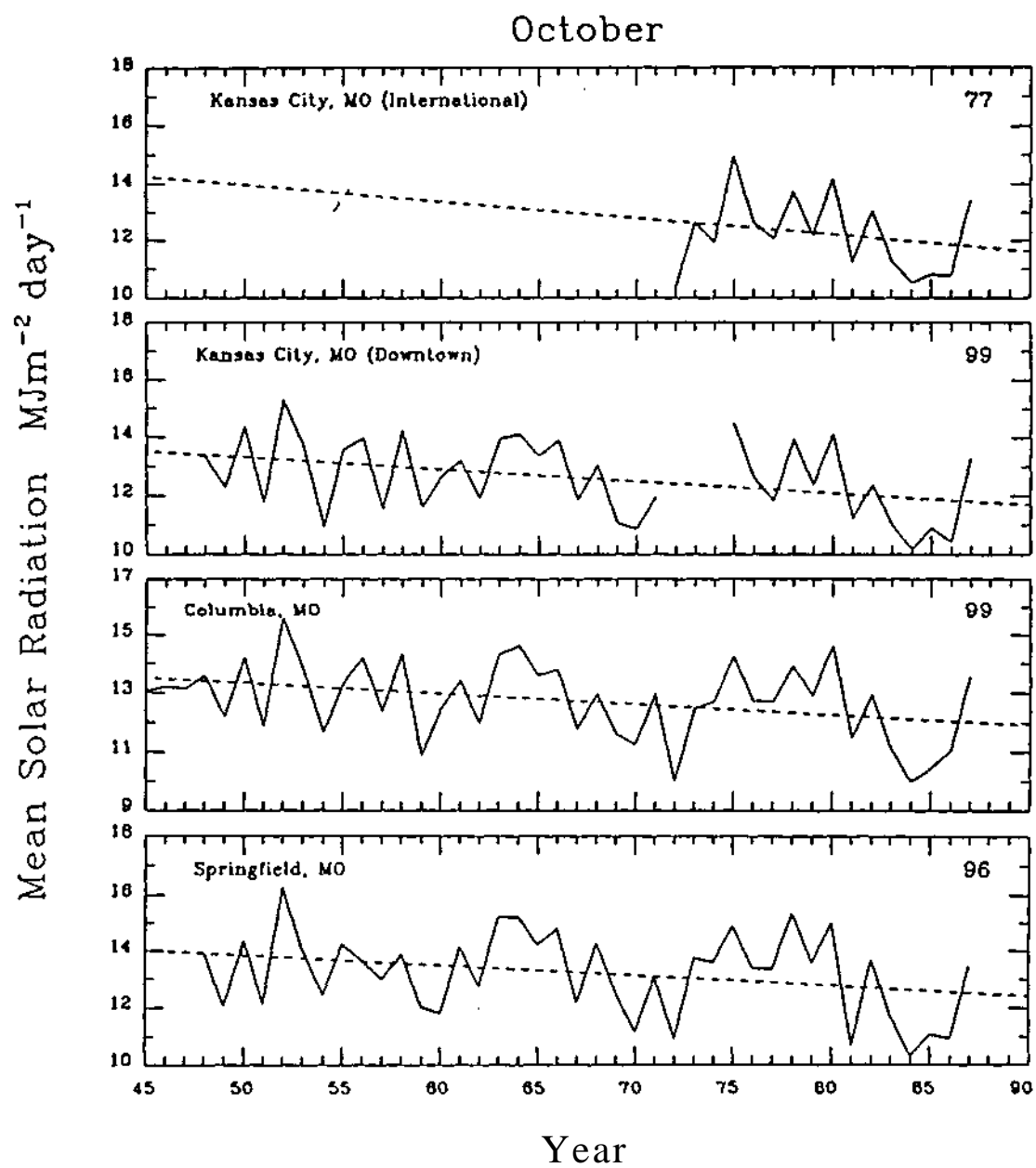


Fig. E.46. As in Fig. E.1.

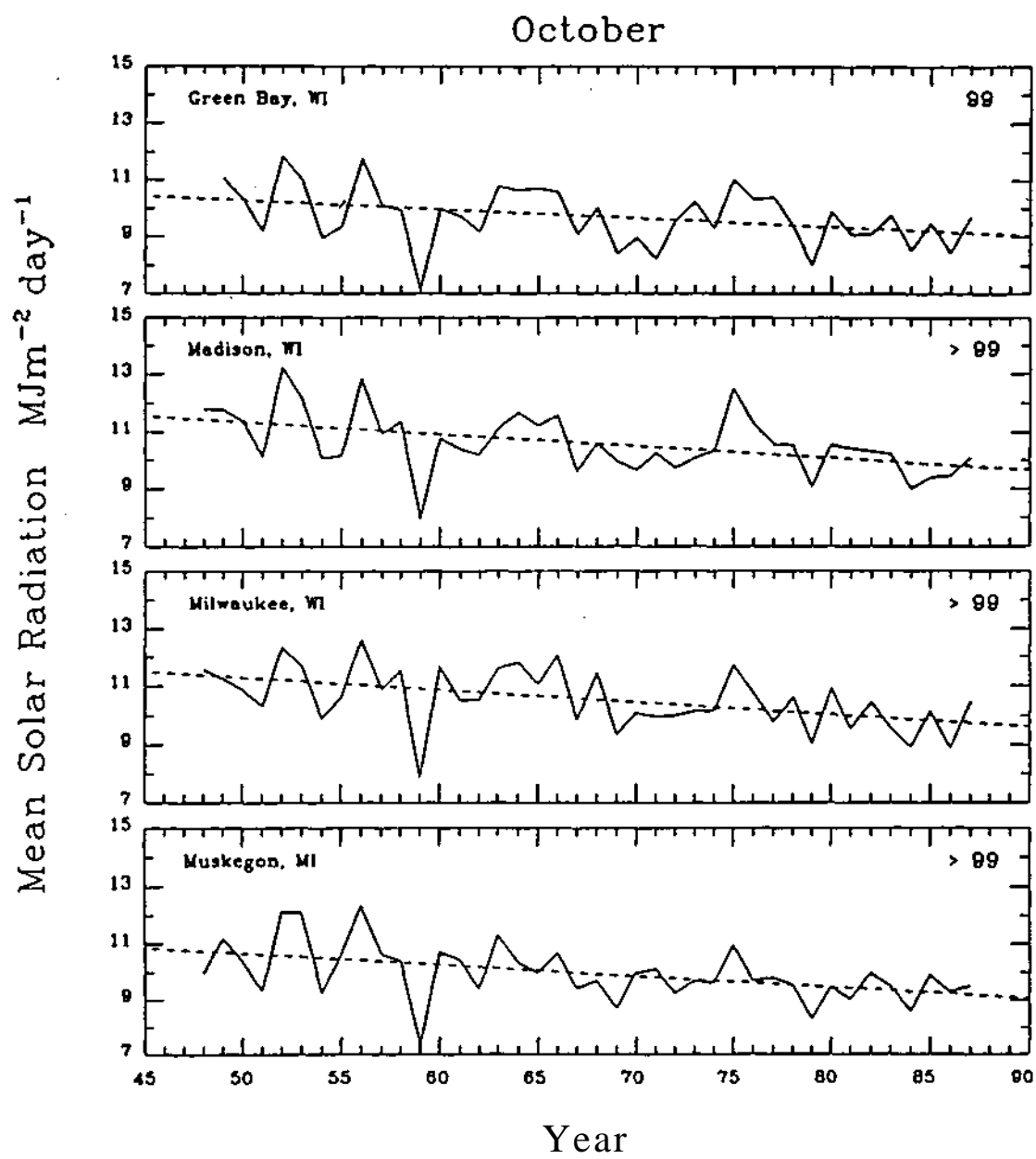


Fig. E.47. As in Fig. E.1.

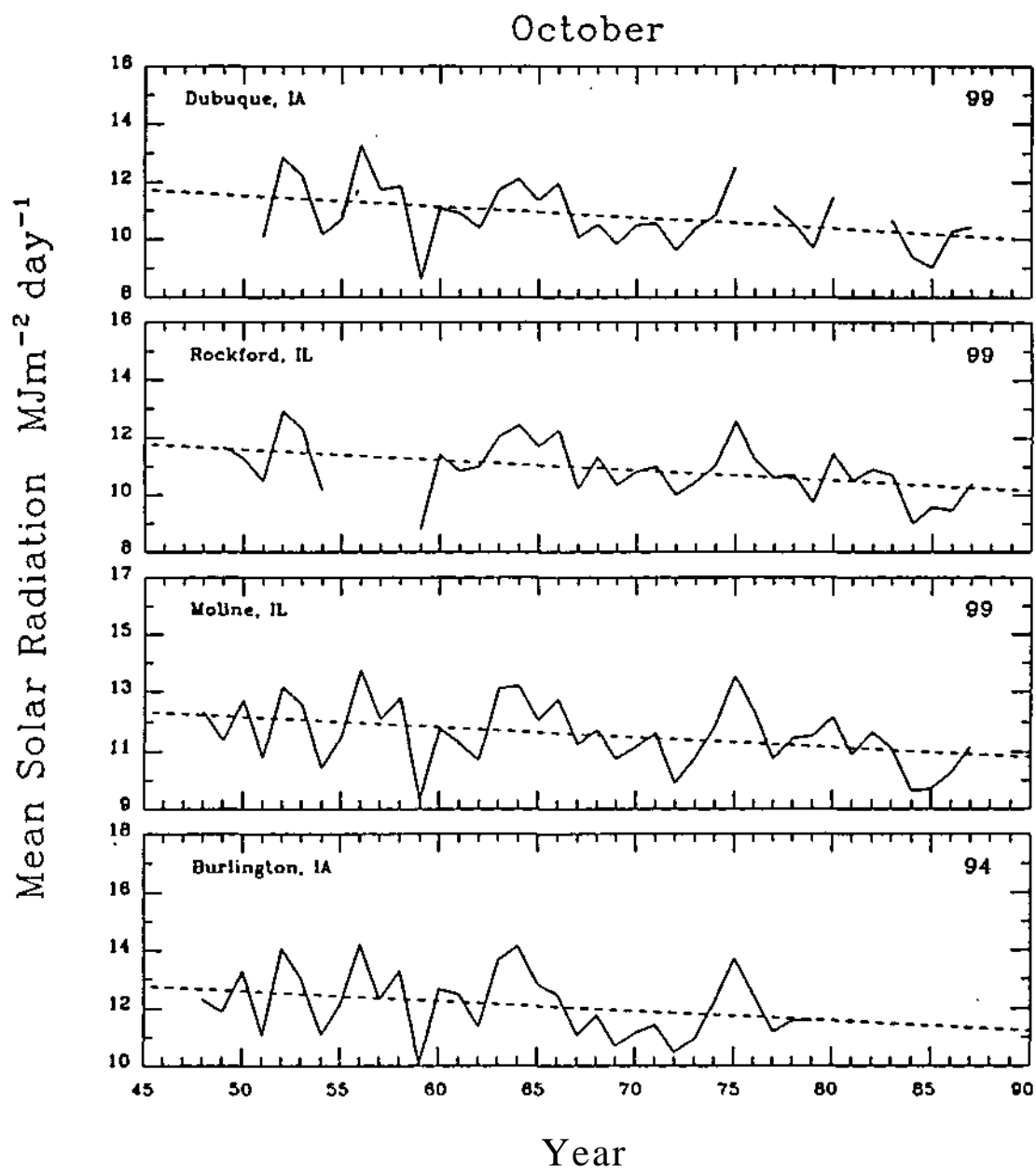


Fig. E.48. As in Fig. E.1.

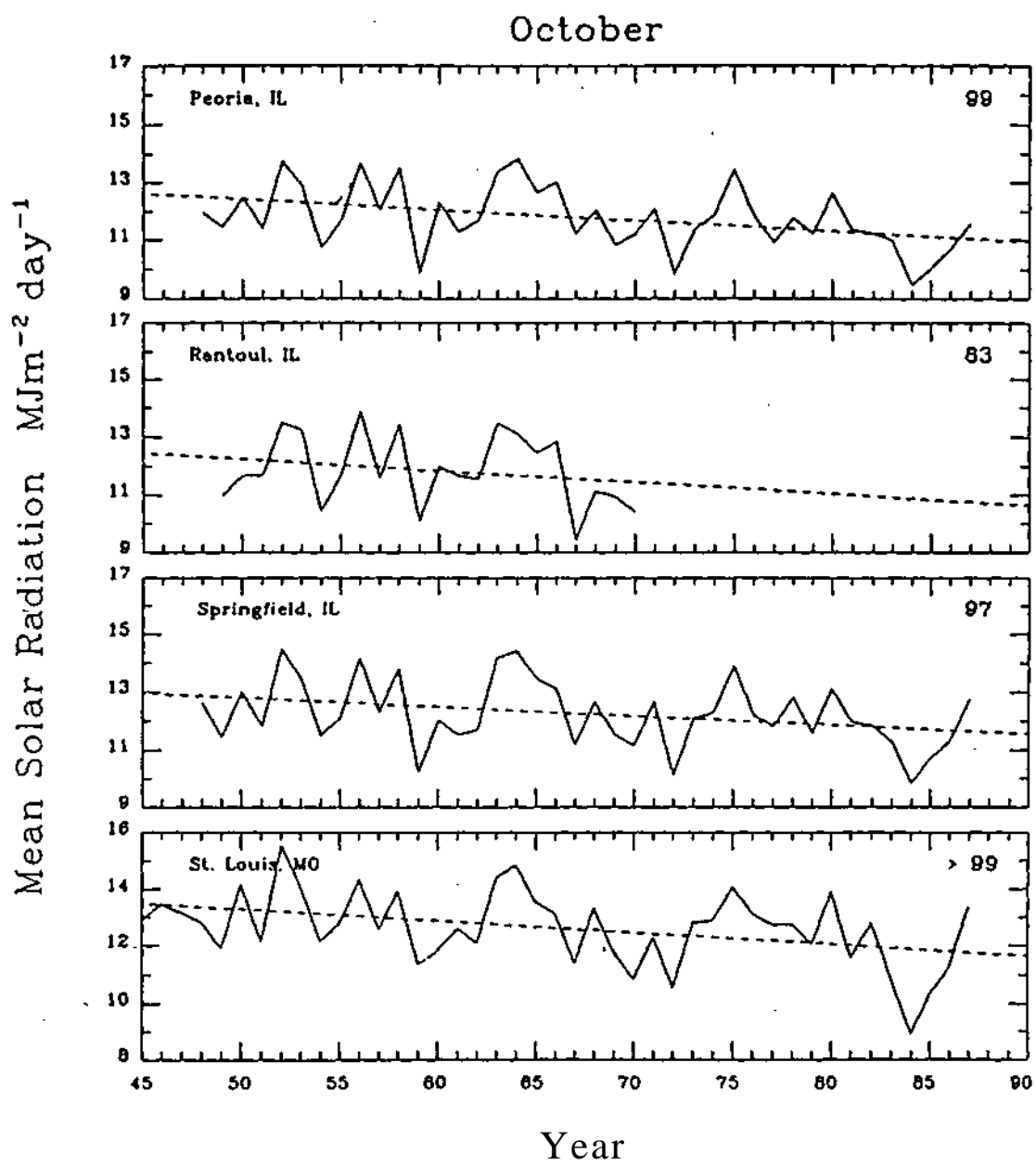


Fig. E.49. As in Fig. E.1.

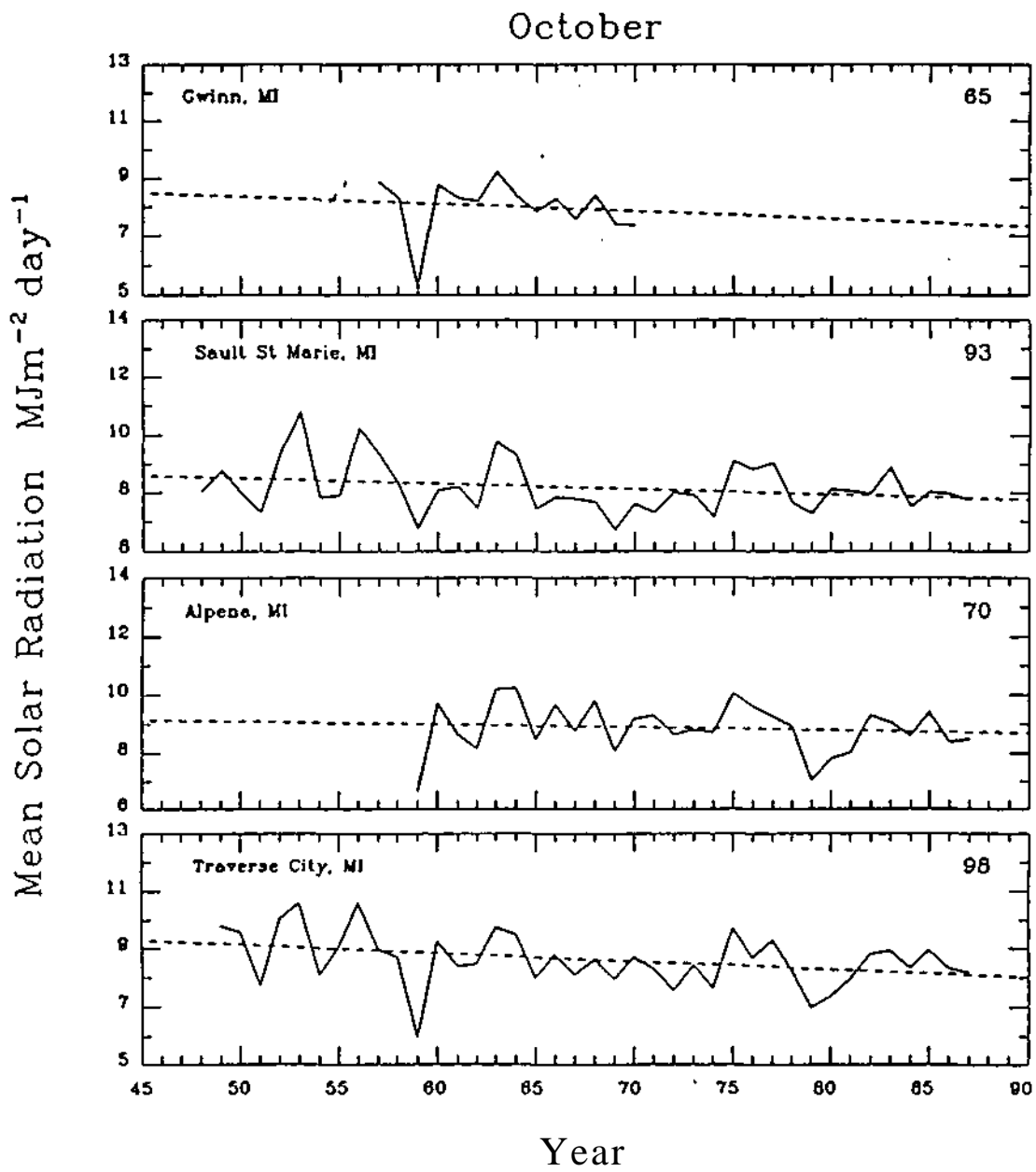


Fig. E.50. As in Fig. E.1.

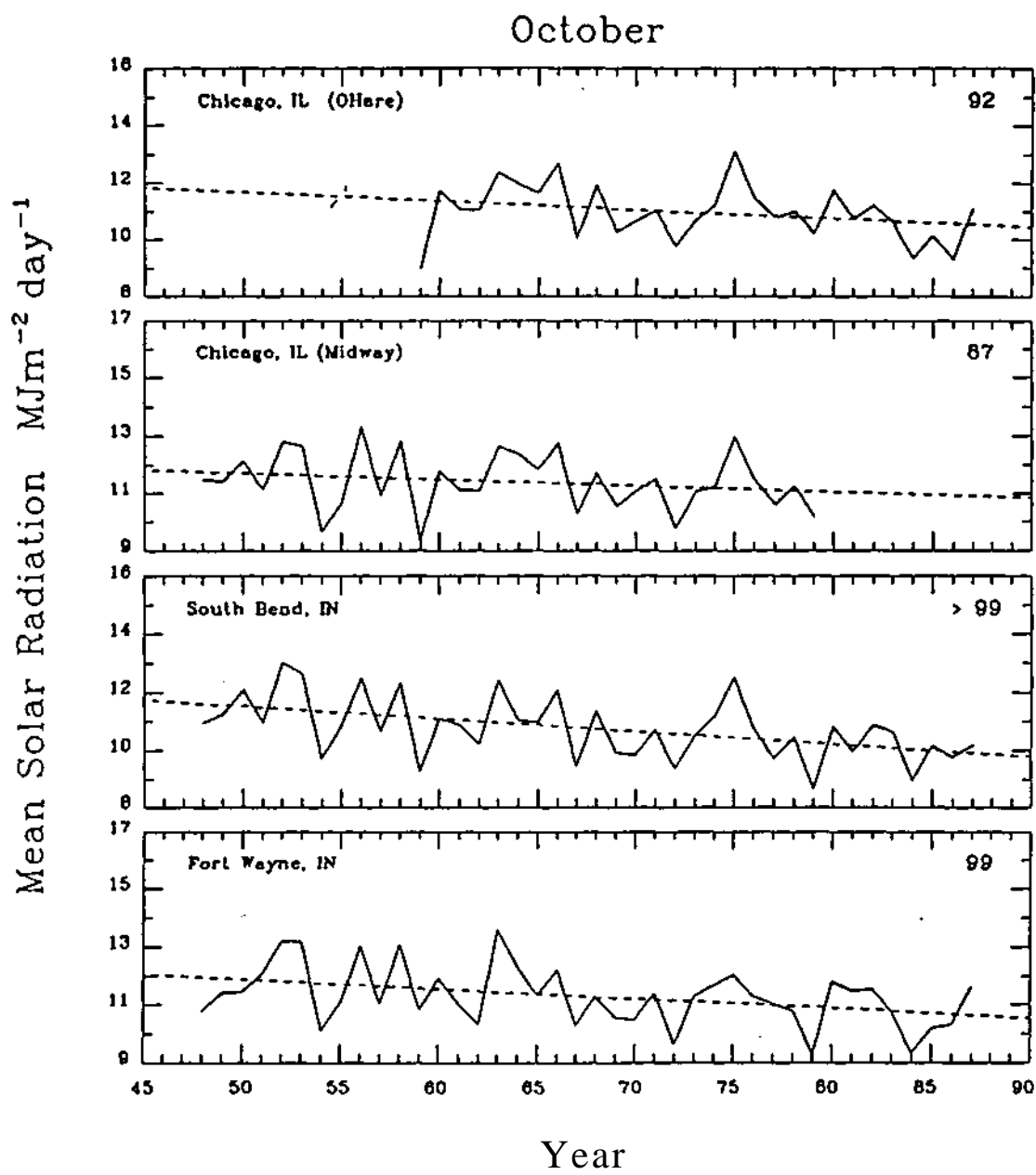


Fig. E.51. As in Fig. E.1.

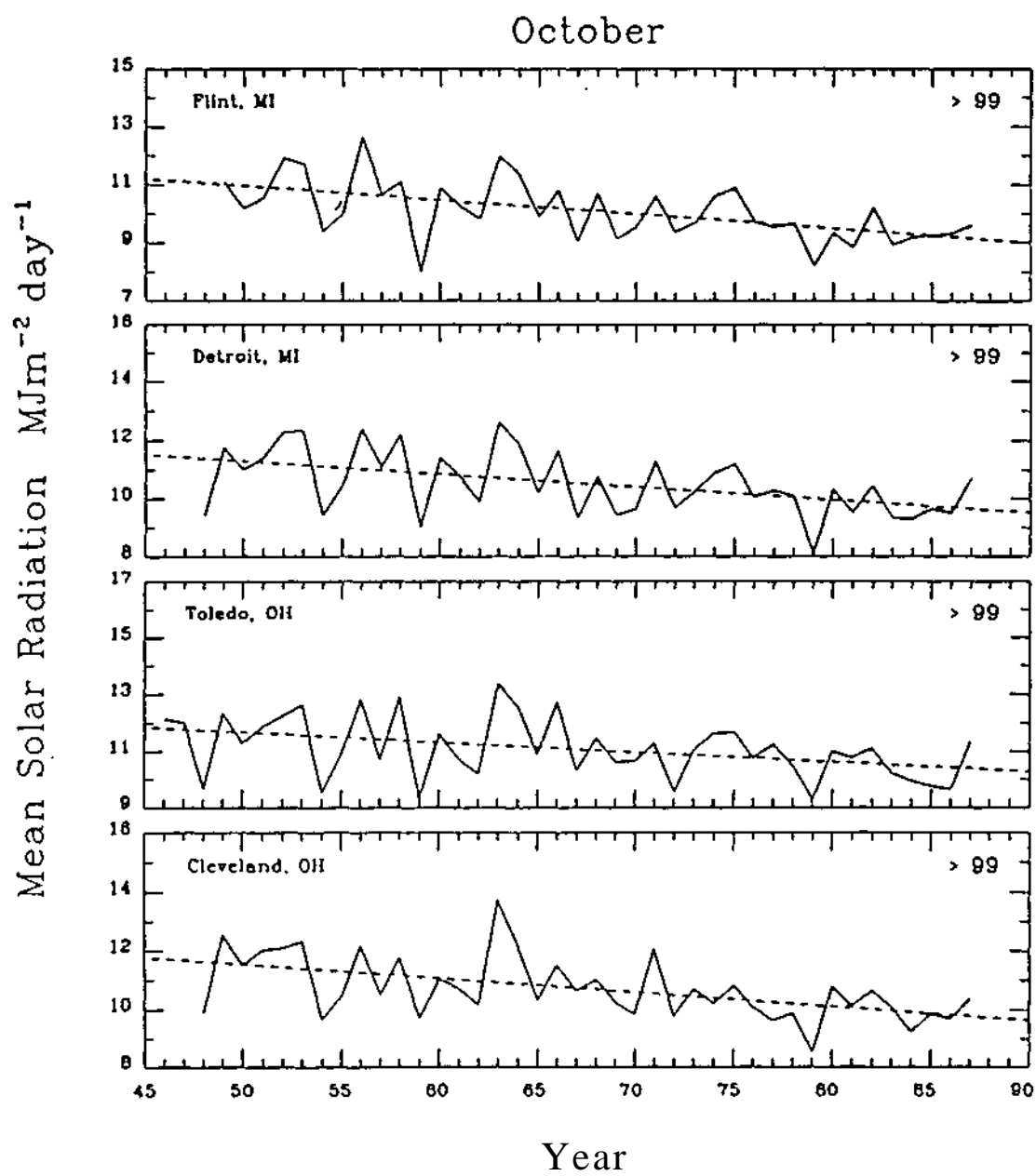


Fig. E.52. As in Fig. E.1.

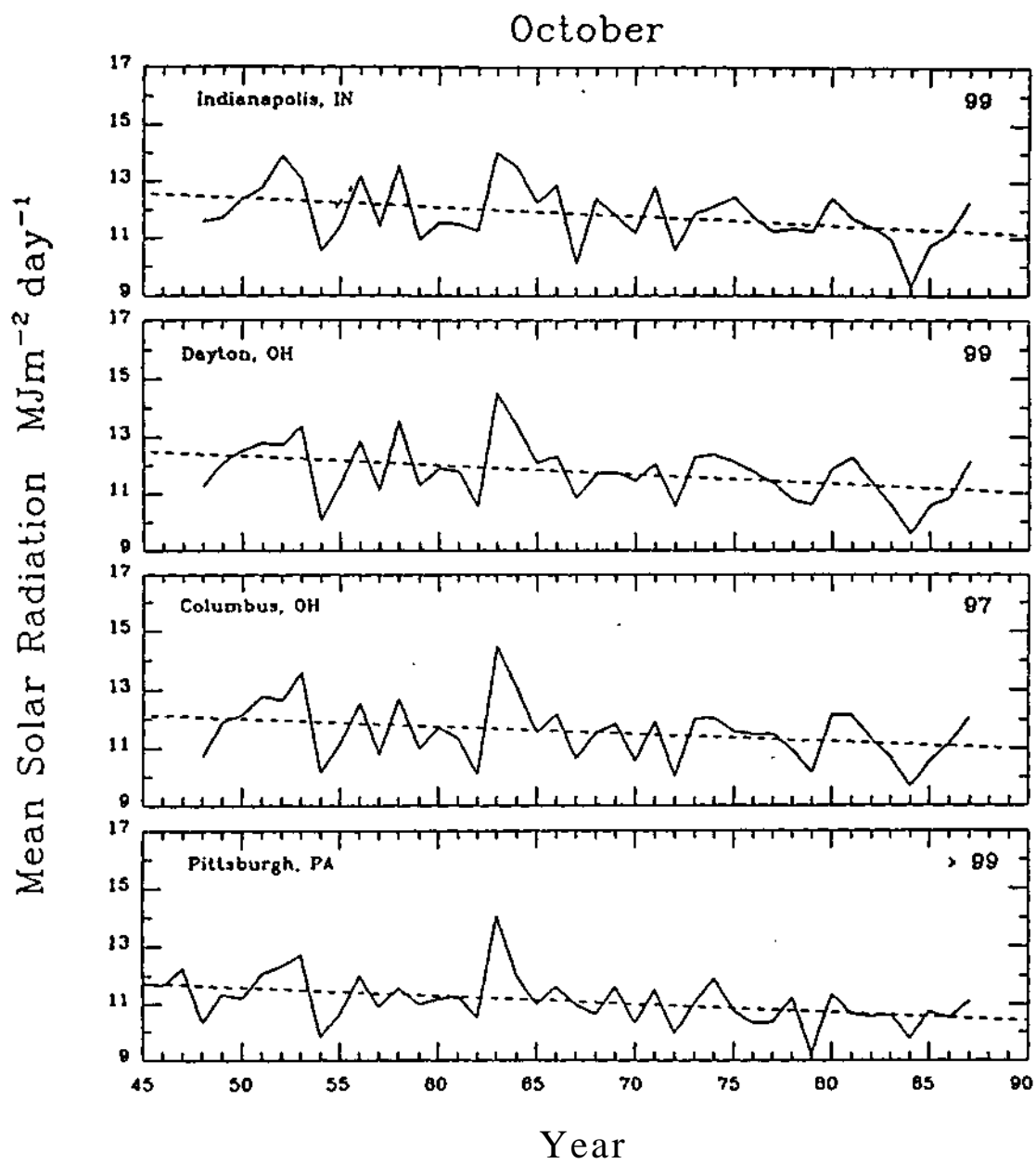


Fig. E.53. As in Fig. E.1.

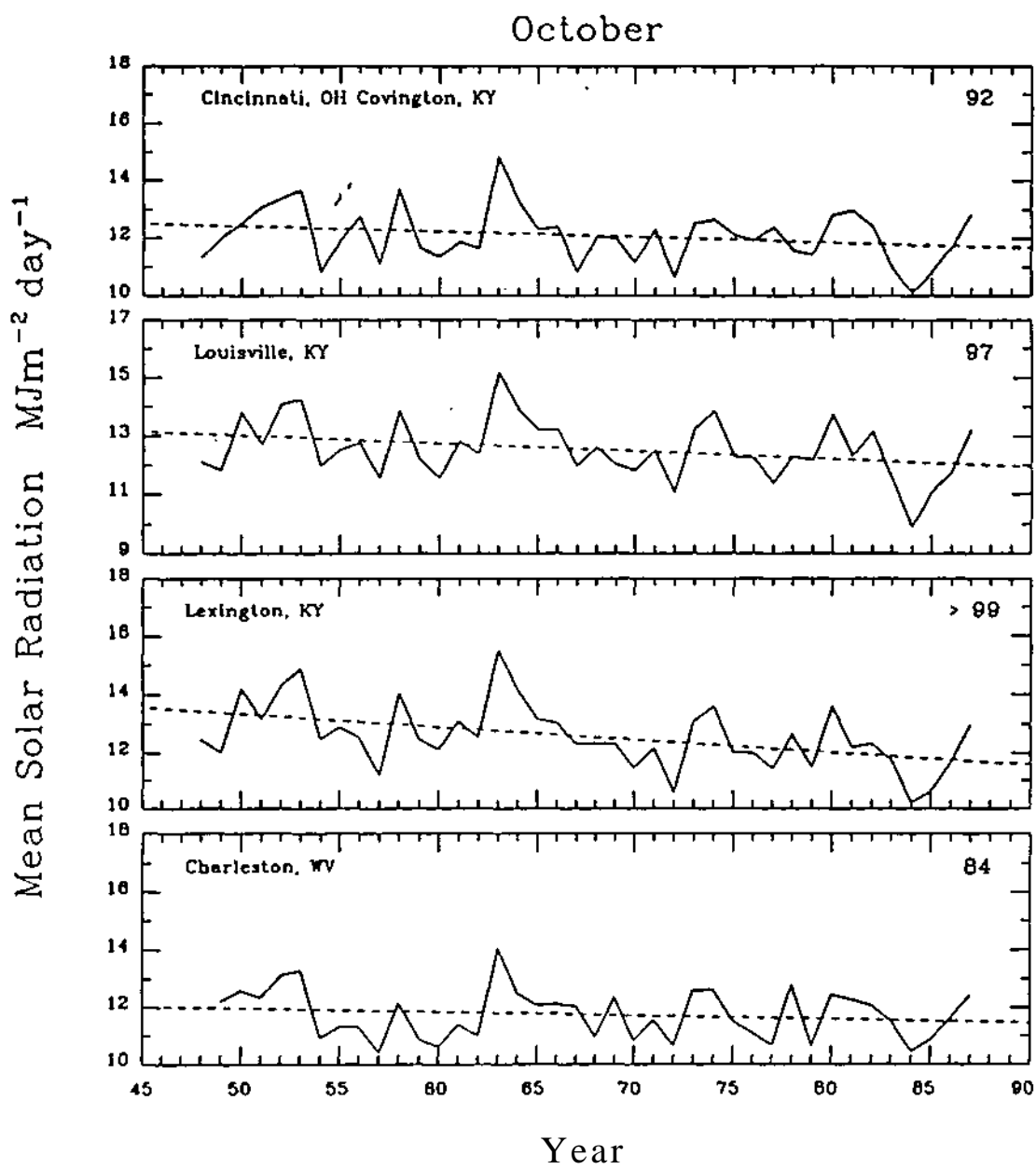


Fig. E.54. As in Fig. E.1.

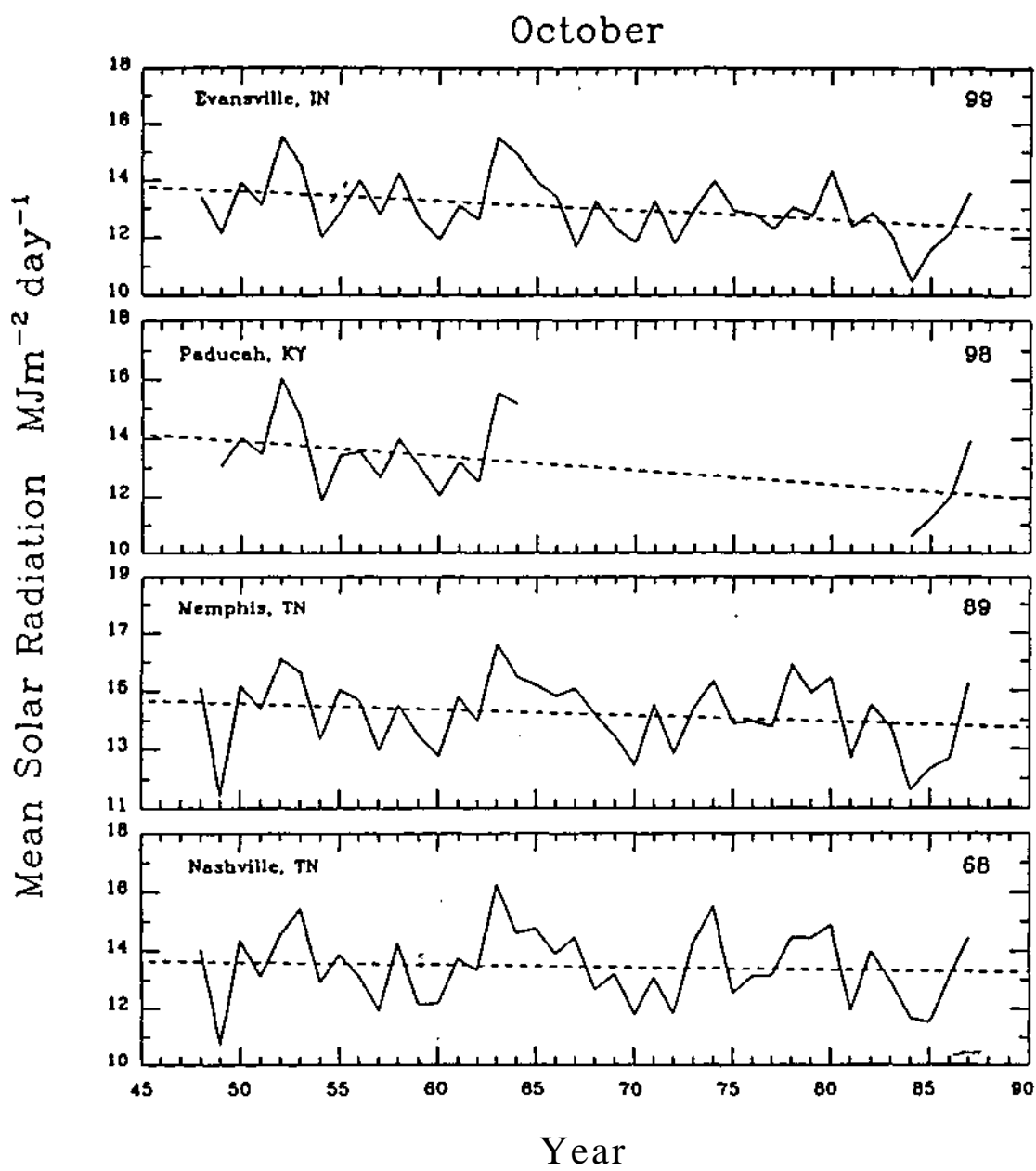


Fig. E.55. As in Fig. E.1.

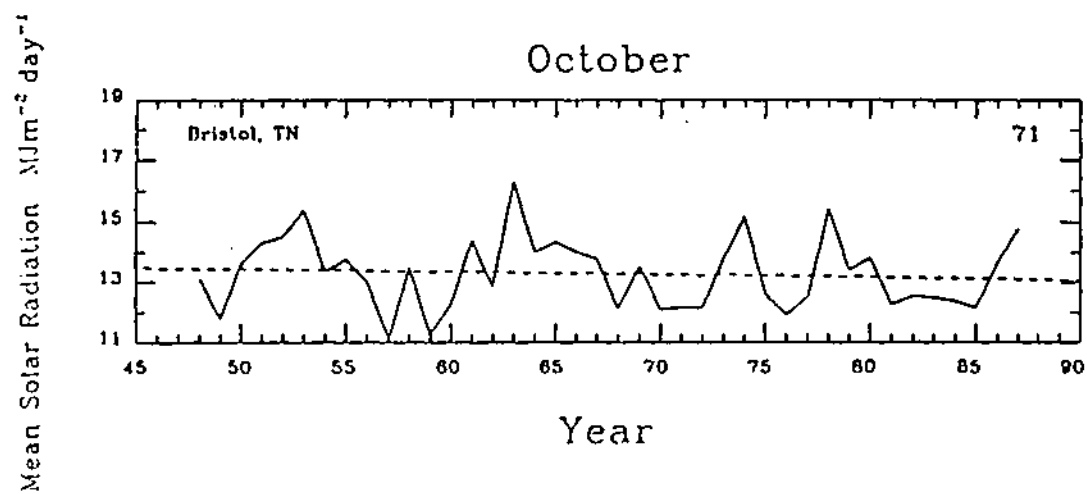


Fig. E.56. As in Fig. E.1.